

# Stability Analysis of Fixed Points of Various Nonlinear Mathematical Models with Chaos Control



By

Muhammad Salman Khan

Department of Mathematics  
Quaid-I-Azam University,  
Islamabad, Pakistan  
2023

# Stability Analysis of Fixed Points of Various Nonlinear Mathematical Models with Chaos Control



By

Muhammad Salman Khan

Supervised By

Dr. Maria Samreen

Department of Mathematics

Quaid-I-Azam University,  
Islamabad, Pakistan

2023

# Stability Analysis of Fixed Points of Various Nonlinear Mathematical Models with Chaos Control



By

**Muhammad Salman Khan**

This dissertation is submitted for the degree of  
Doctor of Philosophy in Mathematics

Supervised By

**Dr. Maria Samreen**

Department of Mathematics

Quaid-I-Azam University,  
Islamabad, Pakistan

2023

## Author's Declaration

I, Muhammad Salman Khan, hereby state that my PhD thesis titled Stability Analysis of Fixed Points of Various Nonlinear Mathematical Models with Chaos Control is my own work and has not been submitted previously by me for taking any degree from the Quaid-I-Azam University Islamabad, Pakistan or anywhere else in the country/world.

At any time if my statement is found to be incorrect even after my graduate the university has the right to withdraw my PhD degree.



Name of Student: Muhammad Salman Khan

Date: 29-May-2023



## **Plagiarism Undertaking**

I solemnly declare that research work presented in the thesis titled "**Stability Analysis of Fixed Points of Various Nonlinear Mathematical Models with Chaos Control**" is solely my research work with no significant contribution from any other person. Small contribution/help wherever taken has been duly acknowledged and that complete thesis has been written by me.

I understand the zero tolerance policy of the HEC and **Quaid-i-Azam University** towards plagiarism. Therefore, I as an Author of the above titled thesis declare that no portion of my thesis has been plagiarized and any material used as reference is properly referred/cited.

I undertake that if I am found guilty of any formal plagiarism in the above titled thesis even afterward of PhD degree, the University reserves the rights to withdraw/revoke my PhD degree and that HEC and the University has the right to publish my name on the HEC/University Website on which names of students are placed who submitted plagiarized thesis.



Student/Author Signature

Name: **Muhammad Salman Khan**

# Stability Analysis of Fixed Points of Various Nonlinear Mathematical Models with Chaos Control

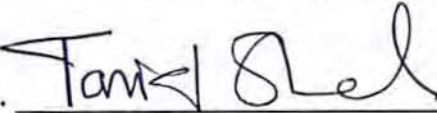
By

**Muhammad Salman Khan**

CERTIFICATE

A THESIS SUBMITTED IN THE PARTIAL FULFILLMENT OF THE  
REQUIREMENTS FOR THE DEGREE OF THE  
DOCTOR OF PHILOSOPHY IN MATHEMATICS

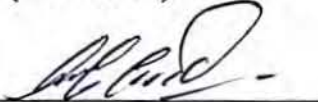
We accept this thesis as conforming to the required standard

1. 

**Prof. Dr. Tariq Shah**  
(Chairman)

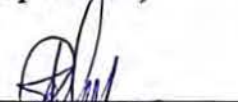
2. 

**Dr. Maria Samreen**  
(Supervisor)

3. 

**Dr. Ghulam Farid**

Department of Mathematics, COMSATS  
University Islamabad, Attock Campus  
(External Examiner)

4. 

**Prof. Dr. Mujeeb ur Rehman**

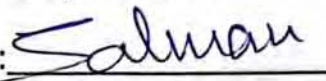
School of Natural Sciences (SNS),  
National University of Sciences and  
Technology (NUST), Islamabad  
(External Examiner)

**Department of Mathematics**  
**Quaid-I-Azam University**  
**Islamabad, Pakistan**  
**2023**

## Certificate of Approval

This is to certify that the research work presented in this thesis entitled Stability Analysis of Fixed Points of Various Nonlinear Mathematical Models with Chaos Control was conducted by **Mr. Muhammad Salman Khan** under the kind supervision of **Dr. Maria Samreen**. No part of this thesis has been submitted anywhere else for any other degree. This thesis is submitted to the Department of Mathematics, Quaid-i-Azam University, Islamabad in partial fulfillment of the requirements for the degree of Doctor of Philosophy in field of Mathematics from Department of Mathematics, Quaid-i-Azam University Islamabad, Pakistan.

Student Name: **Muhammad Salman Khan**

Signature: 

External committee:

a) **External Examiner 1:**

Name: **Dr. Ghulam Farid**

Designation: Associate Professor

Office Address: Department of Mathematics,

COMSATS University Islamabad, Attock Campus

Signature: 

b) **External Examiner 2:**


Name: **Dr. Mujeeb ur Rehman**

Designation: Professor

Office Address: School of Natural Sciences (SNS),

National University of Sciences and Technology

(NUST), Islamabad

Signature: 

c) **Internal Examiner**

Name: **Dr. Maria Samreen**

Designation: Associate Professor


Office Address: Department of Mathematics,

QAU Islamabad.

Signature: 

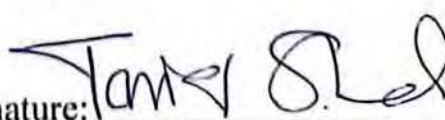
**Supervisor Name:**

**Dr. Maria Samreen**

Signature: 

**Name of Dean/ HOD**

**Prof. Dr. Tariq Shah**

Signature: 

# Acknowledgments

All glory belongs to almighty **Allah**, who has bestowed upon me the strength, wisdom, and perseverance to successfully complete this research endeavor. I would like to express my sincere gratitude and appreciation to the following researchers whose valuable contributions have greatly enriched my research journey:

- 1. Dr. Maria Samreen-**I owe my special thanks to my supervisor for invaluable guidance, support, and mentorship throughout this research journey.
- 2. Dr. Qamar Din-**Your extensive knowledge and technical assistance have been immensely helpful in conducting the necessary experiments and analyzing the results.
- 3. Prof. Mushtaq Hussain-** I am deeply thankful for your critical evaluation and constructive suggestions that have significantly improved the quality and clarity of this work.
- 4. Dr. Muhammad Asif Ashraf-**Your collaboration and fruitful discussions have broadened my understanding of the subject matter and provided me with valuable insights. Your input has been crucial in overcoming research challenges and refining the methodology.
- 5. Dr. Aqib Abbasi-** Your support and encouragement have been a constant source of motivation throughout this research endeavor. Your expertise in the field has been instrumental in shaping my perspective and enhancing the overall quality of this study. I would also like to express my gratitude to my family, friends, and colleagues for their unwavering support and encouragement throughout this journey. Their understanding and encouragement have been invaluable to me.

Finally, I am grateful to my institution which has supported this research, allowing me to pursue my academic and scientific goals.



## *Dedication*

*I dedicate this work to my loving family, and especially to my wife **Maria**, whose unwavering love, understanding, and support have been the driving force behind my academic pursuits. Your encouragement and sacrifices have been the cornerstone of my success, and I am forever grateful for your presence in my life. This achievement would not have been possible without your constant belief in me. Thank you for being my pillar of strength and my source of inspiration.*

## Preface

Several types of research on the qualitative study of nonlinear models have appeared in applied mathematics in past few decades. Moreover, these investigations are mainly focused on theoretical results instead of applications. In this thesis, we are aimed to contribute some research in the qualitative study of nonlinear mathematical models in applied mathematics. In our work, the adopted approach for the qualitative study is simple and easy to understand for readers interested in the qualitative study of nonlinear models, which we encounter in mathematical biology, mathematical ecology, mathematical chemistry and engineering. We have also provided some new theoretical results on the boundedness of solutions, existence of fixed points, stability analysis, bifurcation and chaos control. These significant results were not available in the literature before. It is necessary to analyze the qualitative behaviour of various mathematical models to understand complexities aligned with the qualitative study of dynamical systems. These models may be discrete-time or continuous-time models, depending upon the situation. Many biological and chemical interactions such as prey-predator interactions, plant-herbivore interactions, host-parasite interactions and several interactions are described using discrete and continuous-time models. For example, these models are often used to describe the properties of an epidemic when it arrives in a community and to forecast under which circumstances it will be continued or wiped out from that community. Discrete-time mathematical models are easy to analyze and have rich dynamics compared to their continuous-time counterparts. Hence, it is interesting to analyze the dynamics of such discrete-time mathematical models. In this work, we consider some nonlinear mathematical models in continuous form and then discuss the qualitative behaviour of their discrete-time counterparts.

Furthermore, we have used four different discretization techniques: piecewise arguments, Euler's forward method, nonstandard finite difference scheme, and fractional order discretization. The boundedness character of every positive solution of obtained systems is discussed, and the existence of a positive fixed point is discussed for every system. It is shown that each system undergoes the Neimark-Sacker bifurcation about its positive fixed point. Moreover, some mathematical models also show the existence of period-doubling bifurcation and chaos. It is shown that whenever a discrete-time mathematical model is obtained using a nonstandard finite difference scheme, it is dynamically consistent and exhibits similar dynamics as its continuous-time counterpart. In addition, two generalized hybrid control techniques are presented to overcome the chaos and inconsistent behaviour of mathematical systems. A comparison of generalized hybrid techniques with the old hybrid method shows the effectiveness and wide range of generalized hybrid con-

trol techniques. Finally, some surprising numerical examples are provided to show some exceptional dynamics of discrete-time mathematical models and to justify our theoretical discussion. Let us briefly describe the content of every chapter.

**Chapter 1. Introduction and Preliminaries.** In this chapter, we focus on the basic theory of the dynamical system. Moreover, some beneficial results for the qualitative study of dynamical systems are provided in this chapter.

**Chapter 2. Bifurcation analysis of a discrete-time four-dimensional cubic autocatalator chemical reaction model with coupling through uncatalyzed reactant.** The continuous four-dimensional cubic autocatalator chemical reaction model is examined in this chapter. Using Routh-Hurwitz stability criteria, our major goals are to develop parametric requirements for the local stability of the continuous system and assess if a positive fixed point exists. Using Euler's forward approach and a nonstandard difference scheme, we discretize the continuous model to provide a discrete-time equivalent of the four-dimensional model. We also look at the prerequisites for the positive fixed point's local asymptotic stability in the discrete-time system. Using a generic method for Neimark-Sacker bifurcation analysis, our research shows that the system exhibits a Neimark-Sacker bifurcation at the positive fixed point. In addition, depending on the bifurcation parameter values, we find chaotic dynamics in the discrete-time version of a simplified four-dimensional system. We provide a generalized hybrid control technique that combines parameter perturbation and feedback control to address the Neimark-Sacker bifurcation and chaos. Finally, we offer a number of numerical illustrations to support the conclusions drawn from theory in this chapter. The findings of this chapter have recently been published in an extreme international journal.

**Chapter 3. Bifurcation analysis of a discrete-time phytoplankton-zooplankton model with Holling type-II response and toxicity.** The interaction between phytoplankton and zooplankton plays a vital role in ecology. In this field, discrete-time mathematical models are commonly employed to understand the dynamics of phytoplankton-zooplankton interactions, where generations do not overlap, and new age groups replace older ones at regular intervals. This chapter focuses on converting a continuous-time phytoplankton-zooplankton model into a discrete-time counterpart using a dynamically consistent nonstandard difference scheme to ensure the models' dynamical consistency. Additionally, the chapter explores boundedness conditions for all solutions and establishes the existence of a exceptional positive fixed point. The linearized stability of the obtained system is analyzed with respect to all of its fixed points, and the presence of a Neimark-Sacker bifurcation around the one and only positive equilibrium is demonstrated under specific mathematical circumstances. To control the Neimark-Sacker bifurcation, a comprehensive hybrid control method is applied. Several numerical examples are provided to illustrate the abstract outcomes and match up to the

dynamics of the discrete-time model with its continuous counterpart.

Moreover, the numerical study shows that both the obtained system and its continuous-time counterpart exhibit stability for the same parameter values and instability for the identical parametric values. This consistency in dynamical behavior is evident from the numerical study. Finally, the chapter concludes with a comparison between the modified hybrid method and the previous method. We have published this chapter in a high-quality international journal.

**Chapter 4. Bifurcation analysis of a discrete-time compartmental model for hypertensive or diabetic patients exposed to COVID-19.** In this chapter, we investigate a mathematical model concerning hypertensive or diabetic patients who are exposed to COVID-19. The model is constructed using a set of first-order nonlinear differential equations. To discretize the continuous system, we utilize piecewise constant arguments. We derive local stability conditions for the equilibrium points of the resulting discrete-time mathematical system. Furthermore, we explore the occurrence of period-doubling bifurcation and chaos in the absence of an isolated population. Notably, our system exhibits instability and chaos when the quarantined compartment is empty, which holds biological significance. Additionally, we study the existence of Neimark-Sacker bifurcation at the endemic equilibrium point.

Moreover, through numerical simulations, we observe that the discrete-time mathematical system undergoes period-doubling bifurcation around the endemic equilibrium. To control both the period-doubling bifurcation and Neimark-Sacker bifurcation, we employ a generalized hybrid control methodology. The model serves to emphasize the epidemiological importance of quarantine by illustrating chaos and oscillation within the context of the COVID-19 environment. The results of this chapter are published in an international journal of high quality.

**Chapter 5. Dynamics of a discrete-time fractional-order phytoplankton-zooplankton model with Holling type-II response.** This chapter is devoted to the qualitative study of a continuous-time phytoplankton-zooplankton model with Holling type-II response. Furthermore, we obtained its discrete-time counterpart by using a fractional-order discretization method. The local stability of the obtained system about all of its equilibrium points is discussed. It is proved that the system experience Neimark-Sacker bifurcation about positive equilibrium point under some mathematical conditions. The Neimark-Sacker bifurcation is controlled using two modified hybrid control techniques. Finally, at the end of this chapter, some interesting numerical examples are provided to support our theoretical discussion and explore the effectiveness and feasibility of newly designed control strategies. In addition, a comparison of modified hybrid techniques with the existing hybrid approach is given. This chapter is submitted in an international peer-review journal.



**Chapter 6. Bifurcation analysis and control of chaos in a discrete-time two-trophic plant-herbivore model and dynamical consistency of a nonstandard difference scheme.** In this final chapter, we explore the dynamics of two discrete-time plant-herbivore models. The discrete-time model is obtained by applying Euler's forward method to convert a continuous-time plant-herbivore model. To ensure the dynamic consistency of the discrete-time model, we employ a nonstandard difference scheme.

Furthermore, we discuss the local stability of the system and establish the existence of bifurcation around the positive equilibrium under specific mathematical conditions. In order to effectively manage the occurrence of bifurcation and chaos, we develop a modified hybrid technique. To validate our findings and demonstrate the reliability of the nonstandard difference scheme, we provide several numerical examples at the conclusion of the chapter. The results of this chapter are published in an international journal of high quality.

Every chapter encloses some theorems on a qualitative study of different models, and we have delivered proofs for most of them. The explanations of the literature of each chapter are summarized at the end of each chapter. Moreover, all references for our study are provided in the bibliography section. This bibliography aims mainly to provide a reader with information on further reading. The symbol  $\square$  marks the conclusion of a theorem's proof.

# Contents

<b>1</b>	<b>Introduction and Preliminaries</b>	<b>1</b>
1.1	Some discretization techniques . . . . .	2
1.2	Existence of fixed points . . . . .	3
1.3	Local stability analysis . . . . .	4
1.4	Bifurcation analysis . . . . .	5
1.5	Chaos control . . . . .	6
<b>2</b>	<b>Bifurcation Analysis of a Discrete-Time Four-Dimensional Cubic Autocatalator Chemical Reaction Model with Coupling Through Uncatalysed Reactant</b>	<b>8</b>
2.1	Discretization of model . . . . .	11
2.2	Existence of fixed points . . . . .	11
2.3	Local stability analysis . . . . .	13
2.4	Bifurcation analysis . . . . .	15
2.4.1	Neimark-Sacker bifurcation . . . . .	15
2.5	Chaos control . . . . .	16
2.5.1	A modified technique for chaos control . . . . .	16
2.6	Numerical simulations . . . . .	17
2.7	Concluding remarks . . . . .	26
<b>3</b>	<b>Bifurcation Analysis of a Discrete-Time Phytoplankton-Zooplankton Model with Holling Type-II Response and Toxicity</b>	<b>28</b>
3.1	Discretization of model . . . . .	32
3.2	Boundedness of solutions . . . . .	32
3.3	Existence of fixed points . . . . .	33
3.4	Local stability analysis . . . . .	35
3.5	Bifurcation analysis . . . . .	39
3.5.1	Neimark-Sacker bifurcation . . . . .	39
3.6	Chaos control . . . . .	45
3.6.1	A modified technique for chaos control . . . . .	45

3.6.2	Hybrid technique for chaos control . . . . .	46
3.7	Numerical simulations . . . . .	46
3.8	Concluding remarks . . . . .	55
<b>4</b>	<b>Bifurcation Analysis of a Discrete-Time Compartmental Model for Hypertensive or Diabetic Patients Exposed to COVID-19</b>	<b>58</b>
4.1	Discretization of model . . . . .	59
4.2	Boundedness of solutions . . . . .	60
4.3	Existence of fixed points . . . . .	62
4.4	Local stability analysis . . . . .	66
4.5	Bifurcation analysis . . . . .	67
4.5.1	Period-doubling bifurcation . . . . .	67
4.5.2	Neimark-Sacker bifurcation . . . . .	72
4.6	Chaos control . . . . .	73
4.6.1	A modified technique for chaos control . . . . .	73
4.7	Numerical simulations . . . . .	74
4.8	Concluding remarks . . . . .	81
<b>5</b>	<b>Dynamics of a Discrete-Time Fractional-Order Phytoplankton-Zooplankton Model with Holling Type-II Response</b>	<b>82</b>
5.1	Discretization of model . . . . .	82
5.2	Existence of fixed points . . . . .	84
5.3	Local stability analysis . . . . .	85
5.4	Bifurcation analysis . . . . .	88
5.4.1	Neimark-Sacker bifurcation . . . . .	88
5.5	Chaos control . . . . .	92
5.5.1	A modified technique for chaos control . . . . .	93
5.6	Numerical simulations . . . . .	94
5.7	Concluding remarks . . . . .	101
<b>6</b>	<b>Bifurcation Analysis and Control of Chaos in a Discrete-Time Two-Trophic Plant-Herbivore Model and Dynamical Consistency of a Non-standard Difference Scheme</b>	<b>103</b>
6.1	Discretization of model . . . . .	105
6.2	Existence of fixed points . . . . .	106
6.3	Local stability analysis . . . . .	106
6.4	Bifurcation analysis . . . . .	110
6.4.1	Period-doubling bifurcation . . . . .	110
6.4.2	Neimark-Sacker bifurcation . . . . .	113

6.5	Chaos control . . . . .	118
6.5.1	A modified technique for chaos control . . . . .	118
6.6	Numerical simulations . . . . .	119
6.7	Concluding remarks . . . . .	130



# Chapter 1

## Introduction and Preliminaries

The concept of a dynamical system is the precise formalization of the common logical theory of a deterministic method. The upcoming and past states of several physical, chemical, ecological, biological, economic, and yet societal systems can be predicted to a definite degree by knowing their existing situation and the laws leading their development, followed by the condition that these laws do not transform with the passage of time. Moreover, for solving a dynamical system, an initial point must be given so that it is probable to govern all of its upcoming points. A group of points is recognized as an orbit or a trajectory. Before the arrival of computers, concluding about any trajectory or orbit, it was required to calculate them through some standard methods. These methods were straightforward to apply while solving a linear dynamical system. However, finding the solution of nonlinear dynamical systems by applying these methods was not easy [1].

Mathematical approaches applied to electrical calculating machines have shortened the job of defining the trajectories of a mathematical system. Moreover, it is easy to know their solution trajectories when dealing with a simple dynamical system. However, large numbers of these systems are too complex to understand entirely in terms of distinct orbits. The complexity arises because the structures considered may only be acknowledged roughly, the mathematical parameters of the structure might not be recognized exactly, or expressions may perhaps be absent from the equations. The estimates are used to question the rationality or significance of mathematical solutions [2]. These questions are answered by introducing various techniques in the stability theory of dynamical systems, such as structural stability, Lyapunov stability, or some other techniques. By stability of the dynamical system, we mean that there may be an initial point for which the orbits or trajectories are comparable. In addition, the process for matching trajectories to create the equivalence among them varies with the different ideas of stability theory [3]. The nature of orbit or trajectory could be more important than any specific trajectory. Several trajectories may cover up different solutions of a dynamical system, and some of them may be periodic. In applications, it is frequently needed to count these

types of trajectories or to preserve the whole structure inside a specific trajectory.

Categorizing entirely possible trajectories leads us to the qualitative analysis of a dynamical system, to be precise, properties that remain unchanged by changing coordinates. If we take the nature of orbits as a function of any parameter, it may fulfil an application's criteria. For example, when the value of a parameter is minutely changed from the original value, the dynamical systems could experience the bifurcation, where the dynamical system changes its qualitative behaviour. For instance, it may change its periodic behaviour to irregular motion or see some random and irregular trajectories of the system. In such situations, it could be required to calculate the average, utilizing a lengthy trajectory or multiple dissimilar trajectories. These averages and means are well-defined for ergodic dynamical systems, and a supplementary and comprehensive understanding has been necessary for hyperbolic dynamical systems [4]. Knowing about the probabilistic features of dynamical systems leads us to establish the fundamentals of chaos and statistical mechanics [4]. To study some attractive models in discrete-time and continuous-time dynamical systems, we refer the readers to [5-8].

## 1.1 Some discretization techniques

It is appropriate to explore the dynamics of any biological model by difference equations instead of differential equations when dealing with non-overlapping generations. Furthermore, there is better observation and analysis of chaos in any mathematical system by using difference equations instead of differential equations [9]. Hence, it is interesting to study some mathematical models in discrete form. Recently, Ghanbari and Gölmez-Aguilar [10] have discussed the dynamics of the nutrient-phytoplankton-zooplankton system with variable-order fractional derivatives. Moreover, the authors in [11] have explored the existence of chaos in a cancer model using fractional derivatives through exponential decay and Mittag-Leffler law. Beigi *et al.* [12] have discussed the use of reinforcement learning for effective vaccination strategies of coronavirus disease 2019 (COVID-19). The authors in [13] have analyzed the role of zooplankton dynamics for Southern Ocean phytoplankton biomass and global biogeochemical cycles. We refer the interested reader to [13-15] for further detail on the analysis of various dynamical systems. There are various mathematical techniques for converting the systems of differential equations to their corresponding discrete counterparts. To achieve this goal the usual way is to apply standard difference schemes such as:

- Euler method [16]
- Runge-Kutta method [17]
- Method of piecewise arguments [18]

- Method of Fractional order derivatives [106]
- Nonstandard finite difference schemes [20].

However, numerical inconsistency is experienced with the application of usual finite difference methods. Hence, to avoid this numerical inconsistency, one can apply Mickens's nonstandard finite difference method [20]. In general, whenever a discretization method is used to convert any continuous-time mathematical system into its discrete counterpart, it aims to preserve the following properties of the respective continuous-time system: positivity of results, boundedness, stability of equilibrium points and bifurcations.

## 1.2 Existence of fixed points

In general, studying the dynamics of a nonlinear mathematical model by its exact solution is almost impossible. However, their qualitative study gives us an additional way to study their dynamics. For this type of study, the usual way is to find their fixed points and then discuss the properties of their constant solutions [18]. A dynamical system may have more than one fixed point: the trivial fixed point, boundary fixed points and the unique positive fixed point. From the application point of view, the only one is of central importance: the unique positive fixed point. To find the number of positive real roots of any algebraic equation, we have the following lemma:

**Lemma 1.2.1.** [21] *Assume that  $F_1(X) = c_0 + c_1X + \dots + c_{m-2}X^{m-2} + c_{m-1}X^{m-1} + c_mX^m$  be a mapping with coefficients from real numbers. Formerly, the number of roots for  $F_1$  maybe same as the number of sign variations for  $F_1(X)$  or not more than a positive even integer. Additionally, if the  $F_1(X)$  sign varies once, then  $F_1$  has a precisely unique positive real solution.*

Moreover, the unique positive fixed point may or may not be in closed form (see [22-24]). To prove the existence of the unique positive fixed point of any particular two-dimensional dynamical system and the boundedness of every positive solution, we have the following lemma.

**Lemma 1.2.2.** [38] *Let  $\zeta_m$  fulfills  $\zeta_{m+1} \leq \zeta_m \exp(A(1 - B\zeta_m))$  for each  $m \in [m_1, \infty)$  where  $\zeta_0 > 0$ , with  $A, B > 0$ . Then,*

$$\lim_{m \rightarrow \infty} \sup \zeta_m \leq \frac{1}{AB} \exp(B - 1).$$

Discrete-time dynamical systems are effortlessly implementable for stepwise computer simulations, and they are repeatedly appropriate for modeling investigational statistics that are approximately at all times or previously discrete. In addition, they can symbolize

sudden change in the system's states and probably disordered dynamics, by means of less variables when compared to their continuous-time counterparts [39]. An orbit is the most superficial kind of any fixed point. For the stability state of any mechanical system, a small momentum given to that system results in a restricted motion, for instance, slight swinging, as in the case of a plumb. Moreover, a steady equilibrium state is also stable in an asymptotic manner in any damped system [25].

### 1.3 Local stability analysis

In the case of a linear system, there are many suitable checks for stability. However, in the case of any nonlinear system, the stability can frequently be concluded from its linearized stability [26-28]. The permanency of an orbit in any dynamical system characterizes whether neighbouring (i.e., perturbed) trajectories will stay in a locality of that orbit or be resisted away from it. However, in the case of asymptotic stability, we are also concerned with characterizing the pull of adjacent orbits to this trajectory in the major-time limit [26]. Hence, we have the following lemma for the dynamical study of linearized stability of any two-dimensional discrete-time mathematical system.

**Lemma 1.3.1.** [39] *Let  $M(\xi) = \xi^2 - Tr\xi + Dt$ ,  $M(1) > 0$  and  $(\underline{x}, \underline{y})$  be any equilibrium point of any 2-dimensional discrete-time system. In addition, if  $\xi_1, \xi_2$  are root of  $M(\xi) = 0$ , then:*

(a)  $|\xi_1| < 1$  and  $|\xi_2| < 1 \Leftrightarrow M(-1) > 0$  and  $Dt < 1$ ;

(b)  $1 < |\xi_1|$  and  $1 < |\xi_2| \Leftrightarrow M(-1) > 0$  and  $Dt > 1$ ;

(c)  $|\xi_1| < 1$  and  $|\xi_2| > 1$  or  $(|\xi_1| > 1$  and  $|\xi_2| < 1) \Leftrightarrow M(-1) < 0$ ;

(d)  $\xi_1$  and  $\xi_2$  represent complex conjugates with  $|\xi_1| = 1 = |\xi_2| \Leftrightarrow Tr^2 - 4Dt < 0$  and  $Dt = 1$ .

(e)  $\xi_1 = -1$  and  $|\xi_2| \neq 1 \Leftrightarrow M(-1) = 0$  and  $Dt \neq 1, -1$ ;

As  $\xi_1$  and  $\xi_2$  are characteristic values of  $M(\xi) = 0$ , then the point  $(\underline{x}, \underline{y})$  is sink if  $|\xi_1| < 1$  and  $|\xi_2| < 1$ . Furthermore, it is stable locally asymptotically. The point  $(\underline{x}, \underline{y})$  is known as source (repeller) if  $|\xi_1| > 1$  and  $|\xi_2| > 1$ , and it provides un-stability condition for the given system. The point  $(\underline{x}, \underline{y})$  is a saddle point if  $|\xi_1| < 1$  and  $|\xi_2| > 1$  or  $(|\xi_1| > 1$  and  $|\xi_2| < 1)$ . Finally,  $(\underline{x}, \underline{y})$  is pronounced as non-hyperbolic if condition (d) or (e) is satisfied. Where  $Tr$  and  $Dt$  are respectively trace and determinants of any  $2 \times 2$  jacobian matrix.

In addition, for the study of linearized stability in the dimension higher than two, we have the following result from [40].

**Lemma 1.3.2.** [40] *Assume the fourth degree characteristic equation*

$$\rho^4 + d_1\rho^3 + d_2\rho^2 + d_3\rho + d_4 = 0, \tag{1.3.1}$$



where  $d_1, d_2, d_3, d_4 \in \mathfrak{R}$ . Additionally, let  $\rho_1, \rho_2, \rho_3, \rho_4$  are roots of (1.3.1) and  $D_1$  be any open disk of radius one. Then, the necessary and sufficient conditions that  $\rho_1, \rho_2, \rho_3, \rho_4 \in D_1$  are given as:

$$|d_3 + d_1| < 1 + d_4 + d_2, \quad |d_3 - d_1| < 2(1 - d_4), \quad d_2 - 3d_4 < 3,$$

and

$$d_4 + d_2 + d_4^2 + d_3^2 + d_4^2 d_2 + d_4 d_1^2 < 1 + 2d_4 d_2 + d_3 d_1 + d_4 d_3 d_1 + d_4^3.$$

The qualitative study of a dynamical system leads us to conclude whether it is stable or unstable(experiences the bifurcation). Bifurcation is the mathematical phenomenon produced in any system due to a minimal change in the system's stability. Mathematically, bifurcation arises when parameters change in the fixed point's small neighbourhood. Moreover, for the additional study of the bifurcation concept and recognizing this fantastic behaviour of a discrete-time mathematical system, one can see [27-31].

## 1.4 Bifurcation analysis

A discrete-time mathematical system may experience many types of bifurcations from which the most common are period-doubling bifurcation and Neimark-Sacker bifurcation. In any dynamical system, a period-doubling bifurcation arises as soon as a slight variation in a system's parameters sources a new broken trajectory from a present periodic trajectory. The fresh one takes double the period of the original. Moreover, to study this type of bifurcation concept, the centre manifold theorem is applied after applying standard forms to display the presence and path of this type of bifurcation. Recently, period-doubling bifurcation related to the discrete-time systems has been studied by many authors[32-35]. In addition, closed invariant circles are formed due to Neimark-Sacker bifurcation. Similarly, an individual can locate some isolated periodic orbits as well as tracks that narrowly cover the invariant circle. A supercritical or subcritical bifurcation results in a stable or unstable closed invariant curve. We have the following clear standard for Hopf bifurcation to analyze the Neimark-Sacker bifurcation in any dynamical system of order higher than two [35]. An individual can study Neimark-Sacker bifurcation through this standard without finding the eigenvalues.

**Lemma 1.4.1.** (see [35]) Let  $S_{M+1} = f_\delta(S_M)$ , is any  $N$ -dimensional system and  $\delta \in \mathfrak{R}$  is a bifurcation parameter. Moreover, assume that  $S^*$  is any fixed point of  $f_\delta$ . Let  $G_\delta(\lambda)$  be the characteristic equation of matrix  $J(S^*) = (K_{ij})_{N \times N}$  of  $N$ -dimensional map  $f_\delta$ . Then,  $G_\delta(\lambda)$  is given as

$$G_\delta(\lambda) = \lambda^N + r_1 \lambda^{N-1} + r_2 \lambda^{N-2} + \dots + r_{N-1} \lambda + r_N \quad (1.4.1)$$

with  $r_i = r_i(\delta, S)$ , for  $i \in I$ , where  $I = \{1, 2, 3, \dots, N\}$  and  $S$  is control parameter, which is to be determined. Let  $\Omega_0^\pm(\delta, S) = 1, \Omega_1^\pm(\delta, S), \Omega_2^\pm(\delta, S), \dots, \Omega_N^\pm(\delta, S)$ . be the sequence of determinants defined by  $\Omega_i^\pm(\delta, S) = \det(R_1 \pm R_2)$ , for  $i \in I$ , where  $I = \{1, 2, 3, \dots, N\}$  with

$$R_1 = \begin{pmatrix} 1 & r_1 & r_2 & \dots & r_{i-1} \\ 0 & 1 & r_1 & \dots & r_{i-2} \\ 0 & 0 & 1 & \dots & r_{i-3} \\ \dots & \dots & \dots & \dots & \dots \\ 0 & 0 & 0 & \dots & 1 \end{pmatrix} \quad (1.4.2)$$

$$R_2 = \begin{pmatrix} r_{N-i+1} & r_{N-i+2} & \dots & r_{N-1} & r_N \\ r_{N-i+2} & r_{N-i+3} & \dots & r_N & 0 \\ r_{N-i+3} & r_{N-i+4} & \dots & 0 & 0 \\ \dots & \dots & \dots & \dots & \dots \\ r_N & 0 & 0 & \dots & 0 \end{pmatrix}. \quad (1.4.3)$$

In addition, we have:

$$C_1 : \Omega_{N-1}^-(\delta_0, S) = 0, \Omega_{N-1}^+(\delta_0, S) > 0, \mathbb{G}_{\delta_0}(1) > 0, (-1)^N \mathbb{G}_{\delta_0}(-1) > 0$$

,  $0 < \Omega_i^\pm(\delta_0, S)$ , for  $i \in I_1$ , where  $I_1 = \{N-3, N-5, N-7, \dots, 1\}$  or  $i = N-3, N-5, N-7, \dots, 2$  when  $N$  is even or odd respectively.

$$C_2 : 0 \neq \left[ \frac{d}{d\delta} (\Omega_{N-1}^-(\delta, S)) \right]_{\delta=\delta_0}$$

$C_3$  : Resonance condition  $\cos\left(\frac{2\pi}{n}\right) = \psi$ , or  $\psi \neq \cos\left(\frac{2\pi}{n}\right)$ , where  $n \in \mathbb{N}$  with  $n \geq 3$  and  $\psi = \frac{-1+0.5\mathbb{G}_{\delta_0}(1)\Omega_{N-3}^-(\delta_0, S)}{\Omega_{N-2}^+(\delta_0, S)}$ . Then, the Neimark-Sacker bifurcation exists at  $\delta_0$ .

Under the effects of any bifurcation, the dynamical system may have chaotic dynamics. If the system is in the continuous form, then it must have a dimension greater than two, but in the case of discrete-time systems, chaos can be experienced in the least dimension, namely, one dimension [9].

## 1.5 Chaos control

Specifically in the case of population models, especially when these models are connected to biological interactions and the breeding of various species, the control of bifurcation and chaos in mathematical models is thought to be a crucial component for dynamical systems. Since the population must not encounter any abnormal circumstances in order to survive, discrete-time mathematical systems are more difficult to study in the context of population models than continuous ones. Therefore, it is necessary to employ a chaos-controlling strategy to prevent these abnormalities. There are numerous well-known

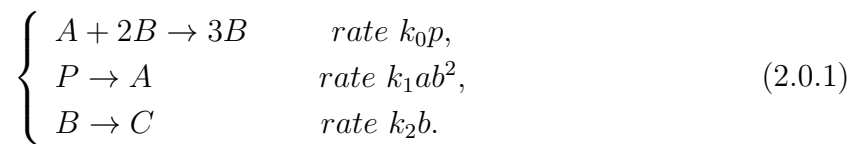
methods that have been developed throughout the years to manage chaos in any discrete dynamical system. These techniques use feedback control and parameter perturbation to steer erratic and unstable trajectories in the direction of stable trajectories. Ott *et al.* [36] provided the OGY approach, which is the most effective and well-known method in the realm of chaos, to regulate period-doubling bifurcation. Later, a number of control techniques were created, [22]. As a result, we talk about the qualitative analysis of several mathematical models in our work. The main topics we covered were boundedness, fixed points, linearized stability, period doubling-bifurcation, Neimark-Sacker bifurcation, and chaos control. Furthermore, the Jury condition is applied to talk about the linearized stability. Standard bifurcation theory is applied to the investigation of period doubling-bifurcation and Neimark-Sacker bifurcation. Additionally, several currently utilized techniques as well as some newly created techniques are used to control bifurcations and chaos.

DRSML QAU

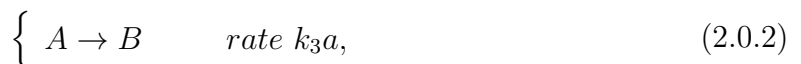
## Chapter 2

# Bifurcation Analysis of a Discrete-Time Four-Dimensional Cubic Autocatalator Chemical Reaction Model with Coupling Through Uncatalysed Reactant

In this chapter, we consider a continuous-time four-dimensional cubic autocatalator chemical reaction model. We obtained a consistent discrete-time counterpart of the four-dimensional cubic autocatalator chemical reaction model by using a nonstandard difference scheme. Mainly, we investigate the existence of fixed points, local stability of fixed points, the existence of Neimark-Sacker bifurcation and chaos control. The results of this chapter are published in an extreme international journal (see [41]). Leach *et al.* [42] have considered a prototype two-cell model using the feedback scheme in every cell being centered on the cubic autocatalator reaction, which is given as



One may obtain a modified version of (2.0.1) by addition of the uncatalysed phase, which is defined as follows:



where the concentrations of the reactants  $A, B$  and  $P$  are respectively represented by  $a, b$  and  $p$ . In addition,  $k_i (i = 0, 1, 2, 3)$  are rate constants [42]. Here, we consider the condition that there is a semi-permeable coating between the cells which permits diffusion of only one from the reactant classes  $B$  or  $A$  at any instant. Moreover, the overall

reaction is catalyzed by using the condition that reactant  $A$  is produced by an only first-order decline from its originator  $P$ . It is assumed that the production of  $A$  from its originator  $P$  at the rate  $k_1ab^2$  is comparatively a slow process. Due to the supposition that the primary concentration of  $P$ , explicitly  $p_0$ , is more significant than the intermediates  $B$  and  $A$  [46]. In these situations, it is standard to consider the "pooled-chemical" estimations and make the additional supposition that the concentration of  $P$  remains the same through its primary value  $p_0$ . Additionally, it is considered that the rate-defining stage, namely, the primary autocatalytic step ( $A+2B \rightarrow 3B$ ), is faster as compared to the uncatalyzed reaction step. However, this additional reaction can significantly influence the total behaviour of the system. A few decades earlier, the authors in [45-50] have widely studied the separated reaction model (2.0.1) in a well-stirred scheme under the effects of pooled-chemical estimation. The authors in [48] and [43] have revealed that this reaction system can show complex behaviour designs.

The authors in [51] have discussed the consequences of the slow decline of the antecedent  $P$  on the overall solution. The authors in [42] have extended the work of [52] on this dual-cell problem centred on the cubic-autocatalator response system (2.0.1). Moreover, in their extended work, they have discussed some consequences that the additional uncatalyzed response stage (2.0.2) had on the inclusive behaviour of the reaction. Merkin *et al.* [47] have shown that with a comparatively small influence, this additional step can ensure a crucial effect on the result of the uncoupled system by keeping the result restricted, by not letting the concentration of  $B \rightarrow 0$  (although it can turn out to be negligible). Adding this additional stage to the uncoupled system has an extreme impact on the oscillatory behaviour, keeping the oscillatory response restricted all over and giving rise to an extra point of Hopf bifurcation. The authors in [52] have presented a complete study of complexity in the dynamical behavior wherever the non catalyzed stage was not involved. Moreover, the authors in [42] have not presented the complete study of complexity in the dynamical behaviour that can ascend due to secondary bifurcations. The equations leading this dual-cell combined system are under the pooled-chemical estimate for the reactant  $P$  (see [42]).

$$\begin{aligned}
\frac{da_1}{dt_1} &= k_0p_0 - k_1b_1^2a_1 - k_3a_1 + D_a(a_2 - a_1), \\
\frac{db_1}{dt_1} &= k_1b_1^2a_1 + k_3a_1 - k_2b_1 + D_b(b_2 - b_1), \\
\frac{da_2}{dt_1} &= k_0p_0 - k_1b_2^2a_2 - k_3a_2 + D_a(a_1 - a_2), \\
\frac{db_2}{dt_1} &= k_1b_2^2a_2 + k_3a_2 - k_2b_2 + D_b(b_1 - b_2),
\end{aligned} \tag{2.0.3}$$

where the diffusion coefficients for autocatalyst  $B$  and reactant  $A$  are  $D_b$  and  $D_a$  respectively through the membrane separating the two cells. Furthermore, to made the

non-dimensional system of equations from (6.0.1), we consider the following transformations [52]:

$$\begin{cases} x_i = a_i \sqrt{\frac{k_1}{k_2}}, \\ y_i = b_i \sqrt{\frac{k_1}{k_2}}, \\ (i = 1, 2), t = k_2 t_1. \end{cases} \quad (2.0.4)$$

The terms arising from the decline of the antecedent  $P$  give growth to a positive dimensionless parameter

$$\mu = \frac{k_0 p_0}{k_2} \sqrt{\frac{k_1}{k_2}}.$$

The addition of the uncatalysed stage gives rise to a dimensionless parameter  $r = \frac{k_3}{k_2}$ , which will, in common, take comparatively lesser values. The combination through  $B$  and  $A$  give rise to the real numbers  $\beta = \frac{D_b}{k_2}$  and  $\alpha = \frac{D_a}{k_2}$ , respectively. Moreover, under these assumptions, the system (6.0.1) takes the following form:

$$\begin{aligned} \frac{dx_1}{dt} &= \mu - x_1 y_1^2 - r x_1 + \alpha(x_2 - x_1), \\ \frac{dy_1}{dt} &= x_1 y_1^2 - y_1 + r x_1 + \beta(y_2 - y_1), \\ \frac{dx_2}{dt} &= \mu - x_2 y_2^2 - r x_2 + \alpha(x_1 - x_2), \\ \frac{dy_2}{dt} &= x_2 y_2^2 - y_2 + r x_2 + \beta(y_1 - y_2), \end{aligned} \quad (2.0.5)$$

with  $x_i, y_i \geq 0$  for every value of  $i = 1, 2$  (see [52]). Some characteristics of the most common case  $\alpha \neq \beta \neq 0$  for system (2.0.5) are considered by Ashkenaz *et al.* [53]. Moreover, the authors in [42] have discussed some qualitative results of the system (2.0.5) by letting pairing either through  $B$  or  $A$  only. Formerly, it was explained by Lech *et al.* [42] that, when pairing is considered by using reactant  $A$  only, we must have to take  $\beta = 0$ , similarly for pairing through autocatalyst  $B$ , we have to take  $\alpha = 0$  in the system (2.0.5). Here, we consider the coupling in the system (2.0.5) through autocatalyst  $B$  by taking  $\alpha = 0$ . In this case the system (2.0.5) takes the following form:

$$\begin{aligned} \frac{du}{dt} &= \mu - uv^2 - ru, \\ \frac{dv}{dt} &= uv^2 + ru - v + \beta(z - v), \\ \frac{dw}{dt} &= \mu - wz^2 - rw, \\ \frac{dz}{dt} &= wz^2 + rw - z + \beta(v - z), \end{aligned} \quad (2.0.6)$$

where  $x_1 = u, x_2 = w, y_1 = v$  and  $y_2 = z$ . Din [6] have discussed the rich dynamics of a discrete-time version of a glycolysis model. Din *et al.* [7] have considered a discrete-time chlorine dioxide-iodine-malonic acid model for study and discussed the complexity

in that mathematical system. In the case of non-overlapping generations, discrete-time mathematical systems give more efficient computational results than their counterparts in the continuous form [54]. Mainly, global stability of system, boundedness of solutions, local asymptotic stability, persistence of solutions and the existence of periodic positive results can be discussed more effortlessly in the case of discrete-time models [56].

## 2.1 Discretization of model

The main benefit of the nonstandard finite difference schemes is to maintain the significant characters of their respective continuous systems. Moreover, the formation of these types of difference schemes is not straightforward, and there is no usual way for their construction, which is probably considered a significant drawback of nonstandard difference schemes [30]. Hence, studying the dynamics of a discrete-time version of (2.0.6) is interesting. By using Euler's forward method, we get the following discrete-time version of the system (2.0.6)

$$\begin{aligned} u_{n+1} &= u_n + \eta (a - u_n v_n^2 - b u_n), \\ v_{n+1} &= v_n + \eta (u_n v_n^2 + b u_n - v_n + c(z_n - v_n)), \\ w_{n+1} &= w_n + \eta (a - w_n z_n^2 - b w_n), \\ z_{n+1} &= z_n + \eta (w_n z_n^2 + b w_n - z_n + c(v_n - z_n)), \end{aligned} \quad (2.1.1)$$

where  $0 < \eta < 1$ . To understand a similar type of discretization, one can study [37-41]. Moreover, by applying a nonstandard finite difference scheme (see Mickens [20]), we get the following form of system (6.1.2).

$$\begin{aligned} u_{n+1} &= \frac{(u_n + \eta\mu)}{(1 + \eta(v_n^2 + r))}, \\ v_{n+1} &= \frac{v_n + \eta(u_n v_n^2 + r u_n + \beta z_n)}{(1 + \eta(1 + \beta))}, \\ w_{n+1} &= \frac{(w_n + \eta\mu)}{(1 + \eta(z_n^2 + r))}, \\ z_{n+1} &= \frac{(z_n + \eta(w_n z_n^2 + r w_n + \beta v_n))}{(1 + \eta(1 + \beta))}. \end{aligned} \quad (2.1.2)$$

## 2.2 Existence of fixed points

From system (2.1.2) one can get the positive fixed point  $(u_*, v_*, w_*, z_*)$ . Additionally,  $(u_*, v_*, w_*, z_*)$  represents the unique positive fixed point of system (2.1.2). Furthermore, this fixed point is given as:

$$(u_*, v_*, w_*, z_*) = \left( \frac{\mu}{r + \mu^2}, \mu, \frac{\mu}{r + \mu^2}, \mu \right).$$

In order to study the stability analysis of system (2.1.2) about the positive fixed point  $(u_*, v_*, w_*, z_*)$ , we have the next theorem. This theorem provides us with a necessary and sufficient condition for all the roots of a real fourth-order polynomial to have a magnitude less than one (see **Theorem 1.5** of [40]).

**Theorem 2.2.1.** *Consider the following biquadratic equation with real coefficients*

$$\rho^4 + d_1\rho^3 + d_2\rho^2 + d_3\rho + d_4 = 0. \quad (2.2.1)$$

Then, by applying **Lemma 1.3.2**, the necessary and sufficient conditions that all the roots of (2.2.1) lie inside the disk of unit radius are given as follows:

$$\begin{cases} |d_3 + d_1| < 1 + d_4 + d_2, \\ |d_3 - d_1| < 2(1 - d_4), \\ d_2 - 3d_4 < 3, \\ d_4 + d_2 + d_4^2 + d_3^2 + d_4^2d_2 + d_4d_1^2 < 1 + 2d_4d_2 + d_3d_1 + d_4d_3d_1 + d_4^3, \end{cases} \quad (2.2.2)$$

where

$$\begin{cases} d_1 = -\left(\frac{2}{1+S\eta} + \frac{2(S+2\eta\mu^2)}{ST}\right), \\ d_2 = \frac{\frac{(S+2\eta\mu^2)^2}{S^2} + \frac{ST(4+T+4S\eta)+4T\eta(1+S\eta)(2+S\eta)\mu^2 - \beta^2\eta^2}{S(1+S\eta)^2}}{T^2}, \\ d_3 = \frac{2S^2((1+S\eta)(1-\beta^2\eta^2)-T) - 4S\eta(1+S\eta)(2+T+S\eta)\mu^2 - 8\eta^2(1+S\eta)^2\mu^4}{S^2T^2(1+S\eta)^2}, \\ d_4 = \frac{S^2(1-\beta^2\eta^2) + 4S\eta(1+S\eta)\mu^2 + 4\eta^2(1+S\eta)^2\mu^4}{S^2T^2(1+S\eta)^2}, \\ S = r + \mu^2 \text{ and } T = 1 + \eta + \beta\eta. \end{cases} \quad (2.2.3)$$

*Proof.* Let  $J_{(u_*, v_*, w_*, z_*)}$  be the jacobian matrix of system (2.1.2) about  $\left(\frac{\mu}{r+\mu^2}, \mu, \frac{\mu}{r+\mu^2}, \mu\right)$  then  $J_{(u_*, v_*, w_*, z_*)}$  has the following mathematical form

$$J_{(u_*, v_*, w_*, z_*)} = \begin{pmatrix} \frac{1}{1+\eta S} & -\frac{2\eta\mu^2}{S(1+\eta S)} & 0 & 0 \\ \frac{\eta S}{T} & \frac{1+\frac{2\eta\mu^2}{S}}{T} & 0 & \frac{\beta\eta}{T} \\ 0 & 0 & \frac{1}{1+\eta S} & -\frac{2\eta\mu^2}{S(1+\eta S)} \\ 0 & \frac{\beta\eta}{T} & \frac{\eta S}{T} & \frac{1+\frac{2\eta\mu^2}{S}}{T} \end{pmatrix}. \quad (2.2.4)$$

The characteristic equation of  $J_{(u_*, v_*, w_*, z_*)}$  is given as

$$\rho^4 + d_1\rho^3 + d_2\rho^2 + d_3\rho + d_4 = 0,$$

where  $d_1, d_2, d_3, d_4$  are given in (2.2.3). Finally, by applying **Theorem 2.2.1**, the positive fixed point  $\left(\frac{\mu}{r+\mu^2}, \mu, \frac{\mu}{r+\mu^2}, \mu\right)$  remains stable locally asymptotically if the following



conditions are fulfilled:

$$\begin{cases} |d_3 + d_1| < 1 + d_4 + d_2, \\ |d_3 - d_1| < 2(1 - d_4), \\ d_2 - 3d_4 < 3, \\ d_4 + d_2 + d_4^2 + d_3^2 + d_4^2 d_2 + d_4 d_1^2 < 1 + 2d_4 d_2 + d_3 d_1 + d_4 d_3 d_1 + d_4^3. \end{cases}$$

□

## 2.3 Local stability analysis

Assume that  $J^*(u_*, v_*, w_*, z_*)$  be jacobian matrix of system (2.0.6) about  $\left(\frac{\mu}{r+\mu^2}, \mu, \frac{\mu}{r+\mu^2}, \mu\right)$  then  $J^*(u_*, v_*, w_*, z_*)$  has the following mathematical form:

$$J^*(u_*, v_*, w_*, z_*) = \begin{pmatrix} -r - \mu^2 & -\frac{2\mu^2}{r+\mu^2} & 0 & 0 \\ r + \mu^2 & 1 - \beta - \frac{2r}{r+\mu^2} & 0 & \beta \\ 0 & 0 & -r - \mu^2 & -\frac{2\mu^2}{r+\mu^2} \\ 0 & \beta & r + \mu^2 & 1 - \beta - \frac{2r}{r+\mu^2} \end{pmatrix}.$$

Additionally, let  $F(\xi) = 0$  be characteristic equation obtained from  $J^*(u_*, v_*, w_*, z_*)$  then it is given as follows:

$$c_4 \xi^4 + c_3 \xi^3 + c_2 \xi^2 + c_1 \xi + c_0 = 0, \quad (2.3.1)$$

where

$$\begin{cases} c_0 = (r + \mu^2)^2 (1 + 2\beta), \\ c_1 = 2((2r(1 + \beta) - 1)\mu^2 + r(1 + r + (2 + r)\beta) + (1 + \beta)\mu^4), \\ c_2 = r(4 + r + 4\beta) + 2(r + 2\beta)\mu^2 + \mu^4 + 1 - 2\beta + \frac{4r^2}{(r+\mu^2)^2} + \frac{4r(-1+\beta)}{r+\mu^2}, \\ c_3 = 2\left(\mu^2 + r + \beta - 1 + \frac{2r}{r+\mu^2}\right), \\ c_4 = 1. \end{cases} \quad (2.3.2)$$

Now, by using Routh-Hurwitz stability criteria for four dimensional system we have the following Routh array [55]:

$$R_a = \begin{pmatrix} c_4 & c_2 & c_0 & 0 \\ c_3 & c_1 & 0 & 0 \\ \frac{c_2 c_3 - c_1 c_4}{c_3} & c_0 & 0 & 0 \\ \frac{-c_0 c_3^2 + c_1 (c_2 c_3 - c_1 c_4)}{c_2 c_3 - c_1 c_4} & 0 & 0 & 0 \\ c_0 & 0 & 0 & 0 \end{pmatrix},$$

where  $c_i$  for  $i = 0, 1, 2, 3, 4$  are given in (2.3.2). For stability of system (2.0.6) about  $\left(\frac{\mu}{r+\mu^2}, \mu, \frac{\mu}{r+\mu^2}, \mu\right)$ , it is necessary that all the elements in the first column of  $R_a$  have same sign [55]. Hence, we have the following result for the local stability of system (2.0.6) about  $\left(\frac{\mu}{r+\mu^2}, \mu, \frac{\mu}{r+\mu^2}, \mu\right)$ .

**Theorem 2.3.1.** [55] Assume the fourth degree characteristic equation

$$c_4\xi^4 + c_3\xi^3 + c_2\xi^2 + c_1\xi + c_0 = 0, \quad (2.3.3)$$

where  $c_0, c_1, c_2, c_3$  and  $c_4$  are given in (2.3.2). Additionally, let  $\xi_1, \xi_2, \xi_3, \xi_4$  are roots of (2.3.6) and  $D_2$  be any open disk of radius one. Then, the necessary and sufficient conditions that  $\xi_1, \xi_2, \xi_3, \xi_4 \in D_2$  are given as:

$$\begin{cases} c_0 > 0, \\ c_3 > 0, \\ c_1(c_2c_3 - c_1c_4) - c_0c_3^2 > 0, \\ c_4 > 0. \end{cases} \quad (2.3.4)$$

**Theorem 2.3.2.** Assume the fourth degree characteristic equation

$$c_4\xi^4 + c_3\xi^3 + c_2\xi^2 + c_1\xi + c_0 = 0. \quad (2.3.5)$$

Additionally, let  $\xi_1, \xi_2, \xi_3, \xi_4$  are roots of (2.3.5) and  $D_2$  be any open disk of radius one. Then,  $\xi_1, \xi_2, \xi_3, \xi_4 \in D_2$  if and only if  $\beta > 0, r > 0$  and  $\mu \geq 1$ .

*Proof.* Assume that  $J^*(u_*, v_*, w_*, z_*)$  be the jacobian matrix of system (2.0.6) about  $(u_*, v_*, w_*, z_*)$ . In addition, suppose  $F(\xi) = 0$  be the characteristic equation obtained from  $J^*(u_*, v_*, w_*, z_*)$ . Then,  $F(\xi) = 0$  can be specified as follows

$$c_4\xi^4 + c_3\xi^3 + c_2\xi^2 + c_1\xi + c_0 = 0, \quad (2.3.6)$$

where  $c_0, c_1, c_2, c_3$  and  $c_4$  are given in (2.3.2). Moreover, from  $J^*(u_*, v_*, w_*, z_*)$  we have

$$\begin{cases} c_0 = (1 + 2\beta)(r + \mu^2)^2, \\ c_1(c_2c_3 - c_1c_4) - c_0c_3^2 = -4(1 + 2\beta)(r(1 + r + \beta) + (-1 + 2r + \beta)\mu^2 + \mu^4)^2 + \alpha_1(\alpha_2 + c_3\alpha_3), \\ c_3 = 2\left(-1 + r + \beta + \mu^2 + \frac{2r}{r + \mu^2}\right), \\ c_4 = 1, \end{cases} \quad (2.3.7)$$

with

$$\begin{cases} \alpha_1 = 2((2r(1 + \beta) - 1)\mu^2 + r(1 + r + (2 + r)\beta) + (1 + \beta)\mu^4), \\ \alpha_2 = -2((2r(1 + \beta) - 1)\mu^2 + r(1 + r + (2 + r)\beta) + (1 + \beta)\mu^4), \\ \alpha_3 = 1 - 2\beta + r(4 + r + 4\beta) + 2(r + 2\beta)\mu^2 + \mu^4 + \frac{4r^2}{(r + \mu^2)^2} + \frac{4r(-1 + \beta)}{r + \mu^2}. \end{cases} \quad (2.3.8)$$

Finally, if we have  $\beta > 0, r > 0$  and  $\mu \geq 1$  then we have

$$c_0, c_1(c_2c_3 - c_1c_4) - c_0c_3^2, c_3 > 0.$$

Consequently, all the conditions of array (2.3.4) are satisfied. Which completes the proof of theorem.  $\square$

## 2.4 Bifurcation analysis

In this section, we examine the parametric situations for the existence of Neimark-Sacker bifurcation about the positive fixed point  $(u_*, v_*, w_*, z_*)$  of system (2.1.2).

### 2.4.1 Neimark-Sacker bifurcation

By using **Lemma 1.4.1** one has the following result for the existence of Neimark-Sacker bifurcation for positive fixed point  $(u_*, v_*, w_*, z_*)$  of system (2.1.2).

**Theorem 2.4.1.** *If the next conditions are satisfied, the positive fixed point  $(u_*, v_*, w_*, z_*)$  of the system (2.1.2) experiences the Neimark-Sacker bifurcation*

$$\begin{cases} 1 \pm d_4 > 0, \\ 1 + d_4^3 - d_4^2(1 + d_2) - d_1^2 d_4 + 2d_2 d_4 + -d_4 - d_2 - d_3^2 + d_1 d_3(1 + d_4) = 0, \\ 1 - d_4^3 - d_4^2 - d_1^2 d_4 + d_4 + d_2 - d_3^2 - d_2 d_4^2 - d_1 d_3(1 - d_4) > 0, \\ 1 + d_1 + d_2 + d_3 + d_4 > 0, \\ 1 - d_1 + d_2 - d_3 + d_4 > 0, \end{cases} \quad (2.4.1)$$

where  $d_1, d_2, d_3$  and  $d_4$  are provided in (2.2.3).

*Proof.* By using **Lemma 1.4.1**, for a discrete-time mathematical system of 4-dimension, we have

$$\begin{cases} A_1 = \begin{pmatrix} 1 & d_1 & d_2 \\ 0 & 1 & d_1 \\ 0 & 0 & 1 \end{pmatrix}, \\ A_2 = \begin{pmatrix} d_2 & d_3 & d_4 \\ d_3 & d_4 & 0 \\ d_4 & 0 & 0 \end{pmatrix}. \end{cases}$$

Moreover, we get the following inequalities and equations:

$$\begin{cases} \square_1^\pm(\eta) = 1 \pm d_4 > 0, \\ \square_3^-(\eta) = 1 + d_4^3 - d_4^2(1 + d_2) - d_1^2 d_4 + 2d_2 d_4 + -d_4 - d_2 - d_3^2 + d_1 d_3(1 + d_4) = 0, \\ \square_3^+(\eta) = 1 - d_4^3 - d_4^2 - d_1^2 d_4 + d_4 + d_2 - d_3^2 - d_2 d_4^2 - d_1 d_3(1 - d_4) > 0, \\ F_\eta(1) = 1 + d_4 + d_3 + d_2 + d_1 > 0, \\ (-1)^4 F_\eta(-1) = 1 - d_4 + d_2 - d_3 + d_1 > 0, \end{cases} \quad (2.4.2)$$

which confirms the existence of Neimark-Sacker bifurcation in system (2.1.2) about  $\left(\frac{\mu}{r+\mu^2}, \mu, \frac{\mu}{r+\mu^2}, \mu\right)$ , whenever  $\eta$  is taken as bifurcation parameter.  $\square$

## 2.5 Chaos control

In this part of chapter, we apply a generalized hybrid control technique which is based on state feedback along with parameter perturbation.

### 2.5.1 A modified technique for chaos control

We consider the following system

$$s_{n+k} = \theta^3 g^{(k)}(s_n, \omega) + (1 - \theta^3)s_n \quad (2.5.1)$$

where  $k \in N$ ,  $s_n \in R^n$ ,  $n \in Z$  and  $0 < \theta < 1$  is control parameter and  $g^{(k)}$  is  $k^{th}$  iteration of  $g(\cdot)$ . Applying technique (2.5.1) on model (2.1.2) we get the following controlled model:

$$\begin{aligned} u_{n+1} &= \theta^3 \frac{(u_n + \eta\mu)}{(1 + \eta(v_n^2 + r))} + (1 - \theta^3)u_n, \\ v_{n+1} &= \theta^3 \frac{v_n + \eta(u_nv_n^2 + ru_n + \beta z_n)}{(1 + \eta(1 + \beta))} + (1 - \theta^3)v_n, \\ w_{n+1} &= \theta^3 \frac{(w_n + \eta\mu)}{(1 + \eta(z_n^2 + r))} + (1 - \theta^3)w_n, \\ z_{n+1} &= \theta^3 \frac{(z_n + \eta(w_n z_n^2 + rw_n + \beta v_n))}{(1 + \eta(1 + \beta))} + (1 - \theta^3)z_n. \end{aligned} \quad (2.5.2)$$

The variational matrix  $J^*$  for (2.5.2) about  $(u_*, v_*, w_*, z_*) = \left(\frac{\mu}{r+\mu^2}, \mu, \frac{\mu}{r+\mu^2}, \mu\right)$  is given as:

$$J^* = \begin{pmatrix} 1 + \theta^3 \left(-1 + \frac{1}{1+\eta(r+\mu^2)}\right) & \frac{2\eta\theta^3\mu^2}{(r+\mu^2)(1+\eta(r+\mu^2))} & 0 & 0 \\ \frac{\eta\theta^3(r+\mu^2)}{1+\eta+\beta\eta} & 1 - \theta^3 + \frac{\theta^3 \left(1 + \frac{2\eta\mu^2}{r+\mu^2}\right)}{1+\eta+\beta\eta} & 0 & j_{11} \\ 0 & 0 & j_{12} & -\frac{2\eta\theta^3\mu^2}{(r+\mu^2)(1+\eta(r+\mu^2))} \\ 0 & \frac{\beta\eta\theta^3}{1+\eta+\beta\eta} & \frac{\eta\theta^3(r+\mu^2)}{1+\eta+\beta\eta} & 1 - \theta^3 + \frac{\theta^3 \left(1 + \frac{2\eta\mu^2}{r+\mu^2}\right)}{1+\eta+\beta\eta} \end{pmatrix}.$$

Where  $j_{11} = \frac{\beta\eta\theta^3}{1+\eta+\beta\eta}$  and  $j_{12} = 1 + \theta^3 \left(\frac{1}{1+\eta(r+\mu^2)} - 1\right)$ . Finally, we have the following result related to the local stability analysis of controlled system (2.5.2) about  $(u_*, v_*, w_*, z_*) = \left(\frac{\mu}{r+\mu^2}, \mu, \frac{\mu}{r+\mu^2}, \mu\right)$ .

**Theorem 2.5.1.** *Consider the following polynomial equation with real coefficients*

$$\rho_1^4 + d_1^*\rho_1^3 + d_2^*\rho_1^2 + d_3^*\rho_1 + d_4^* = 0, \quad (2.5.3)$$

where (2.5.3) is obtained from  $J^*$ . Then, necessary and sufficient conditions that all the roots of (2.5.3) lie inside the disk of unit radius are given as follows:

$$1 + d_4^* + d_2^* > |d_3^* + d_1^*|, \quad |d_3^* - d_1^*| < 2(1 - d_4^*), \quad d_2^* - 3d_4^* < 3,$$

and

$$d_4^* + d_2^* + d_4^{*2} + d_3^{*2} + d_4^{*2}d_2^* + d_4^*d_1^{*2} < 1 + 2d_4^*d_2^* + d_3^*d_1^* + d_4^*d_3^*d_1^* + d_4^{*3}.$$

## 2.6 Numerical simulations

In this part of thesis, the numerical study of dynamics of (2.1.2) is provided.

**Example 2.6.1.** Assume that  $r = 0.0698, \beta = 0.3469, \mu = 0.97993, u_0 = 0.954166, v_0 = 0.97993, w_0 = 0.954166, z_0 = 0.97993$  and  $\eta \in (0, 1]$ . Then, the mathematical system (2.1.2) takes the following form:

$$\begin{aligned}
 u_{n+1} &= \frac{(u_n + \eta 0.97993)}{(1 + \eta (v_n^2 + 0.0698))}, \\
 v_{n+1} &= \frac{v_n + \eta (u_n v_n^2 + 0.0698 u_n + 0.3469 z_n)}{(1 + \eta (1 + 0.3469))}, \\
 w_{n+1} &= \frac{(w_n + \eta 0.97993)}{(1 + \eta (z_n^2 + 0.0698))}, \\
 z_{n+1} &= \frac{(z_n + \eta (w_n z_n^2 + 0.0698 w_n + 0.3469 v_n))}{(1 + \eta (1 + 0.3469))}.
 \end{aligned} \tag{2.6.1}$$

Additionally, in this case the one and only positive fixed point is  $(0.954166, 0.97993, 0.954166, 0.97993)$ . For aforementioned values of parameters one can obtain the jacobian matrix  $J(0.954, 0.979, 0.954, 0.979)$  as follows:

$$J(0.9541, 0.9799, 0.9541, 0.9799) = \begin{pmatrix} 0.75761 & -0.438739 & 0 & 0 \\ 0.225572 & 1.11334 & 0 & 0.075967 \\ 0 & 0 & 0.75761 & -0.438739 \\ 0 & 0.075967 & 0.225572 & 1.11334 \end{pmatrix}.$$

The characteristic polynomial  $P(\rho)$  calculated from  $J(0.95416, 0.9799, 0.95416, 0.9799)$  is given by

$$P(\rho) = 0.884894 - 3.5178\rho + 5.37959\rho^2 - 3.74191\rho^3 + \rho^4. \tag{2.6.2}$$

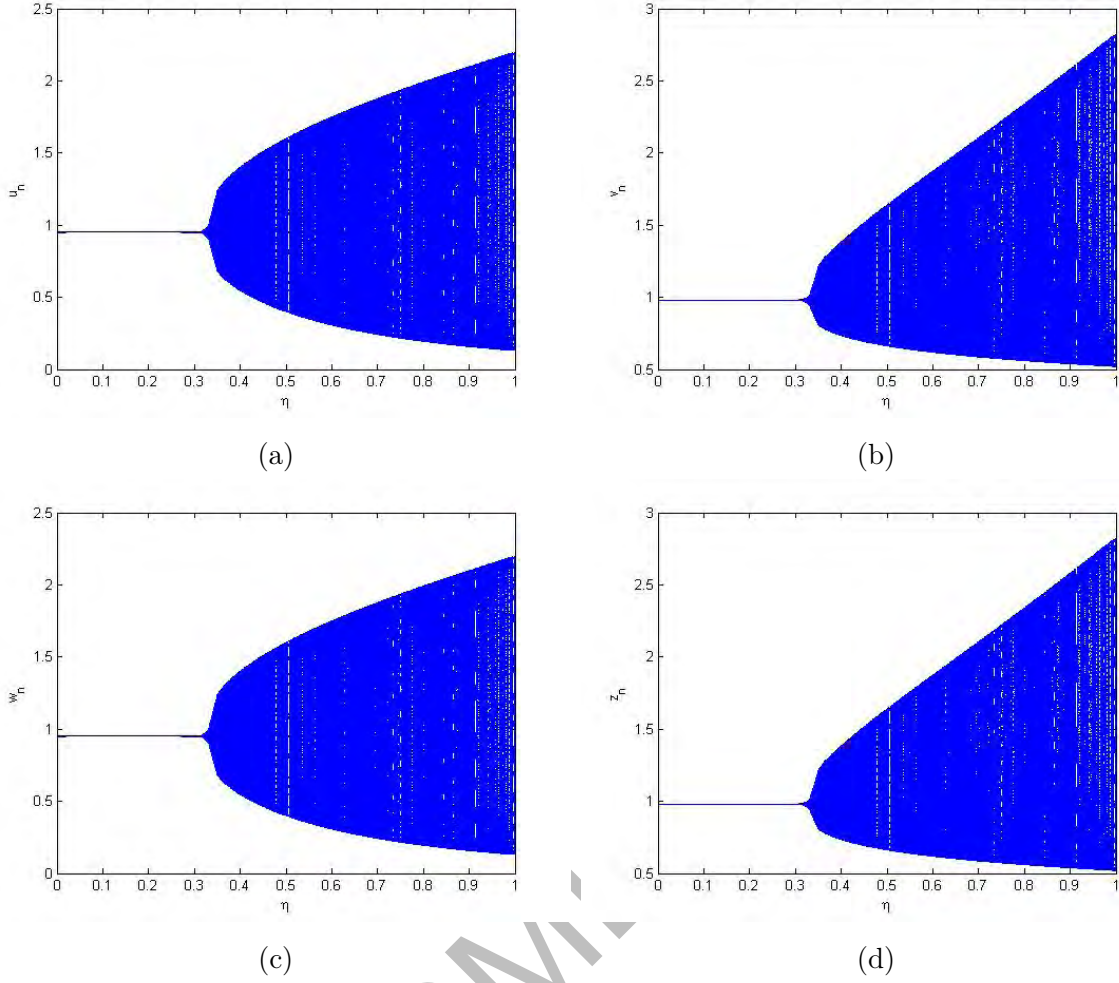


Figure 2.1: Bifurcation diagrams for system (2.1.2) for  $r = 0.0698, \beta = 0.3469, \mu = 0.97993, u_0 = 0.954166, v_0 = 0.97993, w_0 = 0.954166, z_0 = 0.97993$  and  $\eta \in (0, 1]$

Moreover, roots of  $P(\rho) = 0$  are given as  $\rho_1 = 0.897493 - 0.28178\iota, \rho_2 = 0.897493 + 0.28178\iota, \rho_3 = 0.97346 - 0.228858\iota$  and  $\rho_4 = 0.97346 + 0.228858\iota$ , with  $|\rho_{3,4}| = 1, |\rho_{1,2}| \neq 1, d_1 = -3.7419, d_2 = 5.37958, d_3 = -3.5178$ , and  $d_4 = 0.884893$ . In addition, we have

$$\left\{ \begin{array}{l} \square_1^+(\eta) = 1 + d_4 = 1.88489 > 0, \\ \square_1^-(\eta) = 1 - d_4 = 0.115107 > 0, \\ \square_3^-(\eta) = 1 - d_4 - d_2 - d_3^2 + d_4^3 - d_4^2(1 + d_2) - d_1^2d_4 + 2d_2d_4 + d_1d_3(1 + d_4) = 0, \\ \square_3^+(\eta) = 1 + d_4 + d_2 - d_3^2 - d_4^3 - d_4^2 - d_1^2d_4 - d_2d_4^2 - d_1d_3(1 - d_4) = 0.0761663 > 0, \\ F_\eta(1) = 1 + d_1 + d_2 + d_3 + d_4 = 0.00477238 > 0, \\ (-1)^4F_\eta(-1) = 1 - d_1 + d_2 - d_3 + d_4 = 4.52418 > 0. \end{array} \right.$$

Hence, all the conditions for existence of Neimark-Sacker bifurcation is satisfied (see **Theorem 2.4.1**). In this case the graphical behavior of each concentration variable is shown in **Fig. 2.1**. In **Fig. 2.2** some phase portraits are given for variation of  $\eta$  in



Additionally, in this case the one and only positive fixed point is  $(0.954166, 0.97993, 0.954166, 0.97993)$ . For aforementioned values of parameters one can obtain the jacobian matrix  $J(0.954, 0.979, 0.954, 0.979)$  as follows:

$$J(0.95416, 0.9799, 0.9541, 0.9799) = \begin{pmatrix} 0.691371 & -0.558636 & 0 & 0 \\ 0.270997 & 1.13617 & 0 & 0.0912651 \\ 0 & 0 & 0.691371 & -0.558636 \\ 0 & 0.0912651 & 0.270997 & 1.13617 \end{pmatrix}.$$

The characteristic polynomial  $P(\rho)$  calculated from  $J(0.954166, 0.97993, 0.954166, 0.97993)$  is given by

$$P(\rho) = 0.873804 - 3.41293\rho + 5.20537\rho^2 - 3.65508\rho^3 + \rho^4. \quad (2.6.4)$$

Moreover, in this case the equilibrium point  $(0.954166, 0.97993, 0.954166, 0.97993)$  of system (2.6.3) is stable for

$$0 < \theta < 0.8809233539967847.$$

In this case the graphical behavior of each concentration variable is shown in **Fig. 2.4**. Hence, it can be easily seen that bifurcation is controlled for maximum range of controlled parameter  $\theta$  for  $\eta \in (0, 1]$  (see **Fig. 2.4**). Moreover, in **Fig. 2.3** some phase portraits are given for variation of  $\theta$  in  $(0, 1]$ . Hence, it can be easily seen that there exists the Neimark-Sacker bifurcation when  $\theta$  certainly passes through  $\theta = 0.8809233539967847$  (see **Fig. 2.3**). In addition, there is no chance of Neimark-Sacker bifurcation for  $\theta \in (0, 0.8809233539967847)$  (see **Fig. 2.3(a-c)**), and for  $\theta \in (0.8809233539967847, 1)$  the existence of Neimark-Sacker bifurcation in system (2.6.3) can be seen easily (see **Fig. 2.3(d-f)**).



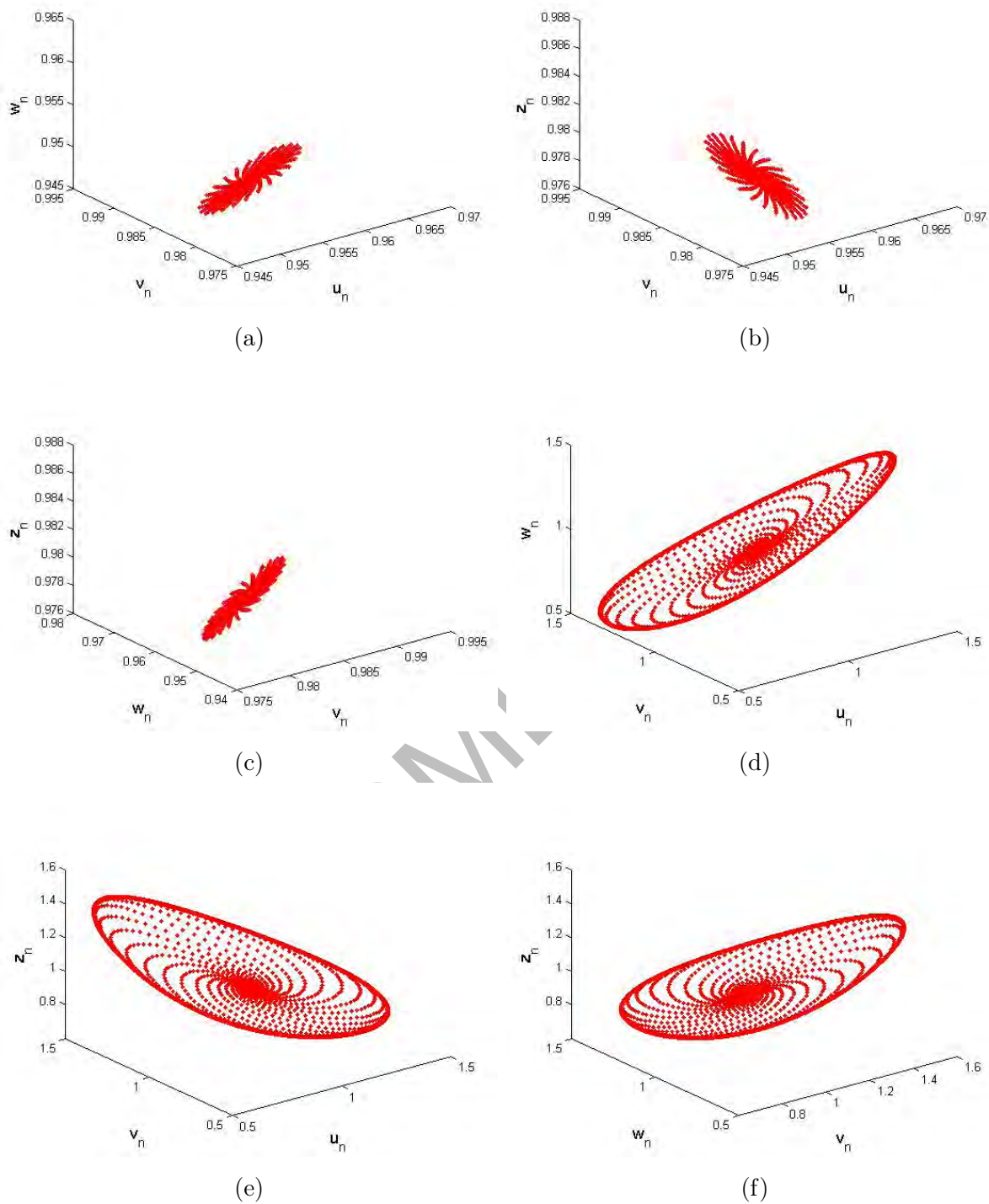


Figure 2.3: Phase portraits for system (2.6.3) for  $\eta \in (0, 1]$ ,  $r = 0.0698$ ,  $\beta = 0.3469$ ,  $\mu = 0.97993$ ,  $u_0 = 0.954166$ ,  $v_0 = 0.97993$ ,  $w_0 = 0.954166$ ,  $z_0 = 0.97993$  and  $\theta \in (0, 1]$

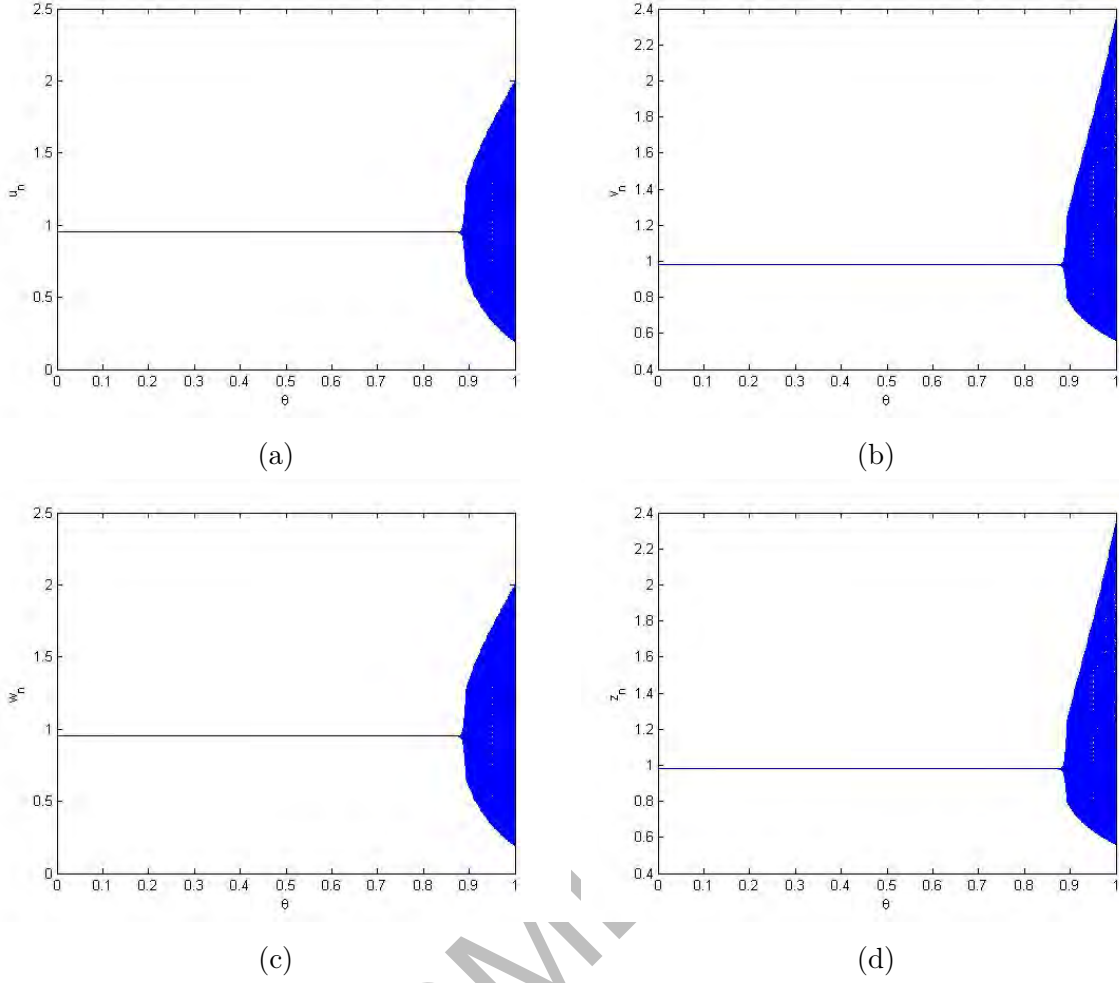


Figure 2.4: Controlled diagrams for system (2.6.3) for  $\eta \in (0, 1]$ ,  $r = 0.0698$ ,  $\beta = 0.3469$ ,  $\mu = 0.97993$ ,  $u_0 = 0.954166$ ,  $v_0 = 0.97993$ ,  $w_0 = 0.954166$ ,  $z_0 = 0.97993$  and  $\theta \in (0, 1]$

**Example 2.6.3.** Assume that  $r = 0.0698$ ,  $\beta = 0.3469$ ,  $\mu = 0.9999$ ,  $u_0 = 1.0007$ ,  $v_0 = 0.97993$ ,  $w_0 = 1.0007$ ,  $z_0 = 0.97993$ . Then, the mathematical system (2.0.6) takes the following form:

$$\begin{aligned}
 \frac{du}{dt} &= 0.97993 - uv^2 - 0.0698u, \\
 \frac{dv}{dt} &= uv^2 + 0.0698u - v + 0.3469(z - v), \\
 \frac{dw}{dt} &= 0.97993 - wz^2 - 0.0698w, \\
 \frac{dz}{dt} &= wz^2 + 0.0698w - z + 0.3469(v - z),
 \end{aligned} \tag{2.6.5}$$

Additionally, in this case the one and only positive fixed point is  $(1.0007, 0.979, 1.0007, 0.979)$ . For aforementioned values of parameters one can obtain the jacobian matrix

$J(1.0007, 0.9793, 1.0007, 0.9793)$  as follows:

$$J(1.0007, 0.9793, 1.0007, 0.9793) = \begin{pmatrix} 0.505244 & -0.990902 & 0 & 0 \\ 0.417249 & 1.26176 & 0 & 0.147812 \\ 0 & 0 & 0.505244 & -0.990902 \\ 0 & 0.147812 & 0.417249 & 1.26176 \end{pmatrix}.$$

The characteristic polynomial  $P(\rho)$  calculated from  $J(1.0007, 0.9793, 1.0007, 0.9793)$  is given by

$$P(\rho) = 1.09892 - 3.692\rho + 5.20237\rho^2 - 3.53402\rho^3 + \rho^4. \quad (2.6.6)$$

In this case the graphical behavior of each concentration variable is shown in **Fig. 2.5**. Moreover, in **Fig. 2.6** some phase portraits are given for different values of  $r$ . It can be easily seen that there exists the system (2.6.5) remains stable about one and only fixed point  $(1.0007, 0.9793, 1.0007, 0.9793)$ . In addition, a three dimensional phase portrait is given in **Fig. 2.6a**.

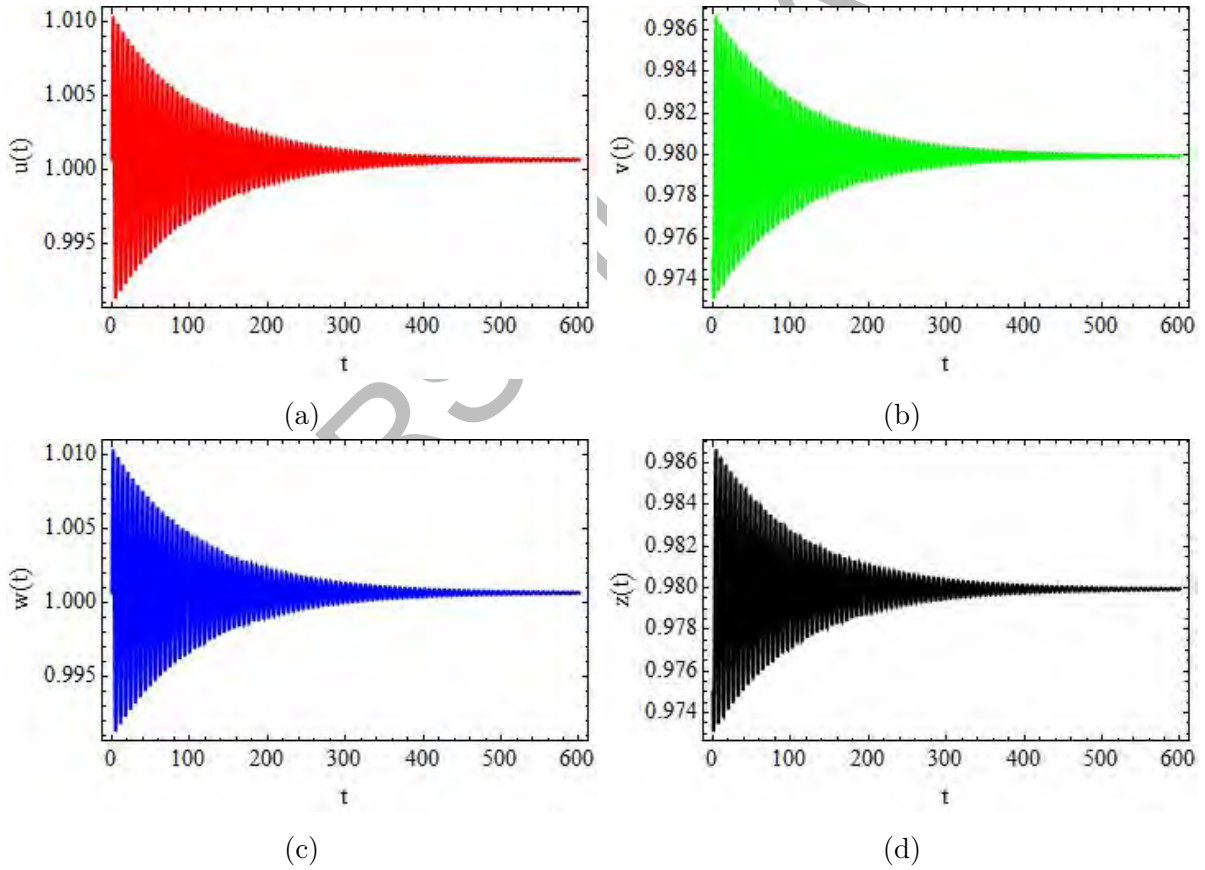


Figure 2.5: Plots of system (2.6.5) for  $r = 0.0698, \beta = 0.3469, \mu = 0.9999, u_0 = 1.0007, v_0 = 0.97993, w_0 = 1.0007, z_0 = 0.97993$

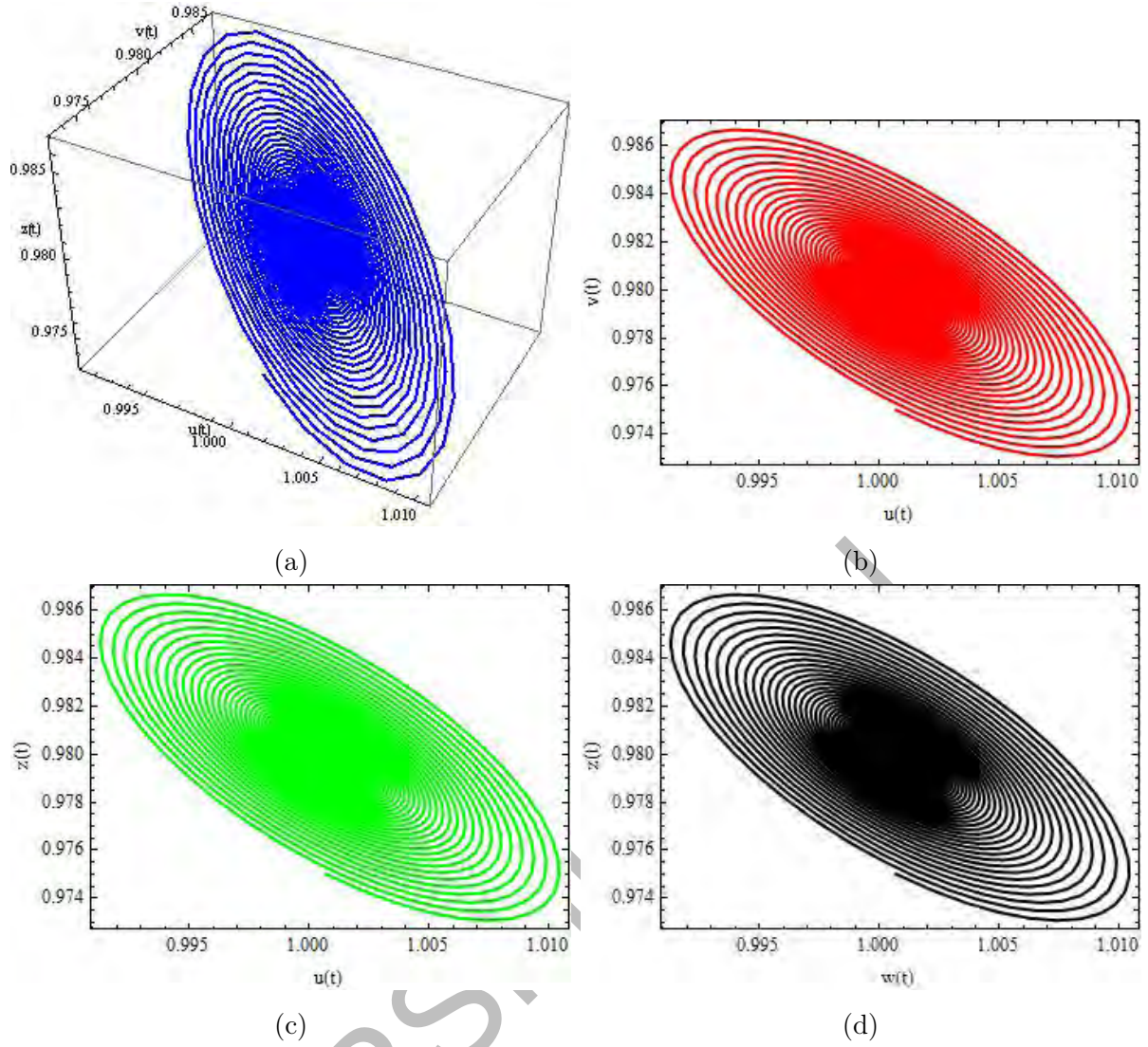


Figure 2.6: Phase portraits for system (2.6.5) for  $r = 0.0698, \beta = 0.3469, \mu = 0.9999, u_0 = 1.0007, v_0 = 0.97993, w_0 = 1.0007, z_0 = 0.97993$

**Example 2.6.4.** Assume that  $r = 0.01275, \beta = 0.3469, \mu = 0.95993, u_0 = 1.0007, v_0 = 0.97993, w_0 = 1.0007, z_0 = 0.97993$ . Then, from mathematical system (2.0.6) we get the one and only positive fixed point  $(1.0007, 0.9793, 1.0007, 0.9793)$  of system (2.0.6). Moreover, for these values of parameters one can obtain the following jacobian matrix  $J(1.0007, 0.9793, 1.0007, 0.9793)$  as follows:

$$J(1.0007, 0.9793, 1.0007, 0.9793) = \begin{pmatrix} 0.506839 & -1.0004 & 0 & 0 \\ 0.414595 & 1.26712 & 0 & 0.147812 \\ 0 & 0 & 0.506839 & -1.0004 \\ 0 & 0.147812 & 0.414595 & 1.26712 \end{pmatrix}.$$

The characteristic polynomial  $P(\rho)$  calculated from  $J(1.0007, 0.9793, 1.0007, 0.9793)$  is



given by

$$P(\rho) = 1.1116 - 3.72793\rho + 5.23903\rho^2 - 3.54791\rho^3 + \rho^4. \quad (2.6.7)$$

In this case the graphical behavior of each concentration variable is shown in **Fig. 2.7**. Moreover, in **Fig. 2.8** some phase portraits are given for variation of  $r$ . Hence, it can be easily seen that there exists the Hopf bifurcation for system (2.5) about one and only fixed point  $(1.0007, 0.9793, 1.0007, 0.9793)$  when the parameter  $r$  certainly passes through 0.01275. In addition, a three dimensional phase portrait is given in **Fig. 2.8a**.

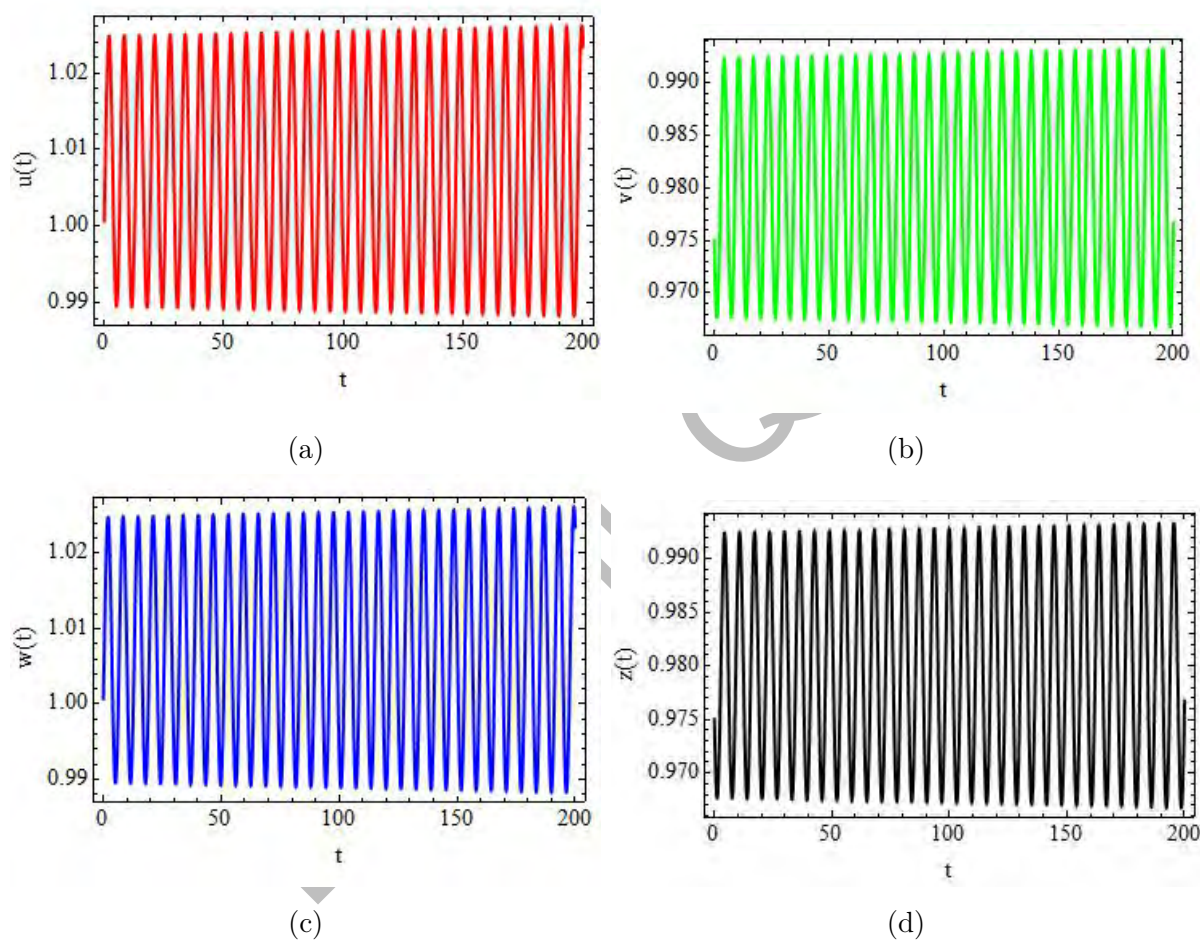


Figure 2.7: Plots of system (2.0.6) for  $r = 0.01275, \beta = 0.3469, \mu = 0.95993, u_0 = 1.0007, v_0 = 0.97993, w_0 = 1.0007, z_0 = 0.97993$

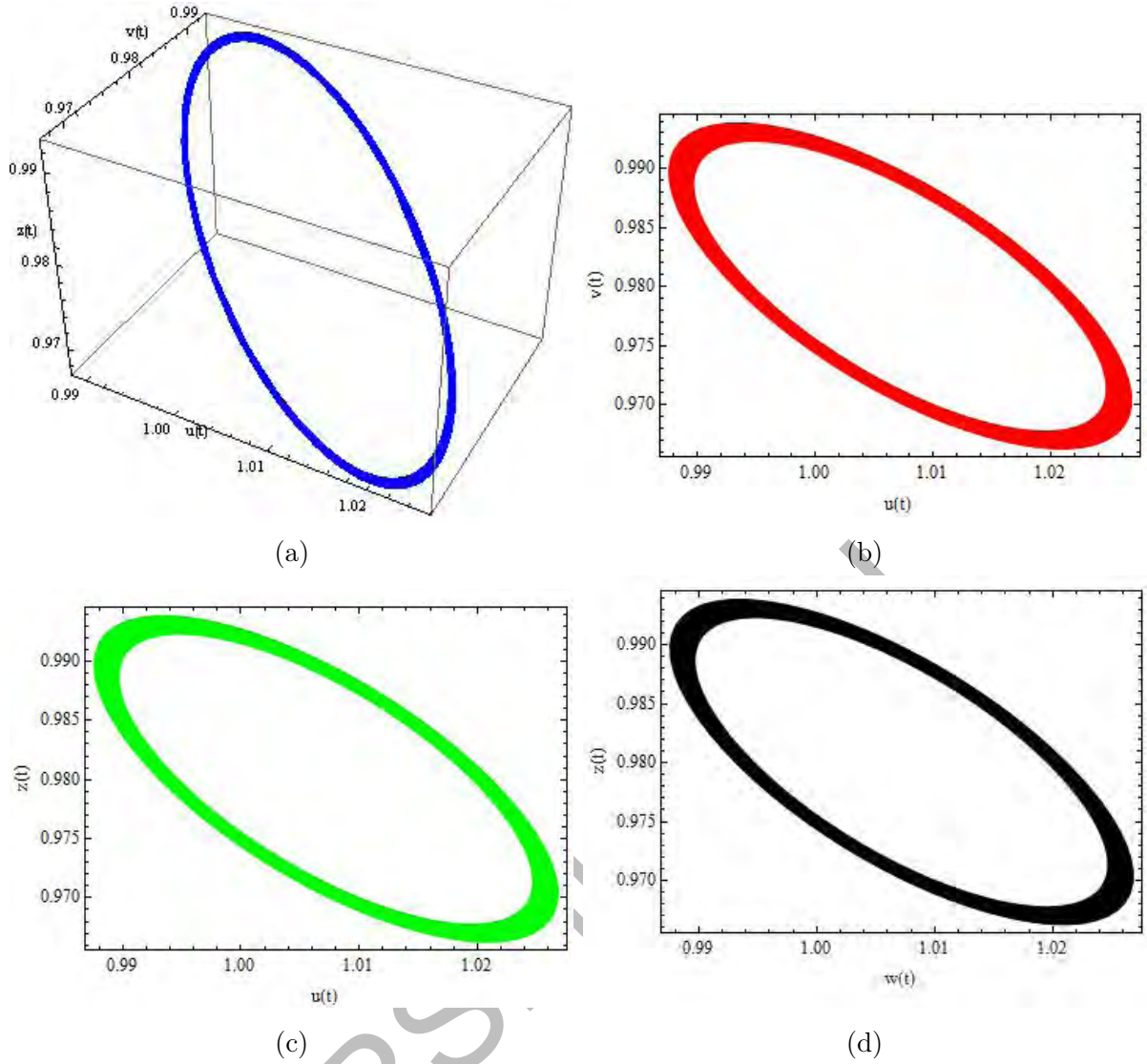


Figure 2.8: Phase portraits for system (2.0.6) for  $r = 0.01275, \beta = 0.3469, \mu = 0.95993$ ,  $u_0 = 1.0007, v_0 = 0.97993, w_0 = 1.0007, z_0 = 0.97993$ .

## 2.7 Concluding remarks

We have studied a two-cell joined cubic autocatalator chemical reaction model [42]. Additionally, during the construction of the basic structure of the model, feedback in every cell is centred on the cubic autocatalator under the effects of pooled-chemical estimations. We have considered the pairing among the cells through autocatalyst  $B$ . We have examined the local stability of a continuous system described by equation (2.0.6) using Routh-Hurwitz stability criteria. To obtain a discrete-time representation of the four-dimensional cubic autocatalator chemical reaction model (2.0.6), we discretized the model using Euler's forward method and a nonstandard difference scheme, ensuring consistency

between the continuous and discrete formulations.

By considering the pairing among the cells based on autocatalyst  $B$ , we have established the existence of a unique fixed point for the system (6.1.2). We have then analyzed the parametric conditions required for the local asymptotic stability of the system (6.1.2) around its positive fixed point. Furthermore, we have demonstrated the occurrence of Neimark-Sacker bifurcation at the positive fixed point of the system (6.1.2) by employing a well-recognized standard for Neimark-Sacker bifurcation analysis, with the bifurcation parameter  $\eta$  playing a crucial role.

In the discrete-time counterpart (6.1.2) of the original four-dimensional system (2.0.6), we have observed the emergence of chaotic dynamics at different levels of the bifurcation parameter  $\eta$ . To effectively manage the Neimark-Sacker bifurcation and chaos, we have devised a generalized hybrid control scheme that combines parameter perturbation and feedback control. The control scheme incorporates the control parameter  $\theta$  to regulate the system's behavior. Finally, we provided some numerical examples to demonstrate theoretical results. From a numerical study of (2.0.6) and (2.1.2), one can see that the system (2.0.6) remains stable for  $\beta, r > 0$  and  $\mu = 1$ , whereas the system (2.1.2) remains unstable under these parametric conditions. Moreover, through the numerical study of the system (2.1.2), one can see that there is no chance for the existence of period-doubling bifurcation, which verifies the consistency of nonstandard difference scheme [20] for mathematical system (2.0.6).

## Chapter 3

# Bifurcation Analysis of a Discrete-Time Phytoplankton-Zooplankton Model with Holling Type-II Response and Toxicity

This chapter is related to the qualitative study of a phytoplankton-zooplankton model using a dynamically consistent nonstandard difference scheme. Moreover, in the qualitative study, discussion on the boundedness of every solution, the local stability analysis, the existence of Neimark-Sacker bifurcation and the control of the Neimark-Sacker bifurcation are part of this chapter. This chapter is published in an international peer-review journal (see [57]).

The study of mathematical models for population dynamics has been considered as a critical area in abstract ecology from the time when the famous Lotka-Volterra model is presented [58]. The learning of organism movement and spreading has to turn out to be a fundamental element for understanding a chain of ecological interrogations associated with the spatiotemporal study of dynamics of populations [59]. Planktons are enormously flexible in abundance, both temporally and spatially. Plankton variability depends on natural and physical procedures for the spatial structure. Biological processes include, for instance, development, grazing and behaviour, and physical practices include, for instance, mixing and lateral stirring and nonlinearity of ecosystems, which entirely contribute to the spatial organization in plankton allocations [60]. Plankton refers to the spontaneously moving and faintly swimming organisms in marine ecology. Commonly, plankton is divided into two species: the phytoplankton species and the zooplankton species. Phytoplankton species are tiny in their size with a single-celled structure [61]. Phytoplankton is beneficial for aquatic life, and they produce half of the oxygen in the world through photosynthesis. Phytoplankton population exert a universal-scale effect on



the atmosphere by transporting  $CO_2$  from water surface to the depth of oceans. Mainly, this process happens due to their death, sinking and primary production [61]. It is observed that algal species rise abundantly in damped, wet and marine environments. The stages of speedy growth, slow stagnation and accelerated decline in cells collectively create an algal bloom. These phenomena of accelerated variation in the density of the phytoplankton population are the central trait in the plankton ecosystem [61]. Even though the sudden emergence and disappearance of blooms are not apparent, but the undesirable effect of damaging algal blooms on the health of humanity, aquatic life and fisheries trade can be seen easily [61].

On the incidence of blooms, phytoplankton and zooplankton interact with each other, and the study of this interaction is the point of focus of many scientific investigations [62]. Phytoplankton produces toxic materials to avert predations by their predators (zooplankton). Furthermore, this has been the topic of interest of many researchers for many decades. Mathematical modelling of interactions between plankton species provides us with an essential, optional method in improving the knowledge of any individual related to the biological and physical mechanisms concerning the ecological study of plankton population [62]. The authors in [63] have considered a plankton-nutrient model related to the aquatic environment by consideration of planktonic blooms. In [64] the authors have examined the influence of periodicity and seasonality on planktonic dynamics. In [65] the authors have presented two mathematical models connected to the plankton ecosystem along with a strong representation of viral septic phytoplankton and viruses. The authors in [66] have contemplated the effect of predation on competitive elimination and the coexistence of competitive predators. Moreover, they presented and explored a one-phytoplankton two-zooplankton model and the harvesting consideration.

Huppert *et al.* [67] have considered a nutrient-phytoplankton model to examine the dynamical behaviour of phytoplankton blooms. In [68] the authors have presented a zooplankton-phytoplankton model with harvesting. Moreover, it has been emphasized that excessive exploitation can result in the extinction of populations, whereas responsible harvesting practices promote the long-term viability of both populations. Additionally, there have been extensive research efforts dedicated to investigating various aspects of phytoplankton-zooplankton models, such as nutrient sources, the toxic effects of plankton species, species survival, and the implications of harvesting [76-80]. When examining the dynamics of phytoplankton-zooplankton models, it is crucial to take into account the inclusion of a lag in toxin production. The authors in [74] have presented a mathematical model including time lag in toxin deliverance by phytoplankton. The work done in [80-83] motivated us to study the dynamics of a phytoplankton-zooplankton population model with toxicity. Moreover, the toxic substance is released by phytoplankton and sometimes by other external sources. We consider the basic phytoplankton-zooplankton

model presented by Chattopadhyay *et al.* [78]. Furthermore, this mathematical model is based on the following conditions.

- We consider that  $z(t)$  and  $p(t)$  are sizes of zooplankton and phytoplankton populations, respectively.
- Zooplankton population eats phytoplankton population and then recycle into their own community. The functional response  $\frac{\alpha p(t)z(t)}{a+p(t)}$  represents the predation rate of zooplankton population on phytoplankton species. Moreover, this predation increases the growth rate of zooplankton and this growth rate is represented by the term  $\frac{\beta p(t)z(t)}{a+p(t)}$ .
- We assume that the zooplankton population becomes infected by eating the infected phytoplankton population. Additionally, the infection in phytoplankton may be produced due to external toxic substances (see [78]).
- We assume that the infection in phytoplankton may be produced due to external toxic substances (see [78]).
- Phytoplankton population has logistic growth [79] in the absence of zooplankton population, where  $r$  is their exponential rate of growth and  $k$  is the maximum carrying capacity of the environment.

Under these conditions we have the following phytoplankton-zooplankton model [78]:

$$\begin{cases} \frac{dp}{dt} = rp(t)\left(1 - \frac{p(t)}{k}\right) - \alpha f(p(t))z(t), \\ \frac{dz}{dt} = \beta f(p(t))z(t) - \delta z(t) - \rho g(p(t))z(t). \end{cases} \quad (3.0.1)$$

Kuang [80] have inspected the limit cycle behaviour in Gauss-type predator-prey systems with Holling type-II response [81]. In addition, he revealed that the study of dynamical properties of predator-prey models using the Holling type response function is better than the study of dynamics of predator-prey models without using Holling response. Generally, Holling type-II response is modelled and described by using rectangular hyperbola, and its mathematical form is given as:

$$\varphi(x) = \frac{x}{a+x},$$

where  $a$  is any constant. By using Holling type-II response we get the following mathematical form of system (3.0.1):

$$\begin{cases} \frac{dp}{dt} = rp(t)\left(1 - \frac{p(t)}{k}\right) - \alpha \frac{p(t)}{a+p(t)}z(t), \\ \frac{dz}{dt} = \beta \frac{p(t)}{a+p(t)}z(t) - \delta z(t) - \rho \frac{p(t)}{a+p(t)}z(t). \end{cases} \quad (3.0.2)$$

- Next, we assumed that phytoplankton's time lag for the production and mediation of toxic substances is zero.
- We are introducing the catchability coefficients  $q_1$  and  $q_2$  for phytoplankton and zooplankton populations, respectively. Generally, the functional form for harvesting is expressed by using the hypothesis of catch-per-unit-effort [82].
- Moreover, introducing  $E$  as the parameter for combined effort for harvesting of population [82].

Then, under these modifications the system (3.0.2) takes the following mathematical form:

$$\begin{cases} \frac{dp}{dt} = rp(t)\left(1 - \frac{p(t)}{k}\right) - \alpha \frac{p(t)}{a+p(t)}z(t) - m_1p^3(t) - q_1Ep(t), \\ \frac{dz}{dt} = \beta \frac{p(t)}{a+p(t)}z(t) - \delta z(t) - \rho \frac{p(t)}{a+p(t)}z(t) - m_2z^2(t) - q_2Ez(t), \end{cases} \quad (3.0.3)$$

where the parameters in system (3.0.3) are non-negative and defined as follows:

- $a$ : constant of partial capturing saturation.
- $\alpha$ : maximal takeover rate of zooplankton on phytoplankton.
- $\beta$ : conversion rate of phytoplankton-zooplankton ( $\beta < \alpha$ ).
- $\rho$ : toxicity rate of phytoplankton per unit biomass.
- $\delta$ : natural rate of death of zooplankton population.

Moreover, the term  $m_1p^3(t)$  appearing in the system (3.0.3) represents the infection produced in the phytoplankton population due to an external toxic substance. In addition,  $\frac{d^2}{dp^2}(m_1p^3) = 6m_1p > 0$  shows an accelerating growth of toxic substance parallel to phytoplankton population. Approximately every individual in the phytoplankton population is increasingly consuming toxic substances. However, the reduction of grazing by zooplankton due to toxicity effect is represented by the term  $m_2z^2(t)$ . Furthermore, the toxicity effect on zooplankton population is less than phytoplankton population, where  $m_1$  and  $m_2$  are toxicity coefficients with  $0 < m_2 < m_1$  [82]. Additionally, if we assume that  $m_2 = 0$  and  $m_1 = m$ , then from (3.0.3) we have

$$\begin{cases} \frac{dp}{dt} = rp(t)\left(1 - \frac{p(t)}{k}\right) - \alpha \frac{p(t)}{a+p(t)}z(t) - mp^2(t), \\ \frac{dz}{dt} = \beta \frac{p(t)}{a+p(t)}z(t) - \delta z(t) - \rho \frac{p(t)}{a+p(t)}z(t), \end{cases} \quad (3.0.4)$$

where,  $\frac{d^2}{dp^2}(mp^2) = 2 > 0$  shows an accelerating growth of toxic substance parallel to phytoplankton population.

### 3.1 Discretization of model

By using Euler's forward method with step size  $h$  we have the following discrete-time version of (3.0.3):

$$\begin{cases} p_{n+1} = p_n + h(rp_n(1 - \frac{p_{n+1}}{k}) - \alpha \frac{p_{n+1}}{a+p_n} z_n - m_1 p_n^2 p_{n+1} - q_1 E p_{n+1}), \\ z_{n+1} = z_n + h(\beta \frac{p_n}{a+p_n} z_n - \delta z_{n+1} - \rho \frac{p_n}{a+p_n} z_{n+1} - m_2 z_n z_{n+1} - q_2 E z_{n+1}), \end{cases} \quad (3.1.1)$$

But, numerical inconsistency is experienced with the application of usual finite difference methods. Hence, to avoid this numerical inconsistency, one can apply nonstandard finite difference method given by Mickens [20]. Hence, by taking into account the original dynamical properties of model (3.0.3), a discrete-time model from (3.0.3) is obtained by using Mickens type non-standard scheme such that it will remain dynamically consistent [30]. Implementing the Mickens type nonstandard scheme on model (3.0.3) we get the following discrete-time mathematical model:

$$\begin{cases} \frac{p_{n+1}-p_n}{h} = rp_n(1 - \frac{p_{n+1}}{k}) - \alpha \frac{p_{n+1}}{a+p_n} z_n - m_1 p_n^2 p_{n+1} - q_1 E p_{n+1}, \\ \frac{z_{n+1}-z_n}{h} = \beta \frac{p_n}{a+p_n} z_n - \delta z_{n+1} - \rho \frac{p_n}{a+p_n} z_{n+1} - m_2 z_n z_{n+1} - q_2 E z_{n+1}, \end{cases} \quad (3.1.2)$$

where  $h > 0$  is taken as step size for nonstandard scheme. Furthermore, (3.1.2) can be written into the following mathematical form:

$$\begin{cases} p_{n+1} = \frac{(1+hr)p_n}{1+h(\frac{r}{k}p_n + \frac{\alpha z_n}{a+p_n} + m_1 p_n^2 + q_1 E)}, \\ z_{n+1} = \frac{(1+h\frac{\beta p_n}{a+p_n})z_n}{1+h(\frac{\rho p_n}{a+p_n} + \delta + m_2 z_n + q_2 E)}. \end{cases} \quad (3.1.3)$$

Moreover, our model (3.1.3) loses its biological consistency whenever  $\beta < \rho$  (see [82]), which is impossible biologically. Hence, for rest of our chapter, we assume that  $a > k$  and  $\beta > \rho$ .

### 3.2 Boundedness of solutions

Suppose that  $p_0 > 0$  and  $z_0 > 0$ , then each solution  $(p_n, z_n)$  of the mathematical system (3.1.3) must satisfies  $p_n > 0$  and  $z_n > 0$  for all  $n \geq 0$ . Then, from first equation of system (3.1.3) it follows that

$$p_{n+1} \leq \frac{(1+hr)p_n}{1 + \frac{hr}{k}p_n}, \quad (3.2.1)$$

consequently, on solving (3.2.1) and then by applying limit we get

$$\lim_{n \rightarrow \infty} \sup p_n \leq k, \quad (3.2.2)$$

for all  $n \geq 0$ . In the same way, from second equation of system (3.1.3) we get

$$\begin{aligned} z_{n+1} &= \frac{(1 + h \frac{\beta p_n}{a+p_n}) z_n}{1 + h(\frac{\rho p_n}{a+p_n} + \delta + m_2 z_n + q_2 E)} \\ &\leq \frac{(1 + h \frac{\beta k}{a+k}) z_n}{1 + h(\frac{\rho k}{a+k} + m_2 z_n)}. \end{aligned}$$

Hence, one can obtain the upper bound for zooplankton population as

$$\lim_{n \rightarrow \infty} \sup z_n \leq \frac{k(\beta - \rho)}{m_2(k + a)}, \quad (3.2.3)$$

for all  $n \geq 0$ . Finally, we have the following theorem about the boundedness of all solutions of (3.1.3)

**Theorem 3.2.1.** *Assume that  $0 < p_0 \leq k$  and  $0 < z_0 \leq \frac{k(\beta - \rho)}{m_2(k + a)}$ , then for all  $n \geq 0$ , every positive solution  $(p_n, z_n)$  of system (3.1.3) is bounded and contained in the set  $[0, k] \times [0, \frac{k(\beta - \rho)}{m_2(k + a)}]$ , whenever  $\beta > \rho$ .*

### 3.3 Existence of fixed points

In order to obtain equilibrium points from system (3.1.3), we consider the following two dimensional system of equations:

$$\begin{cases} \underline{p} = \frac{(1+hr)\underline{p}}{1+h(\frac{r}{k}\underline{p} + \frac{\alpha \underline{z}}{a+\underline{p}} + m_1 \underline{p}^2 + q_1 E)}, \\ \underline{z} = \frac{(1+h \frac{\beta \underline{p}}{a+\underline{p}}) \underline{z}}{1+h(\frac{\rho \underline{p}}{a+\underline{p}} + \delta + m_2 \underline{z} + q_2 E)}. \end{cases} \quad (3.3.1)$$

On solving (3.3.1) one can get the following equilibrium points:  $(0, 0)$  which is extinction point for both populations,  $(\frac{\sqrt{4k^2 m_1 r + r^2 - 4Ek^2 m_1 q_1 - r}}{2km_1}, 0)$  which is extinction equilibrium for zooplankton population and the unique positive equilibrium  $(\underline{p}, \underline{z})$ . Additionally, the first component of equilibrium point  $(\frac{\sqrt{4k^2 m_1 r + r^2 - 4Ek^2 m_1 q_1 - r}}{2km_1}, 0)$  remains positive for  $r > Eq_1$ . Now, the existence and uniqueness of  $(\underline{p}, \underline{z})$  can be studied as follows. We consider the following system of equations

$$\begin{cases} \underline{p} = \frac{(1+hr)\underline{p}}{1+h(\frac{r}{k}\underline{p} + \frac{\alpha \underline{z}}{a+\underline{p}} + m_1 \underline{p}^2 + q_1 E)}, \\ \underline{z} = \frac{(1+h \frac{\beta \underline{p}}{a+\underline{p}}) \underline{z}}{1+h(\frac{\rho \underline{p}}{a+\underline{p}} + \delta + m_2 \underline{z} + q_2 E)}. \end{cases} \quad (3.3.2)$$

Furthermore, from (3.3.2) we get the following pair:

$$\underline{p} = \frac{a(\beta - \rho)}{(\beta - \rho) - (\delta + m_2 \underline{z} + q_2 E)} - a, \quad \underline{z} = \frac{(a + \underline{p})(r - \frac{r\underline{p}}{k} - m_1 \underline{p}^2 - q_1 E)}{\alpha}.$$

From aforementioned pair, we can write

$$F(\underline{p}) = \frac{a(\beta - \rho)}{(\beta - \rho) - (\delta + m_2 f(\underline{p}) + q_2 E)} - a - \underline{p}, \quad (3.3.3)$$

where

$$f(\underline{p}) = \frac{(a + \underline{p})(r - \frac{r\underline{p}}{k} - m_1 \underline{p}^2 - q_1 E)}{\alpha}, \quad (3.3.4)$$

with

$$f(0) = \frac{a(r - q_1 E)}{\alpha} > 0,$$

and

$$F(0) = \frac{a(\delta + m_2 f(0) + q_2 E)}{(\beta - \rho) - (\delta + m_2 f(0) + q_2 E)} > 0.$$

Furthermore, at upper bound and for each  $\lambda \in (0, k]$ , if we have  $(\beta - \rho) > (\delta + m_2 f(\lambda) + q_2 E)$  then

$$F(\lambda) = \frac{a(\delta + m_2 f(\lambda) + q_2 E)}{(\beta - \rho) - (\delta + m_2 f(\lambda) + q_2 E)} - \lambda < 0,$$

where

$$f(\lambda) = -\frac{(a + \lambda)(m_1 r^2 + q_1 E)}{\alpha} < 0.$$

Hence,  $F(\underline{p}) = 0$  has at least one positive real root in  $[0, k]$ . Furthermore, it can be seen that

$$F'(\lambda) = -1 + \frac{a(\beta - \rho)(m_2 f'(\lambda))}{((\beta - \rho) - (\delta + m_2 f(\lambda) + q_2 E))^2} < 0,$$

where

$$f'(\lambda) = -\frac{(a + \lambda)(\frac{r}{k} + 2m_1 \lambda)}{\alpha} + \frac{r - \frac{r\lambda}{k} - m_1 \lambda^2 - q_1 E}{\alpha} < 0,$$

whenever

$$r - q_1 E < \left(\frac{r}{k} + m_1 \lambda\right) \lambda$$

for every  $\lambda \in [0, k]$ . Hence, the equation  $F(\underline{p}) = 0$  has one and only positive solution in  $[0, k]$ .

**Theorem 3.3.1.** Assume that  $0 < p_0 \leq k$  and  $0 < z_0 \leq \frac{k(\beta - \rho)}{m_2(k + a)}$ , then for

$$r - q_1 E < \left(\frac{r}{k} + m_1 \lambda\right) \lambda$$

and

$$r > q_1 E,$$

there exists a unique positive constant solution  $(\underline{p}, \underline{z})$  of system (3.1.3) in  $[0, k] \times \left[0, \frac{k(\beta - \rho)}{m_2(k + a)}\right]$  if and only if for each  $\lambda \in (0, k]$  we have

$$(\beta - \rho) > (\delta + m_2 f(\lambda) + q_2 E).$$

In addition, for  $\lambda = 0$

$$(\beta - \rho) < (\delta + m_2 f(\lambda) + q_2 E).$$

### 3.4 Local stability analysis

In order to discuss the stability analysis of system (3.1.3) about all of its equilibrium points we have to use **Lemma 1.3.1**. We compute the variational matrix  $V_{(p,z)}$  of the system (3.1.3) about each of its fixed point  $(\underline{p}, \underline{z})$ . Moreover,  $V_{(p,z)}$  is given by

$$V_{(p,z)} = \begin{bmatrix} j_{11} & j_{12} \\ j_{21} & j_{22} \end{bmatrix}.$$

In addition, the characteristic polynomial  $\mathbb{M}(\xi)$  of  $V_{(p,z)}$  is:

$$\mathbb{M}(\xi) = \xi^2 - Tr\xi + Dt, \quad (3.4.1)$$

where

$$Tr = (j_{11} + j_{22}),$$

and

$$Dt = j_{11}j_{22} - j_{12}j_{21}.$$

Firstly, we will scrutinize the stability of system (3.1.3) about population free equilibrium point  $(0, 0)$ . The variational matrix  $V_{(p,z)}$  for system (3.1.3) evaluated at  $(0, 0)$  is given by;

$$V_{(0,0)} = \begin{pmatrix} \frac{1+hr}{1+Ehq_1} & 0 \\ 0 & \frac{1}{1+h\delta+Eq_2} \end{pmatrix}.$$

Furthermore,  $V_{(0,0)}$  is a triangular matrix. Hence, the system (3.1.3) has two eigenvalues related to the population free equilibrium point  $(0, 0)$  which are given by  $\xi_1 = \frac{1+hr}{1+Eq_1}$  and  $\xi_2 = \frac{1}{1+h\delta+Eq_2}$ . Where,  $\xi_1$  and  $\xi_2$  are roots of characteristic equation of matrix  $V_{(0,0)}$ . It is clear that  $|\xi_2| = \left| \frac{1}{1+h\delta+Eq_2} \right| < 1$  for all parametric values. Now, by considering the condition  $|\xi_2| < 1$ , and by using **Lemma 1.3.1**, we describe the stability conditions for system (3.1.3) about  $(0, 0)$ .

**Proposition 3.4.1.** *Let  $\xi_1$  and  $\xi_2$  be roots of the characteristic equation of matrix  $V_{(0,0)}$  and  $|\xi_2| < 1$  for all parametric values. Let  $(0, 0)$  be a population free fixed point of system (3.1.3) then  $(0, 0)$  is sink and saddle if and only if we have  $r < Eq_1$  and  $r > Eq_1$ , respectively.*

Next, we will explore the local stability of system (3.1.3) about the zooplankton free equilibrium

$\left( \frac{\sqrt{4k^2mr+r^2-4Ek^2mq_1-r}}{2km}, 0 \right)$ . Clearly, the first component in order pair  $\left( \frac{\sqrt{4k^2mr+r^2-4Ek^2mq_1-r}}{2km}, 0 \right)$  is positive if and only if  $r > q_1E$ . Let  $V_1\left( \frac{\sqrt{4k^2mr+r^2-4Ek^2mq_1-r}}{2km}, 0 \right)$  be the variational matrix of two dimensional system (3.1.3) about the zooplankton free

equilibrium  $(\frac{\sqrt{4k^2mr+r^2-4Ek^2mq_1-r}}{2km}, 0)$ , then  $V_1(\frac{\sqrt{4k^2mr+r^2-4Ek^2mq_1-r}}{2km}, 0)$  has the following mathematical form:

$$V_1(\underline{x}, 0) = \begin{pmatrix} \frac{k^2(1+hr)(1+Ehq_1-hm_1\underline{x}^2)}{(k+Ehkq_1+h\underline{x}(r+km_1\underline{x}))^2} & -\frac{hk^2(1+hr)\alpha\underline{x}}{(a+\underline{x})(k+Ehkq_1+h\underline{x}(r+km_1\underline{x}))^2} \\ 0 & \frac{a+\underline{x}+h\beta\underline{x}}{a+ah\delta+\underline{x}+h(\delta+\rho)\underline{x}+Ehq_2(a+\underline{x})} \end{pmatrix},$$

where  $\underline{x} = \frac{\sqrt{4k^2mr+r^2-4Ek^2mq_1-r}}{2km}$ . Moreover,  $V_1(\underline{x}, 0)$  has the following characteristic polynomial:

$$\mathbb{M}(\xi) = \xi^2 - Tr[V_1(\underline{x}, 0)] + Det[V_1(\underline{x}, 0)], \quad (3.4.2)$$

with

$$Tr[V_1(\underline{x}, 0)] = \frac{a + \underline{x} + h\beta\underline{x}}{a + ah\delta + \underline{x} + h(\delta + \rho)\underline{x} + Ehq_2(a + \underline{x})} + \frac{k^2(1 + hr)(1 + Ehq_1 - hm_1\underline{x}^2)}{(k + Ehkq_1 + h\underline{x}(r + km_1\underline{x}))^2}$$

and

$$Det[V_1(\underline{x}, 0)] = \frac{k^2(1 + hr)(a + \underline{x} + h\beta\underline{x})(1 + Ehq_1 - hm_1\underline{x}^2)}{(a + ah\delta + \underline{x} + h(\delta + \rho)\underline{x} + Ehq_2(a + \underline{x}))(k + Ehkq_1 + h\underline{x}(r + km_1\underline{x}))^2}.$$

Hence, one can have the following proposition about the local stability of system (3.1.3) about the zooplankton free equilibrium  $(\frac{\sqrt{4k^2m_1r+r^2-4Ek^2m_1q_1-r}}{2km_1}, 0)$  by using **Lemma 1.3.1**.

**Proposition 3.4.2.** *Let  $\xi_1$  and  $\xi_2$  be characteristic roots of (3.4.2) and  $r > q_1E$ . Additionally, if  $(\frac{\sqrt{4k^2m_1r+r^2-4Ek^2m_1q_1-r}}{2km_1}, 0) = (\underline{x}, 0)$  be a zooplankton free constant solution of (3.1.3) then:*

- $(\underline{x}, 0)$  remains inside the unit disk if and only if

$$|1 + Ehq_1 - hm_1\underline{x}^2| < \frac{(k + Ehkq_1 + h\underline{x}(r + km_1\underline{x}))^2}{k^2(1 + hr)}, \quad (3.4.3)$$

and

$$\beta\underline{x} < a\delta + (\delta + \rho)\underline{x} + Eq_2(a + \underline{x}). \quad (3.4.4)$$

- $(\underline{x}, 0)$  will lie outside the unit disk if and only if

$$|1 + Ehq_1 - hm_1\underline{x}^2| > \frac{(k + Ehkq_1 + h\underline{x}(r + km_1\underline{x}))^2}{k^2(1 + hr)} \quad (3.4.5)$$

and

$$\beta\underline{x} > a\delta + (\delta + \rho)\underline{x} + Eq_2(a + \underline{x}). \quad (3.4.6)$$



- $(\underline{x}, 0)$  is a saddle point if and only if one of the following pair of the inequalities (3.4.4) and (3.4.5) or (3.4.3) and (3.4.6) is satisfied.
- $(\underline{x}, 0)$  is non hyperbolic if and only if one of the following is satisfied:

$$|1 + Ehq_1 - hm_1\underline{x}^2| = \frac{(k + Ehkq_1 + h\underline{x}(r + km_1\underline{x}))^2}{k^2(1 + hr)}$$

or

$$a\delta + (\delta + \rho - \beta)\underline{x} + Eq_2(a + \underline{x}) = 0.$$

Finally, we are remained with some analysis related to the local stability of system (3.1.3) about the one and only positive fixed point  $(\underline{p}, \underline{z})$ . Moreover, all parametric conditions for the existence of non extinction fixed point  $(\underline{p}, \underline{z})$  are given in **Theorem 3.2.1** and **Theorem 3.3.1**. One can calculate the jacobian matrix  $V_2(\underline{p}, \underline{z})$  of the system (3.1.3) about  $(\underline{p}, \underline{z})$  as follows:

$$V_2(\underline{p}, \underline{z}) = \begin{pmatrix} \frac{k^2(1+hr)((a+\underline{p})^2(1+Ehq_1-hm_1\underline{p}^2)+h\alpha(a+2\underline{p})\underline{z})}{((a+\underline{p})(k+Ehkq_1+h\underline{p}(r+km_1\underline{p}))+hk\alpha\underline{z})^2} & -\frac{h\alpha\underline{p}}{(1+hr)(a+\underline{p})} \\ \frac{h\underline{z}(-\beta+\delta+\rho+Eq_2+m_2\underline{z})^2}{a(\beta+h\beta\delta-\rho+Eh\beta q_2+h\beta m_2\underline{z})} & \frac{\beta+h\beta\delta-\rho+Eh\beta q_2+h\rho m_2\underline{z}}{\beta+h\beta\delta-\rho+Eh\beta q_2+h\beta m_2\underline{z}} \end{pmatrix}.$$

where

$$\underline{z} = \left( \frac{a + \underline{p}}{\alpha} \right) \left( r - r \frac{\underline{p}}{k} - m_1 (\underline{p})^2 - q_1 E \right)$$

and

$$\underline{p} = \frac{a(\beta - \rho)}{(\beta - \rho) - (\delta + m_2\underline{z} + q_2 E)} - a.$$

Let  $M(\xi)$  be the characteristic polynomial for the matrix  $V_2(\underline{p}, \underline{z})$  with

$$\sigma = (-\beta + \delta + \rho + Eq_2) \geq 0, \quad \phi = (\beta + h\beta\delta - \rho + Eh\beta), \quad (1 + hr) = \eta q_2 > 0,$$

$$\psi = \beta + \rho, \quad \text{and } \theta = ((a + \underline{p})(k + ehkq_1 + h\underline{p}(r + km_1\underline{p})) + hk\alpha\underline{z})^2,$$

then we have

$$Tr = 1 - \frac{h\underline{p}((a - k)r + Ekq_1 + \underline{p}(2r + km_1(2a + 3\underline{p})))}{k\eta(a + \underline{p})} + \frac{\phi + h\rho m_2\underline{z}}{\phi + h\beta m_2\underline{z}},$$

and

$$\begin{aligned}
Dt &= \frac{1}{ak\underline{\eta}(a+\underline{p})(\phi+h\beta m_2\underline{z})} (a^2k\underline{\eta}(\phi+h\rho m_2\underline{z})) \\
&- \frac{1}{ak\underline{\eta}(a+\underline{p})(\phi+h\beta m_2\underline{z})} (2ah\underline{p}^2(r+akm_1)(\phi+h\rho m_2\underline{z})) \\
&+ \frac{ak\underline{p}}{ak\underline{\eta}(a+\underline{p})(\phi+h\beta m_2\underline{z})} \left( \left( a\frac{h}{k}r - hr - \eta \right) \phi + Ehq_1(\phi+h\rho m_2\underline{z}) \right) \\
&- \frac{ak\underline{p}}{ak\underline{\eta}(a+\underline{p})(\phi+h\beta m_2\underline{z})} (3hm_1\underline{p}^2(\phi+h\rho m_2\underline{z})) \\
&+ \frac{h\underline{z}\underline{p}}{ak\underline{\eta}(a+\underline{p})(\phi+h\beta m_2\underline{z})} ((a(-ahr+hkr+k\underline{\eta})\rho+hk\underline{\alpha}\underline{z}(2\sigma+m_2\underline{z}))) \\
&+ \frac{h\underline{z}\underline{p}}{ak\underline{\eta}(a+\underline{p})(\phi+h\beta m_2\underline{z})} (hk\underline{\alpha}\sigma^2).
\end{aligned}$$

Taking into account the work done in previous section and by considering the **Theorem 3.3.1**, it follows that

$$\begin{aligned}
\mathbb{M}(1) &= \frac{h^2\underline{p}\underline{z}(m_2(a(\beta-\rho)(Ekq_1+\underline{p}(2r+km_1(2a+3\underline{p}))))+2k\underline{\alpha}\sigma\underline{z}+k\underline{\alpha}m_2\underline{z}^2)}{ak\underline{\eta}(a+\underline{p})(\phi+h\beta m_2\underline{z})} \\
&+ \frac{h^2\underline{p}\underline{z}(k\underline{\alpha}\sigma^2+m_2a(\beta-\rho)(a-k)r)}{ak\underline{\eta}(a+\underline{p})(\phi+h\beta m_2\underline{z})} > 0,
\end{aligned}$$

and

$$\begin{aligned}
\mathbb{M}(-1) &= \frac{-2a\phi\underline{p}}{ak\underline{\eta}(a+\underline{p})(\phi+h\beta m_2\underline{z})} (2k\underline{\eta} - Ehkq_1 - h\underline{p}(2r+km_1(2a+3\underline{p}))) \\
&+ \frac{2ak\underline{\eta} - \underline{p}(h(a-k)r)}{ak\underline{\eta}(a+\underline{p})(\phi+h\beta m_2\underline{z})} (2a\phi + h\underline{z}\alpha\underline{\psi}m_2) \\
&+ \frac{h\underline{z}\alpha\underline{\psi}m_2\underline{p}}{ak\underline{\eta}(a+\underline{p})(\phi+h\beta m_2\underline{z})} (2k\underline{\eta} - Ehkq_1 - h\underline{p}(2r+km_1(2a+3\underline{p}))) \\
&+ \frac{h^2k\underline{\alpha}\sigma\underline{p}\underline{z}}{ak\underline{\eta}(a+\underline{p})(\phi+h\beta m_2\underline{z})} (\sigma + 2m_2\underline{z} + m_2^2\underline{z}^2).
\end{aligned}$$

Hence, the local stability of system (3.1.3) about  $(\underline{p}, \underline{z})$  can be studied with the help of **Lemma 1.3.1** and the following proposition:

**Proposition 3.4.3.** *Let  $a > k$  and  $\beta > \rho$ , then  $(\underline{p}, \underline{z})$  is a positive constant solution of (3.1.3). In addition, suppose*

$$\kappa = 2ak\underline{\eta} - \underline{p}(h(a-k)r - 2k\underline{\eta} + Ehkq_1 + h\underline{p}(2r+km_1(2a+3\underline{p})))$$

then (a) The point  $(\underline{p}, \underline{z})$  remains inside the unit disk if and only if

$$\kappa > \frac{h^2k\underline{\alpha}\sigma\underline{p}\underline{z}(\sigma + 2m_2\underline{z} + m_2^2\underline{z}^2)}{(2a\phi + h\underline{z}\alpha\underline{\psi}m_2)} \quad \text{and} \quad Dt < 1.$$

(b) The point  $(\underline{p}, \underline{z})$  is repeller if and only if

$$\kappa > \frac{h^2 k \alpha \sigma \underline{p} \underline{z} (\sigma + 2m_2 \underline{z} + m_2^2 \underline{z}^2)}{(2a\phi + h \underline{z} a \psi m_2)} \quad \text{and} \quad Dt > 1.$$

(c) The point  $(\underline{p}, \underline{z})$  is a saddle point if and only if

$$\kappa < \frac{h^2 k \alpha \sigma \underline{p} \underline{z} (\sigma + 2m_2 \underline{z} + m_2^2 \underline{z}^2)}{(2a\phi + h \underline{z} a \psi m_2)}.$$

(d) The point  $(\underline{p}, \underline{z})$  is non-hyperbolic if and only if

$h =$

$$\frac{a\phi \underline{p} ((a-k)r + Ekq_1 + \underline{p}(2r + km_1(2a+3\underline{p}))) + ak\eta(\beta - \rho)m_2(a + \underline{p}) \underline{z}}{\underline{p} \underline{z} (k\alpha\sigma^2 - m_2(a\rho((a-k)r + Ekq_1 + \underline{p}(2r + km_1(2a+3\underline{p}))) - 2k\alpha\sigma\underline{z} - k\alpha m_2 \underline{z}^2))}, \quad (3.4.7)$$

and

$$h\underline{p}(Ekq_1 + \underline{p}(2r + km_1(2a+3\underline{p}))) (\phi + h\rho m_2 \underline{z}) + h\underline{p}(a-k)r \neq 2(\phi + h\rho m_2 \underline{z}) k\eta(a + \underline{p}), \quad (3.4.8)$$

$$h\underline{p}((a-k)r + Ekq_1 + \underline{p}(2r + km_1(2a+3\underline{p}))) (\phi + h\rho m_2 \underline{z}) \neq (\phi + h\rho m_2 \underline{z}) k\eta(a + \underline{p}). \quad (3.4.9)$$

## 3.5 Bifurcation analysis

In this section, we use standard theory of bifurcation for the study of Neimark-Sacker bifurcation of system (3.1.3) at  $(\underline{p}, \underline{z})$  (see [87-98]).

### 3.5.1 Neimark-Sacker bifurcation

Let  $\xi_1$  and  $\xi_2$  be roots of (3.4.1), then both of these roots are complex with modulus one if  $(\underline{p}, \underline{z})$  is a non-hyperbolic fixed point under condition (d) of **Proposition 3.4.3**. Hence, (3.1.3) experiences the Neimark-Sacker bifurcation when parameters given in system (3.1.3) vary in the small neighborhood of the following set:

$$\mathcal{U}_* = \{\alpha, \beta, a, k, r, \delta, \rho, m_1, m_2, q_1, q_2, E \in \mathfrak{R}^+ : h \in (0, 1)\},$$

and (3.4.8) and (3.4.9) are satisfied. Let  $(\alpha, \beta, a, k, r, \delta, \rho, m_1, m_2, q_1, q_2, E) \in \mathcal{U}_*$  with

$h =$

$$\frac{a\phi \underline{p} ((a-k)r + Ekq_1 + \underline{p}(2r + km_1(2a+3\underline{p}))) + ak\eta(\beta - \rho)m_2(a + \underline{p}) \underline{z}}{\underline{p} \underline{z} (k\alpha\sigma^2 - m_2(a\rho((a-k)r + Ekq_1 + \underline{p}(2r + km_1(2a+3\underline{p}))) - 2k\alpha\sigma\underline{z} - k\alpha m_2 \underline{z}^2))},$$

then system (3.1.3) can be written as

$$\begin{pmatrix} p \\ z \end{pmatrix} \rightarrow \begin{pmatrix} \frac{(1+hr)p}{1+h(\frac{r}{k}p+\frac{\alpha z}{a+p}+m_1p^2+q_1E)} \\ \frac{(1+h\frac{\beta p}{a+p})z}{1+h(\frac{\rho p}{a+p}+\delta+m_2z+q_2E)} \end{pmatrix}. \quad (3.5.1)$$

Assume that  $(\alpha, \beta, a, k, r, \delta, \rho, m_1, m_2, q_1, q_2, E) \in \mathcal{U}_*$  and by taking  $\check{h}$  as bifurcation parameter, we get the following form of system (3.5.1):

$$\begin{pmatrix} p \\ z \end{pmatrix} \rightarrow \begin{pmatrix} \frac{(1+(h+\check{h})r)p}{1+(h+\check{h})(\frac{r}{k}p+\frac{\alpha z}{a+p}+m_1p^2+q_1E)} \\ \frac{(1+(h+\check{h})\frac{\beta p}{a+p})z}{1+(h+\check{h})(\frac{\rho p}{a+p}+\delta+m_2z+q_2E)} \end{pmatrix}. \quad (3.5.2)$$

where  $|\check{h}| \ll 1$  is very small perturbation parameter. Next, we assume that

$$P = p - \underline{p}, \quad Z = z - \underline{z},$$

then the map (3.5.1) takes the following mathematical form:

$$\begin{pmatrix} P \\ Z \end{pmatrix} \rightarrow \begin{pmatrix} v_{11} & v_{12} \\ v_{21} & v_{22} \end{pmatrix} \begin{pmatrix} P \\ Z \end{pmatrix} + \begin{pmatrix} \check{f}(P, Z) \\ \check{g}(P, Z) \end{pmatrix}, \quad (3.5.3)$$

where

$$\begin{aligned} \check{f}(P, Z) &= v_{13}P^2 + v_{14}PZ + v_{15}Z^2 + v_{16}P^3 + v_{17}P^2Z + v_{18}PZ^2 \\ &\quad + v_{19}Z^3 + O((|P| + |Z|)^4), \\ \check{g}(P, Z) &= v_{23}P^2 + v_{24}PZ + v_{25}Z^2 + v_{26}P^3 + v_{27}P^2Z + v_{28}PZ^2 \\ &\quad + v_{29}Z^3 + O((|P| + |Z|)^4). \end{aligned}$$

Moreover, the coefficients  $v_{ij}$  for  $i = 1, 2, \dots, 9$  and  $j = 1, 2, \dots, 9$  are

$$\begin{aligned} v_{11} &= \frac{k^2(1+h^*r)((a+p)^2+h^*(a+2p)z\alpha+h^*(a+p)^2(-p^2m_1+Eq_1))}{((a+p)(k+h^*pr)+h^*kz\alpha+h^*k(a+p)(p^2m_1+Eq_1))^2}, \\ v_{12} &= \frac{h^*p(1+h^*r)\alpha}{(a+p)(1+x_1)^2}, \\ v_{13} &= \frac{h^{*2}p(1+h^*r)\left(\frac{r}{k}-\frac{z\alpha}{(a+p)^2}+2pm_1\right)^2}{(1+x_1)^3} - \frac{hp(1+h^*r)\left(\frac{2z\alpha}{(a+p)^3}+2m_1\right)}{2(1+x_1)^2} \\ &\quad - \frac{h^*(1+h^*r)\left(\frac{r}{k}-\frac{z\alpha}{(a+p)^2}+2pm_1\right)}{(1+x_1)^2}, \end{aligned}$$

$$\begin{aligned}
v_{14} &= \frac{2h^{*2}\underline{p}(1+h^*r)\alpha\left(\frac{r}{k}-\frac{z\alpha}{(a+p)^2}+2\underline{p}m_1\right)}{(a+p)(1+x_1)^3} + \frac{h^*\underline{p}(1+h^*r)\alpha}{(a+p)^2(1+x_1)^2} \\
&- \frac{h^*(1+h^*r)\alpha}{(a+p)(1+x_1)^2}, \quad v_{15} = \frac{h^{*2}\underline{p}(1+h^*r)\alpha^2}{(a+p)^2(1+x_1)^3}, \\
v_{16} &= -\frac{h^{*3}\underline{p}(1+h^*r)\left(\frac{r}{k}-\frac{z\alpha}{(a+p)^2}+2\underline{p}m_1\right)^3}{(1+x_1)^4} - \frac{h^*(1+h^*r)\left(\frac{2z\alpha}{(a+p)^3}+2m_1\right)}{2(1+x_1)^2} \\
&+ \frac{h^{*2}(1+h^*r)\left(\frac{r}{k}-\frac{z\alpha}{(a+p)^2}+2\underline{p}m_1\right)^2}{(1+x_1)^3} + \frac{h^*\underline{p}(1+h^*r)z\alpha}{(a+p)^4(1+x_1)^2} \\
&+ \frac{h^{*2}\underline{p}(1+h^*r)\left(\frac{2z\alpha}{(a+p)^3}+2m_1\right)\left(\frac{r}{k}-\frac{z\alpha}{(a+p)^2}+2\underline{p}m_1\right)}{(1+x_1)^3}, \\
v_{17} &= -\frac{3h^{*3}\underline{p}\alpha(1+h^*r)\left(\frac{r}{k}-\frac{z\alpha}{(a+p)^2}+2\underline{p}m_1\right)^2}{(a+p)(1+x_1)^4} - \frac{h^*\underline{p}(1+h^*r)\alpha}{(a+p)^3(1+x_1)^2} \\
&- \frac{2h^{*2}\underline{p}\alpha(1+h^*r)\left(\frac{r}{k}-\frac{z\alpha}{(a+p)^2}+2\underline{p}m_1\right)}{(a+p)^2(1+x_1)^3} + \frac{h^*(1+h^*r)\alpha}{(a+p)^2(1+x_1)^2} \\
&+ \frac{h^{*2}\underline{p}\alpha(1+h^*r)\left(\frac{2z\alpha}{(a+p)^3}+2m_1\right)}{(a+p)(1+x_1)^3} + \frac{2h^{*2}\alpha(1+h^*r)\left(\frac{r}{k}-\frac{z\alpha}{(a+p)^2}+2\underline{p}m_1\right)}{(a+p)(1+x_1)^3}, \\
v_{18} &= -\frac{3h^{*3}\underline{p}(1+h^*r)\alpha^2\left(\frac{r}{k}-\frac{z\alpha}{(a+p)^2}+2\underline{p}m_1\right)}{(a+p)^2(1+x_1)^4} - \frac{2h^{*2}\underline{p}(1+h^*r)\alpha^2}{(a+p)^3(1+x_1)^3} \\
&+ \frac{h^{*2}(1+h^*r)\alpha^2}{(a+p)^2(1+x_1)^3}, \quad v_{19} = -\frac{h^{*3}\underline{p}(1+h^*r)\alpha^3}{(a+p)^3(1+x_1)^4}, \\
v_{21} &= \frac{ah^*z(\beta+h^*\beta\delta-\rho+h^*z\beta m_2+ Eh^*\beta q_2)}{(a+p+ah^*\delta+h^*\underline{p}(\delta+\rho)+h^*(a+p)(zm_2+Eq_2))^2}, \\
v_{22} &= \frac{(a+p+h^*\underline{p}\beta)(a+p+ah^*\delta+h^*\underline{p}(\delta+\rho)+ Eh^*(a+p)q_2)}{(a+p+ah^*\delta+h^*\underline{p}(\delta+\rho)+h^*(a+p)(zm_2+Eq_2))^2}, \\
v_{23} &= -\frac{ah^*z(1+h^*(\delta+\rho)+h^*zm_2+ Eh^*q_2)(\beta+h^*\beta\delta-\rho+h^*z\beta m_2+ Eh^*)}{(a+p+ah^*\delta+h^*\underline{p}(\delta+\rho)+h^*(a+p)(zm_2+Eq_2))^3}, \\
v_{24} &= \frac{2h^{*2}z\left(1+\frac{h^*\underline{p}\beta}{a+p}\right)\left(-\frac{p\rho}{(a+p)^2}+\frac{\rho}{a+p}\right)m_2}{(1+x_2)^3} - \frac{h^*\left(1+\frac{h^*\underline{p}\beta}{a+p}\right)\left(-\frac{p\rho}{(a+p)^2}+\frac{\rho}{a+p}\right)}{(1+x_2)^2} \\
&- \frac{h^*z\left(-\frac{h^*\underline{p}\beta}{(a+p)^2}+\frac{h^*\beta}{a+p}\right)m_2}{(1+x_2)^2} + \frac{-\frac{h^*\underline{p}\beta}{(a+p)^2}+\frac{h^*\beta}{a+p}}{1+x_2},
\end{aligned}$$

$$\begin{aligned}
v_{25} &= \frac{h^*(a + \underline{p})(a + \underline{p} + h^*\underline{p}\beta)m_2 (a + \underline{p} + ah^*\delta + h^*\underline{p}(\delta + \rho) + Eh^*(a + \underline{p})q_2)}{(a + \underline{p} + ah^*\delta + h^*\underline{p}(\delta + \rho) + h^*(a + \underline{p})(\underline{z}m_2 + Eq_2))^3}, \\
v_{26} &= -\frac{h^{*3}\underline{z} \left(1 + \frac{h^*\underline{p}\beta}{a + \underline{p}}\right) \left(-\frac{\underline{p}\rho}{(a + \underline{p})^2} + \frac{\rho}{a + \underline{p}}\right)^3}{(1 + x_2)^4} - \frac{h^*\underline{z} \left(1 + \frac{h^*\underline{p}\beta}{a + \underline{p}}\right) \left(\frac{6\rho}{(a + \underline{p})^3}\right)}{6(1 + x_2)^2} \\
&+ \frac{h^{*2}\underline{z} \left(-\frac{h^*\underline{p}\beta}{(a + \underline{p})^2} + \frac{h^*\beta}{a + \underline{p}}\right) \left(-\frac{\underline{p}\rho}{(a + \underline{p})^2} + \frac{\rho}{a + \underline{p}}\right)^2}{(1 + x_2)^3} \\
&- \frac{h^*\underline{z} \left(-\frac{h^*\underline{p}\beta}{(a + \underline{p})^2} + \frac{h^*\beta}{a + \underline{p}}\right) \left(\frac{2\underline{p}\rho}{(a + \underline{p})^3} - \frac{2\rho}{(a + \underline{p})^2}\right)}{2(1 + x_2)^2} + \frac{\underline{z} \left(-\frac{6h^*\underline{p}\beta}{(a + \underline{p})^4} + \frac{6h^*\beta}{(a + \underline{p})^3}\right)}{6(1 + x_2)} \\
&+ \frac{h^{*2}\underline{z} \left(1 + \frac{h^*\underline{p}\beta}{a + \underline{p}}\right) \left(\frac{2\underline{p}\rho}{(a + \underline{p})^3} - \frac{2\rho}{(a + \underline{p})^2}\right) \left(-\frac{\underline{p}\rho}{(a + \underline{p})^2} + \frac{\rho}{a + \underline{p}}\right)}{(1 + x_2)^3}, \\
v_{27} &= \frac{ah^*\underline{z} (1 + h^*(\delta + \rho) + h^*\underline{z}m_2 + Eh^*q_2)^2 (h^*\beta\delta - \rho + h^*\underline{z}\beta m_2 + Eh^*)}{(a + \underline{p} + ah^*\delta + h^*\underline{p}(\delta + \rho) + h^*(a + \underline{p})(\underline{z}m_2 + Eq_2))^4}, \\
v_{28} &= -\frac{3h^{*3}\underline{z} \left(1 + \frac{h^*\underline{p}\beta}{a + \underline{p}}\right) \left(-\frac{\underline{p}\rho}{(a + \underline{p})^2} + \frac{\rho}{a + \underline{p}}\right) m_2^2}{(1 + x_2)^4} - \frac{h^* \left(-\frac{h^*\underline{p}\beta}{(a + \underline{p})^2} + \frac{h^*\beta}{a + \underline{p}}\right) m_2}{(1 + x_2)^2} \\
&+ \frac{2h^{*2} \left(1 + \frac{h^*\underline{p}\beta}{a + \underline{p}}\right) \left(-\frac{\underline{p}\rho}{(a + \underline{p})^2} + \frac{\rho}{a + \underline{p}}\right) m_2}{(1 + x_2)^3} + \frac{h^{*2}\underline{z} \left(-\frac{h^*\underline{p}\beta}{(a + \underline{p})^2} + \frac{h^*\beta}{a + \underline{p}}\right) m_2^2}{(1 + x_2)^3}, \\
v_{29} &= \frac{h^{*2}(a + \underline{p})^2(a + \underline{p} + h^*\underline{p}\beta)m_2^2 (ah^*\delta + h^*\underline{p}(\delta + \rho) + Eh^*(a + \underline{p})q_2)}{(a + \underline{p} + ah^*\delta + h^*\underline{p}(\delta + \rho) + h^*(a + \underline{p})(\underline{z}m_2 + Eq_2))^4},
\end{aligned}$$

with

$$\begin{aligned}
x_1 &= h^* \left( \frac{\underline{p}r}{k} + \frac{\underline{z}\alpha}{a + \underline{p}} + \underline{p}^2 m_1 + Eq_1 \right) \\
x_2 &= h^* \left( \delta + \frac{\underline{p}\rho}{a + \underline{p}} + \underline{z}m_2 + Eq_2 \right), \quad h^* = (h + \check{h}).
\end{aligned}$$

The characteristic equation  $M(\xi) = 0$  obtained from jacobian matrix of the mathematical system (3.5.3) about  $(0, 0)$  can be given as:

$$\xi^2 - Tr(\check{h})\xi + Dt(\check{h}) = 0, \quad (3.5.4)$$

where

$$Tr(\check{h}) = 1 - \frac{\bar{h}\underline{p}((a - k)r + Ekq_1 + \underline{p}(2r + km_1(2a + 3\underline{p})))}{k\eta(a + \underline{p})} + \frac{\phi + \bar{h}\rho m_2 \underline{z}}{\phi + \bar{h}\beta m_2 \underline{z}},$$

and

$$\begin{aligned}
Dt(\check{h}) &= \frac{1}{ak\eta(a+p)(\phi + \bar{h}\beta m_2 \underline{z})} (a^2 k \eta (\phi + \bar{h} \rho m_2 \underline{z})) \\
&- \frac{1}{ak\eta(a+p)(\phi + \bar{h}\beta m_2 \underline{z})} (2a\bar{h}\underline{p}^2 (r + akm_1) (\phi + \bar{h}\rho m_2 \underline{z})) \\
&+ \frac{ak\underline{p}}{ak\eta(a+p)(\phi + \bar{h}\beta m_2 \underline{z})} \left( \left( a \frac{\bar{h}}{k} r - \bar{h}r - \eta \right) \phi + E\bar{h}q_1 (\phi + \bar{h}\rho m_2 \underline{z}) \right) \\
&- \frac{ak\underline{p}}{ak\eta(a+p)(\phi + \bar{h}\beta m_2 \underline{z})} (3\bar{h}m_1\underline{p}^2 (\phi + \bar{h}\rho m_2 \underline{z})) \\
&+ \frac{\bar{h}z\underline{p}}{ak\eta(a+p)(\phi + \bar{h}\beta m_2 \underline{z})} \left( (a(-a\bar{h}r + \bar{h}kr + k\eta)\rho + \bar{h}k\alpha\underline{z}(2\sigma + m_2\underline{z})) \right) \\
&+ \frac{\bar{h}z\underline{p}}{ak\eta(a+p)(\phi + \bar{h}\beta m_2 \underline{z})} (\bar{h}k\alpha\sigma^2),
\end{aligned}$$

where  $\bar{h} = h + \check{h}$ . As  $(\alpha, \beta, a, k, r, \delta, \rho, m_1, m_2, q_1, q_2, E) \in \mathcal{U}_*$ , then roots of (3.5.4) are pair of complex numbers  $\xi_1$  and  $\xi_2$  such that  $|\xi_1| = |\xi_2| = 1$ . Then immediately it can be seen that:

$$\check{\rho}(\check{h}) = \frac{Tr(\check{h})}{2} + \frac{i}{2} \sqrt{4Dt(\check{h}) - Tr^2(\check{h})}.$$

Furthermore, one can have  $\check{\rho}^m(0) \neq 1 \forall m \in \{1, 2, 3, 4\}$  if and only if

$$Tr(\check{h}) = 1 - \frac{\bar{h}\underline{p}((a-k)r + Ekq_1 + \underline{p}(2r + km_1(2a + 3\underline{p})))}{k\eta(a+p)} + \frac{\phi + \bar{h}\rho m_2 \underline{z}}{\phi + \bar{h}\beta m_2 \underline{z}} \neq \pm 2, 0, 1. \quad (3.5.5)$$

Since  $(\alpha, \beta, a, k, r, \delta, \rho, m_1, m_2, q_1, q_2, E) \in \mathcal{U}_*$ , and (3.4.8), (3.4.9) are satisfied, the condition (3.5.5) is automatically satisfied and

$$|\xi_1| = |\check{\rho}(\check{h})| = \sqrt{Dt(\check{h})}, \quad \left( \frac{d\sqrt{Dt(\check{h})}}{d\check{h}} \right)_{\check{h}=0} \neq 0.$$

Finally, to convert the linear part of (3.5.3) into canonical matrix form at  $\check{h} = 0$ , we consider the following similarity transformation:

$$\begin{pmatrix} P \\ Z \end{pmatrix} = \begin{pmatrix} v_{12} & 0 \\ \ell - v_{11} & -\wp \end{pmatrix} \begin{pmatrix} X \\ Y \end{pmatrix}. \quad (3.5.6)$$

where

$$\ell = \frac{Tr(0)}{2},$$

and

$$\wp = \frac{\sqrt{4Dt(0) - Tr^2(0)}}{2}.$$

Then, from (3.5.6) we have

$$\begin{pmatrix} X \\ Y \end{pmatrix} = \begin{pmatrix} \frac{1}{v_{12}} & 0 \\ \frac{\ell-v_{11}}{\wp v_{12}} & -\frac{1}{\wp} \end{pmatrix} \begin{pmatrix} P \\ Z \end{pmatrix}. \quad (3.5.7)$$

By using transformation (3.5.6), one has the next authoritative form of system (3.5.3):

$$\begin{pmatrix} X \\ Y \end{pmatrix} \rightarrow \begin{pmatrix} \ell & -\wp \\ \wp & \ell \end{pmatrix} \begin{pmatrix} X \\ Y \end{pmatrix} + \begin{pmatrix} \check{F}(X, Y) \\ \check{G}(X, Y) \end{pmatrix}, \quad (3.5.8)$$

where

$$\begin{aligned} \check{F}(X, Y) &= \frac{v_{16}P^3}{v_{12}} + \frac{v_{17}P^2Z}{v_{12}} + \frac{v_{13}P^2}{v_{12}} + \frac{v_{18}PZ^2}{v_{12}} + \frac{v_{14}PZ}{v_{12}} + \frac{Z^3v_{19}}{v_{12}} + \frac{Z^2v_{15}}{v_{12}} \\ &+ O((|X| + |Y|)^4), \end{aligned}$$

$$\begin{aligned} \check{G}(X, Y) &= \left( \frac{(\ell - v_{11})v_{16}}{v_{12}\wp} - \frac{v_{26}}{\wp} \right) P^3 + \left( \frac{(\ell - v_{11})v_{17}}{v_{12}\wp} - \frac{v_{27}}{\wp} \right) P^2Z \\ &+ \left( \frac{(\ell - v_{11})v_{13}}{v_{12}\wp} - \frac{v_{23}}{\wp} \right) P^2 + \left( \frac{(\ell - v_{11})v_{18}}{v_{12}\wp} - \frac{v_{28}}{\wp} \right) PZ^2 \\ &+ \left( \frac{(\ell - v_{11})v_{14}}{v_{12}\wp} - \frac{v_{24}}{\wp} \right) PZ + \left( \frac{(\ell - v_{11})v_{19}}{v_{12}\wp} - \frac{v_{29}}{\wp} \right) Z^3 \\ &+ \left( \frac{(\ell - v_{11})v_{15}}{v_{12}\wp} - \frac{v_{25}}{\wp} \right) Z^2 + O((|X| + |Y|)^4), \end{aligned}$$

where  $P = v_{12}X$  and  $Z = (\ell - v_{11})X - \wp Y$ . Hence, by standard theory of normal form for analysis of bifurcation, one can calculate the first Lyapunov exponent at  $(X, Y) = (0, 0)$  as follows:

$$\Omega = \left( \left[ -Re \left( \frac{(1 - 2\xi_1)\xi_2^2}{1 - \xi_1} \theta_{20}\theta_{11} \right) - \frac{1}{2}|\theta_{11}|^2 - |\theta_{02}|^2 + Re(\xi_2\theta_{21}) \right] \right)_{\hbar=0},$$

where

$$\theta_{20} = \frac{1}{8} \left[ i \left( \check{G}_{XX} - \check{G}_{YY} - 2\check{F}_{XY} \right) - \check{F}_{YY} + \check{F}_{XX} + 2\check{G}_{XY} \right],$$

$$\theta_{11} = \frac{1}{4} \left[ i \left( \check{G}_{XX} + \check{G}_{YY} \right) + \check{F}_{XX} + \check{F}_{YY} \right],$$

$$\theta_{02} = \frac{1}{8} \left[ i \left( \check{G}_{XX} - \check{G}_{YY} + 2\check{F}_{XY} \right) - \check{F}_{YY} + \check{F}_{XX} - 2\check{G}_{XY} \right],$$

$$\begin{aligned} \theta_{21} &= \frac{1}{16} \left( \check{F}_{XXX} + \check{F}_{XYX} + \check{G}_{XXY} + \check{G}_{YYX} \right) \\ &+ \frac{i}{16} \left( \check{G}_{XXX} + \check{G}_{XYX} - \check{F}_{XXY} - \check{F}_{YYX} \right). \end{aligned}$$

Due to aforementioned analysis, one can have the following theorem (See [28-33]).



**Theorem 3.5.1.** *Assume that (3.4.7), (3.4.8) and (3.4.9) are satisfied and  $\Omega \neq 0$ , then the unique positive fixed point  $(\underline{p}, \underline{z})$  of mathematical system (3.1.3) undergoes Neimark-Sacker bifurcation. Additionally, if  $\Omega < 0$ , then for  $h > \check{h}$  an attracting invariant closed curve bifurcates from fixed point  $(\underline{p}, \underline{z})$  and if  $\Omega > 0$ , then for  $h < \check{h}$  a repelling invariant closed curve bifurcates from fixed point  $(\underline{p}, \underline{z})$ .*

## 3.6 Chaos control

In this section, we have discussed two different methods for controlling the Neimark-Sacker bifurcation in the system (3.1.3).

### 3.6.1 A modified technique for chaos control

We consider the following  $n$ -dimensional discrete-time dynamical system:

$$Z_{n+k} = L^3 g^{(h)}(Z_n, \mu) + (1 - L^3)Z_n \quad (3.6.1)$$

with  $Z_n \in \mathfrak{R}^n$ ,  $n \in Z$ ,  $h \in Z$ ,  $\mu \in \mathfrak{R}$  is a bifurcation parameter and  $0 < L < 1$  is a control parameter. In addition,  $g^{(h)}$  is  $k$ th value of  $g(\cdot)$ . By application of (3.6.1) on system (3.1.3) we get the following system:

$$\begin{cases} p_{n+1} = L^3 \left( \frac{(1+hr)p_n}{1+h\left(\frac{r}{k}p_n + \frac{\alpha z_n}{a+p_n} + m_1 p_n^2 + q_1 E\right)} \right) + (1 - L^3)p_n, \\ z_{n+1} = L^3 \left( \frac{(1+h\frac{\beta p_n}{a+p_n})z_n}{1+h\left(\frac{\rho p_n}{a+p_n} + \delta + m_2 z_n + q_2 E\right)} \right) + (1 - L^3)z_n. \end{cases} \quad (3.6.2)$$

Furthermore, the system (3.6.2) and system (3.1.3) have same constant solutions. Additionally, the jacobian matrix of (3.6.2) about  $(\underline{p}, \underline{z})$  is given as follows:

$$\begin{pmatrix} 1 - \frac{hL^3 p \left( (a-k)r + ekq_1 + p(2r + km_1(2a+3p)) \right)}{k(1+hr)(a+p)} & -\frac{hL^3 \alpha p}{(1+hr)(a+p)} \\ \frac{hL^3 z (-\beta + \delta + \rho + eq_2 + m_2 z)^2}{a(\beta + h\beta\delta - \rho + eh\beta q_2 + h\beta m_2 z)} & \frac{\beta + h\beta\delta - \rho + eh\beta q_2 + h(\beta - L^3\beta + L^3\rho)m_2 z}{\beta + h\beta\delta - \rho + eh\beta q_2 + h\beta m_2 z} \end{pmatrix}. \quad (3.6.3)$$

The following theorem describes the necessary and sufficient condition for local stability of the system (3.6.2) about  $(\underline{p}, \underline{z})$ .

**Theorem 3.6.1.** *The positive constant solution  $(\underline{p}, \underline{z})$  of the system (3.6.2) is stable locally asymptotically  $\iff$  the following inequality holds true.*

$$|Tr| < 1 + Dt < 2,$$

where,  $Tr$  and  $Dt$  are trace and determinant of (3.6.3) respectively.

### 3.6.2 Hybrid technique for chaos control

In this subsection, we apply the hybrid technique [95] on the system (3.1.3) to control the Neimark-Sacker bifurcation. Moreover, this method is used as control strategy by many researchers for controlling the period-doubling bifurcation, Neimark-Sacker bifurcation and chaos under the effects of period-doubling bifurcation (see [100-104]). By application of hybrid method [95] on the system (3.1.3) we get the following system:

$$\begin{cases} p_{n+1} = S_1 \left( \frac{(1+hr)p_n}{1+h\left(\frac{r}{k}p_n + \frac{\alpha z_n}{a+p_n} + m_1 p_n^2 + q_1 E\right)} \right) + (1 - S_1)p_n, \\ z_{n+1} = S_1 \left( \frac{(1+h\frac{\beta p_n}{a+p_n})z_n}{1+h\left(\frac{\rho p_n}{a+p_n} + \delta + m_2 z_n + q_2 E\right)} \right) + (1 - S_1)z_n, \end{cases} \quad (3.6.4)$$

where,  $0 < S_1 < 1$  is a control parameter. Furthermore, the system (3.6.4) and system (3.1.3) have same constant solutions. Additionally, the jacobian matrix of (3.6.4) about  $(\underline{p}, \underline{z})$  is given as follows:

$$\begin{pmatrix} 1 - \frac{hS_1 p((a-k)r + ekq_1 + p(2r + km_1(2a + 3p)))}{k(1+hr)(a+p)} & -\frac{hS_1 \alpha p}{(1+hr)(a+p)} \\ \frac{hS_1 z(-\beta + \delta + \rho + eq_2 + m_2 z)^2}{a(\beta + h\beta\delta - \rho + eh\beta q_2 + h\beta m_2 z)} & \frac{\beta + h\beta\delta - \rho + eh\beta q_2 + h(\beta - S_1\beta + S_1\rho)m_2 z}{\beta + h\beta\delta - \rho + eh\beta q_2 + h\beta m_2 z} \end{pmatrix}. \quad (3.6.5)$$

### 3.7 Numerical simulations

In this section, the numerical study of dynamics of (3.1.3) is provided. Particularly, in this section we will study the existence and direction of Neimark-Sacker bifurcation by using numeric values of parameters.

**Example 3.7.1.** Assume that  $a = 2.0099$ ,  $q_1 = 0.0189$ ,  $q_2 = 1.2994$ ,  $r = 10.5923$ ,  $E = 0.9959$ ,  $k = 1.3997$ ,  $\beta = 98.499$ ,  $\alpha = 2.9999$ ,  $\delta = 0.0384$ ,  $\rho = 10.5842$ ,  $m_1 = 0.6222$ ,  $m_2 = 0.4422$ ,  $p_0 = 0.105348$ ,  $z_0 = 6.8884251$  and  $h \in (0, 1]$ . In this case the extinction equilibrium and non extinction equilibrium for zooplankton population are  $(\underline{x}, 0) = (1.26553, 0)$  and  $(\underline{p}, \underline{z}) = (0.1053484, 6.888425)$  respectively. Then, from system (3.1.3) we have

$$\lim_{n \rightarrow \infty} \sup p_n \leq k = 1.3997,$$

for all  $n \geq 0$ . Then, by using the value  $k = 1.3997$  in second equation of system (3.1.3) we get

$$\lim_{n \rightarrow \infty} \sup z_n \leq \frac{k(\beta - \rho)}{m_2(k + a)} = 81.61590194902372,$$

for all  $n \geq 0$ . Hence, we have  $(0.1053484, 6.888425) \in [0, k] \times \left[0, \frac{k(\beta - \rho)}{m_2(k + a)}\right]$  for  $\beta > \rho$ , which verifies **Theorem 3.2.1**. Additionally, we have

$$f(0) = \frac{a(r - q_1 E)}{\alpha} = 7.084113606170539 > 0$$

and

$$F(0) = \frac{a(\delta + m_2 f(0) + q_2 E)}{(\beta - \rho) - (\delta + m_2 f(0) + q_2 E)} = 0.10754185654404144 > 0.$$

Furthermore, for  $\lambda = 1.3997$  we have  $(\beta - \rho) = 88.34599$  and  $(\delta + m_2 f(\lambda) + q_2 E) = 4.465067496648613$  then  $(\beta - \rho) > (\delta + m_2 f(\lambda) + q_2 E)$  and we get

$$F(\lambda) = \frac{a(\delta + m_2 f(\lambda) + q_2 E)}{(\beta - \rho) - (\delta + m_2 f(\lambda) + q_2 E)} - \lambda = -1.2921581434559586 < 0,$$

where

$$f(\lambda) = -\frac{(a + \lambda)(m_1 r^2 + q_1 E)}{\alpha} = -79.36413532682512 < 0.$$

Moreover, we have

$$F'(\lambda) = -1 + \frac{a(\beta - \rho)(m_2 f'(\lambda))}{((\beta - \rho) - (\delta + m_2 f(\lambda) + q_2 E))^2} = -1.0580185510185083 < 0,$$

where

$$f'(\lambda) = -\frac{(a + \lambda)\left(\frac{r}{k} + 2m_1 \lambda\right)}{\alpha} + \frac{r - \frac{r\lambda}{k} - m_1 \lambda^2 - q_1 E}{\alpha} = -10.993342080620321 < 0,$$

which verifies **Theorem 3.3.1**.

**Example 3.7.2.** Assume that  $a = 2.0099$ ,  $q_1 = 0.0189$ ,  $q_2 = 1.2994$ ,  $r = 10.5923$ ,  $E = 0.9959$ ,  $k = 1.3997$ ,  $\beta = 98.499$ ,  $\alpha = 2.9999$ ,  $\delta = 0.0384$ ,  $\rho = 10.5842$ ,  $m_1 = 0.6222$ ,  $m_2 = 0.4422$ ,  $p_0 = 0.105348$ ,  $z_0 = 6.8884251$  and  $h \in (0, 1]$ . Then, the mathematical system (3.1.3) takes the following form:

$$\begin{cases} p_{n+1} = \frac{(1+10.5923h)p_n}{1+h\left(\frac{10.5923}{1.3997}p_n + \frac{2.9999z_n}{2.0099+p_n} + 0.6222p_n^2 + 0.0188\right)}, \\ z_{n+1} = \frac{(1+h\frac{98.499p_n}{2.0099+p_n})z_n}{1+h\left(\frac{10.5842p_n}{2.0099+p_n} + 0.0384 + 0.4422z_n + 1.2941\right)}. \end{cases} \quad (3.7.1)$$

Additionally, in this case the extinction equilibrium and non extinction equilibrium for zooplankton population are  $(\underline{x}, 0) = (1.26553, 0)$  and  $(\underline{p}, \underline{z}) = (0.1053484, 6.888425)$  respectively. In this case the graphical behavior of both population variables is shown in **Figure 3.2**. In addition, **Figure 3.2c** represent the maximum Lyapunov exponent for system (3.7.1). In **Figure 3.3** some phase portraits are given for variation of  $h$  in  $(0, 1]$ . Hence, it can be easily seen that there exists the Neimark-Sacker bifurcation when  $h$  certainly passes through  $h = 0.38022$  (see **Figure 3.3b**). For aforementioned values of parameters, the jacobian matrix  $V_2(\underline{p}, \underline{z})$  for system (3.7.1) is given as follows:

$$V_2(0.1053484433, 6.88842511) = \begin{pmatrix} 0.9751639697174742 & -0.01143564868241927 \\ 36.869495419357726 & 0.5871690414953413 \end{pmatrix}.$$

The characteristic equation  $M(\xi) = 0$  for  $V_2(0.1053484433, 6.88842511)$  is

$$\xi^2 - 1.8038899298174336\xi + 1 = 0. \quad (3.7.2)$$

On solving (3.7.2) one can get  $\xi_1 = 0.7811665056064 + 0.6196705420078i$  and  $\xi_2 = 0.7811665056064 - 0.6196705420078i$  with  $|\xi_1| = |\xi_2| = 1$ . In addition, we have

$$\mathbb{M}(-1) = 3.556545701326458 > 0$$

and

$$\mathbb{M}(1) = 0.43187967890082724 > 0.$$

From (3.5.3) we have

$$\begin{aligned} \check{f}(P, Z) &= 0.105348 + 0.974755 P - 0.0116237 Z - 0.256573 P^2 - 0.099269 PZ \\ &+ 0.001282 Z^2 - 0.142822 P^3 + 0.10288 P^2 Z + 0.010039 PZ^2 \\ &- 0.000141506 Z^3 + O((|P| + |Z|)^4), \end{aligned}$$

and

$$\begin{aligned} \check{g}(P, Z) &= 6.88842 + 0.574993 Z + 37.95688 P - 43.12450 P^2 + 3.450296 PZ \\ &- 0.0354763 Z^2 + 48.99565 P^3 - 2.366456 P^2 Z - 0.1893441 PZ^2 \\ &+ 0.00218884 Z^3 + O((|P| + |Z|)^4). \end{aligned}$$

Finally, when system (3.5.3) is converted into canonical form (3.5.6) then we obtain the following matrix:

$$\begin{bmatrix} \frac{1}{v_{12}} & 0 \\ \frac{\ell - v_{11}}{\wp v_{12}} & -\frac{1}{\wp} \end{bmatrix} = \begin{bmatrix} -0.01143564869 & 0 \\ -0.1939974644 & -0.6196705420078615 \end{bmatrix}$$

with

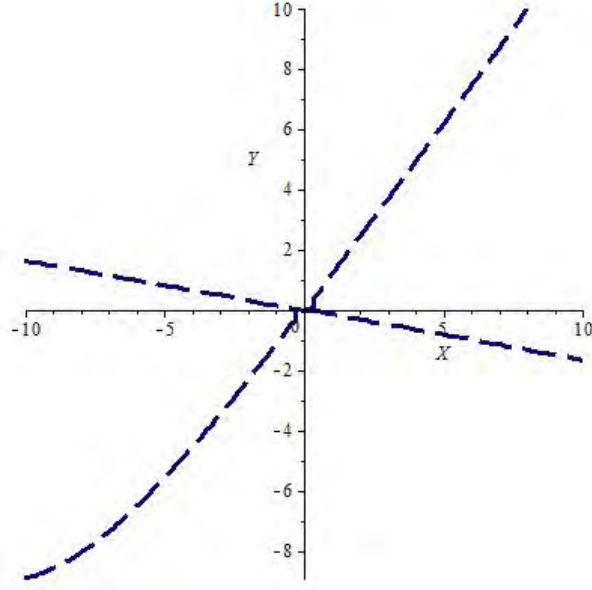
$$\begin{bmatrix} \frac{1}{v_{12}} & 0 \\ \frac{\ell - v_{11}}{\wp v_{12}} & -\frac{1}{\wp} \end{bmatrix}^{-1} = \begin{bmatrix} -87.4458482512197577 & 0.0 \\ 27.3762776879404903 & -1.61376075222132043 \end{bmatrix}.$$

Furthermore, from (3.5.8) we have

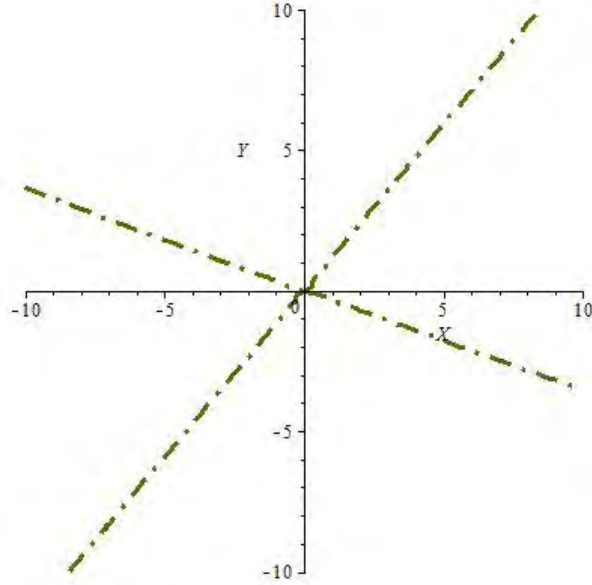
$$\begin{aligned} \check{F}(X, Y) &= 22.073323320819 P^2 + 8.5402951060818 PZ - 0.1103358266003 Z^2 \\ &+ 12.2871550765 P^3 - 8.85102538857 P^2 Z - 0.8636988319698 PZ^2 \\ &+ 0.012173994624 Z^3 + O((|X| + |Y|)^4) \end{aligned}$$

and

$$\begin{aligned} \check{G}(X, Y) &= 61.114564266701 P^2 - 8.141785570023 PZ + 0.0908219975961 Z^2 \\ &- 81.22561954155 P^3 + 6.52880078485 P^2 Z + 0.571452207625 PZ^2 \\ &- 0.0072969596695 Z^3 + O((|X| + |Y|)^4). \end{aligned}$$



(a) Plot for  $\check{F}(X, Y)$ .



(b) Plot for  $\check{G}(X, Y)$ .

Figure 3.1: Plots for  $\check{F}(X, Y)$  and  $\check{G}(X, Y)$  for  $a = 2.0099, q_1 = 0.0189, q_2 = 1.2994, r = 10.5923, E = 0.9959, k = 1.3997, \beta = 98.499, \alpha = 2.9999, \delta = 0.0384, \rho = 10.5842, m_1 = 0.6222, m_2 = 0.4422$  and  $h \in (0, 1]$

Additionally, plots for  $\check{F}(X, Y)$  and  $\check{G}(X, Y)$  with solution at  $(0, 0)$  are represented in **Figure 3.1a** and **Figure 3.1b** respectively. where  $P = (-0.1162370758)X$  and  $Z = (-0.1998810610)X - (0.6334408575)Y$ . Finally, we get

$$\theta_{20} = \frac{1}{8} \left[ \check{F}_{XX} + i \left( \check{G}_{XX} - \check{G}_{YY} - 2\check{F}_{XY} \right) - \check{F}_{YY} + 2\check{G}_{XY} \right] = 0.005831 - 0.019066i,$$

$$\begin{aligned}\theta_{11} &= \frac{1}{4} \left[ i \left( \check{G}_{XX} + \check{G}_{YY} \right) + \check{F}_{YY} + \check{F}_{XX} \right] = -0.01195 + 0.013959i, \\ \theta_{02} &= \frac{1}{8} \left[ i \left( \check{G}_{XX} - \check{G}_{YY} + 2\check{F}_{XY} \right) - \check{F}_{YY} + \check{F}_{XX} - 2\check{G}_{XY} \right] = 0.02389 - 0.00182i, \\ \theta_{21} &= \frac{i}{16} \left( \check{G}_{XYY} + \check{G}_{XXX} - \check{F}_{XXY} - \check{F}_{YY} \right) \\ &\quad + \frac{1}{16} \left( \check{F}_{XXX} + \check{F}_{XYY} + \check{G}_{XXY} + \check{G}_{YY} \right) = 0.00755 + 0.00574i.\end{aligned}$$

and

$$\begin{aligned}\Omega &= \left( \left[ -Re \left( \frac{(1-2\xi_1)\xi_2^2}{1-\xi_1} \theta_{20}\theta_{11} \right) - \frac{1}{2} |\theta_{11}|^2 - |\theta_{02}|^2 + Re(\xi_2\theta_{21}) \right] \right)_{\hat{h}=0} \\ &= -0.00138464412 < 0.\end{aligned}$$

Hence, the condition for existence of Neimark-Sacker bifurcation is satisfied ( see **Theorem 3.5.1**).

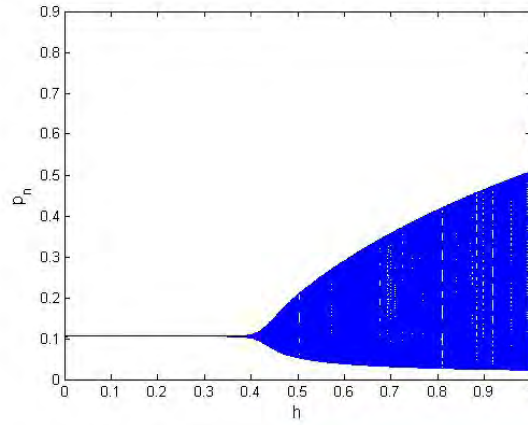
**Example 3.7.3.** This example is related to the study of control of Neimark-Sacker bifurcation by using generalized hybrid technique (3.6.1). To show effectiveness of generalized technique we have used the values of parameters same as we have used in **Example 3.7.1**. Consider the following systems of difference equations

$$\begin{cases} p_{n+1} = L^3 \left( \frac{(1+10.5923h)p_n}{1+h \left( \frac{10.5923}{1.3997} p_n + \frac{2.9999z_n}{2.0099+p_n} + 0.6222p_n^2 + 0.0188 \right)} \right) + (1-L^3)p_n, \\ z_{n+1} = L^3 \left( \frac{(1+h \frac{98.499p_n}{2.0099+p_n})z_n}{1+h \left( \frac{10.5842p_n}{2.0099+p_n} + 0.0384 + 0.4422z_n + 1.2941 \right)} \right) + (1-L^3)z_n. \end{cases} \quad (3.7.3)$$

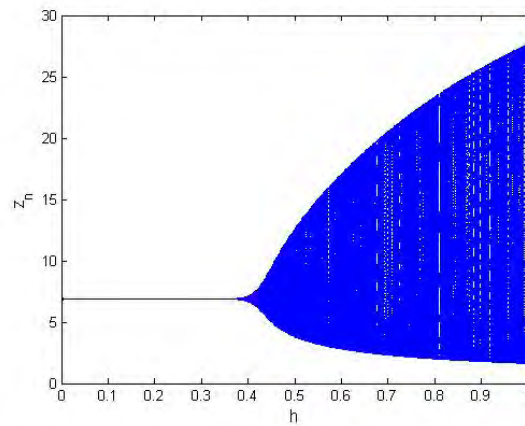
where  $a = 2.0099$ ,  $q_1 = 0.0189$ ,  $q_2 = 1.2994$ ,  $r = 10.5923$ ,  $E = 0.9959$ ,  $k = 1.3997$ ,  $\beta = 98.499$ ,  $\alpha = 2.9999$ ,  $\delta = 0.0384$ ,  $\rho = 10.5842$ ,  $m_1 = 0.6222$ ,  $m_2 = 0.4422$ ,  $h = 0.699909$ . In addition,  $0 < L < 1$  is the control parameter. Furthermore, for system (3.7.3) we have  $(\underline{p}, \underline{z}) = (0.1053484433, 6.88842511)$ , which is unique positive constant solution of original system (3.1.3). Additionally, controlled diagrams for zooplankton and phytoplankton populations by using models (3.7.3) respectively shown in **Figure 3.4b** and **Figure 3.4a**. Finally, it can be seen that the stability of initial system (3.1.3) is victoriously regained for large range of control parameter by using generalized hybrid control method (see **Figure 3.4**).

**Example 3.7.4.** This example is related to the study of control of Neimark-Sacker bifurcation by using hybrid technique [95] of control. Consider the following systems of difference equations

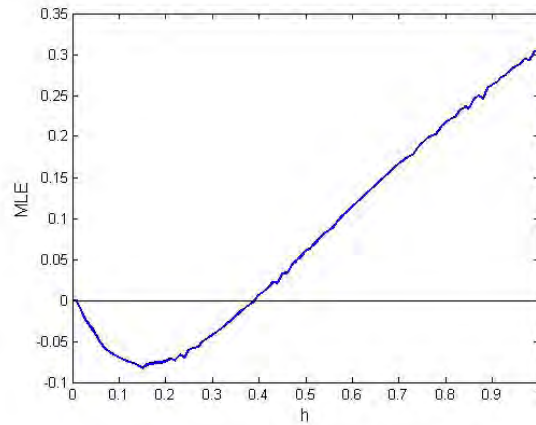
$$\begin{cases} p_{n+1} = S_1 \left( \frac{(1+10.5923h)p_n}{1+h \left( \frac{10.5923}{1.3997} p_n + \frac{2.9999z_n}{2.0099+p_n} + 0.6222p_n^2 + 0.0188 \right)} \right) + (1-S_1)p_n, \\ z_{n+1} = S_1 \left( \frac{(1+h \frac{98.499p_n}{2.0099+p_n})z_n}{1+h \left( \frac{10.5842p_n}{2.0099+p_n} + 0.0384 + 0.4422z_n + 1.2941 \right)} \right) + (1-S_1)z_n. \end{cases} \quad (3.7.4)$$



(a) Bifurcation diagram for  $p_n$ .

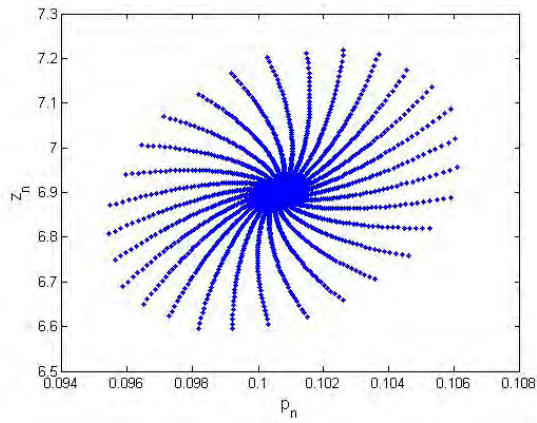


(b) Bifurcation diagram for  $z_n$ .

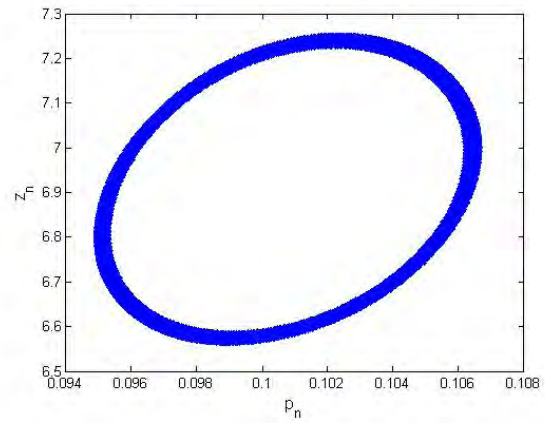


(c) MLE for system (3.1.3).

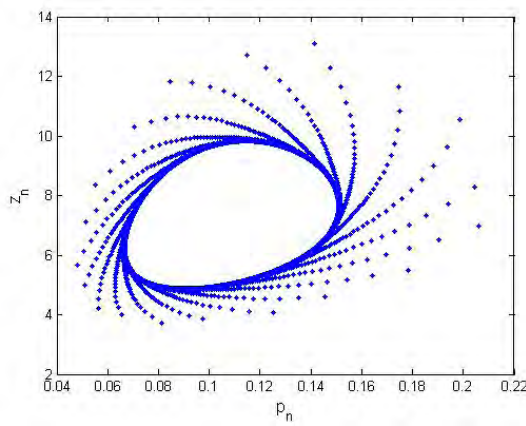
Figure 3.2: Plots of system (3.1.3) for  $a = 2.0099, q_1 = 0.0189, q_2 = 1.2994, r = 10.5923, E = 0.9959, k = 1.3997, \beta = 98.499, \alpha = 2.9999, \delta = 0.0384, \rho = 10.5842, m_1 = 0.6222, m_2 = 0.4422$  and  $h \in (0, 1)$



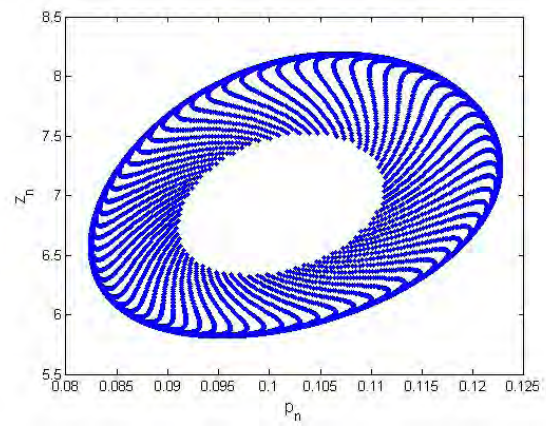
(a)



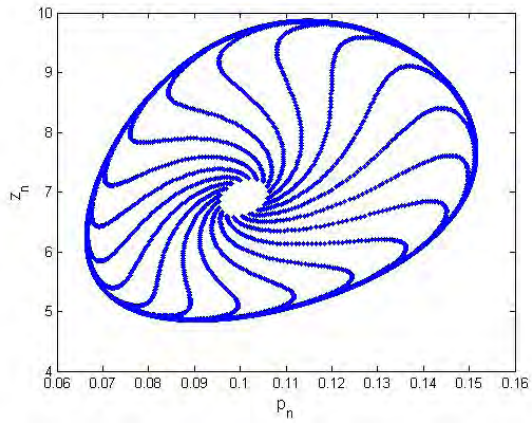
(b)



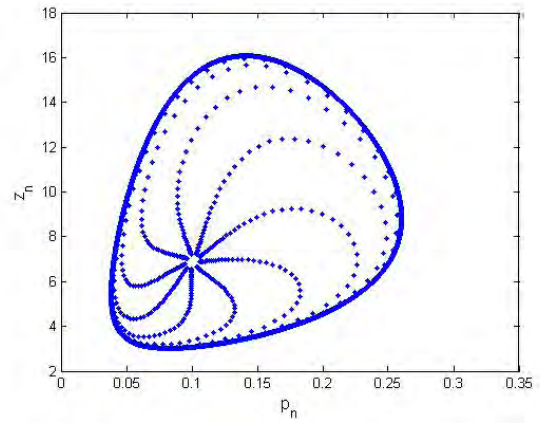
(c)



(d)



(e)



(f)

Figure 3.3: Phase portraits of system (3.1.3) for  $a = 2.0099$ ,  $q_1 = 0.0189$ ,  $q_2 = 1.2994$ ,  $r = 10.5923$ ,  $E = 0.9959$ ,  $k = 1.3997$ ,  $\beta = 98.499$ ,  $\alpha = 2.9999$ ,  $\delta = 0.0384$ ,  $\rho = 10.5842$ ,  $m_1 = 0.6222$ ,  $m_2 = 0.4422$  and  $h \in (0, 1]$



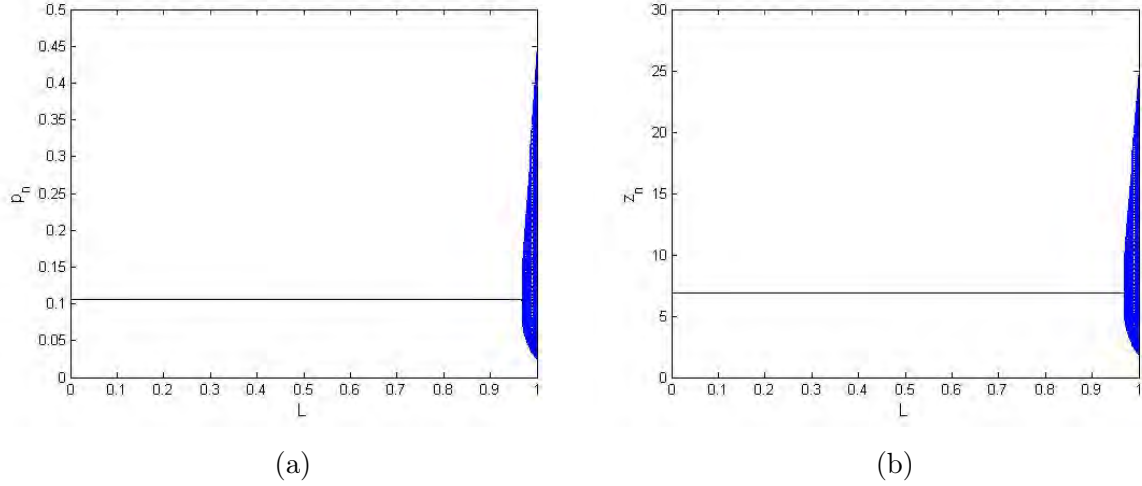


Figure 3.4: Controlled diagrams for system (3.7.3) for  $a = 2.0099, q_1 = 0.0189, q_2 = 1.2994, r = 10.5923, E = 0.9959, k = 1.3997, \beta = 98.499, \alpha = 2.9999, \delta = 0.0384, \rho = 10.5842, m_1 = 0.6222, m_2 = 0.4422, h = 0.699909$  and  $L \in (0, 1]$

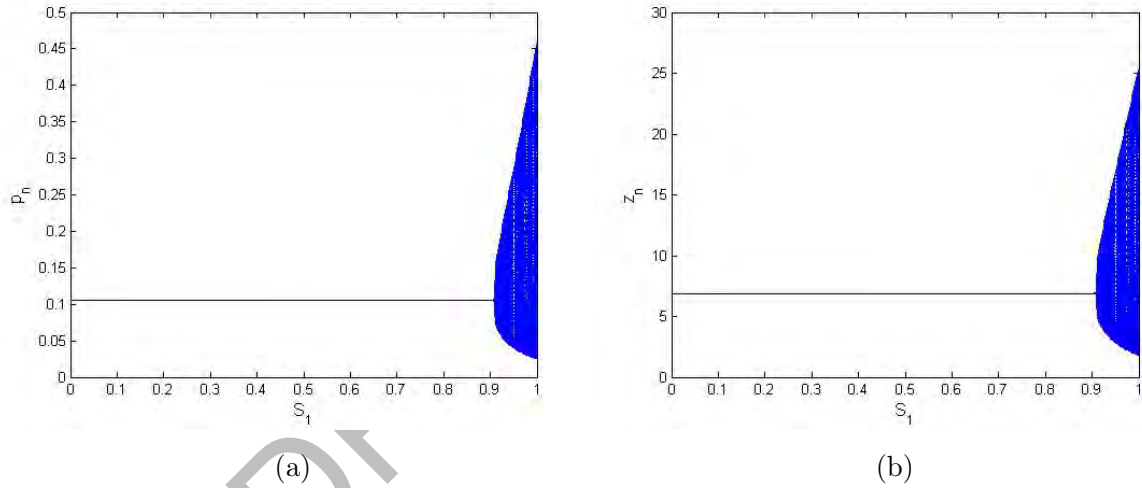


Figure 3.5: Controlled diagrams for system (3.7.4) for  $a = 2.0099, q_1 = 0.0189, q_2 = 1.2994, r = 10.5923, E = 0.9959, k = 1.3997, \beta = 98.499, \alpha = 2.9999, \delta = 0.0384, \rho = 10.5842, m_1 = 0.6222, m_2 = 0.4422, h = 0.699909$  and  $S_1 \in (0, 1)$

where  $a = 2.0099, q_1 = 0.0189, q_2 = 1.2994, r = 10.5923, E = 0.9959, k = 1.3997, \beta = 98.499, \alpha = 2.9999, \delta = 0.0384, \rho = 10.5842, m_1 = 0.6222, m_2 = 0.4422, h = 0.699909$ . In addition,  $0 < S_1 < 1$  is the control parameter. Furthermore, for system (3.7.4) we have  $(\underline{p}, \underline{z}) = (0.1053484433, 6.88842511)$ , which is unique positive constant solution of original system (3.1.3). Additionally, controlled diagrams for zooplankton and phytoplankton populations for system (3.7.4) are respectively shown in **Figure 3.5b** and **Figure 3.5a**.

Table 3.1: Comparison between modified hybrid method (3.6.1) and hybrid method [95] for  $L, S_1 \in (0, 1]$  and  $a = 2.0099, q_1 = 0.0189, q_2 = 1.2994, r = 10.5923, E = 0.9959, k = 1.3997, \beta = 98.499, \alpha = 2.9999, \delta = 0.0384, \rho = 10.5842, m_1 = 0.6222, m_2 = 0.4422, h \in (0, 1]$

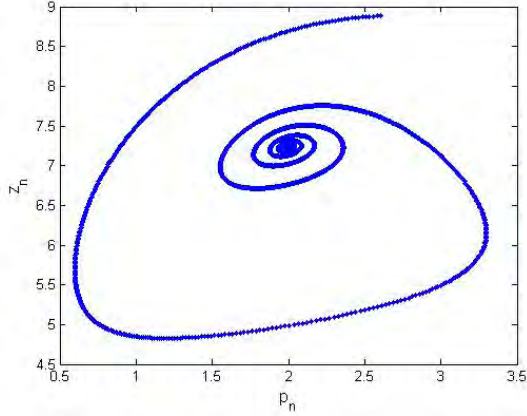
$h \in (0, 1]$	Controlled interval $I_1$ for (3.7.3)	Controlled interval $I_2$ for (3.7.4)
0.48889569	$0 < L < 0.99288325491279$	$0 < S_1 < 0.97880134847096$
0.58889569	$0 < L < 0.983282763587931$	$0 < S_1 < 0.95068201684448$
0.68889569	$0 < L < 0.97635403882826$	$0 < S_1 < 0.93072628972275$
0.78889569	$0 < L < 0.97111704728074$	$0 < S_1 < 0.91582972183557$
0.88889569	$0 < L < 0.96701917628990$	$0 < S_1 < 0.90428485868004$
0.98889569	$0 < L < 0.96372500134675$	$0 < S_1 < 0.89507489723917$

**Example 3.7.5.** In this example a comparison between generalized hybrid method and hybrid method [95] is given. From **Example 3.7.3**, and **Example 3.7.4** we have considered two discrete-time mathematical models (3.7.3) and (3.7.4) respectively. Moreover, in this case we have taken  $L, S_1 \in (0, 1]$  and  $a = 2.0099, q_1 = 0.0189, q_2 = 1.2994, r = 10.5923, E = 0.9959, k = 1.3997, \beta = 98.499, \alpha = 2.9999, \delta = 0.0384, \rho = 10.5842, m_1 = 0.6222, m_2 = 0.4422, h \in (0, 1]$ .

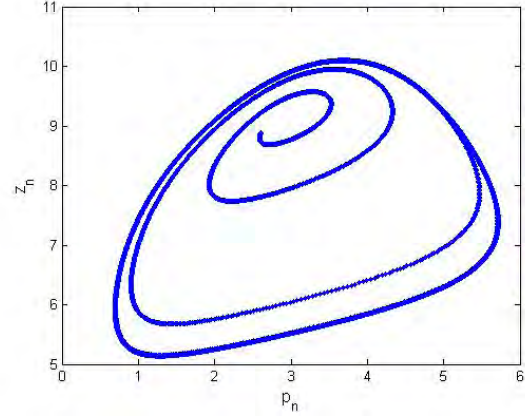
Form both systems (3.7.3) and (3.7.4) we get  $(\underline{p}, \underline{z}) = (0.1053484433, 6.88842511)$  as unique positive fixed point. Additionally, from **Table 3.1** one can observe that  $|I_1| > |I_2|$  for each variation of parameter  $h$  in  $(0, 1]$ . Where  $I_1$  and  $I_2$  are controlled intervals corresponding to controlled systems (3.7.3) and (3.7.4), respectively. Hence, it can be seen from **Table 3.1** that generalized hybrid method (3.6.1) is much better than the old hybrid method [95].

**Example 3.7.6.** In this example, we study a comparison between the dynamics of system (3.0.3) and (3.1.3). For case (i) we take  $a = 2.1, q_1 = 0.09, q_2 = 0.3, r = 1.5, c = 0.14, k = 100, \beta = 0.5, \alpha = 0.69, \delta = 0.001, \rho = 0.1, m_2 = 0.021$  and  $m_1 = 0.06$ , then we get the fixed point  $(\underline{p}, \underline{z}) = (2.3059, 7.38854)$  which is unique positive constant solution of (3.0.3) and (3.1.3). Moreover, for initial conditions  $p_0 = 2.3059$  and  $z_0 = 7.38854$ , **Figure 3.6a** and **Figure 3.7b** are plotted for system (3.1.3) and (3.0.3) respectively. Consequently, it can be seen that system (3.1.3) and (3.0.3) are stable at  $(\underline{p}, \underline{z}) = (2.3059, 7.38854)$ , for  $m_1 = 0.06$  (see **Figure 3.6a** and **Figure 3.7b**). In addition, for case (ii) we take  $m_1 = 0.025$  and  $a = 2.1, q_1 = 0.09, q_2 = 0.3, r = 1.5, c = 0.14, k = 100, \beta = 0.5, \alpha = 0.69, \delta = 0.001, \rho = 0.1, m_2 = 0.021$ , we get the fixed point  $(\underline{p}, \underline{z}) = (2.8059, 8.8854)$  which is unique positive constant solution of (3.0.3) and (3.1.3). Hence, it can be seen that both systems (3.0.3) and (3.1.3) are unstable at  $(\underline{p}, \underline{z}) = (2.8059, 8.8854)$  (see **Figure 3.6b** and **Figure 3.7a**). Finally, **Figure 3.6c** and **Figure 3.6d** shows the existence of Neimark-

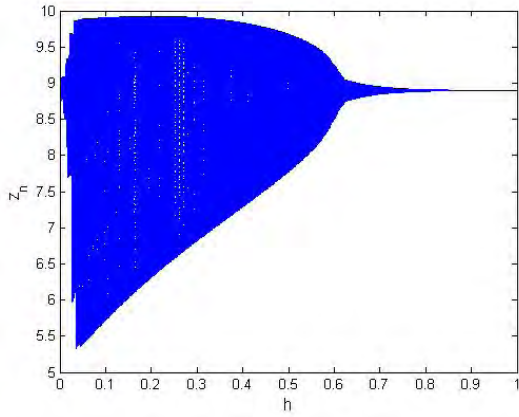
Sacker bifurcation in system (3.1.3) for lower values of step-size  $h$ . Additionally, **Figure 3.7c** and **Figure 3.7d** shows that both variables  $p(t)$  and  $z(t)$  from system (3.0.3) are unstable at  $(\underline{p}, \underline{z}) = (2.8059, 8.8854)$  (see [82]).



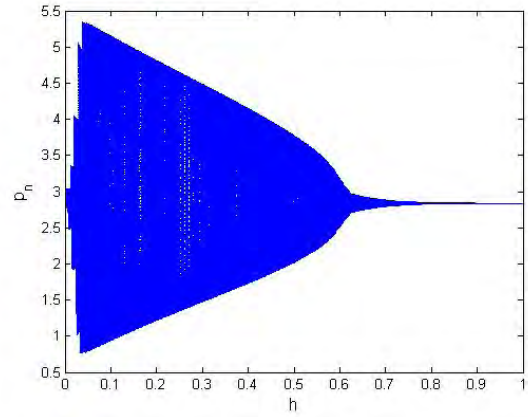
(a) Phase portrait for  $m_1 = 0.06$



(b) Phase portrait for  $m_1 = 0.025$



(c) Bifurcation diagram for  $m_1 = 0.025$

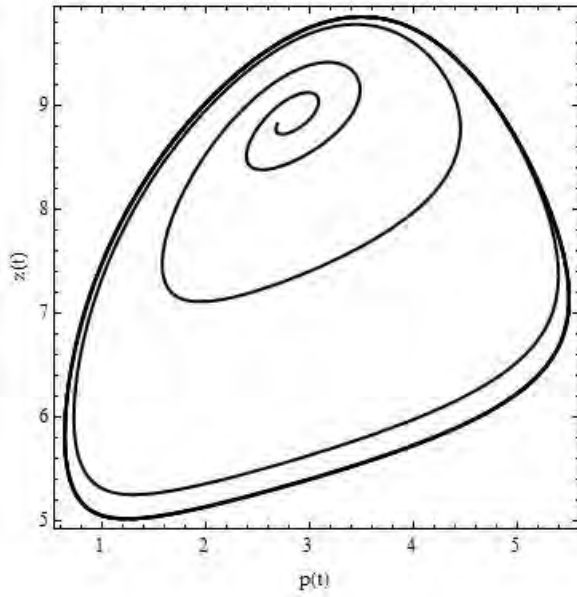


(d) Bifurcation diagram for  $m_1 = 0.025$

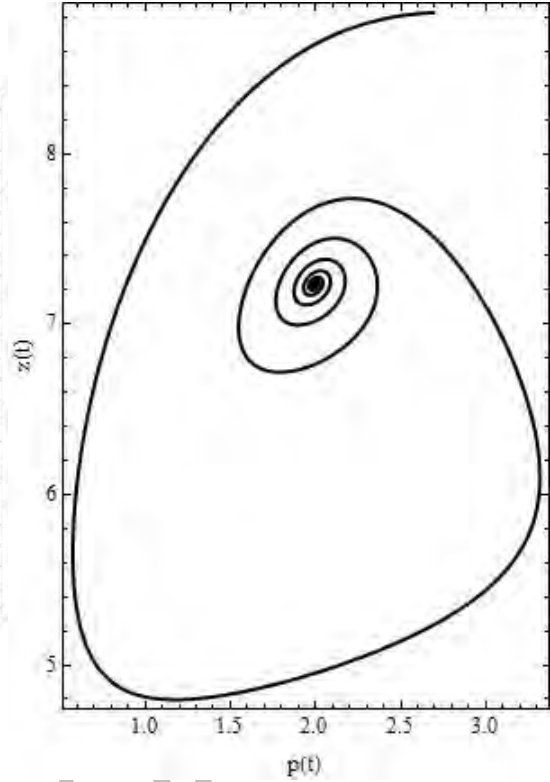
Figure 3.6: Bifurcation diagrams and phase portraits for system (3.1.3) for  $a = 2.1, q_1 = 0.09, q_2 = 0.3, r = 1.5, c = 0.14, k = 100, \beta = 0.5, \alpha = 0.69, \delta = 0.001, \rho = 0.1, m_2 = 0.021$  and  $h = 0.0399909$

### 3.8 Concluding remarks

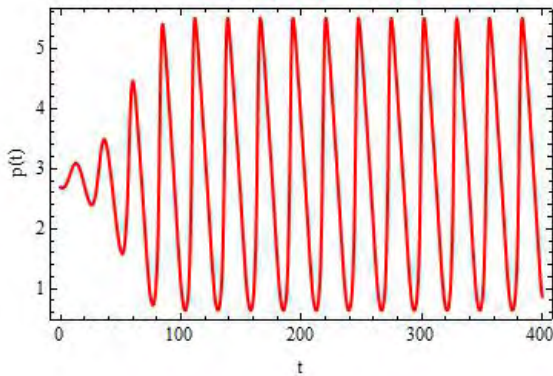
We study the dynamics of a discrete-time phytoplankton-zooplankton model [82]. Firstly, by implementing nonstandard difference scheme we obtained a discrete-time version of the model presented in [82]. It is proved that each solution of system (3.1.3) is bounded and contained in a rectangular region (see **Theorem 3.2.1**). Moreover, it is shown that there exist a unique positive fixed point of system (3.1.3) which is contained in that rectangular region (see **Theorem 3.3.1**). In addition, local stability of system (3.1.3) about each



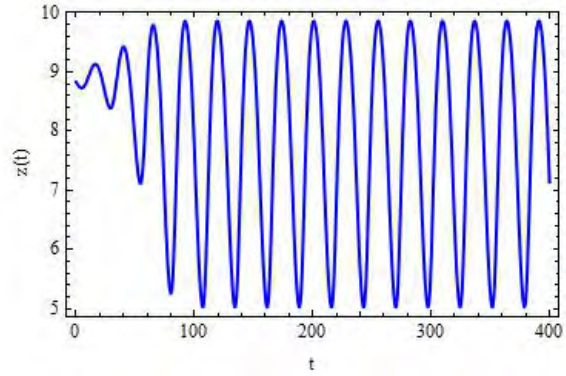
(a) Phase portrait for  $m_1 = 0.025$



(b) Phase portrait for  $m_1 = 0.06$



(c) Plot of  $p(t)$  for  $m_1 = 0.025$



(d) Plot of  $z(t)$  for  $m_1 = 0.025$

Figure 3.7: Plots and phase portraits for system (3.0.3) for  $a = 2.1, q_1 = 0.09, q_2 = 0.3, r = 1.5, c = 0.14, k = 100, \beta = 0.5, \alpha = 0.69, \delta = 0.001, \rho = 0.1$  and  $m_2 = 0.021$ .

of its fixed point is discussed. To prove complexity in mathematical system (3.1.3), the existence of Neimark-Sacker bifurcation for unique positive fixed point is shown mathematically. Neimark-Sacker bifurcation is effectively controlled by using two different methods, namely, generalized hybrid control method and hybrid control method [95]. In order to verify our theoretical investigations, a comprehensive numerical simulation is provided at the end of chapter. In **Example 3.7.2** the numeric validation of **Theorem**

**3.2.1** and **Theorem 3.3.1** is provided. It is numerically and graphically shown that system (3.1.3) experiences the Neimark-Sacker bifurcation for large range of step-size  $h$ . In addition, two examples are provided related to the control of Neimark-Sacker bifurcation. In order to provide a clearer understanding of our theoretical findings and to compare the dynamics between the discrete-time model (5.1.3) and its continuous counterpart (3.0.2), we present a set of numerical examples. Additionally, we conduct a numerical study, specifically in **Example 3.7.6**, where we observe that the obtained system (5.1.3) and its continuous-time counterpart (3.0.2) exhibit stability for the same parameter values, and conversely, they demonstrate instability for corresponding parametric values. This numerical analysis serves as additional evidence to support the observed dynamical consistency in our derived system (5.1.3). For the study of both cases in **Example 3.7.6**, the parametric values are taken from [82]. It is shown that system (3.0.3) and (3.1.3) are stable for the values of  $m_1$  greater than or equal to  $m_1 = 0.06$  and these systems are unstable whenever  $m_1 < 0.06$ . In addition, our numerical study showed that the generalized hybrid method (3.6.1) is superior then hybrid method [95]. In addition, it is based on feedback control and it has brought back the stability of system (3.1.3) for large ranges of parameters. Moreover, from numerical study can be seen that the generalized hybrid method (3.6.1) is suitable for controlling the Neimark-Sacker bifurcation. At last, a comparison between generalized hybrid method (3.6.1) and hybrid method [95] is provided in **Table 3.1**. Moreover, from **Figure 3.4**, **Figure 3.5** and **Table 3.1** it can be seen that the generalized hybrid control technique have restored the stability of the system (3.1.3) for maximum range of control parameter.

## Chapter 4

# Bifurcation Analysis of a Discrete-Time Compartmental Model for Hypertensive or Diabetic Patients Exposed to COVID-19

Here, we consider a continuous-time model for COVID-19 transmission. We consider three mutually exclusive classes, namely, susceptible class (A): which is tested for diabetes or hypertension, exposed class (B), and quarantined class (C). Moreover, all parametric values related to our mathematical system are provided in **Table 4.1**. The findings of this chapter are published in a top-quality international journal (see [18]). Under these considerations, we have the following model

$$\begin{aligned}A'(t) &= KA(t) - \delta_1 A(t)B(t) - \frac{\delta_2 A(t)B(t)}{\alpha + A(t)} - \frac{\delta_4 A(t)C(t)}{b + A(t)} - dA^2(t), \\B'(t) &= \delta_1 A(t)B(t) + \frac{\beta_2 A(t)B(t)}{\alpha + A(t)} - \frac{\delta_3 B(t)C(t)}{\gamma + B(t)} - dB(t), \\C'(t) &= \frac{r_1 \delta_3 C(t)B(t)}{\gamma + B(t)} + \frac{r_2 \delta_4 A(t)C(t)}{\beta + A(t)} - dC(t),\end{aligned}\tag{4.0.1}$$

with,  $A \geq 0$ ,  $B \geq 0$ , and  $C \geq 0$ . Here, parameter  $K$  represents the birth rate for a new individual. In addition, the death rate for each individual in their particular class is represented by a uniform rate parameter  $d$ .  $\frac{\delta_2 AB}{\alpha + A}$  represents the saturated rate where  $\alpha$  is the constant of saturation, and  $\delta_2$  is the infection force, as shown in the following flow diagram:

Notations	Clarification	Parametric values	
$K$	Birth rate	$+ve$	Assumed
$\delta_1$	Transmission rate of individuals from $A \rightarrow B$	0.9	Calculated
$\delta_2$	Infection rate	0.001	Assumed
$\delta_3$	Rate at which exposed persons get quarantined	0.80	Calculated
$\delta_4$	Rate at which susceptible persons get quarantined	0.60	Calculated
$\alpha, \beta, \gamma$	Half-saturation constants	2, 10, 0.4	Assumed
$r_1, r_2$	Conversion efficiency	1, 2	Assumed

Table 4.1: Definitions of parameters and their respective values

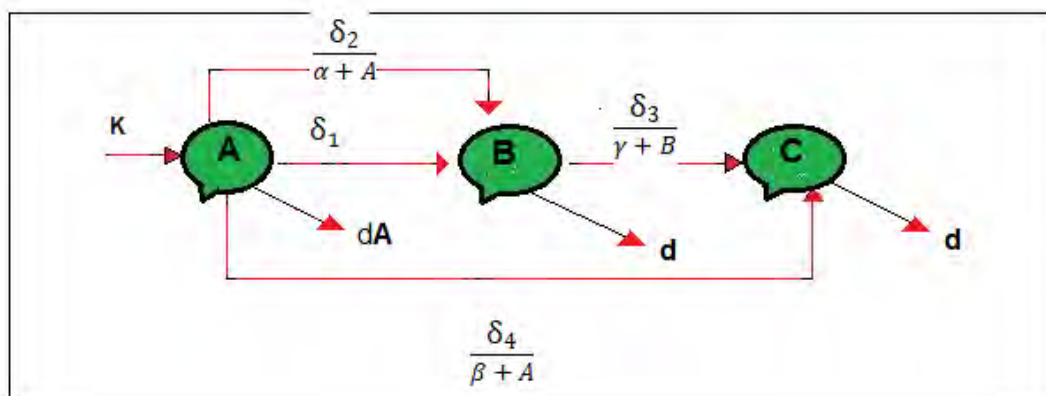


Figure 4.1: Flow diagram representing the shifting of any individual from one class to other class.

The study conducted in [101] examines the qualitative behavior of model (4.0.1) through the application of the Z-control technique for chaos control. Furthermore, the authors delve into the exploration of various foundational models related to Z-control. These include a comprehensive model proposed by Samanta [96] and a prey-predator model investigated by Alzahrani et al. [97].

## 4.1 Discretization of model

In [98], the authors have explained that Euler's forward method is not appropriate for discretizing every continuous-time dynamical system. Moreover, it violates the consistency of the original model, and different types of bifurcations occur for the maximum

range of the step-size parameter. Hence, a different discretization technique must be required to eliminate this lack, which is as follows: Supposing that the ordinary evolution rates in every compartment vary at the fixed lag of time. Then by using the technique of piecewise constant arguments (see [99]) for differential equations, system (4.0.1) can be written as:

$$\begin{aligned}\frac{1}{A(t)}A'(t) &= K - \delta_1 B(t) - \frac{\delta_2 B(t)}{\alpha + A(t)} - \frac{\delta_4 C(t)}{b + A(t)} - dA(t), \\ \frac{1}{B(t)}B'(t) &= \delta_1 A(t) + \frac{\beta_2 A(t)}{\alpha + A(t)} - \frac{\delta_3 C(t)}{\gamma + B(t)} - d, \\ \frac{1}{C(t)}C'(t) &= \frac{r_1 \delta_3 B(t)}{\gamma + B(t)} + \frac{r_2 \delta_4 A(t)}{\beta + A(t)} - d,\end{aligned}\tag{4.1.1}$$

with  $[t]$  as integer part of  $t$  and  $t \in (0, 1)$ . In addition, by taking integration of system (4.1.1) on  $[m, m + 1)$  with  $m \in \mathbb{W}$  one have the following system:

$$\begin{aligned}A(t) &= A_m e^{[K - \delta_1 B_m - \frac{\delta_2 B_m}{\alpha + A_m} - \frac{\delta_4 C_m}{b + A_m} - dA_m](t-m)}, \\ B(t) &= B_m e^{[\delta_1 A_m + \frac{\beta_2 A_m}{\alpha + A_m} - \frac{\delta_3 C_m}{\gamma + B_m} - d](t-m)}, \\ C(t) &= C_m e^{[\frac{r_1 \delta_3 B_m}{\gamma + B_m} + \frac{r_2 \delta_4 A_m}{\beta + A_m} - d](t-m)}.\end{aligned}\tag{4.1.2}$$

Formally, by taking limit  $t \rightarrow m + 1$ , we have the next from of system (4.1.2):

$$\begin{aligned}A_{m+1} &= A_m e^{K - \delta_1 B_m - \frac{\delta_2 B_m}{\alpha + A_m} - \frac{\delta_4 C_m}{b + A_m} - dA_m}, \\ B_{m+1} &= B_m e^{\delta_1 A_m + \frac{\beta_2 A_m}{\alpha + A_m} - \frac{\delta_3 C_m}{\gamma + B_m} - d}, \\ C_{m+1} &= C_m e^{\frac{r_1 \delta_3 B_m}{\gamma + B_m} + \frac{r_2 \delta_4 A_m}{\beta + A_m} - d}.\end{aligned}\tag{4.1.3}$$

## 4.2 Boundedness of solutions

This section focuses on proving the boundedness of all positive solutions  $(A_m, B_m, C_m)$ . To achieve this goal, we introduce the following lemma.

**Lemma 4.2.1.** *Each solution  $(A_m, B_m, C_m)$  of the system (4.1.3) is uniformly bounded, whenever for any finite  $\Upsilon \in \mathfrak{R}$ , we take*

$$\lim_{m \rightarrow \infty} \sup B_m \leq \Upsilon.$$

*Proof.* Let  $A_0 > 0$ ,  $B_0 > 0$  and  $C_0 > 0$  then every solution  $(A_m, B_m, C_m)$  of mathematical system (4.1.3) fulfills  $A_m > 0$ ,  $B_m > 0$  and  $C_m > 0$  for every  $m \geq 0$ . Primarily, from



leading equation of the system (4.1.3) one can write

$$\begin{aligned}
A_{m+1} &= A_m \exp\left(K - \delta_1 B_m - \frac{\delta_2 B_m}{\alpha + A_m} - \frac{\delta_4 C_m}{\beta + A_m} - dA_m\right) \\
&\leq A_m \exp\left(K - \delta_1 B_m - \frac{\delta_2 B_m}{\alpha + A_m} - dA_m\right) \\
&\leq A_m \exp(K - dA_m) \\
&= A_m \exp\left(K\left(1 - \frac{d}{K}A_m\right)\right).
\end{aligned}$$

Then, by using **Lemma 1.2.2** we have

$$\lim_{m \rightarrow \infty} \sup A_m \leq \frac{1}{d} \exp(K - 1) = F(\text{say}).$$

From last equation of the system (4.1.3) we get

$$\begin{aligned}
C_{m+1} &= C_m \exp\left(\frac{r_1 \delta_3 B_m}{\gamma + B_m} + \frac{r_2 \delta_4 A_m}{\beta + A_m} - d\right) \\
&\leq C_m \exp\left(\frac{r_1 \delta_3}{\gamma + \Upsilon} + \frac{r_2 \delta_4 (K - \delta_1 \Upsilon - \frac{\delta_2 \Upsilon}{\alpha + F} - \frac{\delta_4 C_m}{\beta + F})}{d\beta}\right) \\
&\leq C_m \exp\left(\frac{r_1 \delta_3 \Upsilon}{\gamma + \Upsilon} + \frac{r_2 \delta_4 K}{d\beta} - \frac{r_2 \delta_4^2 K}{d\beta(\beta + F)} C_m\right) \\
&= C_m \exp\left(\frac{(dK\beta r_1 \delta_3 + r_2 \delta_4 K(\gamma + \Upsilon))}{d\beta(\gamma + \Upsilon)} \left(1 - \frac{r_2 \delta_4^2 K(\gamma + \Upsilon) C_m}{(\beta + F)(d\Upsilon\beta r_1 \delta_3 + r_2 \delta_4 K(\gamma + \Upsilon))}\right)\right).
\end{aligned}$$

By using **Lemma 1.2.2** we have

$$\lim_{m \rightarrow \infty} \sup C_m \leq \frac{1}{\frac{r_2 \delta_4^2 K}{d\beta(\beta + F)}} \exp\left(\frac{(d\Upsilon\beta r_1 \delta_3 + r_2 \delta_4 K(\gamma + \Upsilon))}{d\beta(\gamma + \Upsilon)} - 1\right).$$

□

By using the method of mathematical induction, one has the following lemma.

**Lemma 4.2.2.** *Let us assume  $0 < A_0 < \frac{1}{d} \exp(K - 1)$ , with  $0 < B_0 < K$  and*

$$0 < C_0 < \frac{1}{\frac{r_2 \delta_4^2 K}{d\beta(\beta + F)}} \exp\left(\frac{(d\Upsilon\beta r_1 \delta_3 + r_2 \delta_4 K(\gamma + \Upsilon))}{d\beta(\gamma + \Upsilon)} - 1\right),$$

*then  $[0, \frac{1}{d} \exp(K - 1)] \times [0, \Upsilon] \times [0, \frac{1}{\frac{r_2 \delta_4^2 K}{d\beta(\beta + F)}} \exp\left(\frac{(d\Upsilon\beta r_1 \delta_3 + r_2 \delta_4 K(\gamma + \Upsilon))}{d\beta(\gamma + \Upsilon)} - 1\right)]$  each result of the system (4.1.3) the form  $(A_m, B_m, C_m)$  is invariant.*

### 4.3 Existence of fixed points

In this part of thesis, we consider fixed points  $(A, B, C)$  of the system (4.1.3), obtained from the following mathematical system:

$$\begin{aligned} A^* &= A^* e^{K - \delta_1 B^* - \frac{\delta_2 B^*}{\alpha + A^*} - \frac{\delta_4 C^*}{b + A^*} - d A^*}, \\ B^* &= B^* e^{\delta_1 A^* + \frac{\beta_2 A^*}{\alpha + A^*} - \frac{\delta_3 C^*}{\gamma + B^*} - d}, \\ C^* &= C^* e^{\frac{r_1 \delta_3 B^*}{\gamma + B^*} + \frac{r_2 \delta_4 A^*}{\beta + A^*} - d}. \end{aligned} \quad (4.3.1)$$

From system (4.3.1) individual can have six fixed points  $(0, 0, 0)$ ,  $(\frac{K}{d}, 0, 0)$ ,  $(0, \frac{\gamma d}{r_1 \delta_3 - d}, \frac{\gamma d r_1}{d - r_1 \delta_3})$ ,  $(\frac{d\beta}{(r_2 \delta_4 - d)}, 0, \frac{\beta r_2 (K r_2 \delta_4 - \beta d^2 - d)}{(r_2 \delta_4 - d)^2})$ ,  $(\bar{A}, \bar{B}, 0)$ , and positive fixed point  $(A^*, B^*, C^*)$ .

**Remark 4.3.1.** *The fixed point  $(0, \frac{\gamma d}{r_1 \delta_3 - d}, \frac{\gamma d r_1}{d - r_1 \delta_3})$  of system (4.1.3) does not exist as for every  $r_1, \delta_3, d > 0$  one of its components from  $\frac{\gamma d}{r_1 \delta_3 - d}$  or  $\frac{\gamma d r_1}{d - r_1 \delta_3}$  becomes negative.*

Assume the following jacobian matrix

$$J = \begin{bmatrix} l_{11} & l_{12} & l_{13} \\ l_{21} & l_{22} & l_{23} \\ l_{31} & l_{32} & l_{33} \end{bmatrix}$$

of system (4.1.3) about  $(A^*, B^*, C^*)$ . Then, from  $J$  in consequence we get

$$\mathbb{G}(\psi) = \psi^3 - S_1 \psi^2 + S_2 \psi - S_3, \quad (4.3.2)$$

with

$$S_1 = (l_{11} + l_{22} + l_{33}),$$

$$S_2 = L_{11} + L_{22} + L_{33},$$

and

$$S_3 = \det(J).$$

Where, the minor determinants  $L_{11}$ ,  $L_{22}$  and  $L_{33}$  are obtained from variational matrix  $J$ . Firstly, we analyze the stability of fixed point  $(0, 0, 0)$ . The variational matrix  $J_1$  for fixed point  $(0, 0, 0)$  is specified as

$$J_1 = \begin{pmatrix} e^K & 0 & 0 \\ 0 & \frac{1}{e^d} & 0 \\ 0 & 0 & \frac{1}{e^d} \end{pmatrix}.$$

Additionally, from  $J_1$  we have  $\psi_1 = e^K$ ,  $\psi_2 = \frac{1}{e^d}$  and  $\psi_3 = \frac{1}{e^d}$ , with  $|\varphi_1| > 1$  and  $|\psi_2| = |\psi_3| < 1$  for all values of parameters. Hence, we have the following result about the stability of  $(0, 0, 0)$ .

**Proposition 4.3.1.** *Assume that  $(0, 0, 0)$  be any fixed point of (4.1.3) then for each value of  $K, d > 0$  it remains unstable.*

Next, we study the stability of system (4.1.3) about  $(\frac{K}{d}, 0, 0)$ . The jacobian matrix  $J_2$  about  $(\frac{K}{d}, 0, 0)$  is specified as:

$$J_2 = \begin{pmatrix} 1 - K & -\frac{K\delta_1}{d} - \frac{K\delta_2}{K+\alpha d} & -\frac{K\delta_4}{K+\beta d} \\ 0 & e^{-d+\frac{K\delta_1}{d}+\frac{K\delta_2}{K+\alpha d}} & 0 \\ 0 & 0 & e^{-d-\frac{Kr_2\delta_4}{K+\beta d}} \end{pmatrix}.$$

Then, from characteristic polynomial  $\mathbb{G}(\psi)$  of  $J_2$  we have three solutions, namely,  $\psi_1 = 1 - K$ ,  $\psi_2 = \frac{1}{e^{d-\frac{K\delta_1}{d}-\frac{K\delta_2}{K+\alpha d}}}$  and  $\psi_3 = \frac{1}{e^{d+\frac{Kr_2\delta_4}{K+\beta d}}}$ . Formally, we conclude the following result.

**Proposition 4.3.2.** *Assuming the fixed point  $(\frac{K}{d}, 0, 0)$  of system (4.1.3) we have;*

- *The point  $(\frac{K}{d}, 0, 0)$  remains stable for  $|\psi_1|, |\psi_2|, |\psi_3| < 1 \iff$   
 $0 < K < 2$  and  $d^2(K + \alpha d) > K(\delta_1(K + \alpha d) + d\delta_2)$ .*
- *The fixed point  $(\frac{K}{d}, 0, 0)$  remains unstable for every  
 $K > 2$ .*

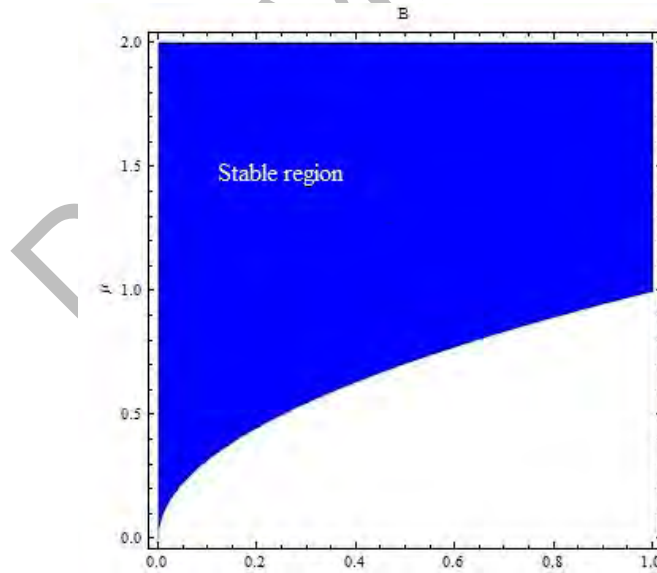


Figure 4.2: Stability region for  $(\frac{K}{d}, 0, 0)$  for  $\alpha = 2, \beta = 10, \delta_1 = 0.99, \gamma = 0.4, \delta_2 = 0.01, \delta_3 = 0.80, \delta_4 = 0.60, r_1 = 1, r_2 = 2, K \in (0, 1), d \in (0, 2)$  with  $A_0 = 0.995, B_0 = 0.38855$  and  $C_0 = 0.3455$ .

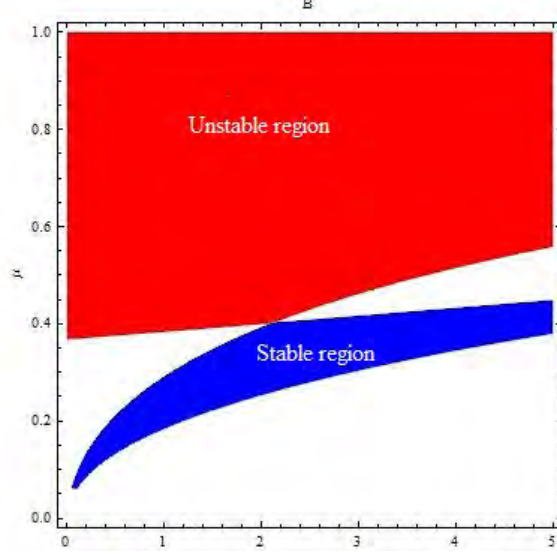


Figure 4.3: Region plot for  $\left(\frac{\beta d}{r_2 \delta_4 - d}, 0, \frac{\beta r_2 (K r_2 \delta_4 - d(K + \beta d))}{(d - r_2 \delta_4)^2}\right)$  for  $\alpha = 2, \beta = 10, \delta_1 = 0.99, \gamma = 0.4, \delta_2 = 0.01, \delta_3 = 0.80, \delta_4 = 0.60, r_1 = 1, r_2 = 2, K \in (0, 1), d \in (0, 2)$  with  $A_0 = 0.995, B_0 = 0.38855$  and  $C_0 = 0.3455$ .

By considering the fixed point  $\left(\frac{\beta d}{r_2 \delta_4 - d}, 0, \frac{\beta r_2 (K r_2 \delta_4 - d(K + \beta d))}{(d - r_2 \delta_4)^2}\right)$  of system (4.1.3) we get the following jacobian matrix:

$$J_3 = \begin{pmatrix} 1 + \frac{d(K + \beta d)}{r_2 \delta_4} + \frac{2\beta d^2}{d - r_2 \delta_4} & \beta d \left( \frac{\delta_1}{d - r_2 \delta_4} + \frac{\delta_2}{\alpha d - \beta d - \alpha r_2 \delta_4} \right) & -\frac{d}{r_2} \\ 0 & e^{-d} \left( \frac{\beta d \delta_1}{-d + r_2 \delta_4} + \frac{\beta d \delta_2}{(\beta - \alpha)d + \alpha r_2 \delta_4} + \frac{\beta r_2 \delta_3 (d(K + \beta d) - K r_2 \delta_4)}{\gamma (d - r_2 \delta_4)^2} \right) & 0 \\ \frac{e^{-2d} (d(K + \beta d) - K r_2 \delta_4)}{\delta_4} & -\frac{\beta e^{-2d} r_1 r_2 \delta_3 (d(K + \beta d) - K r_2 \delta_4)}{\gamma (d - r_2 \delta_4)^2} & e^{-2d} \end{pmatrix}.$$

The roots of  $\mathbb{G}(\tau) = 0$  are

$$\tau_1 = \frac{1}{e^{-d} \frac{\beta d \delta_1}{r_2 \delta_4 - d} - \frac{\beta d \delta_2}{(\beta - \alpha)d + \alpha r_2 \delta_4} - \frac{\beta r_2 \delta_3 (d(K + \beta d) - K r_2 \delta_4)}{\gamma (d - r_2 \delta_4)^2}},$$

$$\tau_2, \tau_3 = \frac{(\alpha_{11} \pm \sqrt{\alpha_{12} + \alpha_{13}})}{e^{2d} 2 r_2 \delta_4 (d - r_2 \delta_4)},$$

where,  $\mathbb{G}(\tau) = 0$  is characteristic equation of  $J_3$  and

$$\begin{cases} \alpha_{11} = e^{2d} d^2 (K + \beta d) + d (1 + e^{2d} (1 - K + \beta d)) r_2 \delta_4 - (1 + e^{2d}) r_2^2 \delta_4^2, \\ \alpha_{12} = (e^{2d} d^2 (K + \beta d) + r_2 \delta_4 (d + e^{2d} d (1 - K + \beta d) - (1 + e^{2d}) r_2 \delta_4))^2, \\ \text{and} \\ \alpha_{13} = (d^2 (1 + d) (K + \beta d) - r_2 \delta_4 (d(K - 1 + 2Kd + \beta(d - 1)d) + (Kd - 1)r_2 \delta_4)) \\ (4e^{2d} r_2 \delta_4 (r_2 \delta_4 - d)). \end{cases} \quad (4.3.3)$$

**Proposition 4.3.3.** Taking the fixed point  $\left(\frac{\beta d}{r_2\delta_4-d}, 0, \frac{\beta r_2(Kr_2\delta_4-d(K+\beta d))}{(d-r_2\delta_4)^2}\right)$  of system (4.3.1) and  $\tau_1, \tau_2$  and  $\tau_3$  as roots of  $J_3$  we find  $\left(\frac{\beta d}{r_2\delta_4-d}, 0, \frac{\beta r_2(Kr_2\delta_4-d(K+\beta d))}{(d-r_2\delta_4)^2}\right)$  stable

$$d > \frac{\beta d \delta_1}{r_2\delta_4 - d} + \frac{\beta d \delta_2}{(\beta - \alpha)d + \alpha r_2\delta_4} + \frac{\beta r_2\delta_3 (d(K + \beta d) - Kr_2\delta_4)}{\gamma (d - r_2\delta_4)^2}$$

and

$$|(\alpha_{11} \pm \sqrt{\alpha_{12} + \alpha_{13}})| < e^{2d} 2r_2\gamma_4 (d - r_2\delta_4)$$

with  $d > r_2\delta_4$  and  $\alpha_{11}, \alpha_{12}$ , and  $\alpha_{13}$  are specified in (4.3.3).

From a biological view, we must have to find a positive result of (4.3.1). Hence, we do care to find at least a positive solution of the system (4.3.1). Formally, from the system (4.3.1), we have

$$B^* = -\gamma \left(1 + \frac{r_1\delta_3(\beta + A^*)}{d(\beta + S^*) + r_2\delta_4 + A^* - r_1\delta_3(\beta + A^*)}\right)$$

and

$$Q^* = \frac{-(\gamma + B^*)}{\delta_3} \left(d - \left(\delta_1 + \frac{\delta_2}{(\alpha + A^*)}\right) A^*\right),$$

such that  $A^*$  is obtained from the cubic equation:

$$h(t) = E_{11}t^3 + F_{11}t^2 + G_{11}t + H_{11}, \quad (4.3.4)$$

with

$$\begin{cases} E_{11} = d(r_1\delta_3 + r_2\delta_4 - d), \\ F_{11} = (K - (\alpha + \beta)d)(d - r_1\delta_3) - (K - \alpha d)r_2\delta_4 + \gamma\delta_1(d + (r_1 - r_2)\delta_4), \\ G_{11} = ((\alpha + \beta)K - \alpha\beta d)(d - r_1\delta_3) - (\gamma dr_1 + \alpha Kr_2)\delta_4 + (d + (r_1 - r_2)\delta_4)\gamma\delta_2 \\ \quad + ((\alpha + \beta)d + \alpha(r_1 - r_2)\delta_4)\gamma\delta_1, \\ H_{11} = (\alpha\beta(K + \gamma\delta_1) + \gamma\beta\delta_3)d - \alpha r_1(\beta K\delta_3 + d\gamma\delta_4). \end{cases} \quad (4.3.5)$$

From **Lemma 1.2.1**, we get the following lemma for presence of the positive real solution of equation  $h(t)$  in (4.3.4).

**Lemma 4.3.1.** There exist one and only positive real root of polynomial  $h(t)$  given in (4.3.4)  $\iff$  one of the following is satisfied: *i.*  $E_{11} < 0, F_{11} < 0, G_{11} < 0, H_{11} > 0$ . *ii.*  $E_{11} < 0, F_{11} > 0, G_{11} > 0, H_{11} > 0$ .

**Lemma 4.3.2.** Assume that  $A^*$  is any solution of (4.3.4). Then, from **Lemma 4.3.1**, one can see that the system (4.0.1) has only one positive solution if conditions

$$r_1\delta_3 + r_2\delta_4 < d < (r_2 - r_1)\delta_4$$

and

$$K < d$$

are satisfied.

*Proof.* The positive fixed point of (4.1.3) satisfies the algebraic equations that are similar to its counterpart in continuous form (see (4.0.1)). For system (4.0.1), the validation is given in [101].  $\square$

## 4.4 Local stability analysis

Consider the variational matrix  $J_4$  of system the (4.1.3) about fixed point  $(A^*, B^*, C^*)$ .

$$J_4 = \begin{pmatrix} 1 + A^* \left( \frac{\delta_2 B^*}{(\alpha + A^*)^2 - d} + \frac{\delta_4 C^*}{(\beta + A^*)^2} \right) & -A^* \left( \delta_1 + \frac{\delta_2}{\alpha + A^*} \right) & -\frac{\delta_4 A^*}{\beta + A^*} \\ \frac{B^* (\alpha \delta_2 + \delta_1 (\alpha + A^*)^2)}{(\alpha + A^*)^2} & \frac{(\gamma + B^*)^2 + \delta_3 B^* C^*}{(\gamma + B^*)^2} & -\frac{\delta_3 B^*}{\gamma + B^*} \\ -\frac{\beta r_2 \delta_4 C^*}{(\beta + A^*)^2} & \frac{\gamma r_1 \delta_3 C^*}{(\gamma + B^*)^2} & 1 \end{pmatrix}. \quad (4.4.1)$$

Moreover, the following theorem offers us an essential condition for all of the solutions of any fundamental equation of degree 3 to have mod one (see, **Theorem 5** from [100]).

**Theorem 4.4.1.** *Let us consider the following third-degree equation*

$$\mathbb{G}(\psi) = \psi^3 - S_1 \psi^2 + S_2 \psi - S_3, \quad (4.4.2)$$

with  $S_1, S_2, S_3 \in \mathfrak{R}$ . Then, every root of (4.4.2) remain in the interior of a unit disk  $\iff$

$$\begin{cases} |S_1 + S_3| < 1 + S_2, \\ |S_1 - 3S_3| < 3 - S_2, \\ S_3^2 + S_2 - S_1 S_3 < 1. \end{cases} \quad (4.4.3)$$

**Theorem 4.4.2.** *The endemic fixed point  $(A^*, B^*, C^*)$  of the dynamical system (4.1.3) is stable locally and asymptotically if we have:*

$$\begin{cases} |S_1 + S_3| < 1 + S_2, \\ |S_1 - 3S_3| < 3 - S_2, \\ S_3^2 + S_2 - S_1 S_3 < 1. \end{cases}$$

where

$$\begin{cases} S_1 = 3 + \frac{\delta_3 B^* C^*}{\mu^2} + \left( \frac{\delta_2 B^*}{\epsilon^2} + \frac{\delta_4 C^*}{\eta^2} - d \right) A^*, \\ S_2 = 3 + \frac{\gamma r_1 \delta_3^2 B^* C^*}{\mu^3} + A^* \left( \frac{(\epsilon^3 \delta_1^2 + \epsilon(2 + (\alpha + \epsilon)\delta_1)\delta_2 + \alpha \delta_2^2) B^*}{\epsilon^3} - 2d + \delta_4 C^* \left( \frac{\eta - \beta r_2 \delta_4}{\eta^3} + \frac{1}{(\eta)^2} \right) \right) \\ + \frac{\epsilon_3 B^* C^* (\epsilon^2 - d \epsilon_4^2 C^* A^* + (2\epsilon^2 + (\delta_2 B^* - d \epsilon^2) A^*) (\eta)^2)}{\epsilon^2 \mu^2 (\eta)^2}, \end{cases} \quad (4.4.4)$$

$$\left\{ \begin{array}{l} S_3 = \frac{1}{\epsilon^3 \eta^3 \mu^3} (\epsilon^3 \eta^3 (\mu^3 + \delta_3 (\mu + \gamma r_1 \delta_3)) B^* C^*) \\ + \frac{1}{\epsilon^3 \eta^3 \mu^3} ((\eta^3 \mu^3 (\epsilon^3 \delta_1^2 + \epsilon (1 + (\alpha + \epsilon) \delta_1) \delta_2 + \alpha \delta_2^2)) B^* - d \epsilon^3) \\ - \frac{\epsilon}{\epsilon^3 \eta^3 \mu^3} (\beta \epsilon^2 \mu^3 r_2 \delta_4^2 + \eta^3 \delta_3 (\mu + \gamma r_1 \delta_3) B^* (d \epsilon^2 - \delta_2 B^*)) \\ + \frac{1}{\epsilon^3 \eta^3 \mu^3} (\eta \mu \delta_4 (-\mu^2 \epsilon^2 + (\beta \epsilon \mu r_2 (\epsilon \delta_1 + \delta_2) + \gamma \eta r_1 (\epsilon^2 \delta_1 + \alpha \delta_2)) \delta_3 B^*) C^*) \\ + \frac{\mu^3 \delta_3 \delta_4}{\epsilon^3 \eta^3 \epsilon^3} (\gamma \eta r_1 \delta_3 + \mu (\eta - \beta r_2 \delta_4)) B^* (C^*)^2 A^*, \\ a + A^* = \epsilon, \\ b + A^* = \eta, \\ \text{and} \\ \mu = d + B^*. \end{array} \right. \quad (4.4.5)$$

*Proof.* Now, we have the next variational matrix of system (4.1.3) about  $(A^*, B^*, C^*)$

$$J_4 = \begin{pmatrix} 1 + A^* \left( \frac{\delta_2 B^*}{(\alpha + A^*)^2 - d} + \frac{\delta_4 C^*}{(\beta + A^*)^2} \right) & -A^* \left( \delta_1 + \frac{\delta_2}{\alpha + A^*} \right) & -\frac{\delta_4 A^*}{\beta + A^*} \\ \frac{B^* (\alpha \delta_2 + \delta_1 (\alpha + A^*)^2)}{(\alpha + A^*)^2} & \frac{(\gamma + B^*)^2 + \delta_3 B^* C^*}{(\gamma + B^*)^2} & -\frac{\delta_3 B^*}{\gamma + B^*} \\ -\frac{\beta r_2 \delta_4 C^*}{(\beta + A^*)^2} & \frac{\gamma r_1 \delta_3 C^*}{(\gamma + B^*)^2} & 1 \end{pmatrix}.$$

Formally, the characteristic equation  $\mathbb{G}(\psi)$  from  $J_4$  is specified as:

$$\mathbb{G}(\psi) = \psi^3 - S_1 \psi^2 + S_2 \psi - S_3, \quad (4.4.6)$$

where  $S_1, S_2$  and  $S_3$  are specified in (4.4.4) and (4.4.5). Hence, from **Theorem 4.4.1**, one can see that the positive fixed point of the dynamical system (4.1.3) is stable locally and asymptotically if we have:

$$\begin{cases} |S_1 + S_3| < 1 + S_2, \\ |S_1 - 3S_3| < 3 - S_2, \\ S_3^2 + S_2 - S_1 S_3 < 1. \end{cases}$$

□

## 4.5 Bifurcation analysis

In this part of thesis, we are focused on the analysis of bifurcation of the system (4.1.3) when evaluated at  $(A^*, B^*, C^*)$ . All conditions for the presence of  $(A^*, B^*, C^*)$  are provided in **Lemma 1.2.2** and **Lemma 4.3.2**. Moreover, this part of thesis is related to the study of period-doubling bifurcation experienced by system (4.1.3) about its quarantined free fixed point.

### 4.5.1 Period-doubling bifurcation

In recent times, many researchers have studied the period-doubling bifurcation in the qualitative analysis of discrete-time mathematical models (see [103-108]). Under the

suppositions that  $K > d$  and  $C_M \rightarrow 0, \forall M$ , we study the following set:

$$\Omega_1 = \{\alpha, K, \gamma, \delta_1, \delta_2 \in \mathfrak{R}^+ : d = f(\bar{A}, \bar{B}, \alpha, K, \gamma, \delta_1, \delta_2)\}.$$

Then, the fixed point  $(\bar{A}, \bar{B}, 0)$  of system (4.1.3) experiences the period-doubling bifurcation such that  $d$  is taken as bifurcation parameter, and it varies in a slight neighborhood of  $\hat{d}$ , which is given as

$$\hat{d} = f(\bar{A}, \bar{B}, \alpha, K, \gamma, \delta_1, \delta_2).$$

Besides, the system (4.1.3) is categorized uniformly employing the following mapping:

$$\begin{pmatrix} A \\ B \end{pmatrix} \rightarrow \begin{pmatrix} Ae^{K-\delta_1 B - \frac{\delta_2 B}{\alpha+A} - dA} \\ Be^{\delta_1 A + \frac{\delta_2 A}{\alpha+A} - d} \end{pmatrix}. \quad (4.5.1)$$

To argue and investigate the period-doubling bifurcation for fixed point  $(\bar{A}, \bar{B}, 0)$  of (4.5.1), we assume that  $\alpha, K, \gamma, \delta_1, \delta_2, \hat{d} \in \Phi_1$ . At that time, it seems that

$$\begin{pmatrix} A \\ B \end{pmatrix} \rightarrow \begin{pmatrix} Ae^{K-\delta_1 B - \frac{\delta_2 B}{\alpha+A} - \hat{d}A} \\ Be^{\delta_1 A + \frac{\delta_2 A}{\alpha+A} - \hat{d}} \end{pmatrix}. \quad (4.5.2)$$

By letting  $\bar{d}$  as a bifurcation parameter, the perturbation of map (4.5.2) can be defined with the following map:

$$\begin{pmatrix} A \\ B \end{pmatrix} \rightarrow \begin{pmatrix} Ae^{K-\delta_1 B - \frac{\delta_2 B}{\alpha+A} - (\hat{d} + \bar{d})A} \\ Be^{\delta_1 A + \frac{\delta_2 A}{\alpha+A} - (\hat{d} + \bar{d})} \end{pmatrix} \quad (4.5.3)$$

with  $|\bar{d}| \ll 1$ , is a least perturbation parameter. By letting  $X = A - \bar{A}$  and  $Y = B - \bar{B}$ . Then, by using (4.5.3) we get the following mapping:

$$\begin{pmatrix} X \\ Y \end{pmatrix} \rightarrow \begin{pmatrix} \kappa_{11} & \kappa_{12} \\ \tau_{21} & \tau_{22} \end{pmatrix} \begin{pmatrix} X \\ Y \end{pmatrix} + \begin{pmatrix} g_1(X, Y, \bar{d}) \\ g_2(X, Y, \bar{d}) \end{pmatrix}, \quad (4.5.4)$$

where, the fixed point of (4.5.4) is at  $(0, 0)$  and we have

$$\begin{aligned} g_1(X, Y, \bar{d}) &= \kappa_{13}X^2 + \kappa_{14}XY + \kappa_{15}X\bar{d} + \kappa_{16}Y^2 + \kappa_{17}\bar{\mu}Y + \kappa_{18}\bar{\mu}^2 + \kappa_{19}X^3 + \kappa_{20}X^2Y \\ &+ \kappa_{21}\bar{d}X^2 + \kappa_{22}XY^2 + \kappa_{23}XY\bar{d} + \kappa_{24}X\bar{d}^2 + \kappa_{25}Y\bar{d}^2 + \kappa_{26}\bar{d}^3 \\ &+ O((|X| + |Y| + |\bar{d}|)^4), \\ g_2(X, Y, \bar{d}) &= \tau_{13}X^2 + \tau_{14}XY + \tau_{15}Y\bar{d} + \tau_{16}\bar{d}^2 + \tau_{17}X^3 + \tau_{18}X^2Y + \tau_{19}\bar{d}X^2 + \tau_{20}\bar{d}XY \\ &+ \tau_{21}\bar{d}^2X + \tau_{22}Y\bar{d}^2 + \tau_{23}\bar{d}^3 + O((|X| + |Y| + |\bar{d}|)^4), \end{aligned}$$



with

$$\begin{cases} \kappa_{11} = \bar{A} \left( \frac{\bar{B}\delta_2}{(\alpha+\bar{A})^2} - \bar{d} \right), \quad \kappa_{12} = -\bar{A} \left( \delta_1 + \frac{\delta_2}{\alpha+\bar{A}} \right), \\ \kappa_{13} = \frac{1}{2} \left( \bar{d}(\bar{A}\bar{d} - 2) + \frac{\bar{B}\delta_2(2(\alpha+\bar{A})(\alpha-\bar{A})(\alpha+\bar{A})\bar{d} + \bar{B}\bar{A}\delta_2)}{(\alpha+\bar{A})^4} \right), \\ \kappa_{14} = \left( -\delta_1 - \frac{\delta_2}{\alpha+\bar{A}} \right) + \frac{\bar{A}\delta_2}{(\alpha+\bar{A})^2} + \bar{A} \left( \frac{\delta_2\bar{B}}{(\alpha+\bar{A})^2} - \bar{d} \right) \left( -\delta_1 - \frac{\delta_2}{\alpha+\bar{A}} \right), \\ \kappa_{15} = \bar{A} \left( \bar{A}\bar{d} - 2 - \frac{\bar{B}\bar{A}\delta_2}{(\alpha+\bar{A})^2} \right), \\ \kappa_{16} = \frac{\bar{A}((\alpha+\bar{A})\delta_1 + \delta_2)^2}{2(\alpha+\bar{A})^2}, \quad \kappa_{17} = \frac{\bar{A}^2((\alpha+\bar{A})\delta_1 + \delta_2)}{\alpha+\bar{A}}, \quad \kappa_{18} = \frac{\bar{A}^3}{2}, \\ \kappa_{19} = \frac{1}{6} \left( \frac{\bar{B}\delta_2(3(\alpha+\bar{A})^2(-2\alpha-2\alpha(\alpha+\bar{A})\bar{d} + \bar{A}(\alpha+\bar{A})^2\bar{d}^2) + \bar{B}\delta_2(-3(\alpha+\bar{A})(-\alpha+\bar{A} + \bar{A}(\alpha+\bar{A})\bar{d}) + \bar{B}\bar{A}\delta_2))}{(\alpha+\bar{A})^6} \right) \\ + \frac{1}{6} (\bar{d}^2(3 - \bar{A}\bar{d})), \\ \kappa_{20} = \frac{\delta_2}{(\alpha+\bar{A})^2} + \left( \frac{\delta_2\bar{B}}{(\alpha+\bar{A})^2} - \bar{d} \right) \left( -\delta_1 - \frac{\delta_2}{\alpha+\bar{A}} \right) - \frac{\bar{S}\beta_2}{(\alpha+\bar{S})^3} - \frac{S\beta_2 E(-\beta_1 - \frac{\delta_2}{\alpha+\bar{A}})}{(\alpha+\bar{A})^3} + \frac{A \left( \frac{\delta_2\bar{B}}{(\alpha+\bar{A})^2} - \bar{d} \right) \delta_2}{(\alpha+\bar{A})^2} \\ + \frac{1}{2} \bar{A} \left( \frac{\delta_2\bar{B}}{(\alpha+\bar{A})^2} - \bar{d} \right)^2 \left( -\delta_1 - \frac{\delta_2}{\alpha+\bar{A}} \right), \\ \kappa_{21} = -1 + \frac{B\bar{A}^2\delta_2}{(\alpha+\bar{A})^3} + 2\bar{A} \left( \bar{d} - \frac{B\delta_2}{(\alpha+\bar{A})^2} \right) - \frac{1}{2} \bar{A}^2 \left( \bar{d} - \frac{\bar{B}\alpha_2}{(\alpha+\bar{A})^2} \right)^2, \\ \kappa_{22} = -\frac{((\alpha+\bar{A})\delta_1 + \delta_2)((\alpha+\bar{A})^3(-1+A\bar{d})\delta_1 + (\alpha+\bar{A})(-\alpha+\bar{A} + \bar{A}(\alpha+\bar{A})\bar{d} - \bar{B}\bar{A}\delta_1)\delta_2 - \bar{B}\bar{A}\delta_2^2)}{2(\alpha+\bar{A})^4}, \\ \kappa_{23} = 2\bar{A} \left( \delta_1 + \frac{\delta_2}{\alpha+\bar{A}} \right) - \frac{\bar{A}^2}{(\alpha+\bar{A})^2} + \bar{A}^2 \left( \frac{\delta_2\bar{B}}{(\alpha+\bar{A})^2} - \bar{d} \right) \left( \delta_1 + \frac{\delta_2}{\alpha+\bar{A}} \right), \\ \kappa_{24} = \frac{1}{2} \bar{A}^2 \left( 3 - \bar{A}\bar{d} + \frac{\bar{B}\bar{A}\delta_2}{(\alpha+\bar{A})^2} \right), \\ \kappa_{25} = -\frac{\bar{A}^3((\alpha+\bar{A})\delta_1 + \delta_2)}{2(\alpha+\bar{A})}, \quad \kappa_{26} = -\frac{\bar{A}^4}{6}, \\ \tau_{11} = \bar{B} \left( \delta_1 + \frac{\alpha\delta_2}{(\alpha+\bar{A})^2} \right), \quad \tau_{12} = 1, \quad \tau_{13} = \frac{\bar{B}((\alpha+\bar{A})^4\delta_1^2 + 2\alpha(\alpha+\bar{A})(-1+(\alpha+\bar{A})\delta_1)\delta_2 + \alpha^2\delta_2^2)}{2(\alpha+\bar{A})^4}, \\ \tau_{14} = \delta_1 + \frac{\alpha\delta_2}{(\alpha+\bar{A})^2}, \\ \tau_{15} = -1, \quad \tau_{16} = \frac{\bar{B}}{2}, \quad \tau_{17} = \frac{\bar{B}(-6\bar{A}(\alpha+\bar{A})^2\delta_2 + 6(\alpha+\bar{A})^3\delta_2 - 6\alpha(\alpha+\bar{A})\delta_2((\alpha+\bar{A})^2\delta_1 + \alpha\delta_2) + ((\alpha+\bar{A})^2\delta_1 + \alpha\delta_2)^3)}{6(\alpha+\bar{A})^6}, \\ \tau_{18} = \frac{-2\alpha(\alpha+\bar{A})\delta_2 + ((\alpha+\bar{A})^2\delta_1 + \alpha\delta_2)^2}{2(\alpha+\bar{A})^4}, \quad \tau_{19} = -\frac{\bar{B}((\alpha+\bar{A})^4\delta_1^2 + 2\alpha(\alpha+\bar{A})(-1+(\alpha+\bar{A})\delta_1)\delta_2 + \alpha^2\delta_2^2)}{2(\alpha+\bar{A})^4}, \\ \tau_{20} = -\delta_1 - \frac{\alpha\delta_2}{(\alpha+\bar{A})^2}, \quad \tau_{21} = \frac{1}{2} \bar{B} \left( \delta_1 + \frac{\alpha\delta_2}{(\alpha+\bar{A})^2} \right), \quad \tau_{22} = \frac{1}{2}, \quad \tau_{23} = -\frac{\bar{B}}{6}. \end{cases}$$

Let  $\psi_1$  and  $\psi_2$  are characteristic roots for system (4.5.2) then, we get the next translation;

$$\begin{pmatrix} X \\ Y \end{pmatrix} = N \begin{pmatrix} U \\ V \end{pmatrix}, \quad (4.5.5)$$

where

$$N = \begin{bmatrix} -\bar{A} \left( \delta_1 + \frac{\delta_2}{\alpha+\bar{A}} \right) & -\bar{A} \left( \delta_1 + \frac{\delta_2}{\alpha+\bar{A}} \right) \\ \bar{A}\bar{d} - \frac{\bar{B}\bar{A}\delta_2}{(\alpha+\bar{A})^2} - 1 & \psi_2 - \bar{A} \left( \frac{\bar{B}\delta_2}{(\alpha+\bar{A})^2} - \bar{d} \right) \end{bmatrix}$$

be a nonsingular matrix. With the application of transformation (4.5.5), the equation (4.5.4) becomes:

$$\begin{pmatrix} U \\ V \end{pmatrix} \rightarrow \begin{pmatrix} -1 & 0 \\ 0 & \psi_2 \end{pmatrix} \begin{pmatrix} U \\ V \end{pmatrix} + \begin{pmatrix} f(U, V, \bar{d}) \\ g(U, V, \bar{d}) \end{pmatrix}, \quad (4.5.6)$$

where

$$\begin{aligned}
f(U, V, \bar{d}) &= \left( \frac{(\psi_2 - \kappa_{11}) \kappa_{26}}{\kappa_{12} (\psi_2 + 1)} - \frac{\tau_{23}}{\psi_2 + 1} \right) \bar{d}^3 + \left( \frac{(\psi_2 - \kappa_{11}) \kappa_{24}}{\kappa_{12} (\psi_2 + 1)} - \frac{\tau_{21}}{\psi_2 + 1} \right) \bar{d}^2 X \\
&+ \left( \frac{(\psi_2 - \kappa_{11}) \kappa_{25}}{\kappa_{12} (\psi_2 + 1)} - \frac{\tau_{22}}{\psi_2 + 1} \right) \bar{d}^2 Y + \left( \frac{(\psi_2 - \kappa_{11}) \kappa_{18}}{\kappa_{12} (\psi_2 + 1)} - \frac{\tau_{16}}{\psi_2 + 1} \right) \bar{d}^2 \\
&+ \left( \frac{(\psi_2 - \kappa_{11}) \kappa_{21}}{\kappa_{12} (\psi_2 + 1)} - \frac{\tau_{19}}{\psi_2 + 1} \right) \bar{d} X^2 + \left( \frac{(\psi_2 - \kappa_{11}) \kappa_{23}}{\kappa_{12} (\psi_2 + 1)} - \frac{\tau_{20}}{\psi_2 + 1} \right) \bar{d} XY \\
&+ \frac{(\psi_2 - \kappa_{11}) \kappa_{15} \bar{d} X}{\kappa_{12} (\psi_2 + 1)} + \left( \frac{(\psi_2 - \kappa_{11}) \kappa_{17}}{\kappa_{12} (\psi_2 + 1)} - \frac{\tau_{15}}{\psi_2 + 1} \right) Y \bar{d} \\
&+ \left( \frac{(\psi_2 - \kappa_{11}) \kappa_{19}}{\kappa_{12} (\psi_2 + 1)} - \frac{\tau_{17}}{\psi_2 + 1} \right) X^3 + \left( \frac{(\psi_2 - \kappa_{11}) \kappa_{20}}{\kappa_{12} (\psi_2 + 1)} - \frac{\tau_{18}}{\psi_2 + 1} \right) X^2 Y \\
&+ \left( \frac{(\psi_2 - \kappa_{11}) \kappa_{13}}{\kappa_{12} (\psi_2 + 1)} - \frac{\tau_{13}}{\psi_2 + 1} \right) X^2 + \frac{(\psi_2 - \kappa_{11}) \kappa_{22} X Y^2}{\kappa_{12} (\psi_2 + 1)} \\
&+ \left( \frac{(\psi_2 - \kappa_{11}) \kappa_{14}}{\kappa_{12} (\psi_2 + 1)} - \frac{\tau_{14}}{\psi_2 + 1} \right) XY + \frac{(\psi_2 - \kappa_{11}) \kappa_{16} Y^2}{\kappa_{12} (\psi_2 + 1)} \\
&+ O((|U| + |V| + |\bar{d}|)^4),
\end{aligned}$$

$$\begin{aligned}
g(U, V, \bar{d}) &= \left( \frac{(1 + \kappa_{11}) \kappa_{26}}{\kappa_{12} (\psi_2 + 1)} + \frac{\tau_{23}}{\psi_2 + 1} \right) \bar{d}^3 + \left( \frac{(1 + \kappa_{11}) \kappa_{24}}{\kappa_{12} (\psi_2 + 1)} + \frac{\tau_{21}}{\psi_2 + 1} \right) \bar{d}^2 X \\
&+ \left( \frac{(1 + \kappa_{11}) \kappa_{25}}{\kappa_{12} (\psi_2 + 1)} + \frac{\tau_{22}}{\psi_2 + 1} \right) \bar{d}^2 Y + \left( \frac{(1 + \kappa_{11}) \kappa_{18}}{\kappa_{12} (\psi_2 + 1)} + \frac{\tau_{16}}{\psi_2 + 1} \right) \bar{d}^2 \\
&+ \left( \frac{(1 + \kappa_{11}) \kappa_{21}}{\kappa_{12} (\psi_2 + 1)} + \frac{\tau_{19}}{\psi_2 + 1} \right) \bar{d} X^2 + \left( \frac{(1 + \kappa_{11}) \kappa_{23}}{\kappa_{12} (\psi_2 + 1)} + \frac{\tau_{20}}{\psi_2 + 1} \right) \bar{d} XY \\
&+ \frac{(1 + \kappa_{11}) \kappa_{15} \bar{d} X}{\kappa_{12} (\psi_2 + 1)} + \left( \frac{(1 + \kappa_{11}) \kappa_{17}}{\kappa_{12} (\psi_2 + 1)} + \frac{\tau_{15}}{\psi_2 + 1} \right) Y \bar{d} \\
&+ \left( \frac{(1 + \kappa_{11}) \kappa_{19}}{\kappa_{12} (\psi_2 + 1)} + \frac{\tau_{17}}{\psi_2 + 1} \right) X^3 + \left( \frac{(1 + \kappa_{11}) \kappa_{20}}{\kappa_{12} (\psi_2 + 1)} + \frac{\tau_{18}}{\psi_2 + 1} \right) X^2 Y \\
&+ \left( \frac{(1 + \kappa_{11}) \kappa_{13}}{\kappa_{12} (\psi_2 + 1)} + \frac{\tau_{13}}{\psi_2 + 1} \right) X^2 + \frac{(1 + \kappa_{11}) \kappa_{22} X Y^2}{\kappa_{12} (\psi_2 + 1)} \\
&+ \left( \frac{(1 + \kappa_{11}) \kappa_{14}}{\kappa_{12} (\psi_2 + 1)} + \frac{\tau_{14}}{\psi_2 + 1} \right) XY + \frac{(1 + \kappa_{11}) \kappa_{16} Y^2}{\kappa_{12} (\psi_2 + 1)} \\
&+ O((|U| + |V| + |\bar{d}|)^4),
\end{aligned}$$

where

$$\kappa_{12}(V + U) = X, \quad (\psi_2 - \kappa_{11})V - (1 + \kappa_{11})U = Y.$$

Let  $\mathcal{U}^c(0, 0, 0)$  be the center manifold of (4.5.6) anticipated at  $(0, 0)$  in a least neighborhood of  $\bar{\eta} = 0$ . At that time  $\mathcal{U}^c(0, 0, 0)$  can be expected as follows:

$$\{(U, V, \bar{d}) \in \mathbb{R}^3 : V = K_{11}U^2 + K_{12}U\bar{d} + K_{13}\bar{d}^2 + O((|\bar{d}| + |U|)^3)\} = \mathcal{U}^c(0, 0, 0),$$

where

$$K_{11} = \frac{1}{1 - \psi_2} \left( \left( \frac{(1 + \kappa_{11}) \kappa_{13}}{\kappa_{12} (\psi_2 + 1)} + \frac{\tau_{13}}{\psi_2 + 1} \right) \kappa_{12}^2 - \left( \frac{(1 + \kappa_{11}) \kappa_{14}}{\kappa_{12} (\psi_2 + 1)} + \frac{\tau_{14}}{\psi_2 + 1} \right) \kappa_{12} (1 + \kappa_{11}) \right) \\ + \frac{1}{1 - \psi_2} \frac{(1 + \kappa_{11}) \kappa_{16} (1 + \kappa_{11})^2}{\kappa_{12} (\psi_2 + 1)},$$

$$K_{12} = \frac{1}{1 - \psi_2} \left( \frac{(1 + \kappa_{11}) \kappa_{15}}{\psi_2 + 1} - \left( \frac{(1 + \kappa_{11}) \kappa_{17}}{\kappa_{12} (\psi_2 + 1)} + \frac{\tau_{15}}{\psi_2 + 1} \right) (1 + \kappa_{11}) \right),$$

$$K_{13} = \frac{1}{1 - \psi_2} \left( \frac{(1 + \kappa_{11}) \kappa_{18}}{\kappa_{12} (\psi_2 + 1)} + \frac{\tau_{16}}{\psi_2 + 1} \right).$$

Hence, the restricted map to  $\mathcal{U}^c(0, 0, 0)$  is described as follows:

$$F : U \rightarrow -U + G_{11}U^2 + G_{12}U\bar{d} + G_{13}U^2\bar{d} + G_{14}U\bar{d}^2 + G_{15}U^3 + O((|U| + |\bar{d}|)^4),$$

where

$$G_{11} = \left( \frac{(\psi_2 - \kappa_{11}) \kappa_{13}}{\kappa_{12} (\psi_2 + 1)} - \frac{\tau_{13}}{\psi_2 + 1} \right) \kappa_{12}^2 - \left( \frac{(\psi_2 - \kappa_{11}) \kappa_{14}}{\kappa_{12} (\psi_2 + 1)} - \frac{\tau_{14}}{\psi_2 + 1} \right) \kappa_{12} (1 + \kappa_{11}) \\ + \frac{(\psi_2 - \kappa_{11}) \kappa_{16} (1 + \kappa_{11})^2}{\kappa_{12} (\psi_2 + 1)},$$

$$G_{12} = \frac{(\xi_2 - \theta_{11}) \theta_{15}}{\xi_2 + 1} - \left( \frac{(\xi_2 - \theta_{11}) \theta_{17}}{\theta_{12} (\xi_2 + 1)} - \frac{\phi_{15}}{\xi_2 + 1} \right) (1 + \theta_{11}),$$

$$G_{13} = \left( \frac{(\psi_2 - \kappa_{11}) \kappa_{21}}{\kappa_{12} (\psi_2 + 1)} - \frac{\tau_{19}}{\psi_2 + 1} \right) \kappa_{12}^2 - \left( \frac{(\psi_2 - \kappa_{11}) \kappa_{23}}{\kappa_{12} (\psi_2 + 1)} - \frac{\tau_{20}}{\psi_2 + 1} \right) \kappa_{12} (1 + \kappa_{11}) \\ + \frac{(\psi_2 - \kappa_{11}) \kappa_{15} K_1}{\psi_2 + 1} + \left( \frac{(\psi_2 - \kappa_{11}) \kappa_{17}}{\kappa_{12} (\psi_2 + 1)} - \frac{\tau_{15}}{\psi_2 + 1} \right) (\psi_2 - \kappa_{11}) K_1 \\ + 2 \left( \frac{(\psi_2 - \kappa_{11}) \kappa_{13}}{\kappa_{12} (\psi_2 + 1)} - \frac{\tau_{13}}{\psi_2 + 1} \right) \kappa_{12}^2 K_2 + \left( \frac{(\psi_2 - \kappa_{11}) \kappa_{14}}{\kappa_{12} (\psi_2 + 1)} - \frac{\tau_{14}}{\psi_2 + 1} \right) \kappa_{12} (\psi_2 - \kappa_{11}) K_2 \\ - \left( \frac{(\psi_2 - \kappa_{11}) \kappa_{14}}{\kappa_{12} (\psi_2 + 1)} - \frac{\tau_{14}}{\psi_2 + 1} \right) \kappa_{12} K_2 (1 + \kappa_{11}) - 2 \frac{(\psi_2 - \kappa_{11}) \kappa_{16} (1 + \kappa_{11}) (\psi_2 - \kappa_{11}) K_2}{\kappa_{12} (\psi_2 + 1)}$$

$$G_{14} = \left( \frac{(\psi_2 - \kappa_{11}) \kappa_{24}}{\kappa_{12} (\psi_2 + 1)} - \frac{\tau_{21}}{\psi_2 + 1} \right) \kappa_{12} - \left( \frac{(\psi_2 - \kappa_{11}) \kappa_{25}}{\kappa_{12} (\psi_2 + 1)} - \frac{\tau_{22}}{\psi_2 + 1} \right) (1 + \kappa_{11}) \\ + \frac{(\psi_2 - \kappa_{11}) \kappa_{15} K_2}{\psi_2 + 1} + \left( \frac{(\psi_2 - \kappa_{11}) \kappa_{17}}{\kappa_{12} (\psi_2 + 1)} - \frac{\tau_{15}}{\psi_2 + 1} \right) (\psi_2 - \kappa_{11}) K_2 \\ + 2 \left( \frac{(\psi_2 - \kappa_{11}) \kappa_{13}}{\kappa_{12} (\psi_2 + 1)} - \frac{\tau_{13}}{\psi_2 + 1} \right) \kappa_{12}^2 K_3 - 2 \frac{(\psi_2 - \kappa_{11}) \kappa_{16} (1 + \kappa_{11}) (\psi_2 - \kappa_{11}) K_3}{\kappa_{12} (\psi_2 + 1)} \\ + \left( \frac{(\psi_2 - \kappa_{11}) \kappa_{14}}{\kappa_{12} (\psi_2 + 1)} - \frac{\tau_{14}}{\psi_2 + 1} \right) \kappa_{12} (\psi_2 - \kappa_{11}) K_3 \\ - \left( \frac{(\psi_2 - \kappa_{11}) \kappa_{14}}{\kappa_{12} (\psi_2 + 1)} - \frac{\tau_{14}}{\psi_2 + 1} \right) \kappa_{12} K_3 (1 + \kappa_{11}),$$

$$G_{15} = \frac{(\psi_2 - \kappa_{11}) \kappa_{26}}{\kappa_{12} (\psi_2 + 1)} + \frac{(\psi_2 - \kappa_{11}) \kappa_{15} K_3}{\psi_2 + 1} + \left( \frac{(\psi_2 - \kappa_{11}) \kappa_{17}}{\kappa_{12} (\psi_2 + 1)} - \frac{\tau_{15}}{\psi_2 + 1} \right) (\psi_2 - \kappa_{11}) K_3 - \frac{\tau_{23}}{\psi_2 + 1}.$$

Finally, we get the following numbers:

$$l_1 = \left( \frac{\partial^2 g_1}{\partial U \partial \bar{d}} + \frac{1}{2} \frac{\partial F}{\partial \bar{d}} \frac{\partial^2 F}{\partial U^2} \right)_{(0,0)} = \frac{((1 + \kappa_{11}) \kappa_{17} - \kappa_{12} \kappa_{15}) (\kappa_{11} - \psi_2) + (1 + \kappa_{11}) \kappa_{12} \tau_{15}}{\kappa_{12} (1 + \psi_2)} \neq 0,$$

and

$$l_2 = \left( \left( \frac{1}{2} \frac{\partial^2 F}{\partial U^2} \right)^2 + \frac{1}{6} \frac{\partial^3 F}{\partial U^3} \right)_{(0,0)} = G_{11}^2 + G_{15} \neq 0.$$

Hence, by the study as mentioned above, we have the next conclusive theorem related to bifurcation of system (4.1.3) about  $(\bar{A}, \bar{B}, 0)$ .

**Theorem 4.5.1.** *If  $l_1 \neq 0$ , then the system (4.1.3) experiences the period-doubling bifurcation about the quarantined free equilibrium  $(\bar{A}, \bar{B}, 0)$  when the parameter  $d$  varies in the least neighborhood of  $\bar{d}$ . Moreover, if  $0 > l_2$  then the period-two trajectories that bifurcate from  $(\bar{A}, \bar{B}, 0)$  are stable, and if  $0 < l_2$ , then these trajectories are unstable.*

## 4.5.2 Neimark-Sacker bifurcation

Here, we will discuss the complex behaviour of the system (4.1.3) about  $(A^*, B^*, C^*)$ . In addition, for this study, we have to show the existence of Neimark-Sacker bifurcation in the system (4.1.3) about  $(S^*, E^*, Q^*)$ . For the study of Neimark-Sacker bifurcation the standard theory of bifurcation is used (see **Chapter 2: Section 2.3**). Hence, by using an obvious standard of bifurcation [35], it is easy to observe that the system (4.1.3) experiences the Neimark-Sacker bifurcation for parameter  $d$  without finding any eigenvalue (see **Lemma 1.4.1**).

**Theorem 4.5.2.** *The positive fixed point of system (4.1.3) experiences the Neimark-Sacker bifurcation if the following conditions are satisfied:*

$$\begin{cases} S_3(S_1 - S_3) + 1 - S_2 = 0, \\ -S_3(S_1 - S_3) + 1 + S_2 > 0, \\ 1 + S_1 + S_2 + S_3 > 0, \\ 1 - S_1 + S_2 - S_3 > 0 \end{cases}$$

where,  $S_1, S_2$  and  $S_3$  are provided in (4.4.4) and (4.4.5).

*Proof.* By using **Lemma 1.4.1**, for  $m = 3$ , and considering the characteristic equation (4.4.2) of the system (4.1.3) evaluated at its positive fixed point, we get the following equalities and inequalities:

$$\begin{cases} \Delta_2^-(d) = 1 - S_2 + S_3(S_1 - S_3) = 0, \\ \Delta_2^+(d) = 1 + S_2 - S_3(S_1 + S_3) > 0, \\ \mathbb{H}_d(1) = 1 + S_1 + S_2 + S_3 > 0, \\ (-1)^3 \mathbb{H}_d(-1) = 1 - S_1 + S_2 - S_3 > 0. \end{cases}$$

□

**Remark 4.5.1.** By taking  $d$  as a bifurcation parameter, the arithmetical rule Neimark-Sacker bifurcation can be established by finding the solutions of equation  $\Delta_2^-(\mu) = 0$ .

## 4.6 Chaos control

This section is related to the control of the chaos and Neimark-sacker bifurcation. Furthermore, a modified hybrid control method (see [22]) is used for the system (4.1.3). In addition, this technique is appropriate to use for every discrete-time system experiencing chaos and period-doubling bifurcation. For the further study of the modified hybrid method, one can see **Chapter 2: Section 2.4**.

### 4.6.1 A modified technique for chaos control

By application of modified hybrid control method on the system (4.1.3) we get the following system:

$$\begin{aligned} A_{m+1} &= h^3 \left( A_m e^{K - \delta_1 B_m - \frac{\delta_2 B_m}{\alpha + A_m} - \frac{\delta_4 C_m}{\beta + A_m} - d A_m} \right) + (1 - h^3) A_m, \\ B_{m+1} &= h^3 \left( B_m e^{\delta_1 A_m + \frac{\delta_2 A_m}{\alpha + A_m} - \frac{\delta_3 C_m}{\gamma + B_m} - d} \right) + (1 - h^3) B_m, \\ C_{m+1} &= h^3 \left( C_m e^{\frac{r_1 \delta_3 B_m}{\gamma + B_m} + \frac{r_2 \delta_4 A_m}{\beta + A_m} - d} \right) + (1 - h^3) C_m \end{aligned} \quad (4.6.1)$$

Furthermore, the system (4.6.1) and (4.1.3) have same fixed points. Moreover, the variational matrix of (4.6.1) about  $(S^*, E^*, Q^*)$  is specified as:

$$\begin{pmatrix} 1 + h^3 A^* \left( d - \frac{\delta_2 e^*}{(\alpha + A^*)^2} - \frac{\delta_4 C^*}{(\beta + A^*)^2} \right) & -h^3 A^* \left( \delta_1 + \frac{\delta_2}{\alpha + A^*} \right) & -\frac{h^3 \delta_4 A^*}{\beta + A^*} \\ \frac{h^3 B^* (\alpha \delta_2 + \delta_1 (\alpha + A^*)^2)}{(\alpha + A^*)^2} & 1 - h^3 + \frac{h^3 ((\gamma + B^*)^2 + \delta_3 B^* C^*)}{(\gamma + B^*)^2} & -\frac{\delta^3 \delta_3 B^*}{\gamma + B^*} \\ -\frac{\beta h^3 r_2 \delta_4 C^*}{(\beta + A^*)^2} & \frac{\gamma h^3 r_1 \delta_3 C^*}{(\gamma + e^*)^2} & 1 \end{pmatrix}. \quad (4.6.2)$$

The positive fixed point  $(A^*, B^*, C^*)$  of the system (4.6.1) is locally asymptotically stable if every solution of the characteristic equation of (4.6.2) lies in the interior of  $D$ . Where  $D$  is an open disk of radius one.

## 4.7 Numerical simulations

This section provides the numerical study for the system (4.1.3). Moreover, this study directly verifies our theoretical analysis and analytic results: which we have proved in previous sections of this chapter.

**Example 4.7.1.** Let  $\alpha = 2, \beta = 10, \delta_1 = 0.99, \gamma = 0.4, \delta_2 = 0.01, \delta_3 = 0.80, \delta_4 = 0.60, r_1 = 1, r_2 = 2$  and  $K > 0$ . Then, the system (4.1.3) can be specified as:

$$\begin{aligned} A_{m+1} &= A_m e^{K - 0.99B_m - \frac{0.01B_m}{2+A_m} - \frac{0.60C_m}{10+A_m} - dA_m}, \\ B_{m+1} &= B_m e^{0.99A_m + \frac{0.01A_m}{2+A_m} - \frac{0.80C_m}{0.4+B_m} - d}, \\ C_{m+1} &= C_m e^{\frac{0.80B_m}{0.4+B_m} + \frac{2(0.60)A_m}{10+A_m} - d}, \end{aligned} \quad (4.7.1)$$

where  $A_0 = 0.91059, B_0 = 0.38854, C_0 = 0.3549$  are primary conditions and  $d > 0$ . In this case bifurcation diagram for  $A_m$  and  $B_m$  are respectively shown in (Fig. 4.7a) and (Fig. 4.7b). In addition, MLE for the presence of bifurcation is provided in (Fig. 4.7c). In (Fig. 4.6), some phase portraits are provided for some values of  $d > 0$ . It can be seen that there exist the Neimark-Sacker bifurcation for a maximum range of bifurcation parameter  $d$ . For values as mentioned earlier of parameters one can obtain the jacobian matrix  $J_3$  is as follows:

$$J_3 = \begin{pmatrix} 1 + 0.91059(0.0021294 - d) & -0.904613 & -0.0500756 \\ 0.286336 & 1.1728 & -0.335248 \\ -0.0357759 & 0.239551 & 1 \end{pmatrix}.$$

Furthermore, the equation  $\mathbb{G}(\psi) = 0$  for  $J_3$  have the following coefficients:

$$S_1 = 3.17946 - 0.91059d,$$

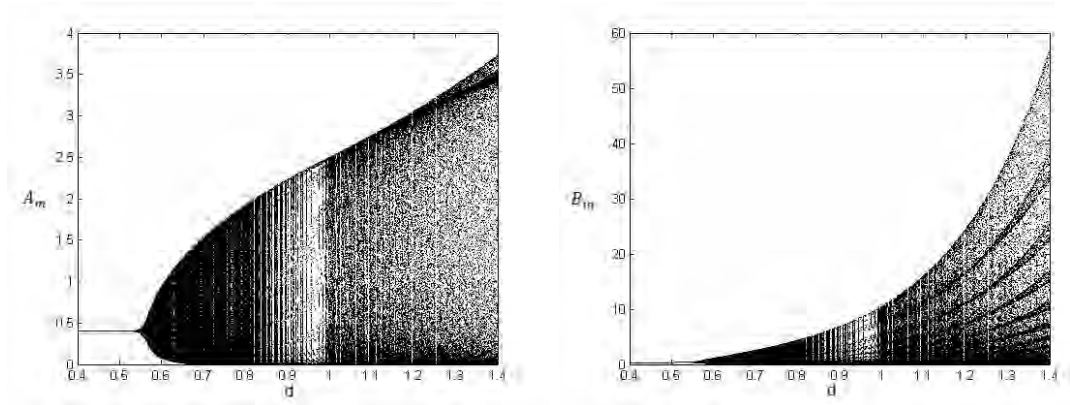
$$S_2 = 3.68735 - 1.97853d,$$

and

$$S_3 = 1.58237 - 1.1377d.$$

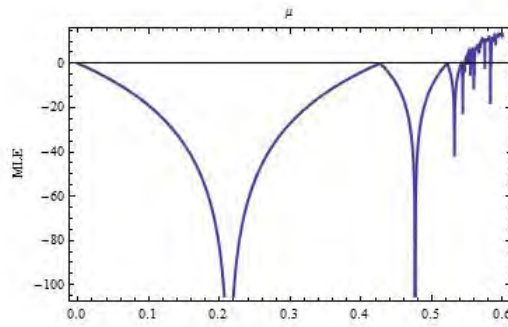
In addition, the fixed point  $(A^*, B^*, C^*)$  remains locally asymptotically stable if and only if we have  $d \in (0.37858611389735736, 1.0675487017977925)$ . In addition, the positive fixed point  $(A^*, B^*, C^*)$  undergoes the Neimark-Sacker bifurcation if we have

$$d \in (1.0675487017977952, 2.3456458284152606).$$



(a) Bifurcation diagram for  $A_m$

(b) Bifurcation diagram for  $B_m$



(c) Lyapunov exponents for system (4.1.3)

Figure 4.4: Bifurcation diagrams for system (4.1.3) for  $K > 0, d > 0, \alpha = 2, \beta = 10, \delta_1 = 0.99, \gamma = 0.4, \delta_2 = 0.01, \delta_3 = 0.80, \delta_4 = 0.60, r_1 = 1, r_2 = 2$ , with  $A_0 = 0.91059, B_0 = 0.38854$ , and  $C_0 = 0.3549$ .

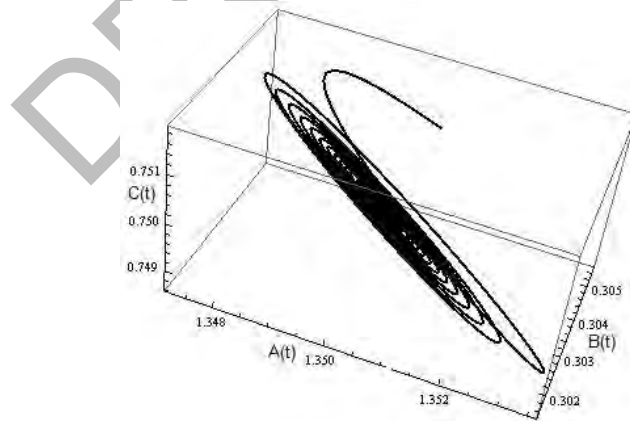


Figure 4.5: 3-dimensional portrait for system (4.7.4) for  $\alpha = 2, \beta = 10, \delta_1 = 0.99, \gamma = 0.4, \delta_2 = 0.01, \delta_3 = 0.80, \delta_4 = 0.60, r_1 = 1, r_2 = 2, K > 0, d > 0$  and  $A_0 = 1.35, B_0 = 0.31, C_0 = 0.75$ .

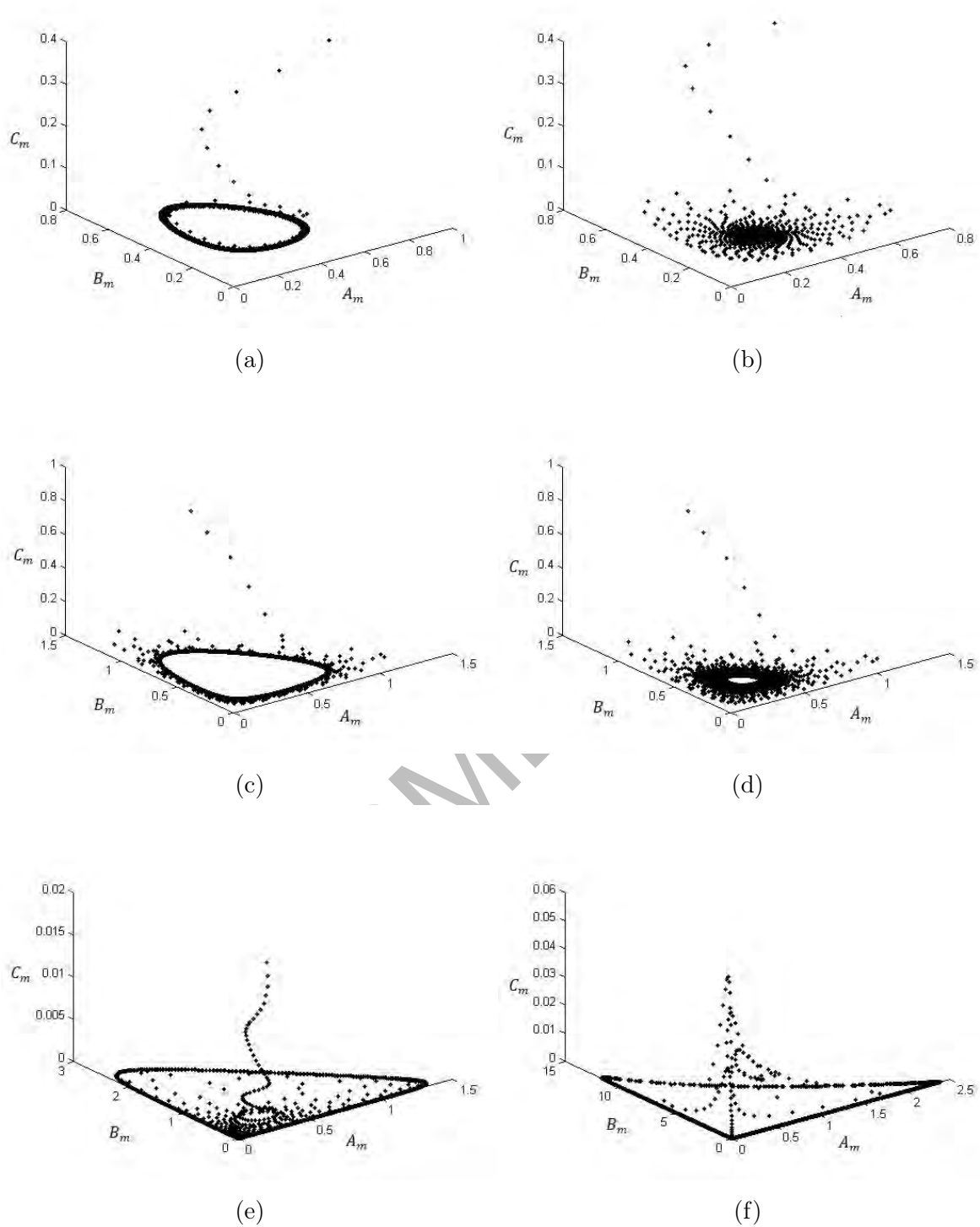


Figure 4.6: Phase portraits of system (4.1.3) for  $K > 0, d > 0, \alpha = 2, \beta = 10, \delta_1 = 0.99, \gamma = 0.4, \delta_2 = 0.01, \delta_3 = 0.80, \delta_4 = 0.60, r_1 = 1, r_2 = 2$ , with  $A_0 = 0.91059, B_0 = 0.38854$ , and  $C_0 = 0.3549$ .

**Example 4.7.2.** Let  $\alpha = 2, \beta = 10, \delta_1 = 0.99, \gamma = 0.4, \delta_2 = 0.01, K > d$  and  $C_m \rightarrow$



$0, \forall m$ . Formally, the system (4.1.3) can be described as:

$$\begin{aligned} A_{m+1} &= A_m e^{K-0.99B_m-\frac{0.01B_m}{2+A_m}-dA_m}, \\ B_{m+1} &= B_m e^{0.99A_m+\frac{0.01A_m}{2+A_m}-d} \end{aligned} \quad (4.7.2)$$

with  $A_0 = 1.4391059$  and  $B_0 = 1.138854$  are initial values. In this case the plots of  $A_m$  and  $B_m$  are given in **Fig. 4.7a** and **Fig. 4.7b**. Additionally, the quarantine free fixed point  $(\bar{A}, \bar{B}, 0)$  undergoes the period-doubling bifurcation for  $d \in (1.269970179, 1.9887756458)$ .

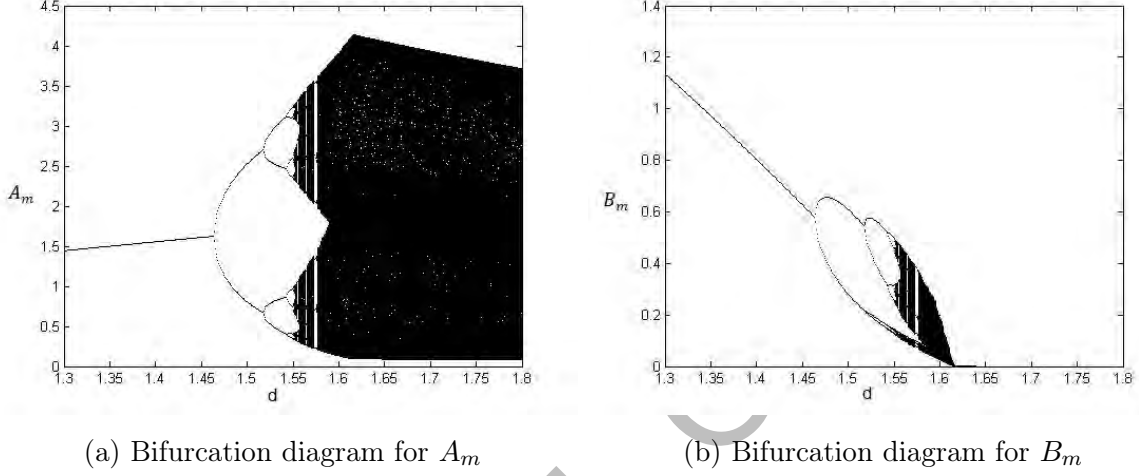


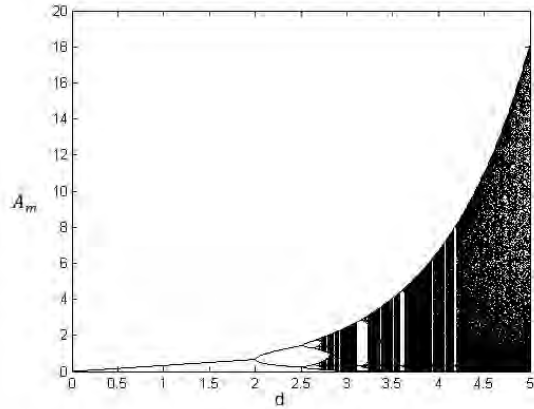
Figure 4.7: Period-doubling bifurcation in system (4.1.3) for  $\alpha = 2, \beta = 10, \delta_1 = 0.99, \gamma = 0.4, \delta_2 = 0.01, K > d$  and  $C_m \rightarrow 0, \forall m$  and  $A_0 = 1.4391059$  and  $B_0 = 1.138854$

**Example 4.7.3.** For system (4.1.3), let  $\beta = 10, \alpha = 2, 0.99 = \delta_1, \gamma = 0.4, \delta_2 = 0.01, \delta_3 = 0.80, \delta_4 = 0.60, r_1 = 1, r_2 = 2, K > 0, d > 0$  with primary conditions are  $A_0 = 1.35, B_0 = 0.31$ , and  $C_0 = 0.75$ . Then, in this case plot of  $A_m$  is shown in (**Fig. 4.8**). Moreover, the system (4.1.3) experiences the period-doubling bifurcation for bigger values of  $d$  (see **Fig. 4.8a**). In addition, the presence of chaos for  $A_m$  is specified in (**Fig. 4.8b**).

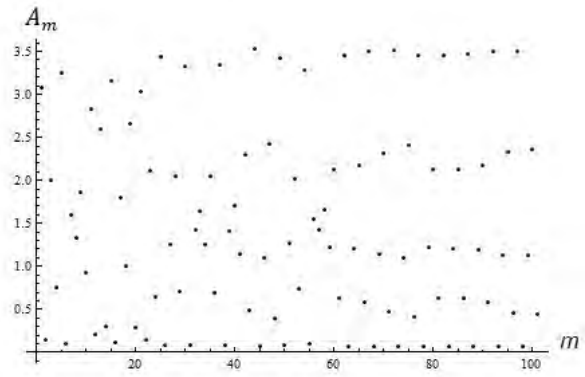
**Example 4.7.4.** Assume that  $\beta = 10, \alpha = 2, 0.99 = \delta_1, \gamma = 0.4, \delta_2 = 0.01, \delta_3 = 0.80, \delta_4 = 0.60, r_1 = 1, r_2 = 2$  and  $K > 0$ . Then, the mathematical system (4.6.1) is specified as:

$$\begin{aligned} A_{m+1} &= h^3(A_m e^{K-0.99B_m-\frac{0.01B_m}{2+A_m}-\frac{0.60C_m}{10+A_m}-dA_m}) + (1-h^3)A_m, \\ B_{m+1} &= h^3(B_m e^{0.99A_m+\frac{0.01A_m}{2+A_m}-\frac{0.80C_m}{0.4+B_m}-d}) + (1-h^3)B_m, \\ C_{m+1} &= h^3(C_m e^{\frac{0.80B_m}{0.4+B_m}+\frac{2(0.60)A_m}{10+A_m}-d}) + (1-h^3)C_m, \end{aligned} \quad (4.7.3)$$

with  $d > 0, h \in (0, 1), A_0 = 0.91059, B_0 = 0.38854$  and  $C_0 = 0.3549$ . In this case the controlled plots for  $A_m$  and  $B_m$  are shown in (**Fig. 4.9**). Hence, one can see that the Neimark-Sacker bifurcation has been controlled for large range of control parameter  $h$ .

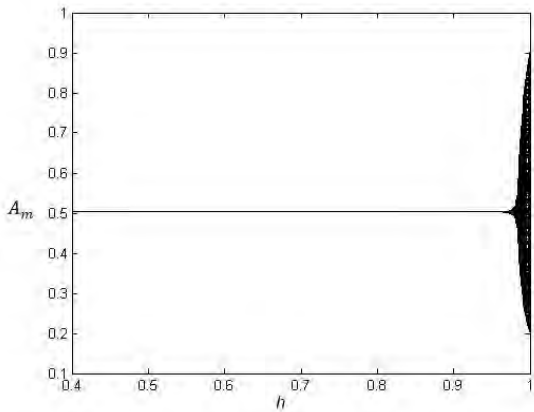


(a) Bifurcation diagram for  $A_m$

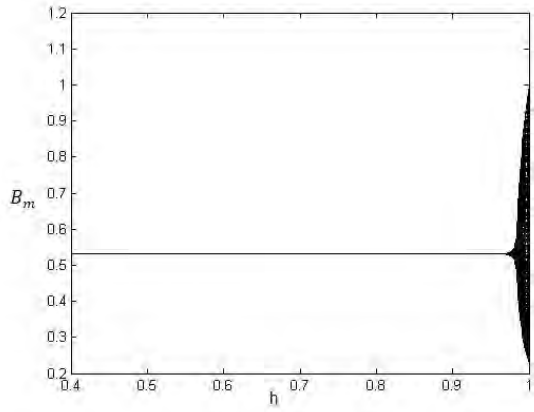


(b) Chaotic plot for  $A_m$

Figure 4.8: Plots for system (4.1.3) for  $\alpha = 2, \beta = 10, \delta_1 = 0.99, \gamma = 0.4, \delta_2 = 0.01, \delta_3 = 0.80, \delta_4 = 0.60, r_1 = 1, r_2 = 2, K > 0, d > 0$  with  $A_0 = 1.35, B_0 = 0.31$ , and  $C_0 = 0.75$ .



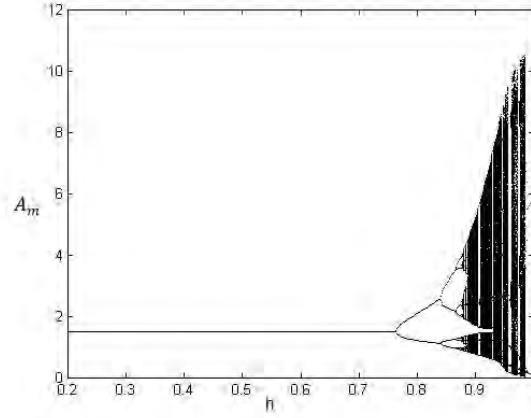
(a) Bifurcation diagram for  $A_m$



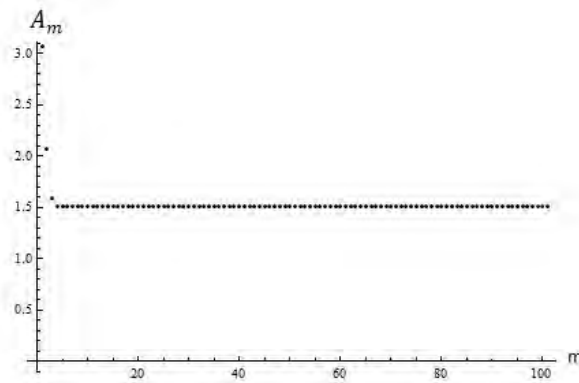
(b) Bifurcation diagram for  $B_m$

Figure 4.9: Control diagrams for system (4.6.1) for  $\alpha = 2, \beta = 10, \delta_1 = 0.99, \gamma = 0.4, \delta_2 = 0.01, \delta_3 = 0.80, \delta_4 = 0.60, r_1 = 1, r_2 = 2, K > 0, d > 0$  and  $A_0 = 0.91059, B_0 = 0.38854, C_0 = 0.3549$ .

**Example 4.7.5.** Let us assume  $\alpha = 2, \beta = 10, \delta_1 = 0.99, \gamma = 0.4, \delta_2 = 0.01, \delta_3 = 0.80, \delta_4 = 0.60, r_1 = 1, r_2 = 2$  and  $K > 0$  in system (4.6.1). Formally, for  $b > 0$  with primary values  $A_0 = 1.35, B_0 = 0.31$ , and  $C_0 = 0.75$  the behavior of  $A_m$  is shown in (Fig. 4.10). Hence, the period-doubling bifurcation is controlled for maximum range of control parameter  $h$ . In addition, from (Fig. 4.10b) it is obvious that the chaos in mathematical system (4.6.1) has been controlled efficiently for maximum range of control parameter  $h$ .



(a) Controlled diagram for  $A_m$



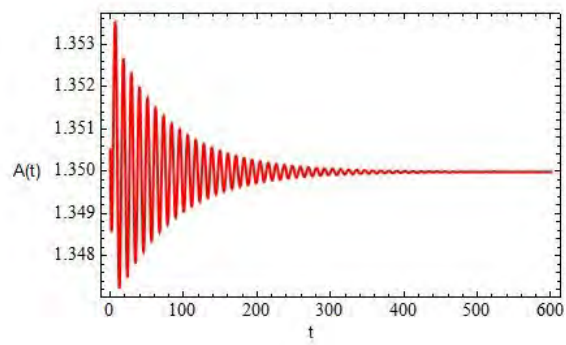
(b) Controlled plot for  $A_m$

Figure 4.10: Controlled plots for (4.6.1) for  $\beta = 10, \alpha = 2, 0.99 = \delta_1, 0.4 = \gamma, \delta_2 = 0.01, \delta_3 = 0.80, \delta_4 = 0.60, r_1 = 1, r_2 = 2, K > 0, d > 0$  and  $A_0 = 1.35, B_0 = 0.31, C_0 = 0.75$ .

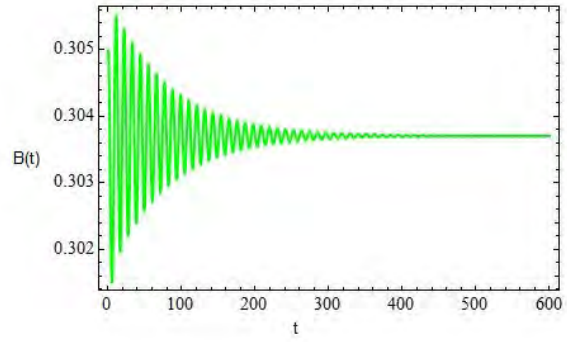
**Example 4.7.6.** Assume that  $\beta = 10, \alpha = 2, 0.99 = \delta_1, 0.4 = \gamma, \delta_2 = 0.01, \delta_3 = 0.80, \delta_4 = 0.60, r_1 = 1, r_2 = 2$  and  $K > 0$ . Then, from system (4.0.1) we get:

$$\begin{aligned}
 A'(t) &= KA(t) - 0.99A(t)B(t) - \frac{0.01A(t)E}{2 + A(t)} - \frac{0.60A(t)C(t)}{10 + A(t)} - dA(t)^2, \\
 B'(t) &= 0.99A(t)B(t) + \frac{0.01A(t)B(t)}{2 + A(t)} - \frac{0.80B(t)C(t)}{0.4 + B(t)} - dB(t), \\
 C'(t) &= \frac{1(0.80)C(t)B(t)}{0.4 + B(t)} + \frac{2(0.60)A(t)Q}{10 + A(t)} - dC(t).
 \end{aligned} \tag{4.7.4}$$

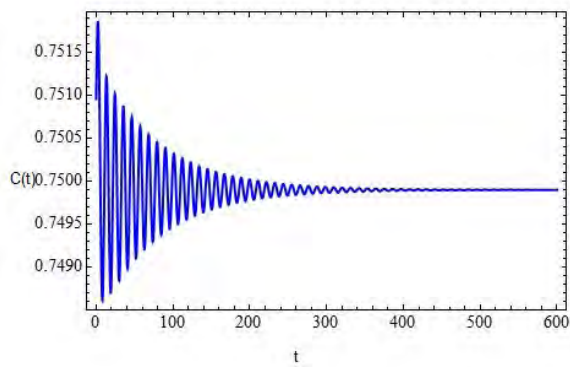
From (Fig. 4.5), it is clear that the system (4.7.4) is stable for  $d \leq 1$ . Moreover, in (Fig. 4.11) the stable plots for every variable, that is,  $A(t)$ ,  $B(t)$  and  $C(t)$  are specified in (Fig. 4.11a), (Fig. 4.11b) and (Fig. 4.11c) respectively. In addition, some phase portraits are also provided in (Fig. 4.11). Finally, it can be observed that the system (4.7.4) experiences an unstable behaviour if the death parameter  $d$  exceeds 1.



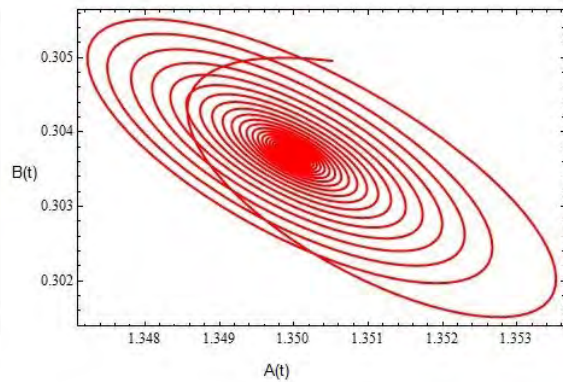
(a)



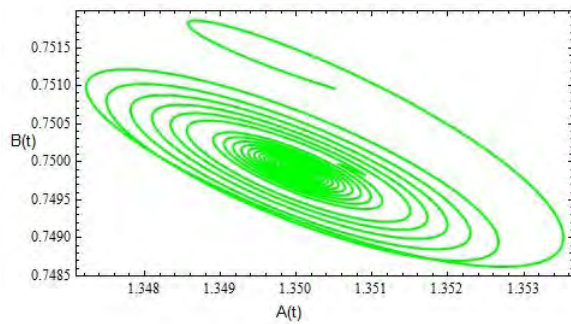
(b)



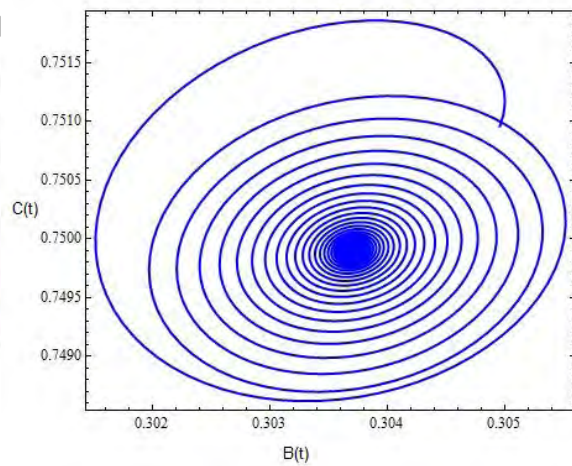
(c)



(d)



(e)



(f)

Figure 4.11: Some plots and phase portraits for system (4.7.4) for  $\beta = 10, \alpha = 2, 0.99 = \delta_1, 0.4 = \gamma, \delta_2 = 0.01, \delta_3 = 0.80, \delta_4 = 0.60, r_1 = 1, r_2 = 2, K > 0, d > 0$  and  $A(0) = 1.35, B(0) = 0.31, C(0) = 0.75$ .

## 4.8 Concluding remarks

We discussed the dynamics of a discrete-time mathematical system for people suffering from diabetes or hypertension and then exposed to coronavirus. For the study of the continuous-time counterpart of our system with Z-control, an individual can see [101]. Firstly, by implementing the method of piecewise constant arguments, we obtained a discrete counterpart of the mathematical system (4.0.1). Moreover, for this chapter, we have taken a case study from India with an initial stage of the coronavirus pandemic at the start of the year 2020 [101]. By taking the situation that the exposed population ( $B$ ) always stay finite, the boundedness for each solution of the system (4.1.3) is shown. A strong result for boundedness is provided in **section 4.2**. The stability analysis of the system (4.1.3) about each of its fixed points is discussed in **section 4.3**. Moreover, some mathematical conditions related to the presence of positive fixed points are given in **Section 4.3**. In **Section 4.4**, the linearized stability of (4.1.3) about its positive fixed point is discussed. It is revealed that for  $C_m \rightarrow 0, \forall m$ , the system (4.1.3) experiences chaos and period-doubling bifurcation (see **Section 4.5**). In the direction to show the complexity in the system (4.1.3), the presence of Neimark-Sacker bifurcation for positive fixed point is proved. A stability association of discrete-time system (4.1.3) with its continuous counterpart (4.0.1) for parameter  $d$  is provided in **Example 4.7.1** and **Example 4.7.3**. One can see that our discrete-time system experiences chaos whenever an exposed person to COVID-19 does not isolate himself, to be exact, for  $C_m \rightarrow 0, \forall m$ . Hence, the system (4.1.3) represents a chaotic system under these conditions, but for system (4.0.1), if  $C(t) \rightarrow 0$ , then system (4.0.1) decreases to a 2-dimensional continuous system, wherein chaos can never be experienced (see [9]). Therefore, our discrete-time mathematical system (4.1.3) will stay bounded when  $B$  is bounded, and it becomes unbounded when  $B$  is unbounded. Additionally, quarantine is necessary for a person infected by coronavirus, such that the system (4.1.3) remains stable.

## Chapter 5

# Dynamics of a Discrete-Time Fractional-Order Phytoplankton-Zooplankton Model with Holling Type-II Response

This chapter examines qualitative findings related to a discrete-time model of phytoplankton-zooplankton dynamics, which incorporates the Holling type-II response. The discrete-time model is obtained by discretizing a continuous-time model using fractional order techniques. The stability of the resulting system is analyzed locally for all equilibrium points, and the presence of a Neimark-Sacker bifurcation around the positive equilibrium is demonstrated based on specific mathematical conditions. To address this bifurcation, two modified hybrid control techniques are proposed. Additionally, numerical examples are presented to validate the theoretical analysis, evaluate the effectiveness and feasibility of the newly developed control strategies, and compare them with an existing hybrid technique.. The findings of this chapter are submitted in an extreme international journal.

### 5.1 Discretization of model

There are many mathematical methods available for discretization of any mathematical model from continuous form to discrete form. Some of them are the following:

- Euler method
- Method of piecewise arguments
- Nonstandard finite difference schemes
- Runge-Kutta method

- Method of Fractional order derivatives.

However, the fractional order differential equations (FOD) provides us a useful tool for modeling genetic effects and many other processes of nature [102]. Many scientific phenomena are modeled by using fractional derivatives such as nonlinear oscillations of earthquake, wave propagation models, hydrologic models and diffusion of wave models [112-114]. Moreover, the study of many natural interactions by FOD is much better than integer order differential equations [102]. Therefore, many researchers have used fractional order differential equations for dynamical study of population models in mathematical biology [115-118]. There are many well known definitions for fractional order derivatives. Among them the most favorable and useful definition is given as follows [109]:

$$\begin{cases} D^\alpha g(t) = \mathfrak{J}^{n-\alpha} D^n g(t), \\ D \equiv \frac{d}{dt}, \end{cases} \quad (5.1.1)$$

where,  $n \in \mathbb{Z}^+$ , and  $\alpha \in (n-1, n)$  is order of of fractional derivative of  $g(t)$ .  $\mathfrak{J}^\theta$  represents the  $\theta$  ordered Riemann-Liouville operator [109], which has the following mathematical form:

$$\mathfrak{J}^\theta f(t) = \frac{1}{\Gamma(\theta)} \int_0^t (t-\varepsilon)^{\theta-1} f(\varepsilon) d\varepsilon, \theta > 0.$$

Here,  $\Gamma(\theta)$  is Euler's gamma function. By applying operator (5.1.1) on system (3.0.2), we get the following system

$$\begin{cases} D^\alpha p(t) = rp(t)(1 - \frac{p(t)}{k}) - \beta \frac{p(t)}{\gamma+p(t)} z(t), \\ D^\alpha z(t) = b \frac{p(t)}{\gamma+p(t)} z(t) - \delta z(t) - \rho \frac{p(t)}{\gamma+p(t)} z(t), \quad t > 0, \end{cases} \quad (5.1.2)$$

where  $p_0 > 0$  and  $z_0 > 0$  are initial conditions. Now, proceeding the discretization by using piecewise arguments (see [29-31]), we get

$$\begin{cases} D^\alpha p(t) = rp([t/s]s)(1 - \frac{p([t/s]s)}{k}) - \beta \frac{p([t/s]s)}{\gamma+p([t/s]s)} z([t/s]s), \\ D^\alpha z(t) = b \frac{p([t/s]s)}{\gamma+p([t/s]s)} z([t/s]s) - \delta z([t/s]s) - \rho \frac{p([t/s]s)}{\gamma+p([t/s]s)} z([t/s]s). \end{cases} \quad (5.1.3)$$

Suppose that  $t \in [0, s)$ , then  $t/s \in [0, 1)$ , and we have

$$\begin{cases} D^\alpha p(t) = rp_0(1 - \frac{p_0}{k}) - \beta \frac{p_0}{\gamma+p_0} z_0, \\ D^\alpha z(t) = b \frac{p_0}{\gamma+p_0} z_0 - \delta z_0 - \rho \frac{p_0}{\gamma+p_0} z_0, \quad t \in [0, s). \end{cases} \quad (5.1.4)$$

On solving (5.1.4), we get the following solution

$$\begin{cases} p_1(t) = p_0 + \frac{t^\alpha}{\alpha\Gamma(\alpha)} \left( rp_0(1 - \frac{p_0}{k}) - \beta \frac{p_0}{\gamma+p_0} z_0 \right), \\ z_1(t) = z_0 + \frac{t^\alpha}{\alpha\Gamma(\alpha)} \left( b \frac{p_0}{\gamma+p_0} z_0 - \delta z_0 - \rho \frac{p_0}{\gamma+p_0} z_0 \right). \end{cases} \quad (5.1.5)$$

For second iteration, we take  $t \in [s, 2s)$  then  $t/s \in [1, 2)$ . Hence, we have

$$\begin{cases} D^\alpha p(t) = rp_1(1 - \frac{p_1}{k}) - \beta \frac{p_1}{\gamma+p_1} z_1, \\ D^\alpha z(t) = b \frac{p_1}{\gamma+p_1} z_1 - \delta z_1 - \rho \frac{p_1}{\gamma+p_1} z_1, \quad t \in [s, 2s). \end{cases} \quad (5.1.6)$$

On solving (5.1.6) we get the following solution

$$\begin{cases} p_1(t) = p_1(s) + \frac{(t-s)^\alpha}{\alpha\Gamma(\alpha)} \left( rp_1(s) \left(1 - \frac{p_1(s)}{k}\right) - \beta \frac{p_1(s)}{\gamma+p_1(s)} z_1(s) \right), \\ z_1(t) = z_1(s) + \frac{(t-s)^\alpha}{\alpha\Gamma(\alpha)} \left( b \frac{p_1(s)}{\gamma+p_1(s)} z_1(s) - \delta z_1(s) - \rho \frac{p_1(s)}{\gamma+p_1(s)} z_1(s) \right). \end{cases} \quad (5.1.7)$$

Repeating this process of discretization  $n$  times, we get the following system

$$\begin{cases} p_{n+1}(t) = p_n(ns) + \frac{(t-ns)^\alpha}{\alpha\Gamma(\alpha)} \left( rp_n(ns) \left(1 - \frac{p_n(ns)}{k}\right) - \beta \frac{p_n(ns)}{\gamma+p_n(ns)} z_n(ns) \right), \\ z_{n+1}(t) = z_n(ns) + \frac{(t-ns)^\alpha}{\alpha\Gamma(\alpha)} \left( b \frac{p_n(ns)}{\gamma+p_n(ns)} z_n(ns) - \delta z_n(ns) - \rho \frac{p_n(ns)}{\gamma+p_n(ns)} z_n(ns) \right), \\ t \in [ns, (n+1)s). \end{cases} \quad (5.1.8)$$

In addition when  $t/s \rightarrow n+1$ , then system (5.1.8) takes the following form:

$$\begin{cases} p_{n+1} = p_n + \frac{s^\alpha}{\alpha\Gamma(\alpha)} \left( rp_n \left(1 - \frac{p_n}{k}\right) - \frac{\beta p_n z_n}{\gamma+p_n} \right), \\ z_{n+1} = z_n + \frac{s^\alpha}{\alpha\Gamma(\alpha)} \left( \frac{bp_n z_n}{\gamma+p_n} - \delta z_n - \frac{\rho p_n z_n}{\gamma+p_n} \right). \end{cases} \quad (5.1.9)$$

The remaining part of the chapter is aimed at: the existence of fixed points and local stability analysis of system (5.1.9), the existence of Neimark-Sacker bifurcation about the positive fixed point of system (5.1.9), the control of Neimark-Sacker bifurcation in the system (5.1.9) by using a modified control strategy, some numerical simulation which strengthens our theoretical discussion.

## 5.2 Existence of fixed points

In order to obtain fixed points of the system (5.1.9), we consider the following two dimensional system of equations:

$$\begin{cases} \frac{s^\alpha}{\alpha\Gamma(\alpha)} \left( rp_* \left(1 - \frac{p_*}{k}\right) - \frac{\beta p_* z_*}{\gamma+p_*} \right) = 0, \\ \frac{s^\alpha}{\alpha\Gamma(\alpha)} \left( \frac{bp_* z_*}{\gamma+p_*} - \delta z_* - \frac{\rho p_* z_*}{\gamma+p_*} \right) = 0. \end{cases} \quad (5.2.1)$$

On solving system (5.2.1) one can obtain three fixed points,  $(p_0, z_0) = (0, 0)$ ,  $(p_1, z_1) = (k, 0)$  and

$$\left( \frac{\gamma\delta}{b - \delta - \rho}, \frac{r\gamma(\rho - b)(k\delta - bk + \gamma\delta + k\rho)}{k\beta(b - \delta - \rho)^2} \right) = (p_*, z_*).$$

Furthermore, if

$$\begin{cases} \rho + \delta < b, \\ \text{and} \\ \gamma\delta < (b - \delta - \rho)k, \end{cases} \quad (5.2.2)$$

then,  $p_* > 0$  and  $z_* > 0$ . In order to discuss the stability of the system (5.1.9) about these fixed points, we compute the variational matrix  $J_{(p,z)}$  of the system (5.1.9) about



each of its fixed point  $(p, z)$ . Moreover,  $J_{(p,z)}$  is

$$J_{(p,z)} = \begin{bmatrix} j_{11} & j_{12} \\ j_{21} & j_{22} \end{bmatrix}.$$

In addition, the characteristic polynomial  $\mathbb{H}(\xi) = 0$  of  $J_{(p,z)}$  is:

$$\mathbb{H}(\xi) = \xi^2 - T\xi + D, \quad (5.2.3)$$

where

$$T = (j_{11} + j_{22}),$$

and

$$D = j_{11}j_{22} - j_{12}j_{21}.$$

### 5.3 Local stability analysis

Firstly, we study the stability conditions for (5.1.9) about the fixed point  $(p_0, z_0)$ . The matrix  $J_{(p,z)}$  evaluated at  $(p_0, z_0)$  is given by;

$$J_{(p_0,z_0)} = \begin{bmatrix} 1 + \frac{rs^\alpha}{\Gamma(1+\alpha)} & 0 \\ 0 & 1 - \frac{s^\alpha\delta}{\Gamma(1+\alpha)} \end{bmatrix}.$$

Furthermore,  $J_{(p_0,z_0)}$  has the following characteristic equation:

$$\mathbb{H}(\xi) = \xi^2 - \xi \left( 2 + \frac{s^\alpha(r - \delta)}{\Gamma(1 + \alpha)} \right) + \frac{(rs^\alpha + \Gamma(1 + \alpha))(-s^\alpha\delta + \Gamma(1 + \alpha))}{\Gamma^2(1 + \alpha)}.$$

$\mathbb{H}(\xi) = 0$  has two characteristic values, namely  $\xi_1 = \frac{rs^\alpha + \Gamma(1 + \alpha)}{\Gamma(1 + \alpha)}$  and  $\xi_2 = \frac{-s^\alpha\delta + \Gamma(1 + \alpha)}{\Gamma(1 + \alpha)}$ . Moreover, it is clear that  $|\xi_1| > 1$  for all parametric values. Hence, by using **Lemma 1.3.1** and by considering the condition  $|\xi_1| > 1$  as a true condition, we are now able to describe stability conditions for (5.1.9) about  $(p_0, z_0)$ .

**Proposition 5.3.1.** *Let  $(p_0, z_0) = (0, 0)$  be an equilibrium point of system (5.1.9) then  $(p_0, z_0)$  is source and saddle iff conditions  $\Gamma(1 + \alpha) > s^\alpha\delta$  and  $2\Gamma(1 + \alpha) < s^\alpha\delta$  respectively holds true.*

Next, our task is to explore of the local stability of system (5.1.9) about the point  $(p_1, z_1)$ . Let  $J_{(p_1,z_1)}$  be the jacobian matrix of system (5.1.9) about the fixed point  $(p_1, z_1)$ , then  $J_{(p_1,z_1)}$  has the following mathematical form:

$$J_{(p_1,z_1)} = \begin{bmatrix} 1 - \frac{rs^\alpha}{\Gamma(1+\alpha)} & -\frac{ks^\alpha\beta}{(k+\gamma)\Gamma(1+\alpha)} \\ 0 & 1 + \frac{s^\alpha(bk - (k+\gamma)\delta - k\rho)}{\alpha(k+\gamma)\Gamma(\alpha)} \end{bmatrix}.$$

Moreover, from  $J_{(p_1, z_1)}$  we can get the following characteristic polynomial:

$$\begin{aligned} \mathbb{H}(\xi) &= \xi^2 - \xi \left( 2 + \frac{s^\alpha (bk - (k + \gamma)(r + \delta) - k\rho)}{(k + \gamma)\Gamma(1 + \alpha)} \right) \\ &\quad - \frac{(s^\alpha (bk - (k + \gamma)\delta - k\rho) + \alpha(k + \gamma)\Gamma(\alpha)) (rs^\alpha - \Gamma(1 + \alpha))}{(k + \gamma)\Gamma^2(1 + \alpha)}. \end{aligned}$$

Hence, by using **Lemma 1.3.1**, one can write the following proposition about the local stability of (5.1.9) about  $(p_1, z_1) = (k, 0)$ .

**Proposition 5.3.2.** *Let  $(p_1, z_1) = (k, 0)$  be a fixed point of system (5.1.9), then:*

- *The point  $(p_1, z_1)$  is stable if and only if*

$$\left\{ \begin{array}{l} rs^\alpha < 2\Gamma(1 + \alpha) \text{ and } s^\alpha bk + (k + r)(s^\alpha \delta + 2\Gamma(1 + \alpha)) > k\rho, \\ \text{or } rs^\alpha > 2\Gamma(1 + \alpha), \text{ and } s^\alpha bk + (k + r)(s^\alpha \delta + 2\Gamma(1 + \alpha)) < k\rho, \\ \text{and} \\ \left( s^\alpha \frac{(b-\rho)}{k+\gamma} + \Gamma(1 + \alpha) - \delta s^\alpha \right) (rs^\alpha - \Gamma(1 + \alpha)) < \Gamma^2(1 + \alpha). \end{array} \right.$$

- *The point  $(p_1, z_1)$  is unstable if and only if*

$$\left\{ \begin{array}{l} rs^\alpha < 2\Gamma(1 + \alpha) \text{ and } s^\alpha bk + (k + r)(s^\alpha \delta + 2\Gamma(1 + \alpha)) > k\rho, \\ \text{or } rs^\alpha > 2\Gamma(1 + \alpha), \text{ and } s^\alpha bk + (k + r)(s^\alpha \delta + 2\Gamma(1 + \alpha)) < k\rho, \\ \text{and} \\ \left( s^\alpha \frac{(b-\rho)}{k+\gamma} + \Gamma(1 + \alpha) - \delta s^\alpha \right) (rs^\alpha - \Gamma(1 + \alpha)) > \Gamma^2(1 + \alpha). \end{array} \right.$$

- *The point  $(p_1, z_1)$  is saddle point if and only if*

$$(rs^\alpha - 2\Gamma(1 + \alpha))(s^\alpha (bk - (k + \gamma)\delta - k\rho) + 2(k + \gamma)\Gamma(1 + \alpha)) > 0.$$

- *The point  $(p_1, z_1)$  can never be non hyperbolic fixed point.*

Ultimately, we have some results related to the local stability of system (5.1.9) about  $(p_*, z_*) = \left( \frac{\gamma\delta}{b-\delta-\rho}, \frac{r\gamma(\rho-b)(k\delta-bk+\gamma\delta+k\rho)}{k\beta(\delta+\rho-b)^2} \right)$ . Furthermore, both components of  $(p_*, z_*)$  are positive if and only if (5.2.2) remains true. One can calculate the jacobian matrix  $J_{(p_*, z_*)}$  of the system (5.1.9) about  $(p_*, z_*)$  as follows:

$$J_{(p_*, z_*)} = \begin{bmatrix} 1 + \frac{rs^\alpha \delta (b(-k+\gamma) + (k+\gamma)\delta + (k-\gamma)\rho)}{\frac{k(b-\rho)(-b+\delta+\rho)\Gamma(1+\alpha)}{r s^\alpha (bk-\gamma\delta-k(\delta+\rho))}} & -\frac{s^\alpha \beta \delta}{b\alpha\Gamma(\alpha) - \alpha\rho\Gamma(\alpha)} \\ \frac{rs^\alpha (bk-\gamma\delta-k(\delta+\rho))}{k\alpha\beta\Gamma(\alpha)} & 1 \end{bmatrix}.$$

Let (5.2.3) is characteristic polynomial obtained from matrix  $J_{(p_*, z_*)}$ , where

$$T = 2 + \frac{rs^\alpha \delta (b(-k + \gamma) + (k + \gamma)\delta + (k - \gamma)\rho)}{k(b - \rho)(-b + \delta + \rho)\Gamma(1 + \alpha)},$$

and

$$D = 1 + \frac{rs^\alpha \delta \left( -s^\alpha (-bk + \gamma\delta + k(\delta + \rho)) + \frac{(b(-k+\gamma)+\gamma(\delta-\rho)+k(\delta+\rho))\Gamma(1+\alpha)}{-b+\delta+\rho} \right)}{k(b-\rho)\Gamma^2(1+\alpha)}.$$

By considering that (5.2.2) is true, and by performing some mathematical calculations it follows that:

$$\mathbb{H}(1) = \frac{rs^{2\alpha} \delta (\gamma - bk + \delta + k(\delta + \rho))}{k(\rho - b)\Gamma^2(1 + \alpha)} > 0,$$

and

$$\mathbb{H}(-1) = 4 + \frac{rs^\alpha \delta \left( -s^\alpha (-bk + \gamma\delta + k(\delta + \rho)) + \frac{2(b(-k+\gamma)+\gamma(\delta-\rho)+k(\delta+\rho))\Gamma(1+\alpha)}{-b+\delta+\rho} \right)}{k(b-\rho)\Gamma^2(1+\alpha)}.$$

Hence, the local stability of system (5.1.9) about  $(p_*, z_*) = \left( \frac{\gamma\delta}{b-\delta-\rho}, \frac{r\gamma(\rho-b)(k\delta-bk+\gamma\delta+k\rho)}{k\beta(\delta+\rho-b)^2} \right)$  can be studied by using the following proposition (see **Lemma 1.3.1**).

**Proposition 5.3.3.** *Let (5.2.2) remains true, then  $(p_*, z_*) = \left( \frac{\gamma\delta}{b-\delta-\rho}, \frac{r\gamma(\rho-b)(k\delta-bk+\gamma\delta+k\rho)}{k\beta(\delta+\rho-b)^2} \right)$  is positive fixed point of (5.1.9). In addition, suppose*

$$\kappa = 2(b(\gamma - k) + \gamma(\delta - \rho) + k(\delta + \rho))\Gamma(1 + \alpha),$$

then:

- The point  $(p_*, z_*)$  is stable fixed point if and only if

$$b(\gamma - k) + r(\delta - \rho) + k(\delta + \rho) < k(\rho - b)\Gamma(1 + \alpha) \quad \text{and} \quad \kappa < 0.$$

- The point  $(p_*, z_*)$  is unstable fixed point if and only if

$$b(\gamma - k) + r(\delta - \rho) + k(\delta + \rho) < k(\rho - b)\Gamma(1 + \alpha) \quad \text{and} \quad \kappa > 0.$$

- The point  $(p_*, z_*)$  is saddle fixed point if and only if

$$\frac{\kappa}{\delta + \rho - b} < 4k(\rho - b)\Gamma^2(1 + \alpha),$$

- The point  $(p_*, z_*)$  is non-hyperbolic if and only if

$$s = \left( \frac{(b(-k+\gamma)+\gamma(\delta-\rho)+k(\delta+\rho))\Gamma(1+\alpha)}{(-b+\delta+\rho)(-bk+\gamma\delta+k(\delta+\rho))} \right)^{\frac{1}{\alpha}},$$

and

$$4k(b-\rho)(-bk + \gamma\delta + k(\delta + \rho))(-b + \delta + \rho)^2 + r\delta(b(-k + \gamma) + \gamma(\delta - \rho) + k(\delta + \rho))^2 < 0. \quad (5.3.1)$$

**Remark 5.3.1.** The system (5.1.9) can never experiences the period-doubling bifurcation as  $\mathbb{H}(-1) < 0$  for all  $a, b, r, k, \gamma, \delta, \rho, \beta > 0$ .

We have the following theorem for the possible validation of **Remark. 5.3.1.**

**Theorem 5.3.1.** Assume that (5.2.2) holds true and  $(\frac{\gamma\delta}{b-\delta-\rho}, \frac{r\gamma(\rho-b)(k\delta-bk+\gamma\delta+k\rho)}{k\beta(\delta+\rho-b)^2})$  be one and only positive fixed point of system (5.1.9) and

$$\mathbb{H}(-1) = 4 + \frac{rs^\alpha\delta \left( -s^\alpha(\gamma\delta - bk + k(\delta + \rho)) + \frac{2(b(\gamma-k)+\gamma(\delta-\rho)+k(\delta+\rho))\Gamma(1+\alpha)}{\delta+\rho-b} \right)}{k(b-\rho)\Gamma^2(1+\alpha)}.$$

Then  $\mathbb{H}(-1) < 0$  for each value of parameters given in (5.1.9). Consequently,  $\mathbb{H}(-1)$  is decreasing for all  $a, b, r, k, \gamma, \delta, \rho, \beta > 0$ .

*Proof.* Assume that (5.2.2) holds true and  $(\frac{\gamma\delta}{b-\delta-\rho}, \frac{r\gamma(\rho-b)(-bk+k\delta+\gamma\delta+k\rho)}{k\beta(-b+\delta+\rho)^2})$  be one and only positive fixed point of system (5.1.9) and

$$\mathbb{H}(-1) = 4 + \frac{rs^\alpha\delta \left( -s^\alpha(\gamma\delta - bk + k(\delta + \rho)) + \frac{2(b(\gamma-k)+\gamma(\delta-\rho)+k(\delta+\rho))\Gamma(1+\alpha)}{\delta+\rho-b} \right)}{k(b-\rho)\Gamma^2(1+\alpha)}.$$

Then  $\mathbb{H}(-1) < 0$  if and only if

$$4 + \frac{rs^\alpha\delta \left( -s^\alpha(\gamma\delta - bk + k(\delta + \rho)) + \frac{2(b(\gamma-k)+\gamma(\delta-\rho)+k(\delta+\rho))\Gamma(1+\alpha)}{\delta+\rho-b} \right)}{k(b-\rho)\Gamma^2(1+\alpha)} < 0 \quad (5.3.2)$$

□

## 5.4 Bifurcation analysis

Here, we will discuss the Neimark-Sacker bifurcation experienced by system (5.1.9) about  $(p_*, z_*)$  under some mathematical conditions.

### 5.4.1 Neimark-Sacker bifurcation

Let  $\xi_1$  and  $\xi_2$  are roots of (5.2.3), then both of these roots are complex conjugates with unit modulus if  $(p_*, z_*)$  is non-hyperbolic fixed point under the last condition (5.3.1) of **Proposition 5.3.3.** Hence (5.1.9) experiences the Neimark-Sacker bifurcation when (5.3.1) is satisfied and parameters given in system (5.1.9) are varied in the small neighborhood of the following set:

$$\mathcal{U}_* = \left\{ \alpha, \beta, b, k, r, s, \gamma, \delta, \rho \in \mathfrak{R}^+, s = \left( \frac{(b(\gamma-k) + \gamma(\delta-\rho) + k(\delta+\rho))\Gamma(1+\alpha)}{(\delta+\rho-k)(\gamma\delta - bk + k(\delta+\rho))} \right)^{\frac{1}{\alpha}} \right\}.$$

Where,  $s \in (0, 1]$ . Let  $(\alpha, \beta, b, k, r, s, \gamma, \delta, \rho) \in \mathcal{U}_*$  with  $s_1 = \left( \frac{(b(\gamma-k)+\gamma(\delta-\rho)+k(\delta+\rho))\Gamma(1+\alpha)}{(\delta+\rho-k)(\gamma\delta-bk+k(\delta+\rho))} \right)^{\frac{1}{\alpha}}$  then system (5.1.9) can be written as;

$$\begin{pmatrix} p \\ z \end{pmatrix} \rightarrow \begin{pmatrix} p + \frac{s_1^\alpha}{\alpha\Gamma(\alpha)} \left( rp(1 - \frac{p}{k}) - \frac{\beta pz}{\gamma+p} \right) \\ z + \frac{s_1^\alpha}{\alpha\Gamma(\alpha)} \left( \frac{bpz}{\gamma+p} - \delta z - \frac{\rho pz}{\gamma+p} \right) \end{pmatrix}. \quad (5.4.1)$$

Consider the perturbation of (5.4.1) by using the parameter  $\hat{s}$ . Moreover, by taking  $\hat{s}$  as bifurcation parameter we get the following form of system (5.4.1):

$$\begin{pmatrix} p \\ z \end{pmatrix} \rightarrow \begin{pmatrix} p + \frac{(s_1+\hat{s})^\alpha}{\alpha\Gamma(\alpha)} \left( rp(1 - \frac{p}{k}) - \frac{\beta pz}{\gamma+p} \right) \\ z + \frac{(s_1+\hat{s})^\alpha}{\alpha\Gamma(\alpha)} \left( \frac{bpz}{\gamma+p} - \delta z - \frac{\rho pz}{\gamma+p} \right) \end{pmatrix}, \quad (5.4.2)$$

where,  $|\hat{s}| \ll 1$ . Next, we consider that  $X = p - \frac{\gamma\delta}{b-\delta-\rho}$ ,  $Y = z - \frac{r\gamma(\rho-b)(k\delta-bk+\gamma\delta+k\rho)}{k\beta(-b+\delta+\rho)^2}$ , then the map (5.4.1) is changed into the following form:

$$\begin{pmatrix} X \\ Y \end{pmatrix} \rightarrow \begin{pmatrix} v_{11} & v_{12} \\ v_{21} & v_{22} \end{pmatrix} \begin{pmatrix} X \\ Y \end{pmatrix} + \begin{pmatrix} j_1(X, Y) \\ j_2(X, Y) \end{pmatrix}, \quad (5.4.3)$$

where

$$\begin{aligned} j_1(X, Y) &= v_{13}X^2 + v_{14}XY + v_{15}X^3 + v_{16}X^2Y + O((|X| + |Y|)^4), \\ j_2(X, Y) &= v_{23}X^2 + v_{24}XY + v_{25}X^3 + v_{26}X^2Y + O((|X| + |Y|)^4), \\ v_{11} &= -\frac{(s_1 + \hat{s})^\alpha r(\gamma b\delta + \gamma\delta^2 - \gamma\delta\rho - b\delta k + \delta^2 k + \delta k\rho)}{(b - \delta - \rho) k (b - \rho) \alpha\Gamma(\alpha)} \\ &\quad + \frac{\alpha\Gamma(\alpha)k(b^2 + b\delta + 2b\rho - \delta\rho - \rho^2)}{(b - \delta - \rho) k (b - \rho) \alpha\Gamma(\alpha)}, \\ v_{12} &= -\frac{(s_1 + \hat{s})^\alpha \beta \delta}{\alpha\Gamma(\alpha) (b - \rho)}, \\ v_{13} &= \frac{(s_1 + \hat{s})^\alpha}{\alpha\Gamma(\alpha)} \left( -\frac{r}{k} + \frac{(bkr - \gamma\delta r - \delta kr - kr\rho)(b - \delta - \rho)}{(b - \rho)^2 k\gamma} \right), \end{aligned}$$

$$\begin{aligned}
v_{14} &= -\frac{(s_1 + \hat{s})^\alpha \beta (b - \delta - \rho)^2}{(b - \rho)^2 \alpha \gamma \Gamma(\alpha)}, \\
v_{15} &= \frac{(s_1 + \hat{s})^\alpha r (-bk + \delta \gamma + \delta k + k\rho) (b - \delta - \rho)^2}{\alpha \Gamma(\alpha) (b - \rho)^3 k \gamma^2}, \\
v_{16} &= \frac{(s_1 + \hat{s})^\alpha \beta (b - \delta - \rho)^3}{\alpha \Gamma(\alpha) (b - \rho)^3 \gamma^2}, \quad v_{21} = -\frac{(-bk + \delta \gamma + \delta k + k\rho) (s_1 + \hat{s})^\alpha r}{k \beta \Gamma(\alpha) \alpha}, \\
v_{22} &= 1, \quad v_{23} = \frac{(b - \delta - \rho) (-bk + \delta \gamma + \delta k + k\rho) r (s_1 + \hat{s})^\alpha}{(b - \rho) k \beta \gamma \alpha \Gamma(\alpha)}, \\
v_{24} &= \frac{(b - \delta - \rho)^2 (s_1 + \hat{s})^\alpha}{(b - \rho) \alpha \Gamma(\alpha) \gamma}, \\
v_{25} &= -\frac{(b - \delta - \rho)^2 (-bk + \delta \gamma + \delta k + k\rho) r (s_1 + \hat{s})^\alpha}{(b - \rho)^2 k \beta \gamma^2 \alpha \Gamma(\alpha)}, \\
v_{26} &= -\frac{(b - \delta - \rho)^3 (s_1 + \hat{s})^\alpha}{(b - \rho)^2 \gamma^2 \alpha \Gamma(\alpha)}.
\end{aligned}$$

The characteristic equation  $\mathbb{H}(\xi) = 0$  generated by the jacobian matrix of (5.4.3) about  $(0, 0)$  can be given as:

$$\xi^2 - T(\hat{s})\xi + D(\hat{s}) = 0, \quad (5.4.4)$$

where

$$T(s_1) = 2 + \frac{r(s_1 + \hat{s})^\alpha \delta (b(\gamma - k) + (k + \gamma)\delta + (k - \gamma)\rho)}{k(b - \rho)(\delta + \rho - b)\Gamma(1 + \alpha)},$$

and

$$D(s_1) = 1 + \frac{r(s_1 + \hat{s})^\alpha \alpha \delta \left( -s^\alpha (\gamma \delta - bk + k(\delta + \rho)) + \frac{(b(\gamma - k) + \gamma(\delta - \rho) + k(\delta + \rho))\Gamma(1 + \alpha)}{\delta + \rho - b} \right)}{k(b - \rho)\Gamma^2(1 + \alpha)}.$$

Assume that  $(\alpha, \beta, b, k, r, s, \gamma, \delta, \rho) \in \mathcal{U}_*$ , then the complex roots for (5.4.4) are computed as follows:

$$\xi_1 = \frac{T(s_1) - i\sqrt{4D(s_1) - T^2(s_1)}}{2}$$

and

$$\xi_2 = \frac{T(s_1) + i\sqrt{4D(s_1) - T^2(s_1)}}{2}.$$

Then it easily follows that

$$|\xi_1| = |\xi_2| = \sqrt{1 + \frac{r(s_1 + \hat{s})^\alpha \alpha \delta \left( -s^\alpha (\gamma \delta - bk + k(\delta + \rho)) + \frac{(b(\gamma - k) + \gamma(\delta - \rho) + k(\delta + \rho))\Gamma(1 + \alpha)}{\delta + \rho - b} \right)}{k(b - \rho)\Gamma^2(1 + \alpha)}}.$$

Moreover, we get

$$\begin{aligned} & \frac{d}{ds_1} \left( \sqrt{1 + \frac{r(s_1 + \hat{s})\alpha\delta \left( -s^\alpha(\gamma\delta - bk + k(\delta + \rho)) + \frac{(b(\gamma-k) + \gamma(\delta-\rho) + k(\delta+\rho))\Gamma(1+\alpha)}{\delta+\rho-b} \right)}{k(b-\rho)\Gamma^2(1+\alpha)}} \right) \Big|_{s_1=0} = \\ & - \frac{r\hat{s}^{\alpha-1}\alpha\delta(b(\gamma-k) + \gamma(\delta-\rho) + k(\delta+\rho))}{2k(b-\rho)(b-\delta-\rho)\Gamma_{1+\alpha}\sqrt{1 + \frac{r\hat{s}^\alpha\delta \left( (-\hat{s})^\alpha(\gamma\delta - bk + k(\delta+\rho)) + \frac{(b(\gamma-k) + \gamma(\delta-\rho) + k(\delta+\rho))\Gamma_{1+\alpha}}{\delta-b+\rho} \right)}{k(b-\rho)\Gamma_{1+\alpha}^2}}} \neq 0. \end{aligned}$$

Since  $|T(0)| < 2$  as  $(\alpha, \beta, b, k, r, s, \gamma, \delta, \rho) \in \mathfrak{U}_*$ . Moreover, a simple computation yields that

$$T(0) = 2 + \frac{r\hat{s}^\alpha\delta(b(\gamma-k) + (k+\gamma)\delta + (k-\gamma)\rho)}{k(b-\rho)(\delta+\rho-b)\Gamma(1+\alpha)},$$

and we suppose that  $T(0) \neq 0$  and  $T(0) \neq 1$ , that is,

$$r\hat{s}^\alpha\delta(b(\gamma-k) + \gamma(\delta-\rho) + k(\delta+\rho)) \neq -2k(b-\rho)(\delta-b+\rho)\Gamma(1+\alpha), \quad (5.4.5)$$

and

$$r\hat{s}^\alpha\delta(b(\gamma-k) + \gamma(\delta-\rho) + k(\delta+\rho)) \neq -k(b-\rho)(\delta+\rho-b)\Gamma(1+\alpha). \quad (5.4.6)$$

Suppose that (5.4.5) and (5.4.6) holds and  $(\alpha, \beta, b, k, r, s, \gamma, \delta, \rho) \in \mathfrak{U}_*$ , then it follows that  $T(0) \neq \pm 2, 0, 1$ , that is,  $\xi_1^m, \xi_2^m \neq 1$  for all  $m \in \{1, 2, 3, 4\}$  at  $s_1 = 0$ . Therefore, both roots of (5.4.4) do not lie in the intersection of the unit circle with the coordinate axes when  $s_1 = 0$ . Furthermore, we suppose that  $\ell = \frac{T(0)}{2}$ , and  $\wp = \frac{1}{2}\sqrt{4D(0) - T^2(0)}$ . Then to convert (5.4.3) into normal form, we consider the next similarity transformation:

$$\begin{pmatrix} X \\ Y \end{pmatrix} = \begin{pmatrix} v_{12} & 0 \\ \ell - v_{11} & -\wp \end{pmatrix} \begin{pmatrix} \phi \\ \psi \end{pmatrix}. \quad (5.4.7)$$

By using transformation (5.4.7), one has the next authoritative form of system (5.4.3):

$$\begin{pmatrix} \phi \\ \psi \end{pmatrix} \rightarrow \begin{pmatrix} \ell & -\wp \\ \wp & \ell \end{pmatrix} \begin{pmatrix} \phi \\ \psi \end{pmatrix} + \begin{pmatrix} \check{f}(\phi, \psi) \\ \check{g}(\phi, \psi) \end{pmatrix}, \quad (5.4.8)$$

where

$$\begin{aligned} \check{f}(\phi, \psi) &= \frac{v_{15}X^3}{v_{12}} + \frac{v_{16}X^2Y}{v_{12}} + \frac{v_{13}X^2}{v_{12}} + \frac{v_{14}XY}{v_{12}} + O((|\phi| + |\psi|)^4), \\ \check{g}(\phi, \psi) &= \left( \frac{(\ell - v_{11})v_{15}}{v_{12}\wp} - \frac{v_{25}}{\wp} \right) X^3 + \left( \frac{(\ell - v_{11})v_{16}}{v_{12}\wp} - \frac{v_{26}}{\wp} \right) X^2Y \\ &+ \left( \frac{(\ell - v_{11})v_{13}}{v_{12}\wp} - \frac{v_{23}}{\wp} \right) X^2 + \left( \frac{(\ell - v_{11})v_{14}}{v_{12}\wp} - \frac{v_{24}}{\wp} \right) YX \\ &+ O((|\phi| + |\psi|)^4). \end{aligned}$$

Where

$$\begin{cases} X = v_{12}\phi, \\ \text{and} \\ Y = (\ell - v_{11})\phi - \wp\psi. \end{cases}$$

Hence, we have the following non-zero real quantities:

$$\Omega = \left( \left[ -\text{Re} \left( \frac{(1 - 2\xi_1)\xi_2^2}{1 - \xi_1} \theta_{20}\theta_{11} \right) - \frac{1}{2}|\theta_{11}|^2 - |\theta_{02}|^2 + \text{Re}(\xi_2\theta_{21}) \right] \right)_{\hat{s}=0},$$

where

$$\begin{cases} \theta_{20} = \frac{1}{8} \left[ \check{f}_{\phi\phi} - \check{f}_{\psi\psi} + 2\check{g}_{\phi\psi} + i \left( \check{g}_{\phi\phi} - \check{g}_{\psi\psi} - 2\check{f}_{\phi\psi} \right) \right], \\ \theta_{11} = \frac{1}{4} \left[ \check{f}_{\phi\phi} + \check{f}_{\psi\psi} + i \left( \check{g}_{\phi\phi} + \check{g}_{\psi\psi} \right) \right], \\ \theta_{02} = \frac{1}{8} \left[ \check{f}_{\phi\phi} - \check{f}_{\psi\psi} - 2\check{g}_{\phi\psi} + i \left( \check{g}_{\phi\phi} - \check{g}_{\psi\psi} + 2\check{f}_{\phi\psi} \right) \right], \\ \theta_{21} = \frac{1}{16} \left[ \check{f}_{\phi\phi\phi} + \check{f}_{\phi\psi\psi} + \check{g}_{\phi\phi\psi} + \check{g}_{\psi\psi\psi} + i \left( \check{g}_{\phi\phi\phi} + \check{g}_{\phi\psi\psi} - \check{f}_{\phi\phi\psi} - \check{f}_{\psi\psi\psi} \right) \right]. \end{cases}$$

Hence, by aforementioned analysis we are now able to discuss the existence and direction of Neimark-Sacker bifurcation in shape of the following theorem [112-118].

**Theorem 5.4.1.** *Assume that (5.4.5) and (5.4.6) holds true, whenever  $s$  varied in small neighborhood of*

$$\hat{s} = \left( \frac{(b(\gamma - k) + \gamma(\delta - \rho) + k(\delta + \rho))\Gamma(1 + \alpha)}{(\delta + \rho - b)(\gamma\delta - bk + k(\delta + \rho))} \right)^{\frac{1}{\alpha}}.$$

Moreover, let

$$\left( \frac{\gamma\delta}{b - \delta - \rho}, \frac{r\gamma(\rho - b)(k\delta - bk + \gamma\delta + k\rho)}{k\beta(b - \delta - \rho)^2} \right) = (p_*, z_*),$$

be unique positive fixed point of system (5.1.9), then the positive fixed point  $(p_*, z_*)$  moves randomly in invariant closed curves produced due to Neimark-Sacker bifurcation. Additionally, if  $\Omega < 0$ , ( $\Omega > 0$ ), respectively, then for  $s > \hat{s}$  an attracting and for  $s < \hat{s}$  a repelling invariant closed curve bifurcate from fixed point.

## 5.5 Chaos control

To control inconsistent, accidental and irregular behavior of any biological system, chaos control is well thought-out to be an applied tool for evading this complex and chaotic behavior. For additional details associated to biological significance of chaos control and its applied use in the actual world, we mention to [22]. In this part thesis, we use a simple chaos control method for system (5.1.9). Furthermore, there are many chaos control techniques for discrete dynamical systems. For additional details connected to these methods, we refer a reader to [105-110].



### 5.5.1 A modified technique for chaos control

We consider a generalized hybrid control technique [22] on system (5.1.9). The generalized hybrid control method [22] is centered on parameter perturbation and a state feedback control technique. By implementing generalized hybrid control methodology (with control parameter  $0 < \mu < 1$ ) to system (5.1.9) we get:

$$\begin{aligned} p_{n+1} &= \mu^3 \left( p_n + \frac{s^\alpha}{\alpha\Gamma(\alpha)} \left( rp_n \left(1 - \frac{p_n}{k}\right) - \frac{\beta p_n z_n}{\gamma + p_n} \right) \right) + (1 - \mu^3) p_n, \\ z_{n+1} &= \mu^3 \left( z_n + \frac{s^\alpha}{\alpha\Gamma(\alpha)} \left( \frac{bp_n z_n}{\gamma + p_n} - \delta z_n - \frac{\rho p_n z_n}{\gamma + p_n} \right) \right) + (1 - \mu^3) z_n. \end{aligned} \quad (5.5.1)$$

Then, system (5.5.1) is controllable provided that its fixed point

$$\left( \frac{\gamma\delta}{b - \delta - \rho}, \frac{r\gamma(\rho - b)(k\delta - bk + \gamma\delta + k\rho)}{k\beta(b - \delta - \rho)^2} \right) = (p_*, z_*),$$

is locally asymptotically stable. Additionally, the jacobian matrix for system (5.5.1) at its positive fixed point  $(p_*, z_*)$  is calculated as follows:

$$\begin{bmatrix} 1 + \frac{rs^\alpha\delta\mu^3(b(-k+\gamma)+(k+\gamma)\delta+(k-\gamma)\rho)}{k(b-\rho)(-b+\delta+\rho)\Gamma(1+\alpha)} & -\frac{s^\alpha\beta\delta\mu^3}{b\alpha\Gamma(\alpha)-\alpha\rho\Gamma(\alpha)} \\ \frac{rs^\alpha\mu^3(bk-\gamma\delta-k(\delta+\rho))}{k\alpha\beta\Gamma(\alpha)} & 1 \end{bmatrix}.$$

**Theorem 5.5.1.** *The positive constant solution  $(p_*, z_*)$  of system (5.5.1) is stable locally asymptotically  $\iff$  the following inequality holds true.*

$$\begin{aligned} & \left| 2 + \frac{rs^\alpha\delta(b(\gamma - k) + (k + \gamma)\delta + (k - \gamma)\rho)\mu^3}{k(b - \rho)(\delta + \rho - b)\Gamma(1 + \alpha)} \right| \\ & < 2 + \frac{rs^\alpha\delta\mu^3 \left( \frac{(b(-k+\gamma)+\gamma(\delta-\rho)+k(\delta+\rho))\Gamma(1+\alpha)}{\delta-b+\rho} - s^\alpha(\gamma\delta - bk + k(\delta + \rho))\mu^3 \right)}{k(b - \rho)\Gamma^2(1 + \alpha)}, \end{aligned}$$

and

$$\frac{(b(\gamma - k) + \gamma(\delta - \rho) + k(\delta + \rho))\Gamma(1 + \alpha)}{\delta - b + \rho} < s^\alpha(\gamma\delta - bk + k(\delta + \rho))\mu^3.$$

Now, we are presenting another modified technique for controlling the bifurcation and chaos. Consider the following generalized hybrid control technique by applying state feedback along with parameter perturbation;

$$Z_{n+k} = \sin \mu_1^m g^{(h)}(Z_n, \eta) + (1 - \sin \mu_1^m) Z_n \quad (5.5.2)$$

where  $h > 0$  is in  $Z$  and  $0 < \mu_1 < 1$  is parameter for controlling the bifurcation appearing in (5.5.2). In addition,  $g^{(h)}$  is  $k$ th iterative value of  $g(\cdot)$ . By application of (5.5.2) for  $m = 1$  on system (5.1.9) we get the following controlled system;

$$\begin{aligned} p_{n+1} &= \sin \mu_1 \left( p_n + \frac{s^\alpha}{\alpha\Gamma(\alpha)} \left( rp_n \left(1 - \frac{p_n}{k}\right) - \frac{\beta p_n z_n}{\gamma + p_n} \right) \right) + (1 - \sin \mu_1) p_n, \\ z_{n+1} &= \sin \mu_1 \left( z_n + \frac{s^\alpha}{\alpha\Gamma(\alpha)} \left( \frac{bp_n z_n}{\gamma + p_n} - \delta z_n - \frac{\rho p_n z_n}{\gamma + p_n} \right) \right) + (1 - \sin \mu_1) z_n. \end{aligned} \quad (5.5.3)$$

Then, system (5.5.1) is controllable provided that its fixed point  $(p_*, z_*)$ , is locally asymptotically stable. Additionally, the jacobian matrix for system (5.5.3) at its positive fixed point  $(p_*, z_*)$  is calculated as follows

$$\begin{bmatrix} 1 + \frac{rs^\alpha \delta(b(-k+\gamma) + (k+\gamma)\delta + (k-\gamma)\rho) \sin \mu_1}{k(b-\rho)(-b+\delta+\rho)\Gamma(1+\alpha)} & -\frac{s^\alpha \beta \delta \sin \mu_1}{b\alpha\Gamma(\alpha) - \alpha\rho\Gamma(\alpha)} \\ \frac{rs^\alpha (bk - \gamma\delta - k(\delta+\rho)) \sin \mu_1}{k\alpha\beta\Gamma(\alpha)} & 1 \end{bmatrix}. \quad (5.5.4)$$

The following theorem describes the necessary and sufficient condition for local stability of the system (5.5.3).

**Theorem 5.5.2.** *The positive constant solution  $(p_*, z_*)$  of system (5.5.3) is stable locally asymptotically  $\iff$  the following inequality holds true.*

$$\begin{aligned} & \left| 2 + \frac{rs^\alpha \delta(b(\gamma - k) + (k + \gamma)\delta + (k - \gamma)\rho) \sin \mu_1}{k(b - \rho)(\delta + \rho - b)\Gamma(1 + \alpha)} \right| \\ & < 2 + \frac{rs^\alpha \delta \sin \mu_1 \left( \frac{(b(-k+\gamma) + \gamma(\delta-\rho) + k(\delta+\rho))\Gamma(1+\alpha)}{\delta-b+\rho} - s^\alpha (\gamma\delta - bk + k(\delta + \rho)) \sin \mu_1 \right)}{k(b - \rho)\Gamma^2(1 + \alpha)}, \end{aligned}$$

and

$$\frac{(b(\gamma - k) + \gamma(\delta - \rho) + k(\delta + \rho))\Gamma(1 + \alpha)}{\delta - b + \rho} < s^\alpha (\gamma\delta - bk + k(\delta + \rho)) \sin \mu_1.$$

## 5.6 Numerical simulations

**Example 5.6.1.** *Assume that  $\rho = 0.599, b = 2.459, k = 1.77, \beta = 2.999, r = 1.992, \alpha = 0.29, \gamma = 2.84, \delta = 0.22$  and  $s \in (0, 1]$ . Then, the mathematical system (5.1.9) takes the following form:*

$$\begin{cases} p_{n+1} = p_n + \frac{s^{0.29}}{0.29\Gamma(0.29)} \left( 1.992p_n \left( 1 - \frac{p_n}{1.77} \right) - \frac{2.999p_n z_n}{2.84 + p_n} \right), \\ z_{n+1} = z_n + \frac{s^{0.29}}{0.29\Gamma(0.29)} \left( \frac{2.459p_n z_n}{2.84 + p_n} - 0.22z_n - \frac{0.599p_n z_n}{2.84 + p_n} \right), \end{cases} \quad (5.6.1)$$

where  $p_0 = 0.380975609$  and  $z_0 = 1.6789467026$  are initial conditions. By substitution of these parametric values one can get  $(p_*, z_*) = (0.380975609, 1.6789467026)$ . In addition, in this situation the graphical behavior of both population variables is shown in (Fig. 5.2). In addition, graphical representation of both population shows the clear existence of Neimark-Sacker bifurcation. (Fig. 5.2c) represents the maximum Lyapunov exponent for system (5.6.1). Moreover, by variation of  $s$  in  $(0, 1]$  the system (5.1.9) have shown interesting graphical behaviors, which are represented in (Fig. 5.1). Hence, it can be seen that the Neimark-Sacker bifurcation exists there when the parameter  $s$  positively crosses the value  $s = 0.3267952585158358$  (see Fig. 5.1b). If

$\mathbb{H}(\xi) = 0$  represents the characteristic equation of system (5.6.1) about the constant solution  $(p_*, z_*) = (0.38097560975, 1.67894670261)$ , then for these parametric values  $\mathbb{H}(\xi) = 0$  has the following form

$$\xi^2 - 1.8038899298174336\xi + 1 = 0. \quad (5.6.2)$$

On solving (5.6.2) one can get  $\xi_1 = -0.901944964908 - 0.431850993139i$  and  $\xi_2 = -0.901944964908 + 0.431850993139i$  with  $|\xi_1| = |\xi_2| = 1$ . Moreover, by performing some mathematical calculation one can obtain

$$\left\{ \begin{array}{l} j_1(X, Y) = 0.3809756100 + 0.803889929 X + 0.467832335 Y - 0.5609220775 X^2 \\ \quad - 0.66020699 XY - 0.1068420362 X^3 + 0.2287371932 X^2 Y \\ \quad + O((|X| + |Y|)^4), \\ j_2(X, Y) = 1.66899367 + 0.9940718649 Y + 0.667846157 X - 0.199557365 X^2 \\ \quad + 0.397776865 XY + 0.05928696739 X^3 - 0.1188586660 X^2 Y \\ \quad + O((|X| + |Y|)^4), \\ \check{f}(\phi, \psi) = -0.2283767669 X^3 + 0.4889298488 X^2 Y - 1.198980992 X^2 \\ \quad - 1.411204274 Y X + O((|\phi| + |\psi|)^4), \\ \text{and} \\ \check{g}(\phi, \psi) = -0.02634731643 X^3 + 0.05380418835 X^2 Y + 0.02644756442 X^2 \\ \quad - 0.1729444352 Y X + O((|\phi| + |\psi|)^4), \end{array} \right.$$

where

$$\left\{ \begin{array}{l} X = v_{12}\phi, \\ \text{and} \\ Y = (\ell - v_{11})\phi - \wp\psi. \end{array} \right.$$

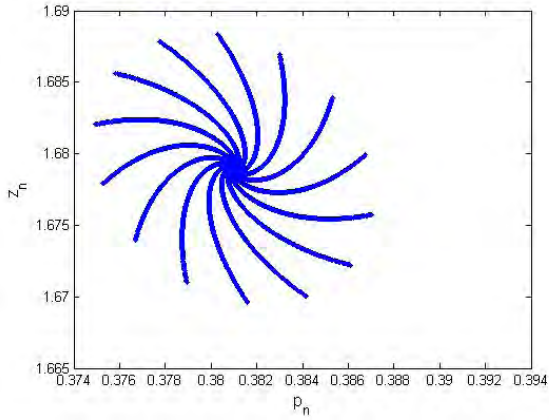
Furthermore, we have

$$\left\{ \begin{array}{l} \theta_{20} = \frac{1}{8} \left[ \check{f}_{\phi\phi} - \check{f}_{\psi\psi} + 2\check{g}_{\phi\psi} + i \left( \check{g}_{\phi\phi} - \check{g}_{\psi\psi} - 2\check{f}_{\phi\psi} \right) \right] = -0.0730534 - 0.071814i, \\ \theta_{11} = \frac{1}{4} \left[ \check{f}_{\phi\phi} + \check{f}_{\psi\psi} + i \left( \check{g}_{\phi\phi} + \check{g}_{\psi\psi} \right) \right] = -0.163577 - 0.00107252i, \\ \theta_{02} = \frac{1}{8} \left[ \check{f}_{\phi\phi} - \check{f}_{\psi\psi} - 2\check{g}_{\phi\psi} + i \left( \check{g}_{\phi\phi} - \check{g}_{\psi\psi} + 2\check{f}_{\phi\psi} \right) \right] = -0.0905237 + 0.0707415i, \\ \theta_{21} = \frac{1}{16} \left[ \check{f}_{\phi\phi\phi} + \check{f}_{\phi\psi\psi} + \check{g}_{\phi\phi\psi} + \check{g}_{\psi\psi\psi} + i \left( \check{g}_{\phi\phi\phi} + \check{g}_{\phi\psi\psi} - \check{f}_{\phi\phi\psi} - \check{f}_{\psi\psi\psi} \right) \right] \\ = -0.00546991 + 0.00519792i \end{array} \right.$$

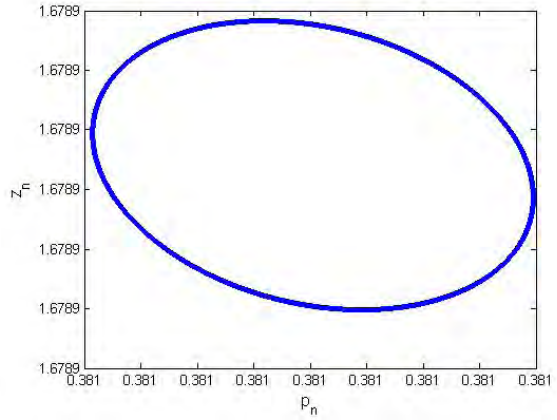
and

$$\Omega = \left( \left[ -\text{Re} \left( \frac{(1 - 2\xi_1)\xi_2^2}{1 - \xi_1} \theta_{20}\theta_{11} \right) - \frac{1}{2} |\theta_{11}|^2 - |\theta_{02}|^2 + \text{Re}(\xi_2\theta_{21}) \right] \right)_{s=0} = -0.01864 < 0.$$

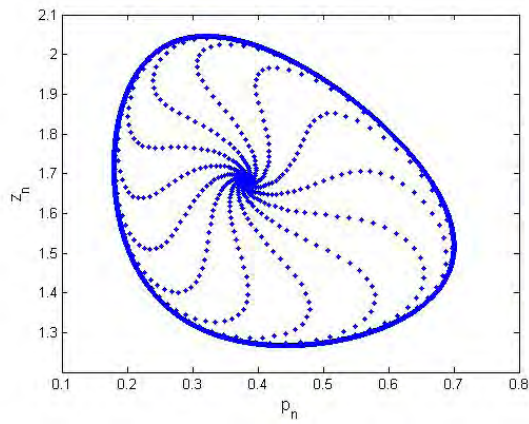
Hence, we have  $\Omega < 0$ , which provides us with numerical proof for the presence of the Neimark-Sacker bifurcation as we have argued in **Theorem 5.4.1**.



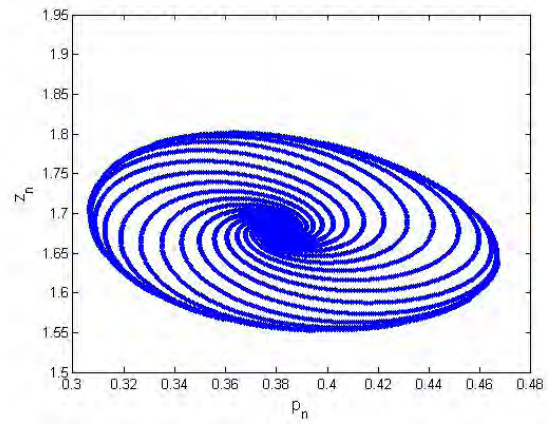
(a) Phase portrait for  $s = 0.3367952585$



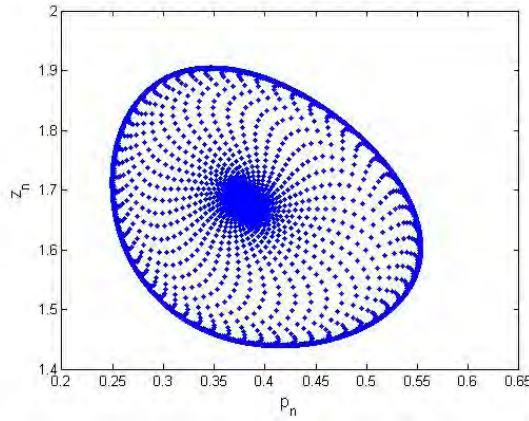
(b) Phase portrait for  $s = 0.3267952585$



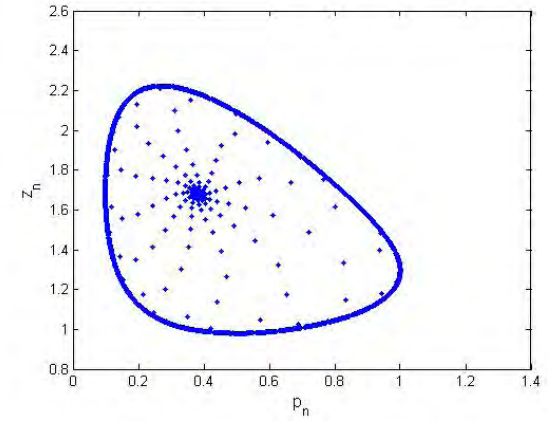
(c) Phase portrait for  $s = 0.4567952585$



(d) Phase portrait for  $s = 0.3667952585$

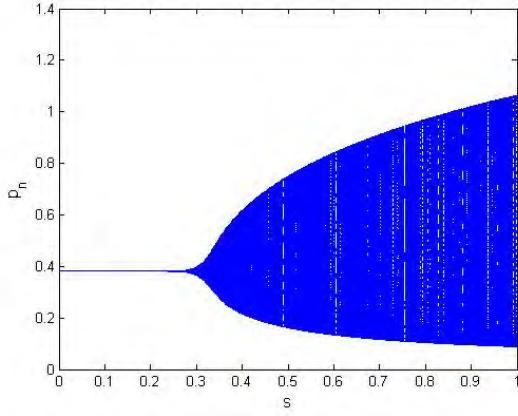


(e) Phase portrait for  $s = 0.5667952585$

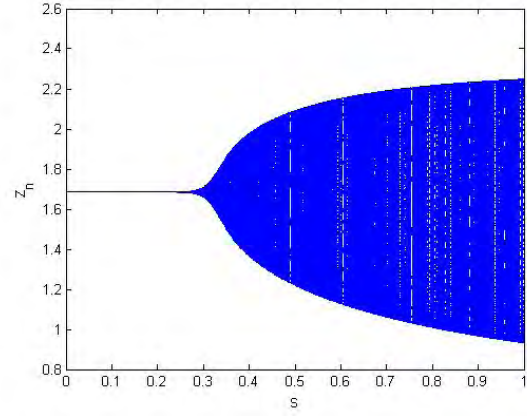


(f) Phase portrait for  $s = 0.8567952585$

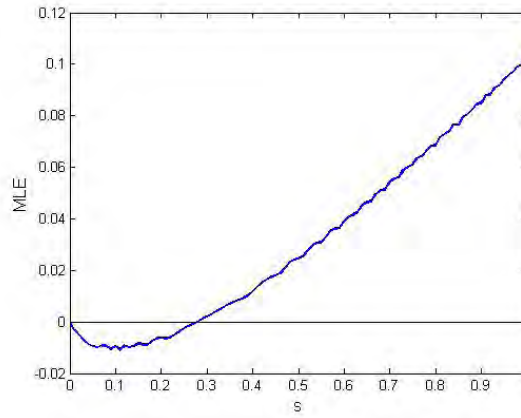
Figure 5.1: Phase portraits for system (5.6.1) for  $\rho = 0.599, b = 2.459, k = 1.77, \beta = 2.999, r = 1.992, \alpha = 0.29, \gamma = 2.84, \delta = 0.22$  and  $s \in (0, 1]$  with initial conditions  $p_0 = 0.380975609$  and  $z_0 = 1.6789467026$ .



(a) Bifurcation diagram for  $p_n$



(b) Bifurcation diagram for  $z_n$



(c) MLE for system (5.6.1)

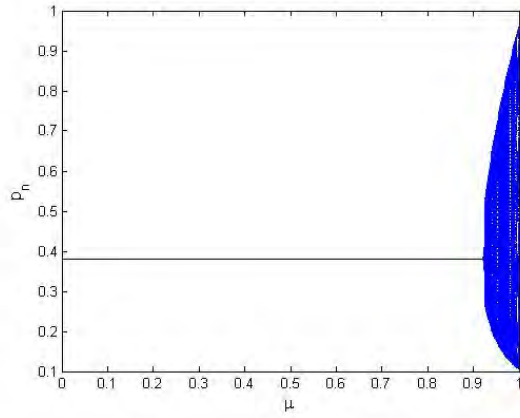
Figure 5.2: Plots for system (5.6.1) for  $\rho = 0.599, b = 2.459, k = 1.77, \beta = 2.999, r = 1.992, \alpha = 0.29, \gamma = 2.84, \delta = 0.22$  and  $s \in (0, 1]$  with initial conditions  $p_0 = 0.380975609$  and  $z_0 = 1.6789467026$ .

**Example 5.6.2.** Consider the following systems of difference equations

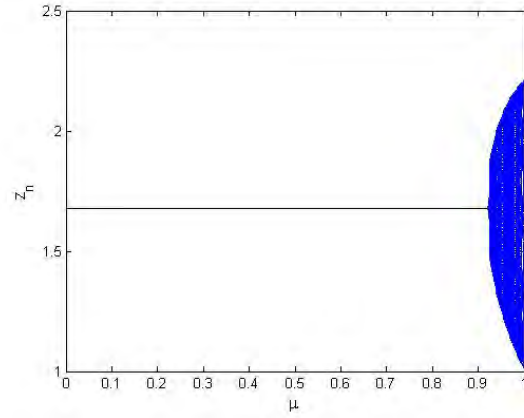
$$\begin{cases} p_{n+1} = \sin \mu_1 \left( p_n + \frac{0.7952585158358^{0.29}}{0.29\Gamma(0.29)} \left( 1.992p_n \left( 1 - \frac{p_n}{1.77} \right) - \frac{2.999p_n z_n}{2.84+p_n} \right) \right) + (1 - \sin \mu_1)p_n, \\ z_{n+1} = \sin \mu_1 \left( z_n + \frac{0.7952585158358^{0.29}}{0.29\Gamma(0.29)} \left( \frac{2.459p_n z_n}{2.84+p_n} - 0.22z_n - \frac{0.599p_n z_n}{\gamma+p_n} \right) \right) + (1 - \sin \mu_1)z_n, \end{cases} \quad (5.6.3)$$

and

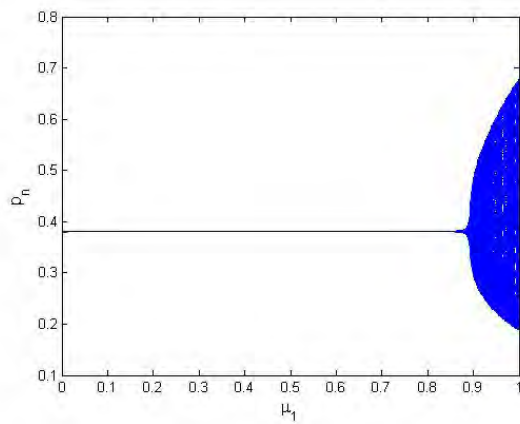
$$\begin{cases} p_{n+1} = \mu^3 \left( p_n + \frac{0.7952585158358^{0.29}}{0.29\Gamma(0.29)} \left( 1.992p_n \left( 1 - \frac{p_n}{1.77} \right) - \frac{2.999p_n z_n}{2.84+p_n} \right) \right) + (1 - \mu^3)p_n, \\ z_{n+1} = \mu^3 \left( z_n + \frac{0.7952585158358^{0.29}}{0.29\Gamma(0.29)} \left( \frac{2.459p_n z_n}{2.84+p_n} - 0.22z_n - \frac{0.599p_n z_n}{2.84+p_n} \right) \right) + (1 - \mu^3)z_n, \end{cases} \quad (5.6.4)$$



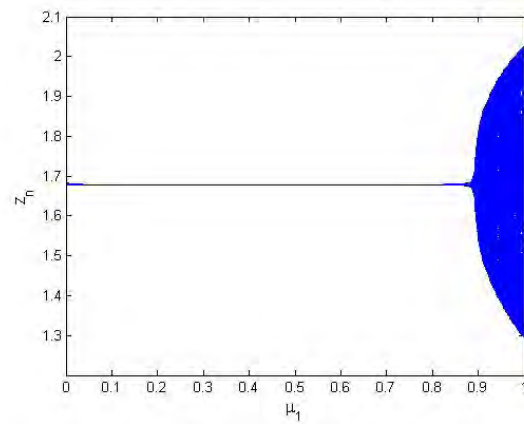
(a) Plot of  $p_n$  for system (5.6.4)



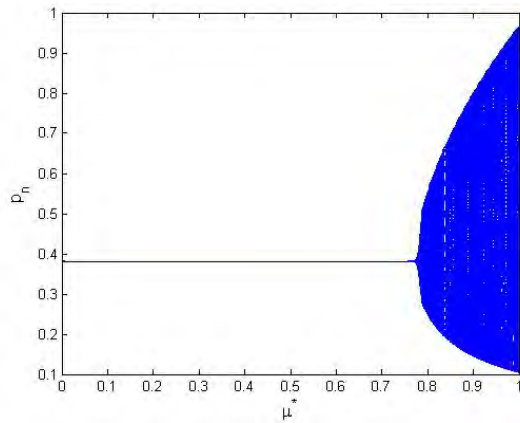
(b) Plot of  $z_n$  for system (5.6.4)



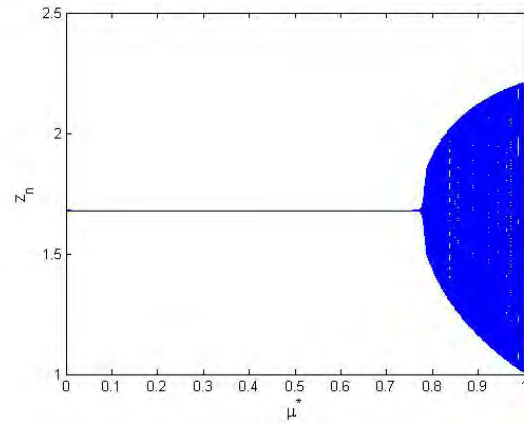
(c) Plot of  $p_n$  for system (5.6.3)



(d) Plot of  $z_n$  for system (5.6.3)



(e) Plot of  $p_n$  for system (5.7.1)

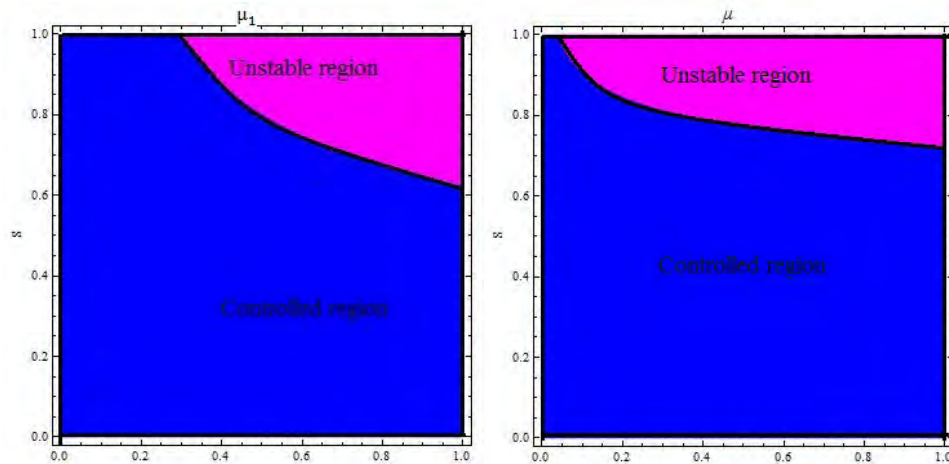


(f) Plot of  $z_n$  for system (5.7.1)

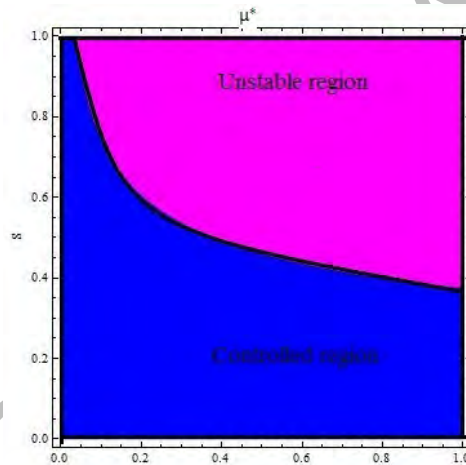
Figure 5.3: Controlled diagrams for  $\rho = 0.599, b = 2.459, k = 1.77, \beta = 2.999, r = 1.992, \alpha = 0.29, \gamma = 2.84, \delta = 0.22$  and  $s \in (0, 1]$  with initial conditions  $p_0 = 0.380975609$  and  $z_0 = 1.6789467026$ .

where  $\rho = 0.599, b = 2.459, k = 1.77, \beta = 2.999, r = 1.992, \alpha = 0.29, \gamma = 2.84, \delta =$

0.22,  $s = 0.7952585158358$ . In addition,  $\mu \in (0, 1]$ ,  $\mu_1 \in (0, 1]$  and  $\mu^* \in (0, 1]$  are parameters used for controlling the bifurcation.



(a) Plot for system (5.6.3) for  $\mu_1 \in (0, 1]$  (b) Plot for system (5.6.4) for  $\mu \in (0, 1]$



(c) Plot for system (5.7.1) for  $\mu^* \in (0, 1]$

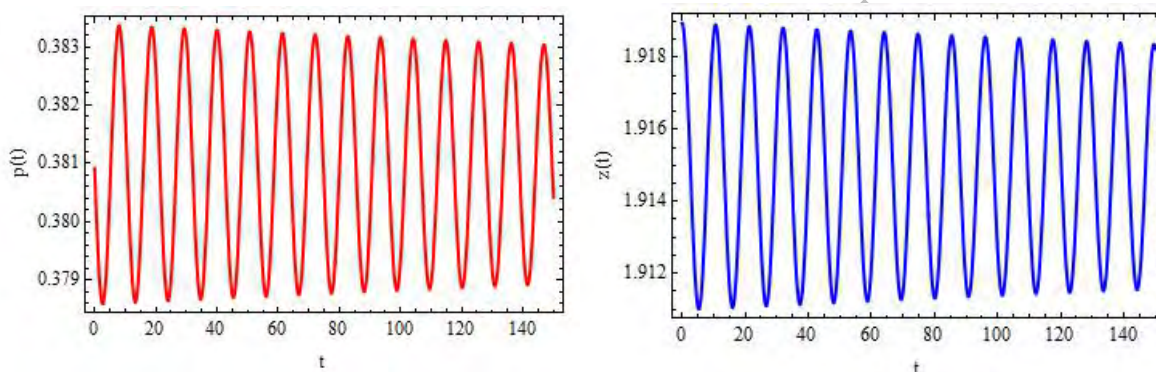
Figure 5.4: Controlled regions for  $\rho = 0.599, b = 2.459, k = 1.77, \beta = 2.999, r = 1.992, \alpha = 0.29, \gamma = 2.84, \delta = 0.22$ , and  $s \in (0, 1]$  with initial conditions  $p_0 = 0.380975609$  and  $z_0 = 1.6789467026$ .

Furthermore, for both systems (5.6.3) and (5.6.4) we get  $(p_*, z_*) = (0.380976, 1.67895)$  which is the unique positive fixed point of original system (5.1.9). Controlled regions for both populations are graphically shown in Fig. 5.3. Furthermore, controlled figures for phytoplankton and zooplankton populations by using models (5.6.3) and (5.6.4) are respectively shown in Fig. 5.3a, Fig. 5.3b and Fig. 5.3c, Fig. 5.3d. Where, the controlled figures for phytoplankton and zooplankton populations by using hybrid method are shown in Fig. 5.3e and Fig. 5.3f respectively. Finally, it can be easily experienced



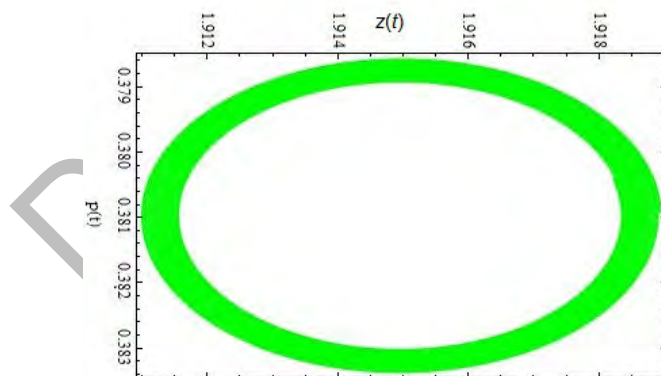
that by using generalized schemes stability of initial system (5.1.9) is gloriously reclaimed for enormous range of control parameter  $\mu$  (see Fig. 5.3).

**Example 5.6.3.** Let  $\rho = 0.599, b = 2.459, k = 3.77, \beta = 2.999, r = 1.992, \alpha = 0.29, \gamma = 2.84$ , and  $\delta = 0.22$ . Then from system (3.0.2) we get  $(p_*, z_*) = (0.380976, 1.917895)$ . Moreover, by taking the initial conditions  $p_0$  and  $z_0$  in the least neighborhood of  $(p_*, z_*)$  an unstable behavior of continuous-time mathematical system (3.0.2) can be seen easily. In addition, the unstable plots for  $p(t)$  and  $z(t)$  are given in Fig. 5.5a and Fig. 5.5b respectively and the Hopf curve for the corresponding system is given in Fig. 5.5c. Hence, it is clear that our continuous-time system (3.0.2) experiences the Hopf bifurcation for similar values of the parameters as we have used for system (5.6.1), which shows the consistency of discretizing technique for our model.



(a) Plot of  $p(t)$  for system (3.0.2)

(b) Plot of  $z(t)$  for system (3.0.2)



(c) Phase portrait for system (3.0.2)

Figure 5.5: Plots of system (3.0.2) for  $\rho = 0.599, b = 2.459, k = 3.77, \beta = 2.999, r = 1.992, \alpha = 0.29, \gamma = 2.84$ , and  $\delta = 0.22$  with initial conditions  $p_0 = 0.380975609$  and  $z_0 = 1.91789467026$ .



Value of $s$	$I_1$	$I_2$	Length of $I_1$	Length of $I_2$
0.595258515	$\mu^* \in (0, 0.840379282)$	$\mu_1 \in (0, 0.9979821)$	0.8403792828	0.997982102
0.695258515	$\mu^* \in (0, 0.803373560)$	$\mu_1 \in (0, 0.9979821)$	0.8033735602	0.997982103
0.795258515	$\mu^* \in (0, 0.772667332)$	$\mu_1 \in (0, 0.8830322)$	0.7726673328	0.883032240
0.895258515	$\mu^* \in (0, 0.746577526)$	$\mu_1 \in (0, 0.8416977)$	0.74657752698	0.841697792
0.995258515	$\mu^* \in (0, 0.723999981)$	$\mu_1 \in (0, 0.8095833)$	0.72399998114	0.809583311

Table 5.1: Comparison between modified hybrid method (5.6.3) and old hybrid method for  $s \in (0, 1]$  and  $\rho = 0.599, b = 2.459, k = 1.77, \beta = 2.999, r = 1.992, \alpha = 0.29, \gamma = 2.84, \delta = 0.22$  with initial points  $x_0 = 0.380976, y_0 = 1.67895$

## 5.7 Concluding remarks

We study some dynamical properties of a phytoplankton-zooplankton model [78]. Firstly, by applying a fractional-order discretization method, we obtained a discrete-time version of the mathematical model presented by Chattopadhyay *et al.* [78]. Consequently, we get some mathematical results related to the presence of a unique positive fixed point. In addition, the local stability of obtained mathematical system (5.1.9) about each of its fixed points is discussed. The existence of Neimark-Sacker bifurcation for a unique positive fixed point is shown mathematically to show the complex behaviour of the mathematical system (5.1.9), and some exceptional numerical examples are provided. It is shown that the system (5.1.9) numerically experiences the Neimark-Sacker bifurcation for an extensive range of parameter  $s$ . It is also shown that the continuous-time system (3.0.2) experiences the Hopf bifurcation for similar values of the parameters, which shows the consistency of discretizing technique for our model (see **Fig. 5.5**). Neimark-Sacker bifurcation is successfully controlled by using three different chaos controlling methods. Our numerical studies have shown that the generalized hybrid methods (5.6.3) and (5.6.4) are improved than hybrid method [95]. In addition, these are based on feedback control and bring back the system's stability for an extensive range of parameters. Moreover, from the numerical study, it is seen that the generalized hybrid methods (5.6.3) and (5.6.4) are more suitable for controlling the Neimark-Sacker bifurcation. Finally, to show the effectiveness of modified techniques, a comparison with the old hybrid control technique [95] is given. By applying the old hybrid method [95] on (5.1.9) and considering the parametric values as in **Example 5.6.2**, we get the following two-dimensional mathematical system:

$$\begin{cases} p_{n+1} = \mu^* \left( p_n + \frac{0.7952585158358^{0.29}}{0.29\Gamma(0.29)} \left( 1.992p_n \left( 1 - \frac{p_n}{1.77} \right) - \frac{2.999p_n z_n}{2.84+p_n} \right) \right) + (1 - \mu^*)p_n, \\ z_{n+1} = \mu^* \left( z_n + \frac{0.7952585158358^{0.29}}{0.29\Gamma(0.29)} \left( \frac{2.459p_n z_n}{2.84+p_n} - 0.22z_n - \frac{0.599p_n z_n}{2.84+p_n} \right) \right) + (1 - \mu^*)z_n, \end{cases} \quad (5.7.1)$$

Value of $s$	$I_1$	$I_3$	Length of $I_1$	Length of $I_3$
0.595258515	$\mu^* \in (0, 0.84037928)$	$\mu \in (0, 0.94368078)$	0.84037928282	0.94368078
0.695258515	$\mu^* \in (0, 0.80337356)$	$\mu \in (0, 0.92962082)$	0.80337356026	0.92962082
0.795258515	$\mu^* \in (0, 0.77266733)$	$\mu \in (0, 0.91762277)$	0.77266733280	0.91762277
0.895258515	$\mu^* \in (0, 0.74657752)$	$\mu \in (0, 0.90717617)$	0.74657752690	0.90717617
0.995258515	$\mu^* \in (0, 0.72399998)$	$\mu \in (0, 0.89793765)$	0.72399998114	0.89793765

Table 5.2: Comparison between modified hybrid method (5.6.4) and old hybrid method for  $s \in (0, 1]$  and  $\rho = 0.599, b = 2.459, k = 1.77, \beta = 2.999, r = 1.992, \alpha = 0.29, \gamma = 2.84, \delta = 0.22$  with initial points  $x_0 = 0.380976, y_0 = 1.67895$

where  $\mu^* \in (0, 1]$  is a control parameter. The bifurcation diagrams for controlled systems (5.6.3), (5.6.4) and (5.7.1) are respectively shown in **Fig. 5.3**. It is seen from **Fig. 5.3** that generalized techniques are much effective than old hybrid techniques. In addition, numerical comparison of generalized control techniques with old hybrid method is given in **Table. 5.1** and **Table. 5.2**. In **Table. 5.1** and **Table. 5.2**,  $I_1$  represents the controlled interval for system (5.7.1) and controlled intervals for system (5.6.3) and (5.6.4) are respectively represented by  $I_2$  and  $I_3$ . It can be seen from these tables that modified models (5.6.3) and (5.6.4) have greater lengths of controlled intervals as compared to the old hybrid system (5.7.1). Moreover, if controlling techniques (5.6.3) and (5.6.4) are applied to (5.1.9) then controlled regions for systems (5.6.3), (5.6.4) and (5.7.1) are respectively shown in **Fig. 5.4a**, **Fig. 5.4b** and **Fig. 5.4c**. Hence, it can be seen from figures **Fig. 5.4a** and **Fig. 5.4b** that the regions formed by using generalized techniques contain the top part of the figure as a controlled region. Hence, from the graphical and tabular comparison of controlling techniques, the feasibility and effectiveness of newly designed hybrid techniques can be seen easily.

## Chapter 6

# Bifurcation Analysis and Control of Chaos in a Discrete-Time Two-Trophic Plant-Herbivore Model and Dynamical Consistency of a Nonstandard Difference Scheme

The findings of this chapter are published in a top-quality international journal (see [83]). Baldwin *et al.* [84] have discussed the unpredictable signalling in plant-herbivore interactions. As plants are leaders of gas interchange, not simply precisely structuring jungles from gases reserved from the atmosphere but also discharging complex posies of impulsive carbon-based compounds (VOCs) back into the atmosphere. This extraordinary aptitude fuels the probability that plants connect through impulsive signals. Generally, the word 'communication' is a burdened word that means unlike things to different investigators; most would agree with the marginal necessity that info is swapped over, nevertheless of 'intent' or suitability significance for each party. Scientists observed twenty years ago that herbivore attacks on plants, as well as nearby plants, cause alterations in the struggle of the affected plants. This also impacts the production of specific compounds that aid in the defense against herbivores. Various studies have suggested that the most effective way of communication in this situation is through the transmission of information through the air or other mediums. This has led to the popular term "speaking trees" being used in the media. However, considering that neighboring plants compete for resources and it is unlikely to be advantageous for them to share information with their adversaries, a more appropriate term for this phenomenon would be "snooping elms." Articles printed in the last two decades have been emphasised in examinations [107-110] and have renewed attention in these singularities. Plant defences against herbivores by the induced role of

the defence is the main topic of focus in ecological science. These defences are activated in plants when they are attacked by herbivores [87]. Induced defences are often grouped into two types: direct and indirect defences. Natural defences by plants are extraction of toxic chemicals, digestibility reducers, poisonous flowers and spines. It is documented that natural defences of plants are observed in more than 100 plant species within their Thirty-four families and these defences have been reported since 1970 [88]. Previous research on natural plant defences shows that plant fitness increases due to herbivore-induced chemical changes [111-117]. On the other hand, indirect protection of plants involves third parties like predators and parasitoids. An illustration of indirect defence is the pull of ants towards plants in search of food. An evident loss in seed production can be seen easily [92].

In a two-trophic plant-herbivore system, an evident loss in seed production can be seen easily [87]. However, parasitoids might act as a steadying mediator in the plant-herbivore system, and a positive increment in seed production can be seen easily [118-120]. It is necessary for survival in the ecosystem that plants and herbivores coexist naturally. Furthermore, nonlinear mathematical models often describe this coexistence [87]. When an ecosystem is disturbed by any factor, it creates a disturbance in the environment [94]. For example, in the absence of herbivore species, the plant population increases without any bound. Hence, in this article, we analyze a two-trophic plant-herbivore interaction model [87]. Let us denote the density of plants by  $x(t)$  and the density of herbivores by  $y(t)$  at any time  $t$ . When there is no herbivore population, then logistically, plant population increases; Where  $r$  is their inherent degree of growing and  $k$  is the carrying ability of the environment for plant species. We assume that the rate at which herbivores eat plants is proportional to the product  $x(t)y(t)$  and is represented by  $\alpha$ . Additionally, assume that  $\beta$  is the conversion factor for herbivores and  $s$  means their death rate. Then, under these assumptions, we are now able to write the mathematical form of the two-trophic plant-herbivore model [87]:

$$\begin{aligned}\frac{dx}{dt} &= \left( r \left( 1 - \frac{x(t)}{k} \right) - \alpha x(t) \right) x(t), \\ \frac{dy}{dt} &= (\beta x(t) - s) y(t).\end{aligned}\tag{6.0.1}$$

Understanding the dynamic relationships between herbivores and plants helps us protect the environment. Hence, the fantastic diversity in the dynamical behaviour of these species attract many researchers; Resulting in some existing theoretical models related to herbivore-plant interactions [119-121]. Furthermore, these theoretical models study plant-herbivore interactions using differential and difference equations [121]. Modelling these interactions by differential and difference equations allows us to explore the complex behaviour produced in these interactions. Moreover, in the case of non-overlapping

generations, the study using discrete-time models is more feasible and has richer dynamics [91-94]. A significant number of researchers use discrete-time models to explore plant-herbivore interactions. For the study of some motivating dynamical properties of plant-herbivore interactions, we refer the reader to [116-121]. In the current article, our purpose is to describe the dynamics of the plant-herbivore model (6.0.1), which is presented by Chattopadhyay *et al.* [87] in differential form. Afterwards, Kartal [99] have given a comparison between discrete-time and continuous-time models by using model (6.0.1). This work presented strong dynamical conditions and a modified chaos control technique to further explain the model (6.0.1). Mukherjee *et al.* [110] studied the dynamical properties produced in a plant-herbivore model with Holling type-II response [81].

## 6.1 Discretization of model

According to Strogatz [9], chaos occurs in a continuous system when it is at least 3-dimensional. Therefore, it is clear that chaos ceased to exist in the system (6.0.1), chaos ceased to exist. HoIn the case of discrete-time maps, chaos can be observed in one dimension. Therefore, it is necessary and interesting to study the qualitative behavior of the discrete-time version of system (6.0.1). By using Euler's forward method with a step size of  $h$ , we obtain the following discrete-time formulation of (6.0.1):

$$\begin{aligned}x_{n+1} &= x_n + h \left( rx_n - \frac{rx_n^2}{k} - \alpha x_n y_n \right), \\y_{n+1} &= y_n + h (\beta x_n y_n - sy_n).\end{aligned}\tag{6.1.1}$$

Furthermore, to understand a similar type of discretization, one can study [91-94]. Shabir *et al.* [30] studied the dynamical consistency of a prey-predator model by using Mickens [20] non-standard difference scheme. Additionally, the author compares the continuous-time prey-predator model with a discrete-time prey-predator model to analyze this dynamical behaviour. Hence, by applying a non-standard difference scheme [20] on the model (6.1.1), we get the following form of system (6.1.1):

$$\begin{aligned}x_{n+1} &= \frac{x_n (1 + rh)}{1 + \frac{rh}{k} x_n + \alpha h y_n}, \\y_{n+1} &= \frac{y_n (1 + \beta h x_n)}{1 + sh}.\end{aligned}\tag{6.1.2}$$

Where  $0 < h < 1$  is step size. The authors in Din *et al.* [6] and Din *et al.* [7] have explored the dynamics of two discrete-time models. Additionally, by taking step size  $h$  as a bifurcation parameter, the author has discussed two different discrete-time models' stability and bifurcation analysis. Furthermore, the author has shown that step size  $h$

can not be used as a controlling parameter for bifurcation in the OGY method [36]. Therefore, we have introduced a modified hybrid control methodology to conquer this deficiency for controlling bifurcation.

## 6.2 Existence of fixed points

Assume that,  $x_{n+1} = x_n = x_*$  and  $y_{n+1} = y_n = y_*$ . Then system (6.1.1) becomes

$$\begin{aligned} rx_* - \frac{rx_*^2}{k} - \alpha x_* y_* &= 0, \\ \beta x_* y_* - sy_* &= 0. \end{aligned} \quad (6.2.1)$$

On solving system (6.2.1) one can obtain three fixed points,  $p_0 = (0, 0)$ ,  $p_1 = (k, 0)$  and the unique positive fixed point  $\underline{p} = \left( \frac{s}{\beta}, \frac{r(k\beta - s)}{k\alpha\beta} \right)$  exists if  $k\beta > s$ . Let

$$F_J(\underline{p}) = \begin{bmatrix} a_{11} & a_{12} \\ a_{21} & a_{22} \end{bmatrix}$$

be the variational matrix about  $\underline{p}$ . Then characteristic polynomial  $\mathbb{H}(\omega)$  of matrix  $F_J(\underline{p})$  is:

$$\mathbb{H}(\omega) = \omega^2 - A_1\omega + A_2, \quad (6.2.2)$$

where

$$A_1 = (a_{11} + a_{22}),$$

and

$$A_2 = a_{11}a_{22} - a_{12}a_{21}.$$

## 6.3 Local stability analysis

Firstly, we explore the stability analysis of the trivial fixed point  $p_0$ . The Jacobian matrix  $F_J(p_0)$  about fixed point  $p_0$ , is given by;

$$F_J(p_0) = \begin{bmatrix} 1 + hr & 0 \\ 0 & 1 - hs \end{bmatrix}.$$

The characteristic polynomial  $\mathbb{H}(\tau)$  obtained from matrix  $F_J(p_0)$  is given by;

$$\mathbb{H}(\tau) = \tau^2 - (2 + h(r - s))\tau + (1 + hr)(hs - 1).$$

In addition,  $\mathbb{H}(\tau) = 0$  has two roots, namely  $\tau_1 = 1 + hr$  and  $\tau_2 = 1 - hs$ , such that  $|\tau_1| > 1$  remains true for all parametric values. By using **Lemma 1.3.1** we conclude the following proposition about the local stability of  $p_0$ .

**Proposition 6.3.1.** *Let  $p_0 = (0, 0)$  be a fixed point of (6.1.1) then;*

- *The point  $p_0$  is exterior of unit disk if and only if*

$$hs > 2.$$

- *The point  $p_0$  is saddle point if and only if*

$$0 < hs < 2$$

- *The point  $p_0$  is non-hyperbolic fix point if and only if*

$$hs = 2.$$

Next, our goal is to explore the local stability of system (6.1.1) about  $p_1 = (k, 0)$ . The matrix of variation  $F_J(p_1)$  evaluated about  $p_1$  can be calculated as:

$$F_J(p_1) = \begin{bmatrix} 1 - hr & -hk\alpha \\ 0 & 1 - hs + hk\beta \end{bmatrix}.$$

Moreover, in this case the quadratic characteristic polynomial  $\mathbb{H}(\varrho)$  obtained from  $F_J(p_1)$  is given by

$$\mathbb{H}(\varrho) = \varrho^2 - (2 - h(r + s - k\beta))\varrho + (hr - 1)(h(s - k\beta) - 1).$$

Clearly,  $\mathbb{H}(\varrho) = 0$  has two roots namely,  $\varrho_1 = 1 - hs$  and  $\varrho_2 = 1 - hs + hk\beta$ . Hence, one has the following proposition for the local stability of  $p_1 = (k, 0)$ .

**Proposition 6.3.2.** *Let  $p_1 = (k, 0)$  be a fixed point of (6.1.1) then:*

- *The point  $p_1$  is interior of unit disk if and only if*

$$0 < hs < 2 \text{ and } -2 < h(k\beta - s) < 2.$$

- *The point  $p_1$  is exterior of unit disk if and only if*

$$hs > 2 \text{ and } k\beta > 2.$$

- *The point  $p_1$  is saddle point if and only if*

$$hs > 2 \text{ and } -2 < h(k\beta - s) < 2 \text{ or } 0 < hs < 2 \text{ and } k\beta > s.$$

- The point  $p_1$  is non-hyperbolic if and only if

$$hs = 2 \text{ and } k\beta > 0.$$

Finally, we have some results related to the local stability of system (6.1.1) about  $\underline{p} = \left( \frac{s}{\beta}, \frac{r(k\beta-s)}{k\alpha\beta} \right)$ . Let  $F_J(\underline{p})$  be the matrix of variation for system (6.1.1) about  $\underline{p}$ . Then  $F_J(\underline{p})$  has the following mathematical form:

$$F_J(\underline{p}) = \begin{pmatrix} 1 - \frac{hrs}{k\beta} & -\frac{hs\alpha}{\beta} \\ \frac{hr(-s+k\beta)}{k\alpha} & 1 \end{pmatrix}.$$

Assume that

$$A_1 = 2 - \frac{hrs}{k\beta},$$

and

$$A_2 = \frac{k\beta + hrs(hk\beta - 1 - hs)}{k\beta}$$

and (6.2.2) is the characteristic polynomial obtained from matrix  $F_J(\underline{p})$  and  $k\beta > s$ . Then, by performing some mathematical operations it follows that:

$$\mathbb{H}(1) = \frac{h^2rs(k\beta - s)}{k\beta} > 0,$$

and

$$\mathbb{H}(-1) = \frac{4k\beta + hrs(hk\beta - 2 - hs)}{k\beta}.$$

Hence, by using **Lemma 1.3.1** we have the next proposition about the local stability of system (6.1.1) about  $\underline{p} = \left( \frac{s}{\beta}, \frac{r(k\beta-s)}{k\alpha\beta} \right)$ .

**Proposition 6.3.3.** Let  $\underline{p} = \left( \frac{s}{\beta}, \frac{r(k\beta-s)}{k\alpha\beta} \right)$  be unique positive fixed point of (6.1.1) then:

- The point  $\underline{p}$  is the point of suction if and only if

$$hrs(2 + hs) < k\beta(4 + h^2rs) \text{ and } k\beta > s.$$

- The point  $\underline{p}$  is repeller if and only if

$$hrs(2 + hs) < k\beta(4 + h^2rs) \text{ and } 1 + hs < hk\beta.$$

- The point  $\underline{p}$  is saddle point if and only if

$$hr > 2$$



- The point  $\underline{p}$  is non-hyperbolic if and only if one of the particular condition holds:

1.

$$h = \frac{rs - \sqrt{r^2s^2 + 4krs^2\beta - 4k^2rs\beta^2}}{krs\beta - rs^2}$$

and

$$hk\beta \neq 1 + hs, \quad hrs(hk\beta - 1 - hs) \neq -2k\beta.$$

2.

$$rs + 4k\beta(s - k\beta) < 0 \quad \text{and} \quad h = \frac{1}{k\beta - s}.$$

Assume that  $s < k\beta$ , then the system (6.1.2) have three equilibrium points, trivial equilibrium  $p_0 = (0, 0)$ , boundary equilibrium  $p_1 = (k, 0)$  and the unique positive equilibrium  $\underline{p} = \left(\frac{s}{\beta}, \frac{r(k\beta - s)}{k\alpha\beta}\right)$ . Furthermore, one can see that  $p_0$  and  $p_1$  are always saddle points. In order to study the behavior of (6.1.2) about  $\underline{p}$ , we assume that  $F(\underline{p})$  be the variational matrix of system (6.1.2) about  $\underline{p}$  such that:

$$F(\underline{p}) = \begin{pmatrix} 1 - \frac{hrs}{k\beta + hkr\beta} & -\frac{hs\alpha}{\beta + hr\beta} \\ -\frac{hrs - hkr\beta}{k\alpha + hks\alpha} & 1 \end{pmatrix}.$$

The second degree characteristic polynomial  $P(\omega)$  calculated by using  $F[\underline{p}]$  is given as:

$$P(\omega) = \omega^2 - \left(2 - \frac{hrs}{k\beta + hkr\beta}\right)\omega + \frac{k(1 + h(r + s + 2hrs))\beta - hrs(1 + 2hs)}{k(1 + hr)(1 + hs)\beta}. \quad (6.3.1)$$

Furthermore, by performing some suitable algebraic manipulation it follows that

$$P(1) = \frac{h^2rs(k\beta - s)}{k(1 + hr)(1 + hs)\beta} > 0, \quad (6.3.2)$$

$$P(-1) = \frac{k(4 + 5h^2rs + 4h(r + s))\beta - hrs(2 + 3hs)}{k(1 + hr)(1 + hs)\beta} > 0, \quad (6.3.3)$$

$$P(0) = \frac{-hrs(1 + 2hs) + k(1 + h(r + s + 2hrs))\beta}{k(1 + hr)(1 + hs)\beta}. \quad (6.3.4)$$

From (6.3.2) it is clear that  $P(1) > 0$  if and only if  $k\beta > s$ . Furthermore, for  $k\beta > s$  we have

$$k(4 + 5h^2rs + 4h(r + s))\beta > hrs(2 + 3hs)$$

**Remark 6.3.1.** As  $P(-1) > 0$ , hence there is no chance of period doubling bifurcation for system (6.1.2) about its unique positive fixed point  $\underline{p}$  (see [30]).

Hence, by using **Lemma 1.3.1** and considering the relations between roots and coefficients of second degree algebraic equation, we have the next result that describes the local stability of the system (6.1.2) about  $\underline{p}$ .

**Proposition 6.3.4.** *Let  $\underline{p}$  be unique positive fixed point of (6.1.2) then:*

1.  $\underline{p}$  is interior of unit circle if and only if

$$k\beta(4 + 5h^2rs + 4h(r + s)) > hrs(2 + 3hs) \text{ and } 1 + hs > 0.$$

2.  $\underline{p}$  is the exterior of the unit circle if and only if

$$k\beta(4 + 5h^2rs + 4h(r + s)) > hrs(2 + 3hs) \text{ and } k\beta h > 1 + 2hs.$$

3.  $\underline{p}$  is non-hyperbolic if and only if

$$h = \frac{1}{k\beta - 2s} \text{ and } s(5hrs + 4s + r) < 4k^2\beta^2(1 + hr).$$

## 6.4 Bifurcation analysis

This section is related to the bifurcation analysis of the system (6.1.1) about its positive fixed point  $\underline{p}$ .

### 6.4.1 Period-doubling bifurcation

Let us assume that (6.2.2) be characteristic equation of (6.1.1) about  $\underline{p}$ . Additionally, assume that  $\omega_1$  and  $\omega_2$  are roots of (6.2.2). Then by using **Lemma 1.3.1** one can see that  $\omega_1 = -1$  and  $|\omega_2| \neq 1$ , if part (1) of **Proposition 6.3.3** holds. Consequently, the system (6.1.1) experiences the period-doubling bifurcation when the parameters in (6.1.1) vary in the least neighborhood of the following set:

$$B_{S1} = \{\alpha, \beta, s, r, k \in \mathfrak{R}^+ : h = \frac{rs - \sqrt{r^2s^2 + 4krs^2\beta - 4k^2rs\beta^2}}{krs\beta - rs^2}, A_2 \neq 1, -1\},$$

Moreover,  $\omega_1$  and  $\omega_2$  are conjugate complex numbers with unit magnitude if the condition (2) of **Proposition 6.3.3** is satisfied. Thus the system (6.1.1) undergoes Neimark-Sacker bifurcation when the parameters in (6.1.1) vary in the least neighborhood of the following set:

$$B_{S2} = \left\{ \alpha, \beta, s, r, k \in \mathfrak{R}^+ : rs + 4k\beta(s - k\beta) < 0, h = \frac{1}{k\beta - s} \right\}.$$

Firstly, we will analyze the flip bifurcation of (6.1.1) about  $\underline{p}$ . Let  $(\alpha, \beta, s, r, k) \in B_{S1}$  are taken arbitrarily and  $h = \frac{rs - \sqrt{r^2 s^2 + 4krs^2\beta - 4k^2 rs\beta^2}}{krs\beta - rs^2}$ . Then the mathematical system (6.1.1) can be defined by the next two-dimensional mapping:

$$\begin{pmatrix} x \\ y \end{pmatrix} \rightarrow \begin{pmatrix} x + h(rx(1 - \frac{x}{k}) - \alpha xy) \\ y + h(\beta xy - sy) \end{pmatrix}. \quad (6.4.1)$$

Taking  $\bar{h}$  as small parameter for bifurcation, then the perturbation of mapping (6.4.1) can be described by the next map:

$$\begin{pmatrix} x \\ y \end{pmatrix} \rightarrow \begin{pmatrix} x + (h + \bar{h})(rx(1 - \frac{x}{k}) - \alpha xy) \\ y + (h + \bar{h})(\beta xy - sy) \end{pmatrix}, \quad (6.4.2)$$

where  $|\bar{h}| \ll 1$ , is a small parameter for perturbation. Taking  $H = x - \frac{s}{\beta}$  and  $P = y - \frac{r(k\beta - s)}{k\alpha\beta}$ , then the mapping (6.4.2) is transformed into the following form:

$$\begin{pmatrix} H \\ P \end{pmatrix} \rightarrow \begin{pmatrix} z_{11} & z_{12} \\ z_{21} & z_{22} \end{pmatrix} \begin{pmatrix} H \\ P \end{pmatrix} + \begin{pmatrix} f_1(H, P, \bar{h}) \\ f_2(H, P, \bar{h}) \end{pmatrix} \quad (6.4.3)$$

where

$$f_1(H, P, \bar{h}) = z_{13}H^2 + z_{14}H\bar{h} + z_{15}HP + z_{16}\bar{h}P + z_{17}HP\bar{h} + z_{18}\bar{h}H^2 + O((|H| + |P| + |\bar{h}|)^4),$$

$$f_2(H, P, \bar{h}) = z_{23}H\bar{h} + z_{24}HP + z_{25}HP\bar{h} + O((|H| + |P| + |\bar{h}|)^4),$$

$$\begin{cases} z_{11} = \frac{\beta k - hrs}{\beta k}, & z_{12} = -\frac{h\alpha s}{\beta}, & z_{21} = \frac{hr(\beta k - s)}{k\alpha}, & z_{22} = 1, & z_{13} = -\frac{hr}{k}, & z_{14} = -\frac{rs}{\beta k}, \\ z_{15} = -h\alpha, & z_{16} = -\frac{\alpha s}{\beta}, & z_{17} = -\alpha, & z_{18} = -\frac{r}{k}, & z_{23} = \frac{r(\beta k - s)}{k\alpha}, & z_{24} = h\beta, & z_{25} = \beta. \end{cases}$$

Next, we consider the following translation:

$$\begin{pmatrix} H \\ P \end{pmatrix} = T \begin{pmatrix} u \\ v \end{pmatrix} \quad (6.4.4)$$

where  $T = \begin{pmatrix} z_{12} & z_{12} \\ -\varsigma & \zeta \end{pmatrix}$  be a nonsingular matrix along with transformation (6.4.4),

then the map (6.4.3) can be written as:

$$\begin{pmatrix} u \\ v \end{pmatrix} \rightarrow \begin{pmatrix} -1 & 0 \\ 0 & \omega_2 \end{pmatrix} \begin{pmatrix} u \\ v \end{pmatrix} + \begin{pmatrix} f(u, v, \bar{h}) \\ g(u, v, \bar{h}) \end{pmatrix}, \quad (6.4.5)$$

with

$$\begin{aligned} f(u, v, \bar{h}) &= \frac{\zeta z_{18}H^2\bar{h}}{z_{12}\eta} + \frac{\zeta z_{13}H^2}{z_{12}\eta} + \left( \frac{\zeta z_{17}}{z_{12}\eta} - \frac{z_{25}}{\eta} \right) HP\bar{h} \\ &+ \left( \frac{\zeta z_{15}}{z_{12}\eta} - \frac{z_{24}}{\eta} \right) HP + \left( \frac{\zeta z_{14}}{z_{12}\eta} - \frac{z_{23}}{\eta} \right) \bar{h}H + \frac{\zeta z_{16}\bar{h}P}{z_{12}\eta} \\ &+ O((|u| + |v| + |\bar{h}|)^4), \end{aligned}$$

$$\begin{aligned}
g(u, v, \bar{h}) &= \frac{\varsigma z_{18} H^2 r}{z_{12} \eta} + \frac{\varsigma z_{13} H^2}{z_{12} \eta} + \left( \frac{\varsigma z_{17}}{z_{12} \eta} + \frac{z_{25}}{\eta} \right) H P \bar{h} \\
&+ \left( \frac{\varsigma z_{15}}{z_{12} \eta} + \frac{z_{24}}{\eta} \right) H P + \left( \frac{\varsigma z_{14}}{z_{12} \eta} + \frac{z_{23}}{\eta} \right) \bar{h} H + \frac{\varsigma z_{16} \bar{h} P}{z_{12} \eta} \\
&+ O(|u| + |v| + |\bar{h}|^4),
\end{aligned}$$

where

$$H = z_{12}(u + v), \quad P = -\varsigma u + \zeta v, \quad \zeta = (\omega_2 - z_{11}), \quad \varsigma = (1 + z_{11}), \quad \eta = \omega_2 + 1.$$

Assume that  $C^m(0, 0, 0)$  be the center manifold of (6.4.5) intended at  $(0, 0)$  in a smallest neighborhood of  $\bar{h} = 0$ , formerly  $C^m(0, 0, 0)$  can be estimated as follows:

$$C^m(0, 0, 0) = \{(u, v, \bar{h}) \in \mathbb{R}^3 : v = m_1 u^2 + m_2 u \bar{h} + m_3 \bar{h}^2 + O(|\bar{h}| + |u|^3)\},$$

where

$$\begin{aligned}
m_1 &= \frac{1}{1 - \omega_2} \left( \frac{\varsigma z_{12} z_{13}}{\eta} - \left( \frac{\varsigma z_{15}}{z_{12} \eta} + \frac{z_{24}}{\eta} \right) z_{12} \varsigma \right), \\
m_2 &= \frac{1}{1 - \omega_2} \left( \left( \frac{\varsigma z_{14}}{z_{12} \eta} + \frac{z_{23}}{\eta} \right) z_{12} - \frac{\varsigma z_{16} \varsigma}{z_{12} \eta} \right), \quad m_3 = 0.
\end{aligned}$$

Hence, we have the following restricted map to the centre manifold  $C^m(0, 0, 0)$  and describe it as follows.

$$G : u \rightarrow -u + k_1 u^2 + k_2 u \bar{h} + k_3 u^2 \bar{h} + k_4 u \bar{h}^2 + k_5 u^3 + O(|u| + |\bar{h}|^4),$$

where

$$\begin{aligned}
k_1 &= \frac{\zeta z_{12} z_{13}}{\eta} - \left( \frac{\zeta z_{15}}{z_{12} \eta} - \frac{z_{24}}{\eta} \right) z_{12} \varsigma, \\
k_2 &= \left( \frac{\zeta z_{14}}{z_{12} \eta} - \frac{z_{23}}{\eta} \right) z_{12} - \frac{\zeta z_{16} \varsigma}{z_{12} \eta}, \\
k_3 &= \frac{\zeta z_{12} z_{18}}{\eta} + 2 \frac{\zeta z_{12} z_{13} m_2}{\eta} - \left( \frac{\zeta z_{17}}{z_{12} \eta} - \frac{z_{25}}{\eta} \right) z_{12} \varsigma \\
&+ \left( \frac{\zeta z_{15}}{z_{12} \eta} - \frac{z_{24}}{\eta} \right) z_{12} \zeta m_2 - \left( \frac{\zeta z_{15}}{z_{12} \eta} - \frac{z_{24}}{\eta} \right) z_{12} m_2 \varsigma \\
&+ \left( \frac{\zeta z_{14}}{z_{12} \eta} - \frac{z_{23}}{\eta} \right) z_{12} m_1 + \frac{\zeta^2 z_{16} m_1}{z_{12} \eta}, \\
k_4 &= \left( \frac{\zeta z_{14}}{z_{12} \eta} - \frac{z_{23}}{\eta} \right) z_{12} m_2 + \frac{\zeta^2 z_{16} m_2}{z_{12} \eta}, \\
k_5 &= \frac{2 \zeta z_{12} z_{13} m_1}{\eta} + \left( \frac{\zeta z_{15}}{z_{12} \eta} - \frac{z_{24}}{\eta} \right) z_{12} m_1 \zeta \\
&- \left( \frac{\zeta z_{15}}{z_{12} \eta} - \frac{z_{24}}{\eta} \right) z_{12} m_1 \varsigma.
\end{aligned}$$

Next, we have the following real numbers:

$$l_1 = \left( \frac{\partial^2 f}{\partial u \partial \bar{h}} + \frac{1}{2} \frac{\partial G}{\partial \bar{h}} \frac{\partial^2 G}{\partial u^2} \right)_{(0,0)} = \left( \frac{\zeta z_{14}}{z_{12} \eta} - \frac{z_{23}}{\eta} \right) z_{12} - \frac{\zeta z_{16} \varsigma}{z_{12} \eta} \neq 0,$$

$$l_2 = \left( \left( \frac{1}{2} \frac{\partial^2 G}{\partial u^2} \right)^2 + \frac{1}{6} \frac{\partial^3 G}{\partial u^3} \right)_{(0,0)} = k_5 + k_1^2 \neq 0. \quad (6.4.6)$$

Hence, by the study as mentioned above, we have the next conclusive theorem related to the existence of period-doubling bifurcation of system (6.1.1) about  $\underline{p}$ .

**Theorem 6.4.1.** *Suppose equation (6.4.6) is met. Under these conditions, as the step size  $h$  varies within a small neighborhood around  $\bar{h}$ , the system (6.1.1) exhibits a period-doubling bifurcation. This bifurcation occurs specifically around the positive fixed point  $\underline{p}$ . Furthermore, the stability of the period-two orbits originating from  $\underline{p}$  depends on the value of  $l_2$ : if  $l_2 > 0$ , the orbits are stable, while if  $l_2 < 0$ , they are unstable.*

## 6.4.2 Neimark-Sacker bifurcation

Next, we deduce some results for the existence and direction of Neimark-Sacker bifurcation. By using **Lemma 1.3.1**, it follows that the characteristic equation  $\mathbb{H}(\omega) = 0$  has two complex roots with modulus one, if condition (2) of **Proposition 6.3.3** is satisfied. Hence the unique positive fixed point  $\underline{p}$  of mathematical system (6.1.1) experiences the Neimark-Sacker bifurcation if parameters in (6.1.1) vary in the smallest neighborhood of  $B_{S_2}$ . Let  $(\alpha, \beta, k, s, r, h) \in B_{S_2}$  then system (6.1.1) can be written as;

$$\begin{pmatrix} x \\ y \end{pmatrix} \rightarrow \begin{pmatrix} x + h_1 (rx (1 - \frac{x}{k}) - \alpha xy) \\ y + h_1 (\beta xy - sy) \end{pmatrix}. \quad (6.4.7)$$

Since  $(\alpha, \beta, k, s, r, h_1) \in B_{S_2}$  and  $h_1 = \frac{1}{k\beta - s}$ . Taking  $\tilde{h}$  as bifurcation parameter and considering the perturbation of (6.4.7) we get the following mathematical system:

$$\begin{pmatrix} x \\ y \end{pmatrix} \rightarrow \begin{pmatrix} x + (h_1 + \tilde{h}) (rx (1 - \frac{x}{k}) - \alpha xy) \\ y + (h_1 + \tilde{h}) (\beta xy - sy) \end{pmatrix}, \quad (6.4.8)$$

where  $|\tilde{h}| \ll 1$  is taken as small perturbation parameter. Next, we assume that  $H = x - \frac{s}{\beta}$ ,  $P = y - \frac{r(k\beta - s)}{k\alpha\beta}$ , then the map (6.4.7) is changed into the following mathematical form:

$$\begin{pmatrix} H \\ P \end{pmatrix} \rightarrow \begin{pmatrix} s_{11} & s_{12} \\ s_{21} & s_{22} \end{pmatrix} \begin{pmatrix} H \\ P \end{pmatrix} + \begin{pmatrix} g_1(H, P) \\ g_2(H, P) \end{pmatrix}, \quad (6.4.9)$$

where

$$\begin{aligned}
g_1(H, P) &= s_{13}H^2 + s_{14}HP + O((|H| + |P|)^4), \\
g_2(H, P) &= s_{23}HP + O((|H| + |P|)^4), \\
s_{11} &= \frac{\beta k - (h_1 + \tilde{h})rs}{\beta k}, \quad s_{12} = -\frac{(h_1 + \tilde{h})\alpha s}{\beta}, \quad s_{21} = \frac{(h_1 + \tilde{h})r(\beta k - s)}{k\alpha}, \\
s_{22} &= 1, \quad s_{13} = -(h_1 + \tilde{h})\alpha, \quad s_{14} = -(h_1 + \tilde{h})\alpha, \quad s_{23} = (h_1 + \tilde{h})\beta.
\end{aligned}$$

The second degree characteristic equation  $\mathbb{H}(\omega) = 0$  of variational matrix of system (6.4.9) estimated at the origin  $(0, 0)$  can be defined as follows:

$$\omega^2 - S(\tilde{h})\omega + M(\tilde{h}) = 0, \quad (6.4.10)$$

where

$$S(\tilde{h}) = 2 - \frac{(\tilde{h} + h_1)rs}{k\beta}, \quad M(\tilde{h}) = \frac{k\beta + (\tilde{h} + h_1)rs \left( (\tilde{h} + h_1)k\beta - 1 - (\tilde{h} + h_1)s \right)}{k\beta}.$$

Since  $(\alpha, \beta, s, k, r, h_1) \in B_{S_2}$ . Then, the zeros  $\omega_1$  and  $\omega_2$  of (6.4.10) are complex conjugates with unit modulus such that  $\omega_1 = \bar{\omega}_2$ . As  $\omega_1$  is the root of (6.4.10) then it has the following mathematical form:

$$\omega_1 = \frac{S(\tilde{h})}{2} + \frac{i}{2} \sqrt{4M(\tilde{h}) - S^2(\tilde{h})}.$$

By performing some mathematical operations it follows that;

$$|\omega_1| = \sqrt{M(\tilde{h})},$$

with

$$\left( \frac{d\sqrt{M(\tilde{h})}}{d\tilde{h}} \right)_{\tilde{h}=0} = \frac{rs(\beta h_1 k - h_1 s - 1) + h_1 r s (k\beta - s)}{2k\beta \sqrt{\frac{k\beta + h_1 r s (\beta h_1 k - h_1 s - 1)}{k\beta}}} \neq 0. \quad (6.4.11)$$

Additionally, it follows that  $|\omega_1| = 1$ , but  $\omega_1^m, \omega_2^m \neq 1$  for all  $m \in \{1, 2, 3, 4\}$  if and only if  $S(0) \neq \pm 2, 0, 1$ . Thus, when  $\tilde{h} = 0$  and the given conditions hold true, the zeros of equation (6.4.10) will consistently lie outside the intersection area of the unit circle and the coordinate axes.

$$2k\beta \neq hrs, k\beta \neq hrs. \quad (6.4.12)$$

Since  $(\alpha, \beta, s, k, r, h_1) \in B_{S_2}$ , we get  $0 < S(0) < 2$ . Thus condition (6.4.12) is satisfied automatically. Moreover, we assume that the condition (6.4.11) is satisfied: Then,

the canonical form of (6.4.9) at  $\tilde{h} = 0$  can be obtained by taking  $\gamma = \frac{S(0)}{2}$ ,  $\delta = \frac{1}{2}\sqrt{4M(0) - S^2(0)}$  and assuming the following similarity transformation:

$$\begin{pmatrix} H \\ P \end{pmatrix} = \begin{pmatrix} s_{12} & 0 \\ \gamma - s_{11} & -\delta \end{pmatrix} \begin{pmatrix} u \\ v \end{pmatrix}. \quad (6.4.13)$$

By using transformation (6.4.13), one has the next authoritative form of system (6.4.9):

$$\begin{pmatrix} u \\ v \end{pmatrix} \rightarrow \begin{pmatrix} \gamma & -\delta \\ \delta & \alpha \end{pmatrix} \begin{pmatrix} u \\ v \end{pmatrix} + \begin{pmatrix} \tilde{f}(u, v) \\ \tilde{g}(u, v) \end{pmatrix}, \quad (6.4.14)$$

where

$$\begin{aligned} \tilde{f}(u, v) &= \frac{Ps_{14}H}{s_{12}} + \frac{s_{13}H^2}{s_{12}} + O((|u| + |v|)^4), \\ \tilde{g}(u, v) &= \frac{(\gamma - s_{11})s_{13}H^2}{s_{12}\delta} + \left( \frac{(\gamma - s_{11})s_{14}}{s_{12}\delta} - \frac{s_{23}}{\delta} \right) PH + O((|u| + |v|)^4). \end{aligned}$$

Where,  $H = s_{12}u$  and  $P = (\gamma - s_{11})u - \delta v$ . Hence, we define the following non-zero real numbers:

$$F = \left( \left[ -Re \left( \frac{(1 - 2\omega_1)\omega_2^2}{1 - \omega_1} \xi_{20}\xi_{11} \right) - \frac{1}{2}(|\xi_{11}|^2 - |\xi_{02}|^2 + Re(\omega_2\xi_{21})) \right] \right)_{\tilde{h}=0},$$

where

$$\begin{aligned} \xi_{20} &= \frac{1}{8} \left[ \tilde{f}_{uu} - \tilde{f}_{vv} + 2\tilde{g}_{uv} + i(\tilde{g}_{uu} - \tilde{g}_{vv} - 2\tilde{f}_{uv}) \right], \\ \xi_{11} &= \frac{1}{4} \left[ \tilde{f}_{uu} + \tilde{f}_{vv} + i(\tilde{g}_{uu} + \tilde{g}_{vv}) \right], \\ \xi_{02} &= \frac{1}{8} \left[ \tilde{f}_{uu} - \tilde{f}_{vv} - 2\tilde{g}_{uv} + i(\tilde{g}_{uu} - \tilde{g}_{vv} + 2\tilde{f}_{uv}) \right], \\ \xi_{21} &= \frac{1}{16} \left[ \tilde{f}_{uuu} + \tilde{f}_{vvv} + \tilde{g}_{uuv} + \tilde{g}_{vvv} + i(\tilde{g}_{uuu} + \tilde{g}_{vvv} - \tilde{f}_{uuv} - \tilde{f}_{vvv}) \right]. \end{aligned}$$

Hence, the aforementioned analysis gives us the following significant result for direction and existence of Neimark-Sacker bifurcation [111]

**Theorem 6.4.2.** *The unique positive fixed point  $\left( \frac{s}{\beta}, \frac{r(k\beta - s)}{k\alpha\beta} \right)$  experiences the Neimark-Sacker bifurcation, whenever  $h$  changes in least neighborhood of  $h_1 = \frac{1}{k\beta - s}$ . In addition, if  $F < 0$ , ( $F > 0$ ), respectively, then an attracting or repelling invariant closed curve bifurcates from the equilibrium point for  $h > h_1$  ( $h < h_1$ ), respectively.*

Now, we have some results related to the existence and direction of Neimark-Sacker bifurcation in system (6.1.2). One can notice that the roots of the characteristic equation (6.3.1) are complex conjugates with modulus one if condition (3) of **Proposition 6.3.4**

is satisfied. Hence, the positive fixed point of the model (6.1.2) experiences the Neimark-Sacker bifurcation if parameters vary in the neighbourhood of the following set

$$\mathfrak{N}_S = \left\{ \alpha, \beta, s, r, k \in \mathfrak{R}^+ : \text{with } s(5hrs + 4s + r) < 4k^2\beta^2(1 + hr) \text{ and } h = \frac{1}{k\beta - 2s} \right\}.$$

Let  $(\alpha, \beta, s, r, k, \bar{h}) \in \mathfrak{N}_S$  then the system (6.1.2) is defined by the next mathematical form

$$\begin{pmatrix} x \\ y \end{pmatrix} \rightarrow \begin{pmatrix} \frac{x(1+\bar{h}r)}{1+\frac{r\bar{h}}{k}x+\alpha\bar{h}y} \\ \frac{y(1+\beta\bar{h}x)}{1+\bar{h}s} \end{pmatrix}. \quad (6.4.15)$$

Where  $\bar{h} = h = \frac{1}{k\beta - 2s}$ . Let  $|\tilde{h}| \ll 1$  be a perturbation parameter, then map (6.4.15) can be expressed as:

$$\begin{pmatrix} x \\ y \end{pmatrix} \rightarrow \begin{pmatrix} \frac{x(1+(\bar{h}+\tilde{h})r)}{1+\frac{r(\bar{h}+\tilde{h})}{k}x+\alpha(\bar{h}+\tilde{h})y} \\ \frac{y(1+\beta(\bar{h}+\tilde{h})x)}{1+(\bar{h}+\tilde{h})s} \end{pmatrix}. \quad (6.4.16)$$

Next, under transformations  $(H, P) = \left(x - \frac{s}{\beta}, y - \frac{r(k\beta-s)}{k\alpha\beta}\right)$ , the mathematical map (6.4.16) is reshaped into the following mathematical map:

$$\begin{pmatrix} H \\ P \end{pmatrix} \rightarrow \begin{pmatrix} r_{11} & r_{12} \\ r_{21} & r_{22} \end{pmatrix} \begin{pmatrix} H \\ P \end{pmatrix} + \begin{pmatrix} R_1(H, P) \\ R_2(H, P) \end{pmatrix}, \quad (6.4.17)$$

where

$$\begin{aligned} R_1(H, P) &= r_{13}H^2 + r_{14}HP + r_{15}P^2 + r_{17}H^3 + r_{17}H^2P + r_{18}HP^2 + r_{19}P^3 \\ &+ O((|H| + |P|)^4), \quad R_2(H, P) = r_{23}HP + O((|H| + |P|)^4), \end{aligned}$$

and

$$\begin{cases} r_{11} = \frac{\beta hkr - hrs + \beta k}{\beta k(hr+1)}, & r_{12} = -\frac{\alpha hs}{\beta(hr+1)}, & r_{21} = \frac{hr(\beta k - s)}{k\alpha(hr+1)}, & r_{22} = 1, \\ r_{13} = -\frac{(\beta hkr - hrs + \beta k)hr}{k^2\beta(hr+1)^2}, & r_{14} = -\frac{(\beta hkr - 2hrs + \beta k)h\alpha}{k\beta(hr+1)^2}, & r_{15} = \frac{h^2\alpha^2s}{\beta(hr+1)^2}, \\ r_{16} = \frac{(\beta hkr - hrs + \beta k)h^2r^2}{k^3\beta(hr+1)^3}, & r_{17} = \frac{(2\beta hkr - 3hrs + 2\beta k)\alpha h^2r}{k^2\beta(hr+1)^3}, \\ r_{18} = \frac{(\beta hkr - 3hrs + \beta k)h^2\alpha^2}{k\beta(hr+1)^3}, & r_{19} = -\frac{h^3\alpha^3s}{\beta(hr+1)^3}, & r_{23} = \frac{\beta h}{hs+1}. \end{cases}$$

The characteristic equation  $\mathbb{P}(\omega) = 0$  of Jacobian matrix  $F(\underline{p})$  of map (6.4.17) computed at  $(0, 0)$  can be described as follows:

$$\omega^2 - M_1(\tilde{h})\omega + M_2(\tilde{h}) = 0 \quad (6.4.18)$$

where

$$M_1(\tilde{h}) = 2 - \frac{(\bar{h} + \tilde{h})rs}{k\beta + (\bar{h} + \tilde{h})kr\beta}$$



and

$$M_2(\tilde{h}) = \frac{-(\bar{h} + \tilde{h})rs(1 + 2(\bar{h} + \tilde{h})s) + k(1 + (\bar{h} + \tilde{h})(r + s + 2(\bar{h} + \tilde{h})rs))\beta}{k(1 + (\bar{h} + \tilde{h})r)(1 + (\bar{h} + \tilde{h})s)\beta}.$$

Since  $(\alpha, \beta, s, k, r, \bar{h}) \in \aleph_S$ . Then roots of  $\mathbb{P}(\omega) = 0$  are calculated as follows:

$$\omega_1, \omega_2 = \frac{M_1(\tilde{h})}{2} \pm \frac{i}{2} \sqrt{4M_2(\tilde{h}) - M_1^2(\tilde{h})}.$$

Therefore, we have

$$|\omega_1| = |\omega_2| = \sqrt{M_2(\tilde{h})},$$

$$\left( \frac{d\sqrt{M_2(\tilde{h})}}{d\tilde{h}} \right)_{\tilde{h}=0} = \frac{rs(\beta h^2kr + \beta h^2ks - rsh^2 - 2h^2s^2 + 2\beta hk - 4hs - 1)}{2k(hr+1)^2(hs+1)^2\beta \left( \sqrt{\frac{2\beta h^2krs - 2rs^2h^2 + \beta hkr + \beta hks - rsh + k\beta}{k(hr+1)(hs+1)\beta}} \right)} \neq 0.$$

Since  $(\alpha, \beta, s, k, r, \bar{h})$  are in  $\aleph_S$ , this implies that  $0 < M_1(0) < 2$ . As a result  $M_1(0) \neq \pm 2, 0, 1$  gives  $\omega_1^m, \omega_2^m \neq 1$  for all  $m = 1, 2, 3, 4$  at  $\tilde{h} = 0$ . Thus, roots of (6.4.18) do not lie in the intersection of the unit circle with the coordinate axes at  $\tilde{h} = 0$  and if the next condition holds true:

$$2k\beta(1 + hr) \neq hrs, k\beta(1 + hr) \neq hrs. \quad (6.4.19)$$

Assume that  $\gamma = \frac{M_1(0)}{2}$ ,  $\delta = \frac{1}{2}\sqrt{4M_2(0) - M_1^2(0)}$ , then normal form of (6.4.17) at  $\tilde{h} = 0$  can be expressed as:

$$\begin{pmatrix} H \\ P \end{pmatrix} = \begin{pmatrix} r_{12} & 0 \\ \gamma - r_{11} & -\delta \end{pmatrix} \begin{pmatrix} u \\ v \end{pmatrix}. \quad (6.4.20)$$

Hence, by using map (6.4.20) one can obtain the next map:

$$\begin{pmatrix} u \\ v \end{pmatrix} \rightarrow \begin{pmatrix} \gamma & -\delta \\ \delta & \gamma \end{pmatrix} \begin{pmatrix} u \\ v \end{pmatrix} + \begin{pmatrix} \tilde{g}_1(u, v) \\ \tilde{g}_2(u, v) \end{pmatrix}, \quad (6.4.21)$$

where

$$\begin{aligned} \tilde{g}_1(u, v) &= \frac{r_{16}H^3}{r_{12}} + \frac{r_{17}H^2P}{r_{12}} + \frac{r_{13}H^2}{r_{12}} + \frac{r_{18}HP^2}{r_{12}} + \frac{r_{14}HP}{r_{12}} + \frac{r_{19}P^3}{r_{12}} + \frac{r_{15}P^2}{r_{12}} \\ &+ O((|u| + |v|)^4), \\ \tilde{g}_2(u, v) &= \frac{(\gamma - r_{11})r_{16}H^3}{r_{12}\delta} + \frac{(\gamma - r_{11})r_{17}H^2P}{r_{12}\delta} + \frac{(\gamma - r_{11})r_{13}H^2}{r_{12}\delta} + \frac{(\gamma - r_{11})r_{18}HP^2}{r_{12}\delta} \\ &+ \left( \frac{(\gamma - r_{11})r_{14}}{r_{12}\delta} - \frac{r_{23}}{\delta} \right) HP + \frac{(\gamma - r_{11})r_{19}P^3}{r_{12}\delta} + \frac{(\gamma - r_{11})r_{15}P^2}{r_{12}\delta} \\ &+ O((|u| + |v|)^4), \end{aligned}$$

where  $H = r_{12}u$  and  $P = (\gamma - r_{11})u - \delta v$ . Therefore, we define the next nonzero real number:

$$F = \left( \left[ -\operatorname{Re} \left( \frac{(1 - 2\omega_1)\omega_2^2}{1 - \omega_1} \tau_{20}\tau_{11} \right) - \frac{1}{2} |\tau_{11}|^2 - |\tau_{02}|^2 + \operatorname{Re}(\omega_2\tau_{21}) \right] \right)_{\bar{h}=0},$$

where

$$\tau_{20} = \frac{1}{8} [\tilde{g}_{1uu} - \tilde{g}_{1vv} + 2\tilde{g}_{2uv} + i(\tilde{g}_{2uu} - \tilde{g}_{2vv} - 2\tilde{g}_{1uv})],$$

$$\tau_{11} = \frac{1}{4} [\tilde{g}_{1uu} + \tilde{g}_{1vv} + i(\tilde{g}_{2uu} + \tilde{g}_{2vv})],$$

$$\tau_{02} = \frac{1}{8} [\tilde{g}_{1uu} - \tilde{g}_{1vv} - 2\tilde{g}_{2uv} + i(\tilde{g}_{2uu} - \tilde{g}_{2vv} + 2\tilde{g}_{1uv})],$$

$$\tau_{21} = \frac{1}{16} [\tilde{g}_{1uuu} + \tilde{g}_{1uvv} + \tilde{g}_{2uuv} + \tilde{g}_{2vvv} + i(\tilde{g}_{2uuu} + \tilde{g}_{2uvv} - \tilde{g}_{1uvv} - \tilde{g}_{1vvv})].$$

Finally, we have the following theorem.

**Theorem 6.4.3.** *Whenever  $h$  varies within a small neighborhood of  $\bar{h} = \frac{1}{k\beta - 2s}$ , a Neimark-Sacker bifurcation occurs at  $\left(\frac{s}{\beta}, \frac{r(k\beta - s)}{k\alpha\beta}\right)$ . Additionally, if  $F < 0$  ( $F > 0$ ), an attracting (repelling) invariant closed curve emerges from the equilibrium point for  $h > \bar{h}$  ( $h < \bar{h}$ ) respectively.*

## 6.5 Chaos control

This section has discussed a generalized hybrid control technique by applying state feedback and parameter perturbation. Moreover, this technique controls the chaos and Neimark-Sacker bifurcation experienced by the system ((6.1.1)) about its positive fixed point.

### 6.5.1 A modified technique for chaos control

In this scenario, we consider a hybrid control technique that combines state feedback and parameter perturbation. The technique is described by the equation below:

$$s_{n+k} = \theta^3 g^{(k)}(s_n, \xi) + (1 - \theta^3)s_n \quad (6.5.1)$$

Here,  $k$  is a positive integer,  $0 < \theta < 1$  is a parameter used to regulate the bifurcation in (6.5.1). Furthermore,  $g^{(k)}$  represents the  $k^{\text{th}}$  iterative value of the function  $g(\cdot)$ . By applying the control strategy (6.5.1) on (6.1.1) and (6.1.2) respectively, one can get the following discrete-time mathematical systems:

$$\begin{aligned} x_{n+1} &= \theta^3 \left( x_n + h \left( rx_n - \frac{rx_n^2}{k} - \alpha x_n y_n \right) \right) + (1 - \theta^3)x_n, \\ y_{n+1} &= \theta^3 (y_n + h(\beta x_n y_n - sy_n)) + (1 - \theta^3)y_n, \end{aligned} \quad (6.5.2)$$

and

$$\begin{aligned} x_{n+1} &= \theta^3 \left( \frac{x_n(1+rh)}{1 + \frac{rh}{k}x_n + \alpha h y_n} \right) + (1 - \theta^3)x_n, \\ y_{n+1} &= \theta^3 \left( \frac{y_n(1 + \beta h x_n)}{1 + s h} \right) + (1 - \theta^3)y_n, \end{aligned} \quad (6.5.3)$$

where  $0 < \theta < 1$  is control parameter. Furthermore, controlled systems (6.5.2) and (6.5.3) are fixed point preservers and their constant solution is same as original system. The variational matrices for (6.5.2) and (6.5.3) evaluated at unique positive fixed point  $\left(\frac{s}{\beta}, \frac{r(k\beta-s)}{k\alpha\beta}\right)$  are respectively:

$$\begin{pmatrix} 1 - \frac{hrs\theta^3}{k\beta} & -\frac{hs\alpha\theta^3}{\beta} \\ \frac{hr(k\beta-s)\theta^3}{k\alpha} & 1 \end{pmatrix} \quad (6.5.4)$$

and

$$\begin{pmatrix} 1 - \frac{hrs\theta^3}{k\beta+hkr\beta} & -\frac{hs\alpha\theta^3}{\beta+hr\beta} \\ \frac{hr(k\beta-s)\theta^3}{k(1+hs)\alpha} & 1 \end{pmatrix}. \quad (6.5.5)$$

The following result properly describes the conditions for local asymptotic stability of one and only positive fixed point  $\left(\frac{s}{\beta}, \frac{r(k\beta-s)}{k\alpha\beta}\right)$  of the controlled system (6.5.2) and (6.5.3).

**Theorem 6.5.1.** *The fixed point  $\left(\frac{s}{\beta}, \frac{r(k\beta-s)}{k\alpha\beta}\right)$  of mathematical system (6.5.2) is locally asymptotically stable if and only if the next condition holds true.*

$$2 > 1 + q > |p|,$$

where,  $p$  and  $q$  are trace and determinant of (6.5.5), respectively. Furthermore, let

$$|p_1| < 1 + q_1 < 2,$$

then the equilibrium  $\left(\frac{s}{\beta}, \frac{r(k\beta-s)}{k\alpha\beta}\right)$  of controlled system (6.5.3) is locally asymptotically stable. Where, trace and determinant of (6.5.4) are respectively represented by  $p_1$  and  $q_1$ .

## 6.6 Numerical simulations

**Example 6.6.1.** *Let  $\alpha = 0.4$ ,  $\beta = 2$ ,  $s = 1.999$ ,  $k = 1$ ,  $r = 2.999$  and  $0 < h < 1$ , in this case we have the following form of system (6.1.1);*

$$\begin{aligned} x_{n+1} &= x_n + h(2.999x_n(1-x_n) - 0.4y_n), \\ y_{n+1} &= y_n + h(2x_ny_n - 1.999y_n). \end{aligned} \quad (6.6.1)$$

Moreover, in this case the system (6.6.1) has unique positive equilibrium point  $\underline{p} = (0.9995, 0.00265075)$ . Additionally, the system (6.6.1) experiences the period-doubling

bifurcation for population variable  $x_n$  and its corresponding bifurcation diagram is given in (Fig. 6.1a) and the maximum Lyapunov exponent is shown in (Fig. 6.1b). Next,  $\mathbb{H}(-1) = 0$ , implies that  $h = 0.667445$  and then by performing some critical computation we have the following consequences for the existence and direction of period-doubling bifurcation. In view of standard theory of period-doubling bifurcation and by considering aforementioned parametric values one can get the following real numbers:  $m_1 = 3.559135287$ ,  $m_2 = -13.47513858$ ,  $m_3 = 0$ ,  $k_1 = 0.5315796793$ ,  $k_2 = -2.98750466$ ,  $k_3 = -11.156205$ ,  $k_4 = -0.46650738$ ,  $k_5 = 3.157005021$ . Hence, we have:  $l_1 = -2.987504665 \neq 0$  and  $l_2 = 3.439581976 > 0$ . Clearly,  $l_2 > 0$ , then the period-two orbits that bifurcate from  $\underline{p} = (0.9995, 0.00265075)$  are stable.

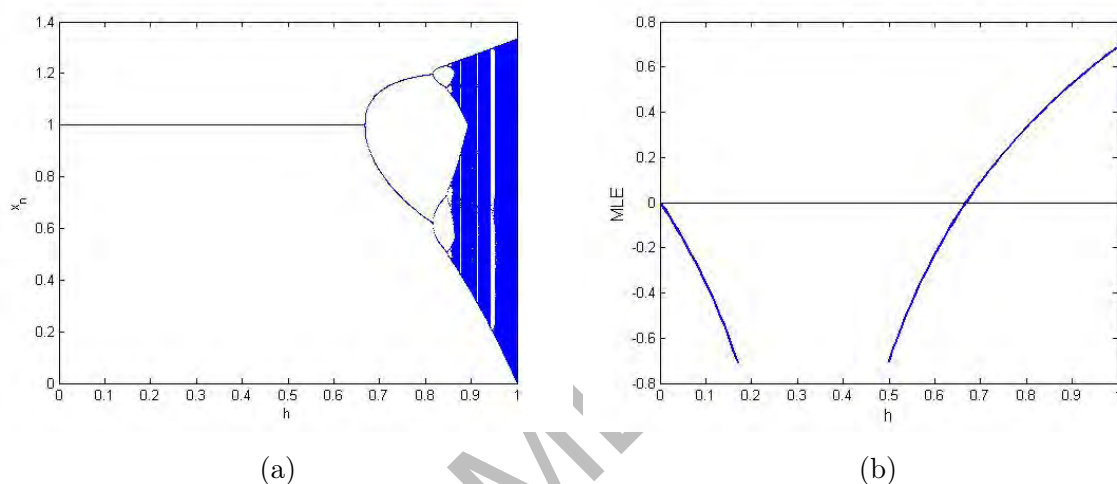


Figure 6.1: Bifurcation diagram and MLE for system (6.6.1)

**Example 6.6.2.** Let  $\beta = 1.299$ ,  $\alpha = 2.599$ ,  $s = 1.099$ ,  $k = 2.099$ ,  $r = 2.495$  and  $0 < h < 1$ . Then the discrete-time system (6.1.1) takes the following mathematical form:

$$\begin{aligned} x_{n+1} &= x_n + h \left( 2.495x_n \left( 1 - \frac{x_n}{2.099} \right) - 2.599y_n \right), \\ y_{n+1} &= y_n + h (1.299x_n y_n - 1.099y_n). \end{aligned} \quad (6.6.2)$$

In this case we get  $\underline{p} = (0.8460354119, 0.5730475087)$  and plots of  $x_n$  and  $y_n$  are given in (Fig. 6.2). Additionally, one can see that the system (6.6.2) experiences the Neimark-Sacker bifurcation for both population variables. Moreover, the maximum Lyapunov exponent is shown in (Fig. 6.2c) and phase portraits for different values of the bifurcation parameter  $h$  are shown in (Fig. 6.3 and Fig. 6.4). One can see from Fig. 6.3a that when  $h$  passes through  $h = 0.6144011954$  then the system (6.6.2) experiences the Neimark-Sacker bifurcation about  $\underline{p}$ . Furthermore, for  $h = 0.9920911954$  and  $h = 0.9344011954$  chaotic attractors are shown which is the confirmation for the existence of chaos produced in system (6.1.1) (see Fig. 6.4g and Fig. 6.4h). The characteristic polynomial of

system (6.1.1) computed at fixed point  $\underline{p} = (0.8460354119, 0.5730475087)$  is given by

$$\mathbb{H}(\omega) = \omega^2 - 1.382127730\omega + 1.$$

Then, roots of  $\mathbb{H}(\omega) = 0$  are  $\omega_{1,2} = 0.6910638648 \pm 0.7227937010i$  with  $|\omega_1| = 1 = |\omega_2|$ . As  $(\beta, \alpha, s, k, r, h) = (1.299, 2.599, 1.099, 2.099, 2.495, 0.6144011954) \in B_{S_2}$  and  $S(0) = 1.382127730$  thus condition (6.4.12) is satisfied. Moreover, some careful calculation gives

$$\tau_{20} = \frac{1}{8} [\tilde{g}_{1uu} - \tilde{g}_{1vv} + 2\tilde{g}_{2uv} + i(\tilde{g}_{2uu} - \tilde{g}_{2vv} - 2\tilde{g}_{1uv})] = -0.0228964 - 0.120618i,$$

$$\tau_{11} = \frac{1}{4} [\tilde{g}_{1uu} + \tilde{g}_{1vv} + i(\tilde{g}_{2uu} + \tilde{g}_{2vv})] = 0.246659 + 0.335853i,$$

$$\tau_{02} = \frac{1}{8} [(\tilde{g}_{2uu} - \tilde{g}_{2vv} + 2\tilde{g}_{1uv})i + \tilde{g}_{1uu} - \tilde{g}_{1vv} - 2\tilde{g}_{2uv}] = 0.269555 + 0.456471i,$$

$$\xi_{21} = \frac{1}{16} [(\tilde{g}_{2uuu} + \tilde{g}_{2uvv} - \tilde{g}_{1uvv} - \tilde{g}_{1vvv})i + \tilde{g}_{1uuu} + \tilde{g}_{1uvv} + \tilde{g}_{2uvv} + \tilde{g}_{2vvv}] = 0,$$

and

$$F = \left( \left[ -\operatorname{Re} \left( \frac{(1 - 2\omega_1)\omega_2^2}{1 - \omega_1} \tau_{20}\tau_{11} \right) - \frac{1}{2} |\tau_{11}|^2 - |\tau_{02}|^2 + \operatorname{Re}(\omega_2\tau_{21}) \right] \right)_{\tilde{h}=0} = -0.270617 < 0.$$

which proves the correctness of **Theorem 6.4.2**.

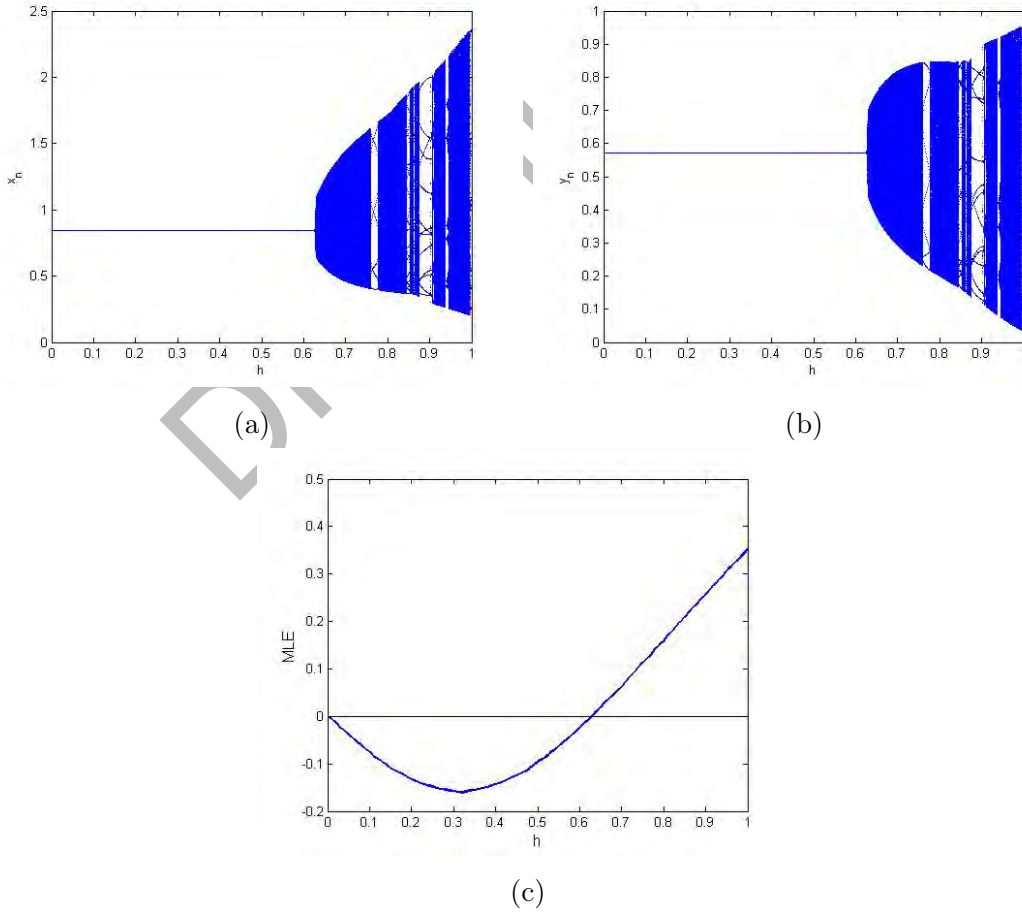
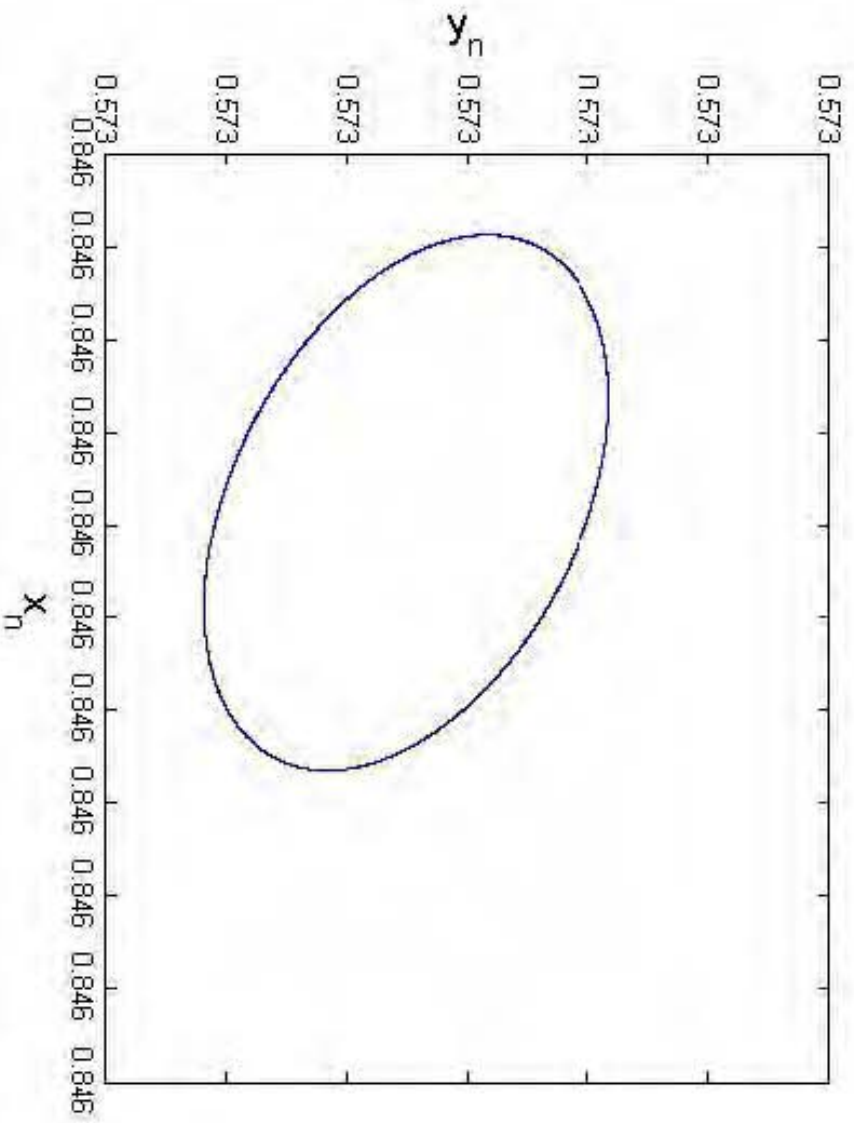
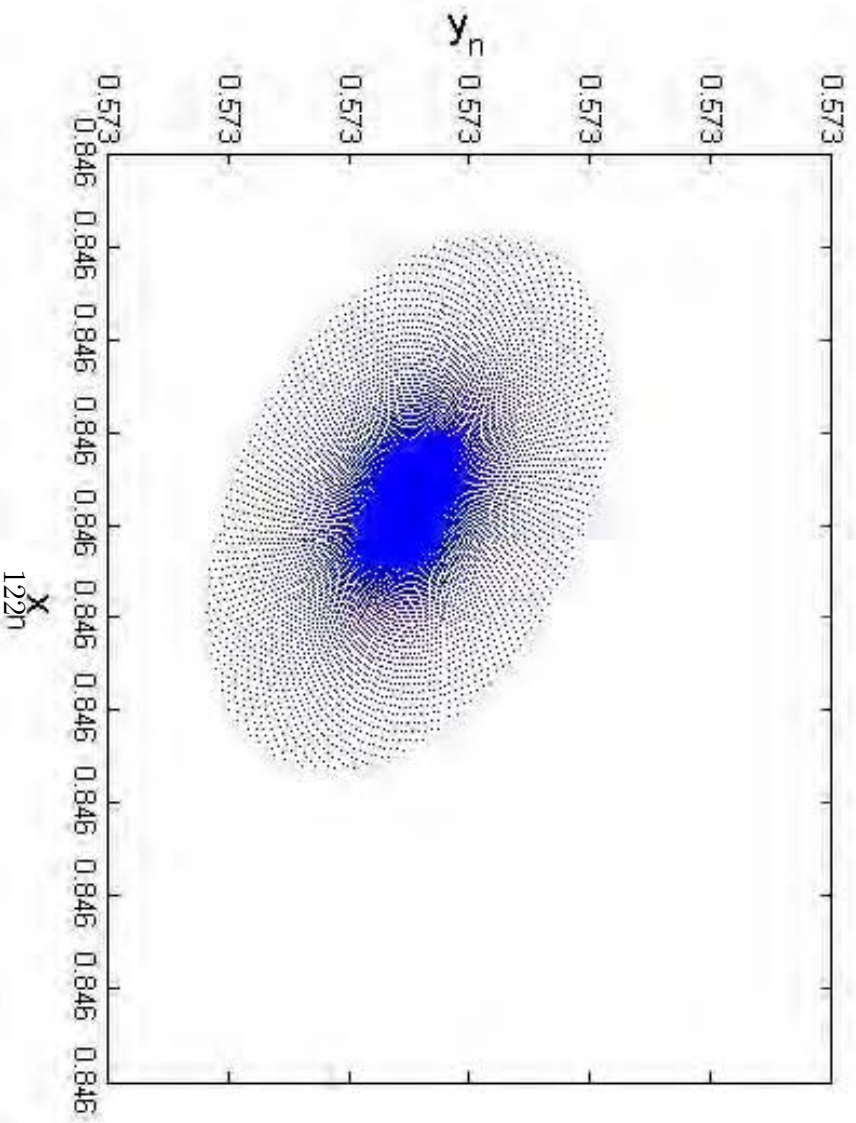


Figure 6.2: Bifurcation diagrams and MLE for system (6.6.2)



(a)



(b)

Figure 6.3: Phase portraits for system (6.1.1) for  $0 < h < 1$  with  $\beta = 1.299$ ,  $\alpha = 2.599$ ,  $s = 1.099$ ,  $k = 2.099$ ,  $r = 2.495$  and initial conditions  $x_0 = 0.8460354119$ ,  $y_0 =$



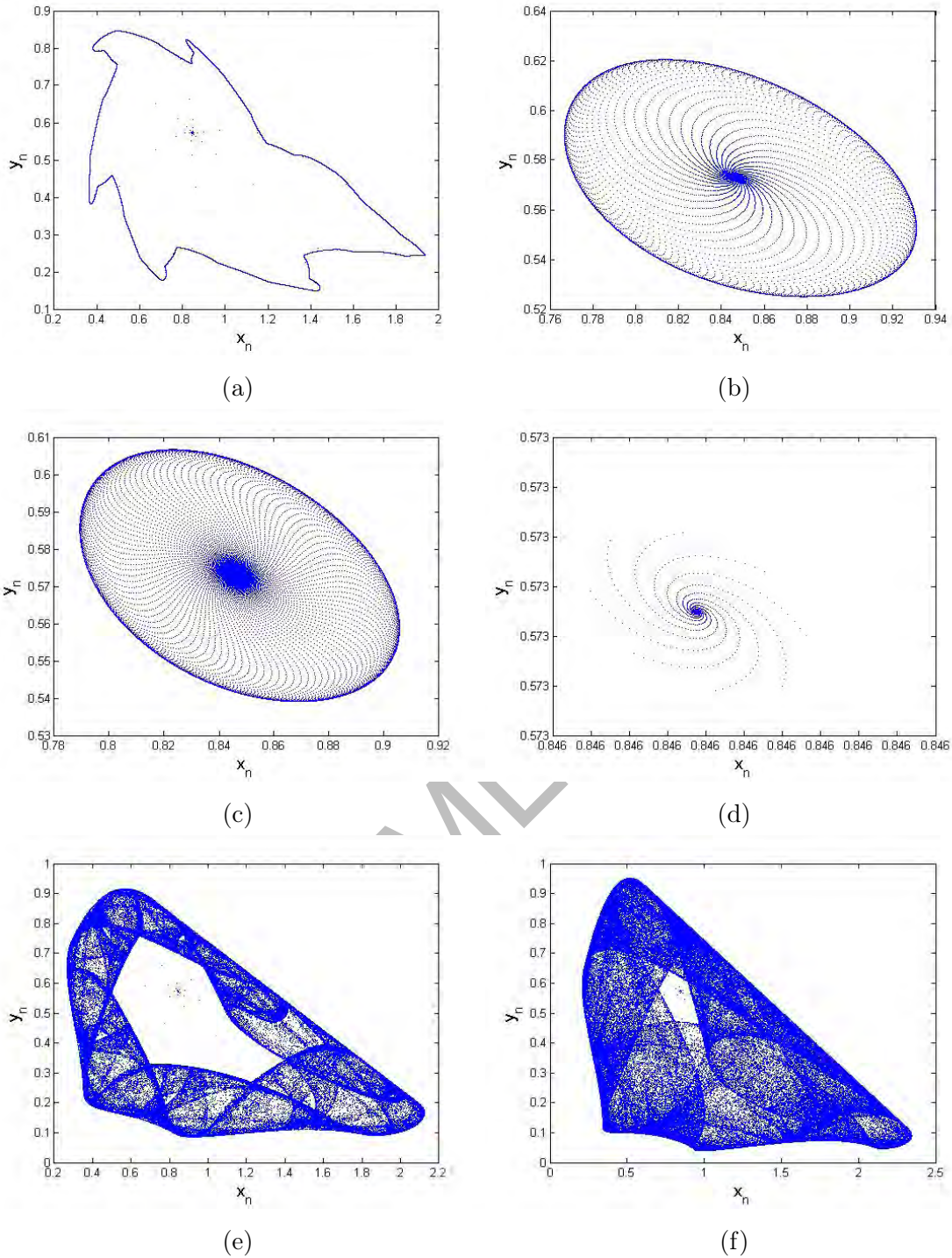


Figure 6.4: Phase portraits for system (6.1.1) for  $0 < h < 1$  with  $\beta = 1.299$ ,  $\alpha = 2.599$ ,  $s = 1.099$ ,  $k = 2.099$ ,  $r = 2.495$  and initial conditions  $x_0 = 0.8460354119$ ,  $y_0 = 0.5730475087$

**Example 6.6.3.** Let  $\beta = 0.999$ ,  $\alpha = 0.599$ ,  $s = 1.679$ ,  $k = 5.999$ ,  $r = 9.95$  and

$0 < h < 1$ . Then, the system (6.1.2) has the following mathematical form:

$$\begin{aligned} x_{n+1} &= \frac{x_n(1 + 9.95h)}{1 + \frac{(9.95)h}{5.999}x_n + 0.599hy_n}, \\ y_{n+1} &= \frac{y_n(1 + 0.999hx_n)}{1 + 1.679h}. \end{aligned} \quad (6.6.3)$$

In this case  $\underline{p} = (1.680680681, 11.89727313)$  and plots of  $x_n$  and  $y_n$  are given in (Fig. 6.5). Additionally, it can be seen from (Fig. 6.5) that both population undergoes Neimark-Sacker bifurcation and their maximum Lyapunov exponent is shown in (Fig. 6.5c). Moreover, some phase portraits for different values of the bifurcation parameter  $h$  are shown in (Fig. 6.6). One can observe that the system (6.6.3) experiences the Neimark-Sacker bifurcation about  $\underline{p} = (1.680680681, 11.89727313)$  when  $h$  passes through  $h = 0.3795064973$  (see Fig. 6.6a). The characteristic polynomial related to the jacobian matrix of system (6.6.3) computed at fixed point  $\underline{p} = (1.680680681, 11.89727313)$  is given by

$$P(\omega) = \omega^2 - 1.778498755\omega + 1.$$

Then, roots of  $P(\omega) = 0$  are  $\omega_{1,2} = 0.8892493774 \pm 0.4574227192i$  with  $|\omega_1| = 1 = |\omega_2|$ . As  $(\beta, \alpha, s, k, r, h) = (0.999, 0.599, 1.679, 5.999, 9.95, 0.3795064973) \in \aleph_S$  and  $M_1(0) = 1.778498755$  : thus condition (6.4.19) is satisfied. Moreover, some careful calculation gives us

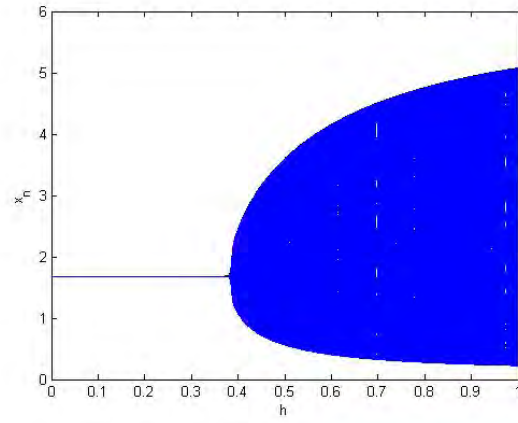
$$\begin{cases} \tau_{20} = \frac{1}{8} [\tilde{g}_{1uu} - \tilde{g}_{1vv} + 2\tilde{g}_{2uv} + i(\tilde{g}_{2uu} - \tilde{g}_{2vv} - 2\tilde{g}_{1uv})] = 0.0000551415 - 0.00223878i, \\ \tau_{11} = \frac{1}{4} [\tilde{g}_{1uu} + \tilde{g}_{1vv} + i(\tilde{g}_{2uu} + \tilde{g}_{2vv})] = -0.00258243 + 0.00160671i, \\ \tau_{02} = \frac{1}{8} [\tilde{g}_{1uu} - \tilde{g}_{1vv} - 2\tilde{g}_{2uv} + i(\tilde{g}_{2uu} - \tilde{g}_{2vv} + 2\tilde{g}_{1uv})] = 0.0073498 + 0.00622883i, \\ \xi_{21} = \frac{1}{16} [\tilde{g}_{1uuu} + \tilde{g}_{1uuv} + \tilde{g}_{2uuu} + \tilde{g}_{2uvv} + i(\tilde{g}_{2uuu} + \tilde{g}_{2uvv} - \tilde{g}_{1uuu} - \tilde{g}_{1vvv})] = \\ 0.0000356238 + 0.0000688866i. \end{cases}$$

and

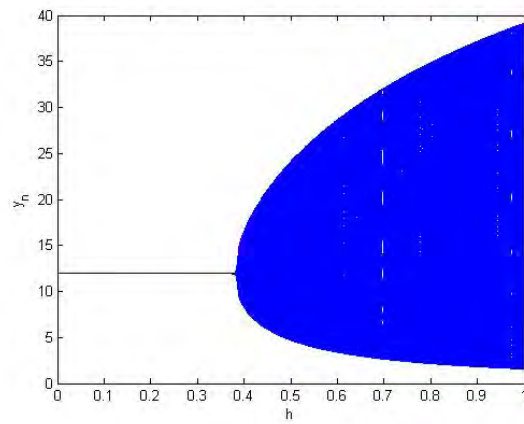
$$F = \left( \left[ -Re \left( \frac{(1 - 2\omega_1)\omega_2^2}{1 - \omega_1} \tau_{20}\tau_{11} \right) - \frac{1}{2} |\tau_{11}|^2 - |\tau_{02}|^2 + Re(\omega_2\tau_{21}) \right] \right)_{\tilde{h}=0} = -0.0000456766 < 0.$$

which verifies the **Theorem 6.4.3**.

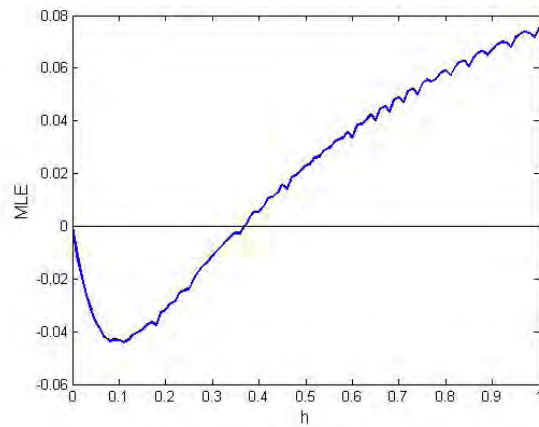




(a)



(b)



(c)

Figure 6.5: Bifurcation diagrams and MLE for system (6.6.3)

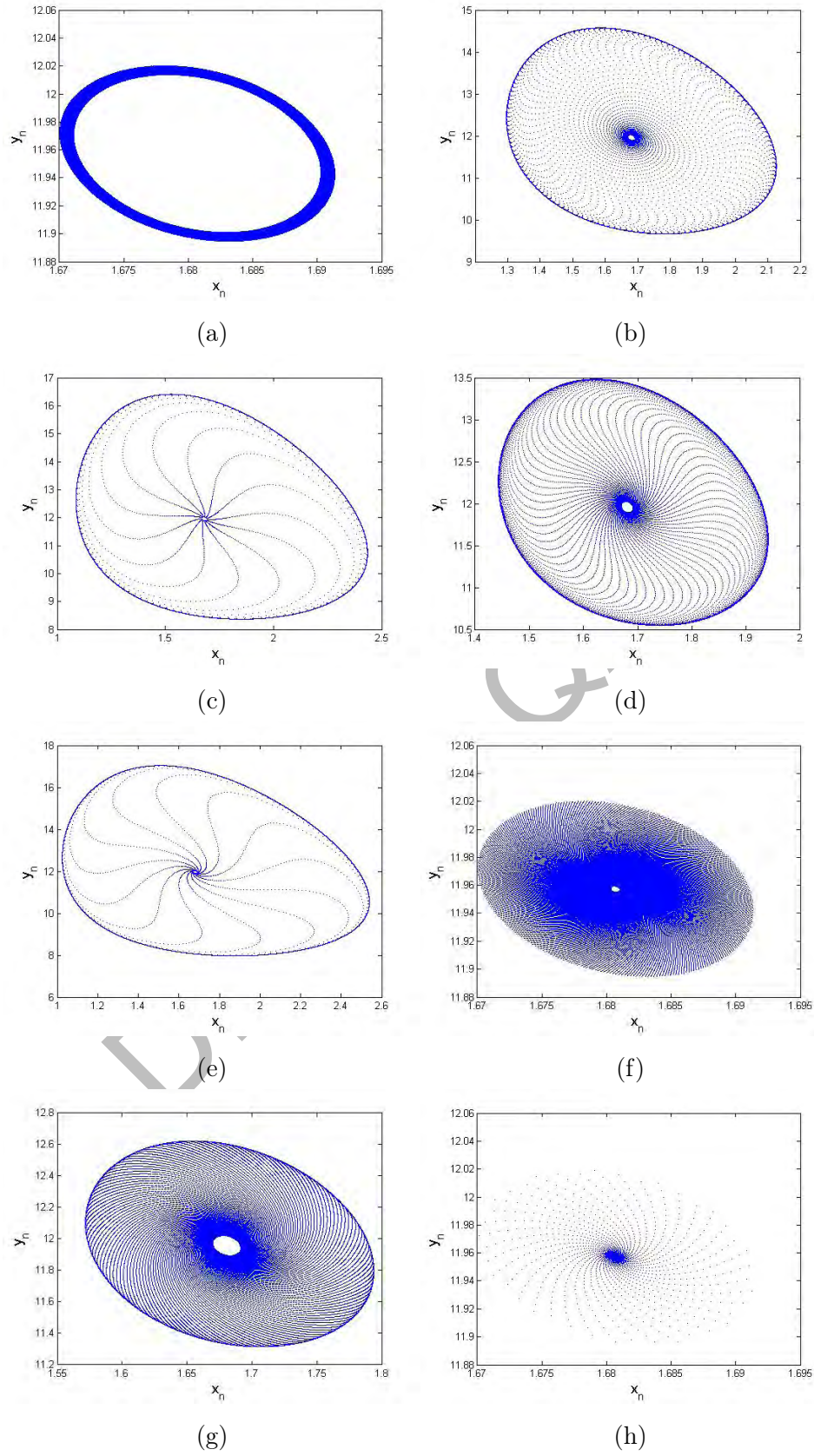
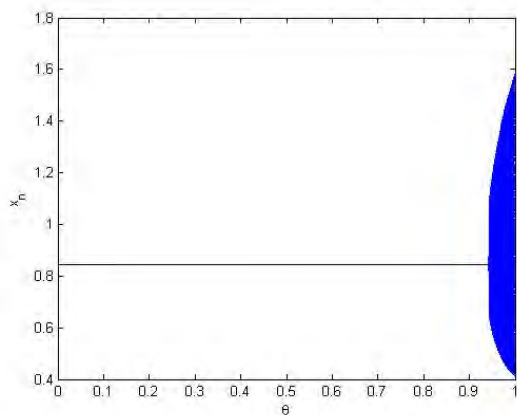


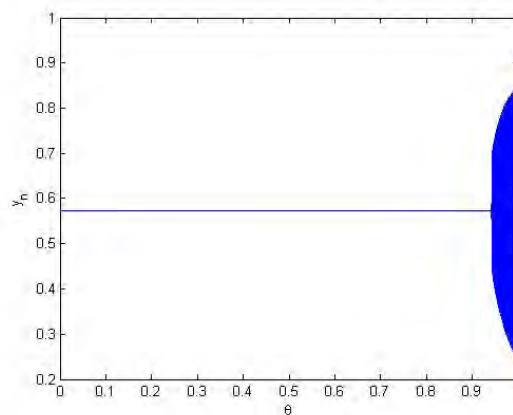
Figure 6.6: Phase portraits for system (6.6.3) for  $0 < h < 1$  with  $\beta = 0.999$ ,  $\alpha = 0.599$ ,  $s = 1.679$ ,  $k = 5.999$ ,  $r = 9.95$  and initial conditions  $x_0 = 1.680680681$ ,  $y_0 = 11.89727313$ .

**Example 6.6.4.** *This example is concerned to the modified hybrid control of Neimark-Sacker bifurcation. By applying the generalized control technique for controlling the Neimark-Sacker bifurcation, we have the following mathematical scheme;*

$$\begin{aligned} x_{n+1} &= \theta^3 \left( x_n + 0.75011954 \left( 2.495x_n - \frac{2.495x_n^2}{2.099} - 2.599x_n y_n \right) \right) + (1 - \theta^3)x_n, \\ y_{n+1} &= \theta^3 (y_n + 0.75011954 (1.299x_n y_n - 1.099y_n)) + (1 - \theta^3)y_n, \end{aligned} \quad (6.6.4)$$

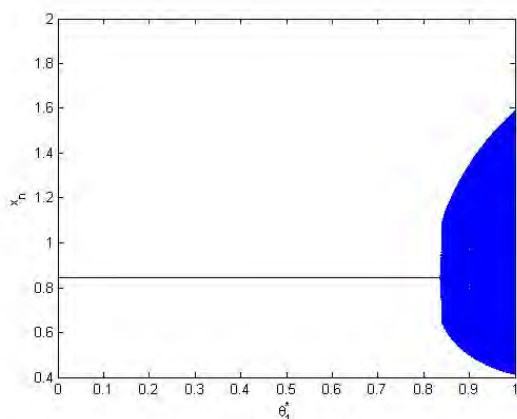


(a) Controlled diagram for  $x_n$

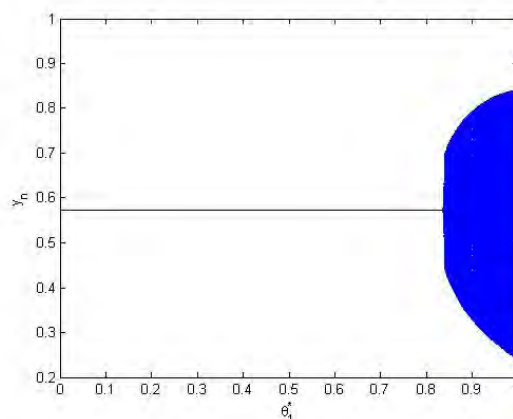


(b) Controlled diagram for  $y_n$

Figure 6.7: Controlled diagrams for system (6.1.1) with  $\theta \in (0, 1)$  with  $(r, k, \alpha, \beta, s, h) = (2.495, 2.099, 2.599, 1.299, 1.099, 0.75011954)$  and initial conditions  $x_0 = 0.8460354119$ ,  $y_0 = 0.5730475087$



(a) Controlled diagram for  $x_n$



(b) Controlled diagram for  $y_n$

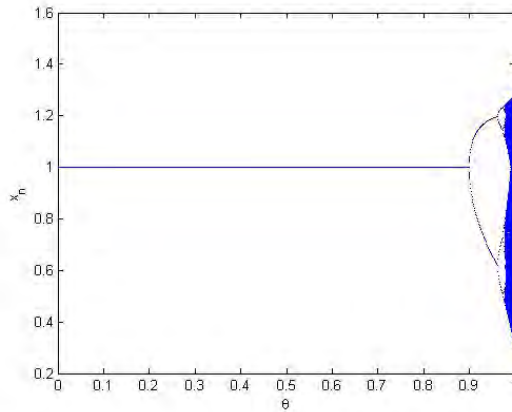
Figure 6.8: Controlled diagrams for system (6.7.1) with  $\theta_1^* \in (0, 1)$  with  $(r, k, \alpha, \beta, s, h) = (2.495, 2.099, 2.599, 1.299, 1.099, 0.75011954)$  with initial values  $x_0 = 0.8460354119$ ,  $y_0 = 0.5730475087$

where  $(r, k, \alpha, \beta, s, h) = (2.495, 2.099, 2.599, 1.299, 1.099, 0.75011954)$  and  $0 < \theta < 1$  is the control parameter. In this case  $\underline{p} = (0.8460354119, 0.5730475087)$  is the unique positive equilibrium point for system (6.6.4). Moreover,  $\underline{p} = (0.8460354119, 0.5730475087)$  is positive fixed point of original map (6.1.1). By utilizing **Lemma 1.3.1**, we can conclude that the controlled map (6.6.4) attains local asymptotic stability only when  $0 < \theta < 0.935637$ . Moreover, an analysis of **Fig. 6.7** readily demonstrates the successful restoration of stability in the original system (6.1.1) across a broad range of the control parameter  $\theta$ .

**Example 6.6.5.** This example is concerned to the implementation of modified hybrid control methodology for controlling the period-doubling bifurcation and chaos. By applying the generalized hybrid control methodology on system (6.1.1), we get the following scheme;

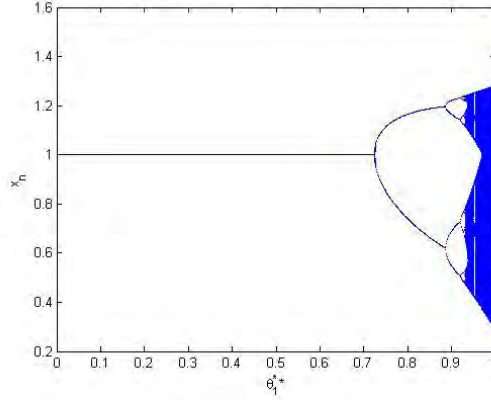
$$\begin{aligned} x_{n+1} &= \theta^3 (x_n + 0.9211954 (2.99x_n - 2.99x_n^2 - 0.4x_n y_n)) + (1 - \theta^3)x_n, \\ y_{n+1} &= \theta^3 (y_n + 0.9211954 (2x_n y_n - 1.999y_n)) + (1 - \theta^3)y_n, \end{aligned} \quad (6.6.5)$$

where  $0 < \theta < 1$  is the control parameter and  $(r, k, \alpha, \beta, s, h) = (2.99, 1, 0.4, 2, 1.999, 0.921)$ . In this case unique positive equilibrium point for (6.6.5) is  $\underline{p} = (0.9995, 0.00262)$ . Furthermore, it is worth noting that  $\underline{p} = (0.9995, 0.00262)$  is a positive fixed point for the original map (6.1.1). Consequently, applying **Lemma 1.3.1**, the controlled map (6.6.5) achieves local asymptotic stability within the range of  $0 < \theta < 0.899062$ . Moreover, the analysis presented in **Fig. 6.9** demonstrates that the stability of the original system (6.1.1) is effectively restored across a broad spectrum of the control parameter  $\theta_2$ .



(a) Controlled diagram for  $x_n$

Figure 6.9: Controlled diagrams for system (6.1.1) with  $\theta \in (0, 1)$  with  $(r, k, \alpha, \beta, s, h) = (2.99, 1, 0.4, 2, 1.999, 0.9211954)$  with initial values  $x_0 = 0.9995$ ,  $y_0 = 0.00262375$

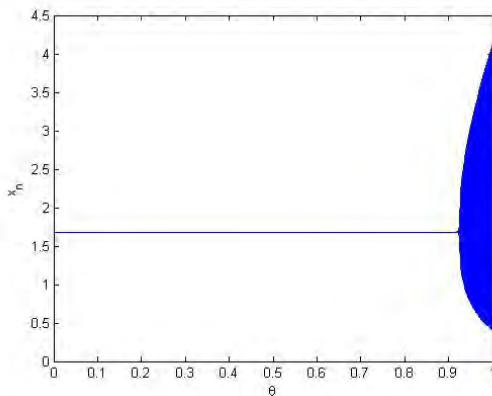


(a) Controlled diagram for  $x_n$

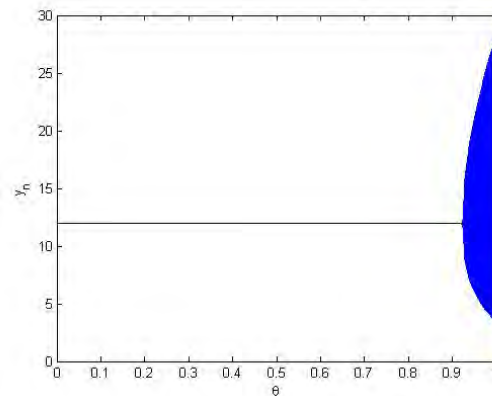
Figure 6.10: Controlled diagrams for system (6.1.1) with  $\theta_1^{**} \in (0, 1)$  with  $(r, k, \alpha, \beta, s, h) = (2.99, 1, 0.4, 2, 1.999, 0.9211954)$  with initial values  $x_0 = 0.9995$ ,  $y_0 = 0.00262375$

**Example 6.6.6.** *In this particular instance, we utilized a modified control technique to manage the Neimark-Sacker bifurcation encountered by system (6.1.2). Consequently, when we apply the modified hybrid control technique to system (6.1.2), we obtain the subsequent mathematical system.*

$$\begin{aligned} x_{n+1} &= \theta^3 \left( \frac{x_n (1 + 9.95(0.59064973))}{1 + \frac{9.95(0.59064973)}{5.999} x_n + 0.599(0.59064973) y_n} \right) + (1 - \theta^3) x_n, \\ y_{n+1} &= \theta^3 \left( \frac{y_n (1 + 0.999(0.59064973) x_n)}{1 + 1.679(0.59064973)} \right) + (1 - \theta^3) y_n, \end{aligned} \quad (6.6.6)$$



(a) Controlled diagram for  $x_n$



(b) Controlled diagram for  $y_n$

Figure 6.11: Controlled diagrams for system (6.1.2) with  $\theta \in (0, 1)$  with  $(r, k, \alpha, \beta, s, h) = (9.95, 5.999, 0.599, 0.999, 1.679, 0.59064973)$  and initial conditions  $x_0 = 1.680680681$ ,  $y_0 = 11.89727313$

Value of h	$I_1$	$I_2$	Length of $I_1$	Length of $I_2$
0.59064973	$0 < \theta < 0.781652763$	$0 < \theta_1 < 0.921166118$	0.781652763	0.921166118
0.69064973	$0 < \theta < 0.724828750$	$0 < \theta_1 < 0.908280151$	0.724828750	0.908280151
0.79064973	$0 < \theta < 0.68237874$	$0 < \theta_1 < 0.880390125$	0.682378743	0.880390125
0.89064973	$0 < \theta < 0.649461101$	$0 < \theta_1 < 0.865999646$	0.649461101	0.865999646

Table 6.1: Comparison between modified hybrid method and old hybrid method [95] for system (6.6.6) for  $h \in (0, 1)$  and  $(r, k, \alpha, \beta, s) = (9.95, 5.999, 0.599, 0.999, 1.679)$  with initial points  $x_0 = 1.680680681$ ,  $y_0 = 11.89727313$

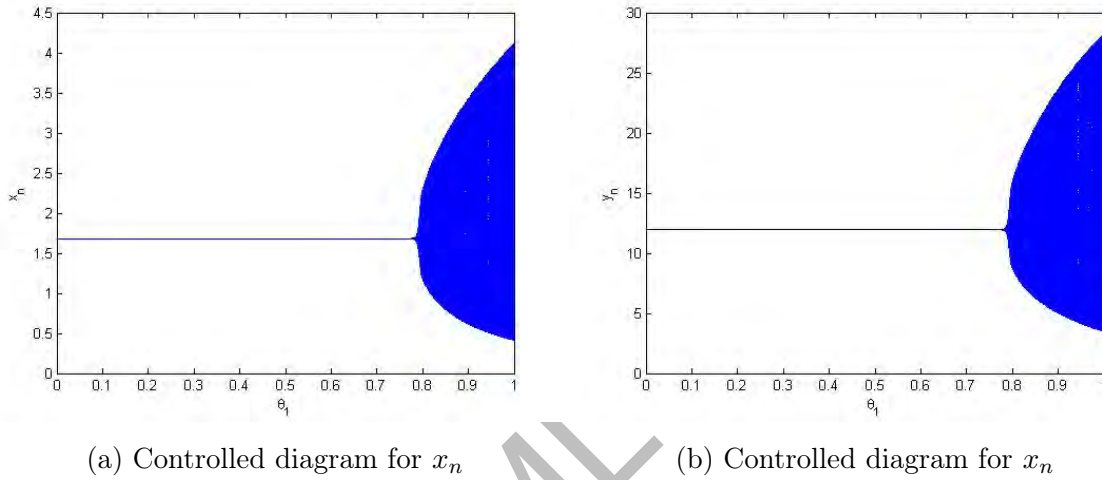


Figure 6.12: Controlled diagrams for system (6.7.2) with  $\theta_1 \in (0, 1)$  with  $(r, k, \alpha, \beta, s, h) = (9.95, 5.999, 0.599, 0.999, 1.679, 0.59064973)$  and initial conditions  $x_0 = 1.680680681$ ,  $y_0 = 11.89727313$

where  $(r, k, \alpha, \beta, s, h) = (9.95, 5.999, 0.599, 0.999, 1.679, 0.59064973)$  and  $0 < \theta < 1$  is the control parameter. In this case  $\underline{p} = (1.680680681, 11.89727313)$  is unique positive equilibrium point for (6.6.6). Additionally,  $\underline{p} = (1.680680681, 11.89727313)$  is positive fixed point of original map (6.1.2). Hence, by using **Lemma 1.3.1** one can see that the controlled system (6.6.6) is locally asymptotically stable if and only if  $0 < \theta < 0.921166$ . Moreover, it can be easily seen that the stability of original system (6.1.2) is successfully restored for maximum range of control parameter  $\theta$  (see **Fig. 6.11**).

## 6.7 Concluding remarks

This chapter has discussed the dynamics of a discrete-time plant-herbivore model proposed by Chattopadhyay *et al.* [87]. We converted a continuous-time plant-herbivore model into its discrete-time counterpart by using Euler's forward method. Furthermore,



Value of h	$I_3$	$I_4$	Length of $I_3$	Length of $I_4$
0.9911954	$0 < \theta < 0.67540166$	$0 < \theta^{**} < 0.87737928$	0.67540166	0.87737928
0.9211954	$0 < \theta < 0.72672423$	$0 < \theta^{**} < 0.89906249$	0.72672423	0.89906249
0.8211954	$0 < \theta < 0.81522013$	$0 < \theta^{**} < 0.93416795$	0.81522013	0.93416795
0.7211954	$0 < \theta < 0.928257475$	$0 < \theta^{**} < 0.97548999$	0.928257475	0.97548999

Table 6.2: Comparison between modified hybrid method and old hybrid method [95] for system (6.6.5) for  $h \in (0, 1)$  and  $(r, k, \alpha, \beta, s) = (2.99, 1, 0.4, 2, 1.999, )$  with initial points  $x_0 = 0.9995$ ,  $y_0 = 0.00262375$

a dynamically consistent discrete-time plant-herbivore model is obtained by using Mickens [20] non-standard difference scheme. Mainly, we studied the linearized stability of systems (6.1.1) and (6.1.2) about all of their equilibrium points. By utilizing the parameter  $h$  as a bifurcation parameter, it has been demonstrated that the discrete-time mathematical system (6.1.1) undergoes Neimark-Sacker bifurcation and period-doubling bifurcation centered around the positive equilibrium  $\underline{p}$ . Additionally, the system (6.1.2) experiences Neimark-Sacker bifurcation solely when  $h$  is employed as a bifurcation parameter, with no possibility of period-doubling bifurcation. Parametric conditions for the existence and direction of both the Neimark-Sacker bifurcation and period-doubling bifurcation have been derived. The main objective of our study is to establish the dynamical consistency of the mathematical system (6.1.2) and develop an improved hybrid control strategy to regulate the Neimark-Sacker bifurcation and period-doubling bifurcation. To demonstrate the effectiveness of this modified technique, a comparison is provided with an existing hybrid control methodology [95]. For this comparison, all parametric values are taken similarly as taken in **Example 6.6.4**, **Example 6.6.5** and **Example 6.6.6**. By applying hybrid scheme [95] on (6.1.1) and (6.1.2), one can get the following discrete-time mathematical systems, respectively;

$$\begin{aligned} x_{n+1} &= \theta_1^{**} \left( x_n + h \left( rx_n - \frac{rx_n^2}{k} - \alpha x_n y_n \right) \right) + (1 - \theta_1^{**})x_n, \\ y_{n+1} &= \theta_1^{**} (y_n + h(\beta x_n y_n - sy_n)) + (1 - \theta_1^{**})y_n, \end{aligned} \quad (6.7.1)$$

and

$$\begin{aligned} x_{n+1} &= \theta_1 \left( \frac{x_n(1+rh)}{1 + \frac{rh}{k}x_n + \alpha h y_n} \right) + (1 - \theta_1)x_n, \\ y_{n+1} &= \theta_1 \left( \frac{y_n(1 + \beta h x_n)}{1 + sh} \right) + (1 - \theta_1)y_n, \end{aligned} \quad (6.7.2)$$

where,  $\theta_1, \theta_1^{**} \in (0, 1]$  are control parameters. Considering the stability criteria from **Lemma 1.3.1** one can see that system (6.7.1) is stable if and only if  $0 < \theta_1^{**} < 0.726724$ ,

where  $\theta_1^{**}$  is control parameters for period-doubling bifurcation. Furthermore, the system (6.7.2) is stable if and only if  $0 < \theta_1 < 0.781653$  where  $\theta_1$  is control parameters for Neimark-Sacker bifurcation. On the other hand, in **example 6.6.4**, **Example 6.6.5** and **Example 6.6.6**, a modified control methodology (6.5.1) is applied to systems (6.1.1) and (6.1.2) for the same parametric values. In this case, a clear regain in the stability of the original system can be seen from regions shown in **Fig. 6.7**, **Fig. 6.9** and **Fig. 6.11**, respectively. Hence, it is seen that the modified control methodology is more efficient than the existing hybrid control scheme and applicable for every class of discrete-time maps. For comparative analysis of control techniques, **Fig. 6.8** and **Fig. 6.12** respectively represent Neimark-Sacker bifurcation related to the system (6.7.1) and (6.7.2). In addition, a controlled diagram for modified control methodology related to period-doubling bifurcation is shown in **Fig. 6.10**. Finally, a comprehensive tabular comparison of controlling techniques is given in **Table. 6.1** and **Table. 6.2**.



# Bibliography

- [1] Strogatz, S. H. (2001). Exploring complex networks. *Nature*, 410(6825), 268-276.
- [2] Katok, A., and Hasselblatt, B. (1995). Introduction to the modern theory of dynamical systems (No. 54). Cambridge University Press.
- [3] Melby, P., Weber, N., & Hilgler, A. (2005). Dynamics of self-adjusting systems with noise. *Chaos: An Interdisciplinary Journal of Nonlinear Science*, 15(3).
- [4] Holmes, P. (1990). Poincaré, celestial mechanics, dynamical-systems theory and chaos. *Physics Reports*, 193(3), 137-163.
- [5] Parthasarathy, S. (1992). Homoclinic bifurcation sets of the parametrically driven Duffing oscillator. *Physical Review A*, 46(4), 2147.
- [6] Din, Q. (2018). Bifurcation analysis and chaos control in discrete-time glycolysis models. *Journal of Mathematical Chemistry*, 56(3), 904-931.
- [7] Din, Q., Donchev, T., & Kolev, D. (2018). Stability, bifurcation analysis and chaos control in chlorine dioxide-iodine-malonic acid reaction. *MATCH Commun. Math. Comput. Chem*, 79(3), 577-606.
- [8] Molgedey, L., Schuchhardt, J., & Schuster, H. G. (1992). Suppressing chaos in neural networks by noise. *Physical review letters*, 69(26), 3717.
- [9] Strogatz, S. H. (1994). *Nonlinear dynamics and chaos: with applications to physics, Biology, Chemistry and Engineering*, 1.
- [10] Ghanbari, B., & Gímez-Aguilar, J. F. (2018). Modeling the dynamics of nutrient-phytoplankton-zooplankton system with variable-order fractional derivatives. *Chaos, Solitons & Fractals*, 116, 114-120.
- [11] Gímez-Aguilar, J. F., López-López, M. G., Alvarado-Martínez, V. M., Baleanu, D., & Khan, H. (2017). Chaos in a cancer model via fractional derivatives with exponential decay and Mittag-Leffler law. *Entropy*, 19(12), 681.

- [12] Beigi, A., Yousefpour, A., Yasami, A., Gilemez-Aguilar, J. F., Bekiros, S., & Jahanshahi, H. (2021). Application of reinforcement learning for effective vaccination strategies of coronavirus disease 2019 (COVID-19). *The European Physical Journal Plus*, 136(5), 1-22.
- [13] Le Quiñirí, C., Buitenhuis, E. T., Moriarty, R., Alvain, S., Aumont, O., Bopp, L., ... & Vallina, S. M. (2016). Role of zooplankton dynamics for Southern Ocean phytoplankton biomass and global biogeochemical cycles. *Biogeosciences*, 13(14), 4111-4133.
- [14] Alderremy, A. A., Gilemez-Aguilar, J. F., Aly, S., & Saad, K. M. (2021). A fuzzy fractional model of coronavirus (COVID-19) and its study with Legendre spectral method. *Results in Physics*, 21, 103773.
- [15] Kumar, S., Kumar, A., Samet, B., Gilemez-Aguilar, J. F., & Osman, M. S. (2020). A chaos study of tumor and effector cells in fractional tumor-immune model for cancer treatment. *Chaos, Solitons & Fractals*, 141, 110321.
- [16] LeVeque, R. J. (2007). *Finite difference methods for ordinary and partial differential equations: steady-state and time-dependent problems*. Society for Industrial and Applied Mathematics.
- [17] Butcher, J. (2007). Runge-kutta methods. *Scholarpedia*, 2(9), 3147.
- [18] Khan, M. S., Ozair, M., Hussain, T., & Gilemez-Aguilar, J. F. (2021). Bifurcation analysis of a discrete-time compartmental model for hypertensive or diabetic patients exposed to COVID-19. *The European Physical Journal Plus*, 136(8), 1-26.
- [19] Yousef, A. M., Rida, S. Z., Gouda, Y. G., & Zaki, A. S. (2019). Dynamical behaviors of a fractional-order predator-prey model with Holling type iv functional response and its discretization. *International Journal of Nonlinear Sciences and Numerical Simulation*, 20(2), 125-136.
- [20] Mickens, R.E., 1994. *Nonstandard finite difference models of differential equations*. world scientific.
- [21] Curtiss, D. R. (1918). Recent extentions of descartes' rule of signs. *Annals of Mathematics*, 251-278.
- [22] Khan, M. S. (2019). Stability, bifurcation and chaos control in a discrete-time prey-predator model with Holling type-II response. *Network Biology*, 9(3), 58.

- [23] Din, Q., Elsadany, A. A., & Khalil, H. (2017). Neimark-Sacker bifurcation and chaos control in a fractional-order plant-herbivore model. *Discrete Dynamics in Nature and Society*, 2017.
- [24] Yang, X. (2006). Uniform persistence and periodic solutions for a discrete predator-prey system with delays. *Journal of Mathematical Analysis and Applications*, 316(1), 161-177.
- [25] Liu, X., & Xiao, D. (2007). Complex dynamic behaviors of a discrete-time predator-prey system. *Chaos, Solitons & Fractals*, 32(1), 80-94.
- [26] Hirsch, M. W., Smale, S., & Devaney, R. L. (2012). *Differential equations, dynamical systems, and an introduction to chaos*. Academic press.
- [27] Grove, E. A., & Ladas, G. (2004). *Periodicities in nonlinear difference equations (Vol. 4)*. CRC Press.
- [28] Din, Q. (2018). Controlling chaos in a discrete-time prey-predator model with Allee effects. *International Journal of Dynamics and Control*, 6(2), 858-872.
- [29] Huang, C., Cao, J., & Xiao, M. (2016). Hybrid control on bifurcation for a delayed fractional gene regulatory network. *Chaos, Solitons & Fractals*, 87, 19-29.
- [30] Shabbir, M. S., Din, Q., Safeer, M., Khan, M. A., & Ahmad, K. (2019). A dynamically consistent nonstandard finite difference scheme for a predator-prey model. *Advances in Difference Equations*, 2019(1), 1-17.
- [31] Din, Q. (2017). Global stability and Neimark-Sacker bifurcation of a host-parasitoid model. *International Journal of Systems Science*, 48(6), 1194-1202.
- [32] Din, Q. (2017). Global stability of Beddington model. *Qualitative theory of dynamical systems*, 16(2), 391-415.
- [33] Din, Q. (2015). Global behavior of a plant-herbivore model. *Advances in Difference Equations*, 2015, 1-12.
- [34] Guckenheimer, J., & Holmes, P. (2013). *Nonlinear oscillations, dynamical systems, and bifurcations of vector fields (Vol. 42)*. Springer Science & Business Media.
- [35] Wen, G. (2005). Criterion to identify Hopf bifurcations in maps of arbitrary dimension. *Physical Review E*, 72(2), 026201.
- [36] Ott, E., Grebogi, C., & Yorke, J. A. (1990). Controlling chaos. *Physical review letters*, 64(11), 1196.

- [37] Singh, H., Dhar, J., & Bhatti, H. S. (2015). Discrete-time bifurcation behavior of a prey-predator system with generalized predator. *Advances in Difference Equations*, 2015(1), 206.
- [38] Yang, X. (2006). Uniform persistence and periodic solutions for a discrete predator-prey system with delays. *Journal of Mathematical Analysis and Applications*, 316(1), 161-177.
- [39] Liu, X., & Xiao, D. (2007). Complex dynamic behaviors of a discrete-time predator-prey system. *Chaos, Solitons & Fractals*, 32(1), 80-94.
- [40] Grove, E.A. and Ladas, G., 2004. Periodicities in nonlinear difference equations (Vol. 4). CRC Press.
- [41] Khan, M. S. (2022). Bifurcation analysis of a discrete-time four-dimensional cubic autocatalator chemical reaction model with coupling through uncatalysed reactant. *MATCH Commun. Math. Comput. Chem*, 87(2), 415-439.
- [42] Leach, J. A., Merkin, J. H., & Scott, S. K. (1992). Two-cell coupled cubic autocatalator: the effect of the uncatalysed reaction. *Dynamics and Stability of Systems*, 7(4), 245-266.
- [43] Forbes, L. K., & Gray, B. F. (1994). Forced oscillations in an exothermic chemical reaction. *Dynamics and Stability of Systems*, 9(3), 253-269.
- [44] Gray, B. F., Roberts, M. J., & Merkin, J. H. (1988). The cubic autocatalator: The influence of the quadratic autocatalytic and the uncatalysed reactions. *Journal of engineering mathematics*, 22(3), 267-284.
- [45] Gray, B. F., Merkin, J. H., & Roberts, M. J. (1989). On the structural stability of the cubic autocatalytic scheme in a closed vessel. *Dynamics and Stability of Systems*, 4(1), 31-54.
- [46] Gray, P., Kay, S. R., & Scott, S. K. (1988). Oscillations of an exothermic reaction in a closed system-I. Approximate (exponential) representation of Arrhenius temperature-dependence. *Proceedings of the Royal Society of London. A. Mathematical and Physical Sciences*, 416(1851), 321-341.
- [47] Merkin, J. H., Needham, D. J., & Scott, S. K. (1987). On the creation, growth and extinction of oscillatory solutions for a simple pooled chemical reaction scheme. *SIAM Journal on Applied Mathematics*, 47(5), 1040-1060.
- [48] Anguelov, R., & Stoltz, S. M. (2017). Stationary and oscillatory patterns in a coupled Brusselator model. *Mathematics and Computers in Simulation*, 133, 39-46.

- [49] Merkin, J. H., Needham, D. J., & Scott, S. K. (1987). On the structural stability of a simple pooled chemical system. *Journal of engineering mathematics*, 21(2), 115-127.
- [50] Tyson, J., & Kauffman, S. (1975). Control of mitosis by a continuous biochemical oscillation: synchronization; spatially inhomogeneous oscillations. *Journal of Mathematical Biology*, 1(4), 289-310.
- [51] Merkin, J. H., Needham, D. J., & Scott, S. K. (1986). Oscillatory chemical reactions in closed vessels. *Proceedings of the Royal Society of London. A. Mathematical and Physical Sciences*, 406(1831), 299-323.
- [52] Leach, J. A., Merkin, J. H., & Scott, S. K. (1991). An analysis of a two-cell coupled nonlinear chemical oscillator. *Dynamics and Stability of Systems*, 6(4), 341-366.
- [53] Ashkenazi, M., & Othmer, H. G. (1977). Spatial patterns in coupled biochemical oscillators. *Journal of Mathematical Biology*, 5, 305-350.
- [54] Liu, X. (2010). A note on the existence of periodic solutions in discrete predator-prey models. *Applied Mathematical Modelling*, 34(9), 2477-2483.
- [55] Routh, E. J. (1877). A treatise on the stability of a given state of motion, particularly steady motion: being the essay to which the Adams prize was adjudged in 1877, in the University of Cambridge. Macmillan and Company.
- [56] Freedman, H. I. (1980). Deterministic mathematical models in population ecology.
- [57] Khan, M. S., Samreen, M., Aydi, H., & De la Sen, M. (2021). Qualitative analysis of a discrete-time phytoplankton-zooplankton model with Holling type-II response and toxicity. *Advances in Difference Equations*, 2021(1), 1-29.
- [58] Zhang, W., & Zhang, G. (2018). Some dynamic models for development of insecticide resistance in insect population. *Comput. Ecol. Softw*, 8(1), 1-6.
- [59] Kareiva, P. (1990). Population dynamics in spatially complex environments: theory and data. *Philosophical Transactions of the Royal Society of London. Series B: Biological Sciences*, 330(1257), 175-190.
- [60] Levin, S. A. (1974). *Dispersion and Population Interactions* The American Naturalist.
- [61] McGillicuddy Jr, D. J. (2010). Models of harmful algal blooms: conceptual, empirical, and numerical approaches. *Journal of marine systems: journal of the European Association of Marine Sciences and Techniques*, 83(3-4), 105.

- [62] Edwards, A. M., & Brindley, J. (1999). Zooplankton mortality and the dynamical behaviour of plankton population models. *Bulletin of mathematical biology*, 61(2), 303-339.
- [63] Mukhopadhyay, B., & Bhattacharyya, R. (2006). Modelling phytoplankton allelopathy in a nutrient-plankton model with spatial heterogeneity. *Ecological modelling*, 198(1-2), 163-173.
- [64] Gao, M., Shi, H., & Li, Z. (2009). Chaos in a seasonally and periodically forced phytoplankton-zooplankton system. *Nonlinear Analysis: Real World Applications*, 10(3), 1643-1650.
- [65] Rhodes, C. J., Truscott, J. E., & Martin, A. P. (2008). Viral infection as a regulator of oceanic phytoplankton populations. *Journal of marine systems*, 74(1-2), 216-226.
- [66] Huppert, A., Olinky, R., & Stone, L. (2004). Bottom-up excitable models of phytoplankton blooms. *Bulletin of Mathematical Biology*, 66, 865-878..
- [67] Pei, Y., Lv, Y., & Li, C. (2012). Evolutionary consequences of harvesting for a two-zooplankton one-phytoplankton system. *Applied Mathematical Modelling*, 36(4), 1752-1765.
- [68] Lv, Y., Pei, Y., Gao, S., & Li, C. (2010). Harvesting of a phytoplankton-zooplankton model. *Nonlinear Analysis: Real World Applications*, 11(5), 3608-3619.
- [69] Zhang, T., & Wang, W. (2012). Hopf bifurcation and bistability of a nutrient-phytoplankton-zooplankton model. *Applied Mathematical Modelling*, 36(12), 6225-6235.
- [70] Jang, S. J., Baglama, J., & Rick, J. (2006). Nutrient-phytoplankton-zooplankton models with a toxin. *Mathematical and Computer Modelling*, 43(1-2), 105-118.
- [71] Edwards, A. M., & Brindley, J. (1996). Oscillatory behaviour in a three-component plankton population model. *Dynamics and stability of Systems*, 11(4), 347-370.
- [72] Ruan, S. (1993). Persistence and coexistence in zooplankton-phytoplankton-nutrient models with instantaneous nutrient recycling. *Journal of Mathematical Biology*, 31, 633-654.
- [73] Jang, S. J. (2000). Dynamics of variable-yield nutrient-phytoplankton-zooplankton models with nutrient recycling and self-shading. *Journal of mathematical biology*, 40, 229-250.

- [74] Chattopadhyay, J., Sarkar, R. R., & El Abdllaoui, A. (2002). A delay differential equation model on harmful algal blooms in the presence of toxic substances. *Mathematical Medicine and Biology: A Journal of the IMA*, 19(2), 137-161.
- [75] Sarkar, R. R., & Chattopadhyay, J. (2003). The role of environmental stochasticity in a toxic phytoplankton-non-toxic phytoplankton-zooplankton system. *Environmetrics: The official journal of the International Environmetrics Society*, 14(8), 775-792.
- [76] Rehim, M., & Imran, M. (2012). Dynamical analysis of a delay model of phytoplankton-zooplankton interaction. *Applied Mathematical Modelling*, 36(2), 638-647.
- [77] Lv, Y., Cao, J., Song, J., Yuan, R., & Pei, Y. (2014). Global stability and Hopf-bifurcation in a zooplankton-phytoplankton model. *Nonlinear Dynamics*, 76, 345-366.
- [78] Chattopadhyay, J., Sarkar, R., Fritzsche-Hoballah, M. E., Turlings, T. C., & Bersier, L. F. (2001). Parasitoids may determine plant fitness: a mathematical model based on experimental data. *Journal of theoretical Biology*, 212(3), 295-302.
- [79] Odum, E. P., & Barrett, G. W. (1971). *Fundamentals of ecology* (Vol. 3, p. 5). Philadelphia: Saunders.
- [80] Kuang, Y. (1988). Limit cycles in Gause-type predator-prey systems.
- [81] Holling, C. S. (1965). The functional response of predators to prey density and its role in mimicry and population regulation. *The Memoirs of the Entomological Society of Canada*, 97(S45), 5-60.
- [82] Zhang, Z., & Rehim, M. (2017). Global qualitative analysis of a phytoplankton-zooplankton model in the presence of toxicity. *International Journal of Dynamics and Control*, 5, 799-810.
- [83] Khan, M. S., Samreen, M., Ozair, M., Hussain, T., Elsayed, E. M., & Güzmez-Aguilar, J. F. (2022). On the qualitative study of a two-trophic plant-herbivore model. *Journal of Mathematical Biology*, 85(4), 34.
- [84] Baldwin, I. T., Kessler, A., & Halitschke, R. (2002). Volatile signaling in plant-herbivore interactions: what is real?. *Current opinion in plant biology*, 5(4), 351-354.
- [85] Pickett, J. A., & Poppy, G. M. (2001). Switching on plant genes by external chemical signals. *Trends in plant science*, 6(4), 137-139.

- [86] Farmer, E. E. (2001). Surface-to-air signals. *Nature*, 411(6839), 854-856.
- [87] Chattopadhyay, J., Sarkar, R., Fritzsche-Hoballah, M. E., Turlings, T. C., & Bersier, L. F. (2001). Parasitoids may determine plant fitness a mathematical model based on experimental data. *Journal of theoretical Biology*, 212(3), 295-302.
- [88] Karban, R., & Baldwin, I. T. (1997). *Induced responses to herbivory*. Chicago: Univ.
- [89] Agrawal, A. A. (1998). Induced responses to herbivory and increased plant performance. *Science*, 279(5354), 1201-1202.
- [90] Agrawal, A. A. (1999). Induced responses to herbivory in wild radish: effects on several herbivores and plant fitness. *Ecology*, 80(5), 1713-1723.
- [91] Agrawal, A. A., & Karban, R. I. C. H. A. R. D. (1999). Why induced defenses may be favored over constitutive strategies in plants. The ecology and evolution of inducible defenses, 10, 000331745.
- [92] Janzen, D. H. (1966). Coevolution of mutualism between ants and acacias in Central America. *Evolution*, 20(3), 249-275.
- [93] Meunier, L., Dalecky, A., Berticat, C., Gaume, L., & McKey, D. (1999). Worker size variation and the evolution of an ant-plant mutualism: comparative morphometrics of workers of two closely related plant-ants, *Petalomyrmex phylax* and *Aphomomyrmex afer* (Formicidae). *Insectes sociaux*, 46, 171-178.
- [94] Choquenot, D., & Parkes, J. (2001). Setting thresholds for pest control: how does pest density affect resource viability?. *Biological Conservation*, 99(1), 29-46.
- [95] Luo, X. S., Chen, G., Wang, B. H., & Fang, J. Q. (2003). Hybrid control of period-doubling bifurcation and chaos in discrete nonlinear dynamical systems. *Chaos, Solitons & Fractals*, 18(4), 775-783.
- [96] Alzahrani, A. K., Alshomrani, A. S., Pal, N., & Samanta, S. (2018). Study of an eco-epidemiological model with Z-type control. *Chaos, Solitons & Fractals*, 113, 197-208.
- [97] Alzahrani, A. K., Alshomrani, A. S., Pal, N., & Samanta, S. (2018). Study of an eco-epidemiological model with Z-type control. *Chaos, Solitons & Fractals*, 113, 197-208.
- [98] Singh, H., Dhar, J., & Bhatti, H. S. (2015). Discrete-time bifurcation behavior of a prey-predator system with generalized predator. *Advances in Difference Equations*, 2015(1), 206.



- [99] Kartal, S. (2016). Dynamics of a plant-herbivore model with differential-difference equations. *Cogent Mathematics*, 3(1), 1136198.
- [100] Din, Q., Elsadany, A. A., & Khalil, H. (2017). Neimark-Sacker bifurcation and chaos control in a fractional-order plant-herbivore model. *Discrete Dynamics in Nature and Society*, 2017.
- [101] Shah, N. H., Sheoran, N., & Jayswal, E. (2020). Z-control on COVID-19-Exposed patients in quarantine. *International Journal of Differential Equations*, 2020, 1-11.
- [102] El-Sayed, A. M., & Gaafar, F. M. (2003). Fractional calculus and some intermediate physical processes. *Applied Mathematics and Computation*, 144(1), 117-126.
- [103] Benson, D. A., Meerschaert, M. M., & Revielle, J. (2013). Fractional calculus in hydrologic modeling: A numerical perspective. *Advances in water resources*, 51, 479-497.
- [104] Sapora, A., Cornetti, P., & Carpinteri, A. (2013). Wave propagation in nonlocal elastic continua modelled by a fractional calculus approach. *Communications in Nonlinear Science and Numerical Simulation*, 18(1), 63-74.
- [105] El-Misiery, A. E. M., & Ahmed, E. (2006). On a fractional model for earthquakes. *Applied mathematics and computation*, 178(2), 207-211.
- [106] Yousef, A. M., Rida, S. Z., Gouda, Y. G., & Zaki, A. S. (2019). Dynamical behaviors of a fractional-order predator-prey model with Holling type iv functional response and its discretization. *International Journal of Nonlinear Sciences and Numerical Simulation*, 20(2), 125-136.
- [107] El-Sayed, A. M. A., & Salman, S. M. (2013). On a discretization process of fractional-order Riccati differential equation. *J. Fract. Calc. Appl*, 4(2), 251-259.
- [108] El Raheem, Z. F., & Salman, S. M. (2014). On a discretization process of fractional-order logistic differential equation. *Journal of the Egyptian Mathematical Society*, 22(3), 407-412.
- [109] Caputo, M. (1967). Linear models of dissipation whose  $Q$  is almost frequency independent-II. *Geophysical Journal International*, 13(5), 529-539.
- [110] Mukherjee, D., Das, P., & Kesh, D. (2011). Dynamics of a plantherbivore model with Holling type-II functional response. *Computational and Mathematical Biology*, 2, 1-9.

- [111] Guckenheimer, J., & Holmes, P. (2013). Nonlinear oscillations, dynamical systems, and bifurcations of vector fields (Vol. 42). Springer Science & Business Media.
- [112] DA SILVA, A. N. G. E. L. A., & RECH, P. C. (2017). Chaos and periodicity in a discrete-time Baier-Sahle model. *Asian Journal of Mathematics and Computer Research*, 123-130.
- [113] Din, Q. (2018). Controlling chaos in a discrete-time prey-predator model with Allee effects. *International Journal of Dynamics and Control*, 6(2), 858-872.
- [114] Barber, N. A., & Marquis, R. J. (2011). Leaf quality, predators, and stochastic processes in the assembly of a diverse herbivore community. *Ecology*, 92(3), 699-708.
- [115] Buckley, Y. M., Rees, M., Sheppard, A. W., & Smyth, M. J. (2005). Stable coexistence of an invasive plant and biocontrol agent: a parameterized coupled plant-herbivore model. *Journal of Applied Ecology*, 42(1), 70-79.
- [116] Feng, Z., Qiu, Z., Liu, R., & DeAngelis, D. L. (2011). Dynamics of a plant-herbivore-predator system with plant-toxicity. *Mathematical Biosciences*, 229(2), 190-204.
- [117] Edelstein-Keshet, L. (1986). Mathematical theory for plant-herbivore systems. *Journal of Mathematical Biology*, 24, 25-58.
- [118] Liu, R., Feng, Z., Zhu, H., & DeAngelis, D. L. (2008). Bifurcation analysis of a plant-herbivore model with toxin-determined functional response. *Journal of Differential Equations*, 245(2), 442-467.
- [119] O'Connell, M. I., Gilbert, B., & Brown, C. J. (2011). Theoretical predictions for how temperature affects the dynamics of interacting herbivores and plants. *The American Naturalist*, 178(5), 626-638..
- [120] Sherratt, J. A., & Murray, J. D. (1991). Mathematical analysis of a basic model for epidermal wound healing. *Journal of mathematical biology*, 29, 389-404..
- [121] Agarwal, R. P., & Wong, P. J. (1997). Advanced topics in difference equations, vol. 404 of. *Mathematics and its Applications*.
- [122] Agiza, H.N., Elabbasy, E.M., El-Metwally, H. & Elsadany, A.A. (2009). Chaotic dynamics of a discrete prey-predator model with Holling type II. *Nonlinear Analysis: Real World Applications*, 10(1), 116-129..

## Turnitin Originality Report

Stability Analysis of Fixed Points of Various Nonlinear Mathematical Models with Chaos Control by Muhammad Salman Khan .

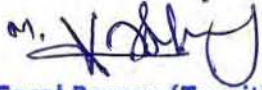



From PhD (PhD DRSMML)

- Processed on 18-Jul-2023 08:38 PKT
- ID: 2132918145
- Word Count: 42030

Similarity Index  
19%  
Similarity by Source

Internet Sources:  
12%  
Publications:  
15%  
Student Papers:  
5%

  
**Focal Person (Turnitin)**  
Quaid-i-Azam University  
Islamabad

  
**ASSOCIATE PROFESSOR**  
Department of Mathematics  
Quaid-i-Azam University  
Islamabad

**sources:**

- 1 2% match (student papers from 01-Nov-2021)  
[Submitted to Higher Education Commission Pakistan on 2021-11-01](#)
- 2 1% match (Internet from 15-Apr-2023)  
<https://advancesincontinuousanddiscretemodels.springeropen.com/articles/10.1186/s13662-021-03599-z/tables/1>
- 3 1% match (Internet from 01-Jan-2022)  
<https://www.pubfacts.com/author/+Samreen>
- 4 < 1% match (student papers from 16-Dec-2016)  
[Submitted to Higher Education Commission Pakistan on 2016-12-16](#)
- 5 < 1% match (student papers from 16-Dec-2016)  
[Submitted to Higher Education Commission Pakistan on 2016-12-16](#)
- 6 < 1% match (student papers from 01-Feb-2016)  
[Submitted to Higher Education Commission Pakistan on 2016-02-01](#)
- 7 < 1% match (student papers from 16-Dec-2016)  
[Submitted to Higher Education Commission Pakistan on 2016-12-16](#)
- 8 < 1% match (student papers from 13-Dec-2016)  
[Submitted to Higher Education Commission Pakistan on 2016-12-13](#)
- 9 < 1% match (student papers from 04-Feb-2021)  
[Submitted to Higher Education Commission Pakistan on 2021-02-04](#)
- 10 < 1% match (student papers from 09-Mar-2017)  
[Submitted to Higher Education Commission Pakistan on 2017-03-09](#)